EFFECTS OF ESSENTIAL AMINO ACIDS SUPPLY AND BODY CONDITION PREPARTUM ON ANTIOXIDANT, INFLAMMATION AND MECHANISTIC TARGET OF RAPAMYCIN PATHWAYS IN ADIPOSE TISSUE DURING THE PERIPARTURIENT PERIOD

BY

YUSHENG LIANG

DISSERTATION

Submitted in partial fulfillment of the requirements
for the degree of Doctor of Philosophy in Animal Sciences
in the Graduate College of the
University of Illinois Urbana-Champaign, 2021

Urbana, Illinois

Doctoral Committee:

Professor Juan J. Loor, Chair and Director of Research
Professor James K. Drackley
Associate Professor Yuan-Xiang Pan
Assistant Professor Joshua C. McCann

ABSTRACT

In non-ruminants, adipose tissue is responsive to amino acid supply, and amino acid can be utilized as fuels, or for protein synthesis regulated in part via insulin and mechanistic target of rapamycin (mTOR) signaling. Nuclear factor, erythroid-derived 2-like 2 (NFE2L2, formerly Nrf2) is a key transcription factor controlling cellular oxidative stress (OS) in non-ruminants. Our research examined the effects of rumen-protected methionine (RPM) supply or body condition prepartum on pathways associated with mTOR and NFE2L2 pathways in subcutaneous adipose tissue (SAT) during the periparturient period, respectively. Sixty multiparous Holstein cows were assigned from –28 to 60 d relative to parturition to a basal diet (control; 1.47 Mcal/kg of DM and 15.3% CP prepartum; 1.67 Mcal/kg and 17.7% CP postpartum) or the control plus ethyl-cellulose RPM. The RPM was fed individually at a rate of 0.09% of DMI prepartum and 0.10% postpartum. Enhanced Met supply led to greater overall mRNA abundance of Gln (*SLC38A1*), Glu (*SLC1A1*), L-type AA (Met, Leu, Val, Phe; *SLC3A2*), and neutral AA (*SLC1A5*) transporters along with greater gene expression of glutathione (GSH) metabolism-related genes. Furthermore, it upregulated protein abundance of insulin-responsive proteins phosphorylated (p) protein kinase B (p-AKT). A diet×day interaction was observed for mTOR protein abundance due to greater values for RPM cows at 30 d postpartum compared with controls. Additionally, supply of Met resulted in an overall upregulation of protein abundance of glutathione peroxidase 1 (GPX1), GPX3, glutathione S-transferase mu 1 (GSTM1), and glutathione S-transferase alpha 4 all related to GSH metabolism. There was a diet×day effect for protein abundance of NFE2L2 and its repressor Kelch-like ECH-associated protein 1 due to lower values at 30 d in cows fed Met versus controls. Therefore, the data suggest that exogenous Met may play a role in activating GSH metabolism and the anti-oxidant NFE2L2 pathways in SAT. Besides, the mTOR

pathway in SAT adapts to the change in the physiologic state during the periparturient period. Twenty-two multiparous Holstein cows were retrospectively classified into a high body condition score (HBCS; n = 11, BCS ≥ 3.5) or normal BCS (NBCS; n = 11, BCS ≤ 3.17) on d 28 before parturition. Cows were fed a corn silage- and wheat straw-based total mixed ration (TMR) during late prepartum and a corn silage- and alfalfa hay-based TMR postpartum. Cows in HBCS had greater overall plasma non-esterified fatty acid concentrations due to marked increases at 7 and 15 d postpartum. Plasma concentrations of reactive oxygen species (ROS) increased after parturition regardless of treatment. Overall ROS concentrations in SAT were greater in HBCS cows. Although HBCS cows had greater overall total protein abundance of NFE2L2 in SAT, the ratio of p-NFE2L2 to total NFE2L2 was lower, suggesting a decrease in the activity of this antioxidant system. Overall mRNA abundance of the GSH metabolism-related genes along with protein abundance of GSTM1 was greater in HBCS cows. Data suggest that HBCS cows might experience greater systemic OS after parturition, while the increased abundance of mRNA and protein components of the GSH metabolism pathway in SAT might help alleviate tissue oxidant status. Overconditioning during the late prepartum period leads to lower activation of AKT (p-AKT/total AKT) and more pronounced lipolysis postpartum; however, adipose tissue in over-conditioned cows might trigger compensatory mechanisms. We further tested the effects of enhanced amino acids (Met, Leu, Ile, Val, Arg) on protein abundance of amino acid transporter, insulin signaling, and GSH metabolism-related proteins with or without challenges (hydrogen peroxide or C2:0-ceramide) using bovine adipose explants. Enhanced amino acid supply promotes the activation of mTOR and may potentially help maintain adipose tissue functionality. Overall, these responses suggested mTOR and NFE2L2 pathways in bovine SAT are responsive to amino acid supply and BCS prepartum.

To My Family

ACKNOWLEDGEMENTS

Four years have almost gone by in a flash! It seems everything just happened yesterday. I appreciated my advisor Dr. Juan J. Loor for his guidance and support both for my research and my life during my Ph.D. study. I also thank Dr. James K. Drackley, Dr. Yuan-Xiang Pan, and Dr. Joshua C. McCann who serve for my committee. Thanks for their time and valuable suggestions for my research.

I appreciate my lab mates and visiting scholars, including Dr. Abdulrahman Alharthi, Dr. Mario Vailati-Riboni, Dr. Fernanda Batistel, Dr. Danielle Coleman, Dr. Ahmed A. Elolimy, Ryan Bucktrout, Dr. Hongyu Dai, Dr. Xinwei Li, Dr. Fang Liu, and Dr. Nana Ma, for their help both in my research and my personal life. Without you, life would lose some of its joy. The times we spent together on the farm, in the lab, and in offices were memorable. I also appreciate my friends Zongyang Li, Nicholas Didycz, Christopher Godas, and Dr. Roman Erdmann for their support and encouragement!

I sincerely thank the China Scholarship Council. This four years' study has not only been a process of gaining knowledge but also a chance to explore a bigger world. I appreciate everything that I have experienced in the last four years, which is invaluable and will have an impact on my whole life. The future is a mystery and you never know what will happen. Be optimistic and be grateful! Please enjoy every day and be well prepared to explore a new world! Stay hungry, stay foolish!

TABLE OF CONTENTS

CHAPTER 1: LITERATURE REVIEW

INTRODUCTION

The periparturient period is the most challenging time during the dairy production cycle (Drackley, 1999). Peripartal cows have decreased dry matter intake (**DMI**); however, they have increased energy requirements due to fetal growth and milk synthesis. Therefore, they experience negative energy balance (**NEB**) and negative amino acid (**AA**) balance and have to mobilize their body fat to satisfy the increased energy demands (Drackley, 1999, Schwab and Broderick, 2017). However, excessive body fat mobilization causes oxidative stress and inflammation and increases the incidence of metabolic diseases such as ketosis and fatty liver (Sordillo et al., 2009, Sordillo and Mavangira, 2014). Additionally, dairy cows are characterized by insulin resistance during the periparturient period (De Koster and Opsomer, 2013). It is noteworthy that cows with high body condition scores exhibit a greater extent of oxidative stress and fat mobilization (Bernabucci et al., 2005).

Previous studies consistently observed that enhanced rumen-protected methionine (**RPM**) could alleviate systemic oxidative stress and inflammation in peripartal cows (Osorio et al., 2014b, Sun et al., 2016, Batistel et al., 2018). In non-ruminants, adipose tissue plays a crucial role in regulating oxidative stress, inflammation, and insulin resistance (Dludla et al., 2019). It has been demonstrated that adipose tissue is also responsible for amino acid metabolism in humans and rodents (Frayn et al., 1991, Herman et al., 2010). Adipose tissue is an insulin-sensitive site and is of great importance to produce free fatty acids (Sechen et al., 1990). Interestingly, a recent study suggests that adipose tissue is a potential site for branched-chain amino acid (**BCAA**) catabolism in dairy cows during early lactation (Webb et al., 2019).

However, whether amino acid metabolism in adipose tissue is responsive to post-ruminal AA supply is largely unknown in dairy cows.

Therefore, our general hypothesis is that adipose tissue plays a role in regulating systemic oxidative stress, inflammation, and insulin resistance in peripartal cows, and that it is affected by BCS and nutritional intervention (e.g., essential AA supply).

Periparturient Period in Dairy Cows

The periparturient period, the most challenging phase in the dairy production cycle, is defined as the period from 3 weeks before to 3 weeks after parturition (Drackley, 1999). This period is characterized by a high incidence of metabolic disorders including fatty liver, ketosis, and milk fever (Sordillo et al., 2009, Sordillo and Mavangira, 2014) which accounts for large economic losses on dairy farms. Peripartal cows exhibit decreased DMI, especially after parturition, resulting in NEB, which at least partly explains increased health issues during the periparturient period. Besides, peripartal cows also show negative AA balance (Schwab and Broderick, 2017). Therefore, it is of great importance to provide adequate nutrients, such as AA, for peripartal cows. Great progress has been made in the area of dairy research including genetics, physiology, and nutrition in the past decades; however, the exact molecular mechanism on impaired health status in peripartal cows is unclear.

Oxidative Stress

Oxidative stress is caused by the imbalance between cellular antioxidants availability and free radicals generation, leading to cell damage (Sies, 1997, Ott et al., 2007). Glutathione (**GSH**) is a major antioxidant in mammal cells (Aquilano et al., 2014). Oxidative stress biomarkers are altered during the periparturient period: for instance, increased concentrations of reactive oxygen species (**ROS**) and thiobarbituric acid-reactive substances, and decreased concentrations of GSH

and β-carotene in plasma, were observed in cows after parturition (Bernabucci et al., 2005, Osorio et al., 2014b, Batistel et al., 2018). Decreased DMI and increased body fat mobilization in peripartal cows are responsible for antioxidants depletion and free radicals generation (Celi, 2011, Osorio et al., 2014b, Sordillo and Mavangira, 2014). Antioxidants/antioxidant precursors (e.g., vitamin E, Met, and Se) supply improves health status and production performance (e.g., milk yield and milk protein content) in peripartal cows (Smith et al., 1997, Sun et al., 2016, Batistel et al., 2017b, Batistel et al., 2018, Zahrazadeh et al., 2018). Therefore, available data suggest that peripartal cows experience oxidative stress and oxidative stress is negatively associated with production performance.

Oxidative stress not only results in decreased lactation performance (e.g., reduced milk fat percentage and fat: protein ratio) in high producing dairy cows (Vázquez-Añón et al., 2008, Zahrazadeh et al., 2018) but also leads to poor calf performance (Jacometo et al., 2015, Ling et al., 2018, Xu et al., 2018, Alharthi et al., 2019), both of which cause economic losses for dairy farmers. Besides, in vitro studies using varied types of bovine cells including mammary epithelial cells, adipocytes, and aortic endothelial cells, demonstrate that oxidative stress induces apoptosis (Trigona et al., 2006, Jin et al., 2016, Song et al., 2016, Ma et al., 2019b, Sun et al., 2019), which might partly explain compromised immunity in peripartal cows (Sordillo and Aitken, 2009). Indeed, it has been well recognized that enhanced antioxidants supply (e.g., vitamin E and β-carotene) reduces the incidence of diseases such as mastitis and metritis in dairy cows (Spears and Weiss, 2008, Yang and Li, 2015). Additionally, recent studies also observed that oxidative stress is positively associated with insulin resistance (Abuelo et al., 2016a, Abuelo et al., 2016b), which potentially makes dairy cows more susceptible to suffer from metabolic

disorders. Thus oxidative stress has a detrimental effect on the well-being of dairy cows and decreases dairy farm profits.

Antioxidative Role of NFE2L2 in Varied Bovine Tissues

Although oxidative stress results in cell damage via impairing cellular macromolecules such as proteins, lipids, and DNA, organisms have their cytoprotective mechanisms in response to redox balance changes (Ma, 2013). In non-ruminants, it is well-known that the antioxidant transcription factor nuclear factor erythroid 2-like 2 (**NFE2L2**) is responsible for regulating oxidative stress via the activation of antioxidant response element-dependent genes such as heme oxygenase 1 (***HMOX1***), NAD(P)H quinone oxidoreductase 1 (***NQO1***), glutathione-S-transferase (***GST***), glutamate-cysteine ligase (***GLC***), and cytochrome P450 (***CYP***) (Bataille and Manautou, 2012, Kansanen et al., 2013, Ma, 2013). The mechanism on how NFE2L2 plays an antioxidative role has been well-reviewed previously (Aleksunes and Manautou, 2007, Kansanen et al., 2013). Briefly, under homeostatic conditions, Kelch-like ECH-associated protein 1 (**KEAP1**) binds to NFE2L2 which contributes to NFE2L2 degradation, consequently suppressing the activation of NFE2L2 (Kansanen et al., 2013). By contrast, ROS overproduction results in the disassociation between KEAP1 and NFE2L2, consequently leading to NFE2L2 activation (Bataille and Manautou, 2012).

The role of NFE2L2 has also been explored in dairy cows under stressful conditions over the past decade. Transcription data reveal that target genes of the NFE2L2 pathway, including glutathione peroxidase 3 (***GPX3***), microsomal glutathione S-transferase 3, superoxide dismutase, catalase (***CAT***), NAD(P)H dehydrogenase, *NQO1*, and *HMOX2*, were markedly upregulated from 3wk prepartum to 1wk postpartum in the liver of dairy cows (Gessner et al., 2013). Likewise, compared to prepartum, greater mRNA abundance related to glutamate-

cysteine ligase catalytic subunit (***GCLC***), glutathione reductase (***GSR***), thioredoxin reductase 1, ferrochelatase, thioredoxin, and *NQO1* along with greater activation of NFE2L2 (p-NFE2L2/NFE2L2) was observed in the bovine mammary gland postpartum (Han et al., 2018b). In vitro studies also showed similar results, for instance, *NFE2L2* silencing in bovine mammary epithelial cells (**BMEC**) led to the accumulation of intracellular ROS concentrations stimulated with hydrogen peroxide (H_2O_2, 600 μ*M*), suggesting that *NFE2L2* plays a role in eliminating ROS in the bovine mammary gland (Ma et al., 2019b). Accumulating evidence demonstrates that oxidative stress induced by H_2O_2 results in apoptosis in BMEC (Jin et al., 2016, Basiricò et al., 2017, Ma et al., 2019b). Except for ROS, in vitro studies using bovine hepatocytes also indicate that non-esterified fatty acids (**NEFA**) and ketone bodies (e.g., β-hydroxybutyrate and acetoacetate) promote the development of oxidative stress and apoptosis (Song et al., 2014, Song et al., 2016, Du et al., 2018). Peripartal cows are characterized by NEB, leading to elevated NEFA and ketone bodies postpartum (Drackley, 1999), which might also explain greater activation of NFE2L2 after parturition. Altogether, the data imply that NFE2L2 potentially plays a role in modulating oxidative stress in different tissues including the liver and mammary gland in dairy cows and the activation of NFE2L2 may help mitigate cell damage under the oxidative stress challenge.

Inflammation

Acute-phase proteins (**APP**), a critical part of acute phase response, are widely used as inflammatory biomarkers in dairy cows. Acute-phase proteins include positive APP, such as haptoglobin and ceruloplasmin, and negative APP, such as albumin and paraoxonase (Ceciliani et al., 2012, Tothova et al., 2014). The liver is a major site for AAP production and peripartal cows have lower liver function along with greater inflammatory responses, thus impaired liver

function may contribute to the increased inflammatory response in peripartal cows (Bionaz et al., 2007, Bertoni et al., 2008). Interestingly, previous studies observed that peripartal cows showed increased inflammatory biomarkers (Sabedra, 2012). Hence, it is likely that inflammatory response during the transition period is one of the adaptive mechanisms for dairy cows to cope with acute metabolic changes. However, inflammation is energy-consuming and it also costs AA to produce antibodies or acute phase proteins (Klasing and Iseri, 2013, Khiaosa-ard et al., 2018). Therefore, prolonged inflammatory response potentially impairs both productive and reproductive performance of high-yielding dairy cows partly due to energy or nutrients limitation. Furthermore, transcription data showed that haptoglobin and pro-inflammatory markers such as C-C motif chemokine ligand 2 ***(CCL2)***, toll-like receptor 4 (***TLR4)***, and tumor necrosis factor (***TNF)*** are increased in liver and adipose tissue in early lactating cows (Loor et al., 2005, Saremi et al., 2012, Vailati Riboni et al., 2015). Thus, available data suggest that dairy cows experience systemic inflammatory responses during the transition period.

Body fat mobilization helps satisfy increased energy requirements in transition cows. However, excessive body fat mobilization leads to increased concentrations of NEFA in plasma which can trigger inflammatory responses in dairy cows. In vitro studies using bovine hepatocytes suggest that high NEFA concentrations result in apoptosis subsequently leading to inflammation (Song et al., 2014, Li et al., 2020). Besides, increased NEFA concentrations disrupt leukocytes and endothelial cell functions of peripartal cows (Contreras et al., 2010). Therefore, excessive accumulation of NEFA at least partly explains increased inflammatory response in peripartal cows. Furthermore, the changes of lipid metabolites (e.g., hydroxy-octadecadienoic acids and hydroxy-eicosatetraenoic acids) may explain increased inflammatory response in dairy cows during the transition period as well (Contreras et al., 2017). Overall, data suggest that lipid

metabolism plays a pivotal role in regulating inflammation in dairy cows during the transition period.

Insulin Resistance

Insulin, a critical growth hormone, regulates anabolic processes such as protein synthesis and glycogen synthesis and plays an important role in modulating systemic glucose homeostasis (Shulman, 2000, Kimball et al., 2002). Insulin resistance is caused by decreased insulin sensitivity or decreased insulin responsiveness or the combination of both, which finally impairs glucose transport in insulin-sensitive tissues (Kahn, 1978). Peripartal cows exhibit decreased DMI around calving especially during early lactation. However, they need more energy/nutrients for fetal growth and mammary gland development before calving and milk synthesis after calving. Thus, actual feed intake is lower than the highly demanding energy requirement for fetal growth and milk production resulting in negative energy/nutrient balance. Transition cows have to mobilize their body energy reserves to support fetal growth and milk production. To some extent, insulin resistance is a compensatory mechanism for dairy cows to cope with increased energy requirements for milk production coupled with decreased DMI (De Koster and Opsomer, 2013). However, excessive insulin resistance leads to increased body fat mobilization which exacerbates oxidative stress and inflammation in dairy cows.

The macrophage is an important immune cell of innate immunity. Generally, there are two classical types of M1 macrophage (classically activated) and M2 macrophage (alternatively activated) (Galván-Peña and O'Neill, 2014). It has been demonstrated that the accumulation of ceramides contributes to the conversion of M2 to M1 macrophage, resulting in an increased inflammatory response in mice (Chaurasia et al., 2016). Accumulating evidence suggests that ceramides are potential mediators in the regulation of insulin resistance in peripartal cows

(McFadden and Rico, 2019). For instance, ceramides accumulate in the plasma and liver of dairy cows during the periparturient period and systemic insulin sensitivity is inversely related to plasma ceramide concentrations (Rico et al., 2017). Insulin resistance is positively associated with body fat mobilization and circulating ceramides, especially in overconditioned cows (Rico et al., 2015), which may potentially contribute to the development of metabolic disorders (McFadden and Rico, 2019). Further studies are needed to demonstrate the role of ceramides in regulating insulin resistance in dairy cows.

The Role of Methionine in Regulating Production Performance and Health

Peripartal cows experience oxidative stress and inflammation which impairs production performance and animal welfare (Sordillo and Mavangira, 2014, Bradford et al., 2015). Additionally, maternal oxidative stress leads to lower immunity and higher incidences of morbidity in their offspring (Ling et al., 2018, Abuelo et al., 2019). Therefore, improving dairy health status plays a pivotal role in the dairy industry. Methionine (**Met**), a limiting AA in lactating cows, plays multiple roles in regulating metabolism and production performance in dairy cows (Coleman et al., 2021). Previous studies observed that a greater supply of RPM enhances DMI, milk yield, and milk protein content (Osorio et al., 2013, 2014a, Batistel et al., 2017b, Batistel et al., 2018). In vitro studies observed that Met addition promotes β-casein synthesis via the activation of the mammalian target of rapamycin (mTOR) due to increased Met availability in BMEC (Nan et al., 2014, Dai et al., 2019), which partly explains increased milk protein yield in RPM cows. Interestingly, calves from the maternal RPM supply group had greater newborn body weight than the control, which may partially due to increased gene expression of nutrient transporters and greater activation of mTOR in the placenta in cows with RPM supply (Batistel et al., 2017a). Transcription data indicate that late pregnancy RPM supply

could enhance calf immunity due to the alteration of mRNA abundance associated with cell adhesion and chemotaxis, oxidative stress, toll-like receptor signaling, and Met metabolism in both polymorphonuclear leukocytes and liver (Jacometo et al., 2017, Jacometo et al., 2018). Overall, RPM supply during late pregnancy not only improves milk yield and protein yield but also calf performance.

Methionine is not only a building block for protein synthesis but also participates in the synthesis of antioxidants such as taurine and GSH via the transsulfuration pathway (Stipanuk, 2004). Indeed, post-ruminal Met supplementation increased Met concentrations in plasma and liver (Zhou et al., 2016a, Batistel et al., 2017a). Moreover, RPM supply downregulated plasma concentration of ROS and upregulated plasma concentrations of ferric-reducing antioxidant power, β-carotene, tocopherol, and total and reduced GSH (Batistel et al., 2018). Similar results were observed by Sun et al. (2016), that RPM increased plasma total antioxidant capacity, GPX activity, and vitamin E. Consistently, transcription data indicate that enhanced RPM upregulates gene expression of key enzymes (e.g., *GCLC* and *GCLM*) associated with GSH synthesis in mammary gland and liver (Osorio et al., 2014a, Han et al., 2018a). Besides, increased mRNA abundance of met cycle including S-adenosyl homocysteine hydrolase and 5-methyltetrahydrofolate-homocysteine methyltransferase was detected in the liver of RMP cows (Osorio et al., 2014b). The data support the idea that reduced systemic oxidative stress is in large part driven by enhancing Met availability and by additional flux of Met through the Met cycle in the liver. It is noteworthy that enhanced RPM improves DMI in dairy cows during the transition period (Osorio et al., 2013, Zhou et al., 2016b, Batistel et al., 2017b), which provides more nutrients and energy, consequently improving health status as well. Overall, enhanced RPM supply during the transition period resulting in elevated circulating Met level, coupled with

increased DMI, contributes to antioxidants synthesis. Further in vitro studies are needed to demonstrate whether the antioxidative responses are caused by Met supply directly.

Adipose Tissue

Adipose tissue is well-known for its role in energy storage. Emerging evidence has demonstrated that adipose tissue plays a crucial role in regulating oxidative stress and inflammation in non-ruminants (Maury and Brichard, 2010, Fernández-Sánchez et al., 2011). Besides, it is also a major insulin sensitivity site, which has an important influence on glucose utilization (Salans et al., 1968). Adipose tissue can be classified into subcutaneous, omental, and mesenteric adipose tissue based on its location. Adipose tissue is responsible for supporting milk synthesis and metabolic regulation (Bell and Bauman, 1997, Zachut, 2015). A previous slaughter study indicates that subcutaneous adipose tissue (**SAT**) is one of the highly mobilized depots in dairy cows during early lactation (Butler-Hogg et al., 1985).

Adipocytes are the dominant cell type in adipose tissue. In humans and rodents, they can be classified as white adipocytes, brown adipocytes, or beige adipocytes based on their function, location, and structure: a white adipocyte has few mitochondria and large lipid droplets while a brown adipocyte has more mitochondria and small lipid droplets (Kajimura et al., 2015, Sidossis and Kajimura, 2015). Brown adipose tissue contributes to converting food energy to heat (Cannon and Nedergaard, 2004). White adipose tissue can be converted to a browning state during cold exposure (Kleiner et al., 2012). Interestingly, a recent study found that brown adipose tissue is positively associated with BCAA consumption in humans and rodents, which is controlled by a mitochondria carrier, SLC25A44, a BCAA transporter (Yoneshiro et al., 2019). Transplantation of normal adipose tissue into globally BCAA transaminase 2 (***BCAT2***) knock-out mice resulted in decreased circulating levels of BCAA, suggesting that white adipose tissue

is responsible for BCAA catabolism (Herman et al., 2010). Altogether, data suggest that adipose tissue plays a role in BCAA utilization. Compared with muscle, liver, and mammary gland, adipose tissue (visceral and subcutaneous) has the most abundant mRNA abundance of the *BCAT2* suggesting that bovine adipose tissue might play a critical role in regulating BCAA catabolism in early lactation (Webb et al., 2019). Future studies are also needed to investigate if brown adipose tissue exists in dairy cows. If it exists, what is the role of brown adipose in regulating immunometabolism in dairy cows?

Besides adipocytes, adipose tissue is also composed of other cell types including eosinophils, endothelial cells, neutrophils, and macrophages (Dam et al., 2016). Obese humans and rodents are characterized by macrophage infiltration in adipose tissue which leads to inflammation and insulin resistance (Kanda et al., 2006, Heilbronn and Campbell, 2008). Furthermore, macrophage polarization has been observed in the adipose tissue of obese mice (Lumeng et al., 2007). Some studies indicate that macrophage infiltration occurs in dairy cow SAT during the transition period and is positively associated with body fat mobilization (De Koster et al., 2018, Newman et al., 2019). In contrast, it has been reported that that macrophage infiltration may not play a critical role in regulating inflammatory response due to low numbers of macrophages observed in SAT (Akter et al., 2012, Häussler et al., 2017). Therefore, the role of macrophage polarization in regulating inflammatory response and in dairy cows merits further study.

Insulin binding to the insulin receptor (**INSR**) triggers a cascade of events in which phosphorylation of protein kinase B (**AKT**) enhances INSR phosphorylation followed by activation of insulin receptor substrate 1, subsequently leading to greater expression of glucose transporter 4 on the plasma membrane to allow for uptake of glucose (Pessin and Saltiel,

2000). Transcription data suggest that gene expression of the insulin signaling pathway in SAT changes through the transition period (Ji et al., 2012). A recent study further confirmed that insulin signaling plays a role in regulating homeorhetic adaptation during the periparturient period (Kenéz et al., 2019). Bovine primary adipocytes challenged with C2:0-ceramide showed impaired insulin sensitivity along with decreased activation of AKT (p-AKT/AKT), an important component of the insulin signaling pathway (Rico et al., 2018). Therefore, ceramides might play a role in regulating insulin resistance in bovine adipose tissue. Dairy cows experience oxidative stress, inflammation, and insulin resistance during the periparturient period (Bernabucci et al., 2005, De Koster and Opsomer, 2013, Bradford et al., 2015). Therefore, it is necessary to investigate the role of adipose tissue in regulating immuometabolism in peripartal cows and how nutritional intervention affects adipose function.

mTOR and Amino Acids

The mammalian target of rapamycin (**mTOR**) plays a critical role in regulating the cellular metabolism by the nutrient-sensing signaling network (Howell and Manning, 2011). Methionine is the first limiting AA in dairy cows and RPM supply contributes to utilizing the AAs more efficiently (Schwab and Broderick, 2017). In non-ruminants, BCAA including leucine, isoleucine, and valine, are essential AAs (Lu et al., 2013) and are key regulators of mTOR which controls protein synthesis and cell growth (Lynch and Adams, 2014). In vitro studies suggest that BCAA play a potential role in regulating protein synthesis via the activation of the mTOR pathway in BMEC (Appuhamy et al., 2012, Dong et al., 2018). In contrast, in vivo studies do not observe positive effects of BCAA supplementation on milk protein synthesis in lactating cows (Appuhamy et al., 2011). Interestingly, research related to obesity suggests that circulating BCAA was associated with insulin resistance (Newgard et al., 2009, McCormack et

al., 2013). Dairy cows experience insulin resistance around calving. However, whether enhanced BCAA supply impairs insulin signaling in dairy cows is unclear.

Evidence shows that adipose tissue is able to catabolize BCAAs in vivo and has an effect on circulating BCAA levels via the alteration of BCAA enzymes (Herman et al., 2010). Branched-chain α-keto acid dehydrogenase kinase (**BCKDK**) regulating the inactivation and phosphorylation of the branched-chain α-keto acid dehydrogenase complex is a rate-limiting one for BCAAs catabolism (Shimomura et al., 2001). Besides, emerging evidence indicates that adipose tissue might be a target organ for BCAA metabolism, including in dairy cows (Webb et al., 2020), particularly during sufficient glucose supplementation (Nichols et al., 2016). A previous study showed that enhanced RPM supply improved milk protein in transition cows (Batistel et al., 2017b). Additionally, in vitro studies indicate that Met supply activates the mTOR pathway in BMEC (Lu et al., 2012, Nan et al., 2014). At least in non-ruminants, the mTOR signaling pathway seems to exert some control on adipose biology and function via regulating aspects of lipid metabolism and adipokine synthesis/secretion (Cai et al., 2016). For instance, adipocyte-specific *mTOR*-silencing in mice led to insulin resistance and inhibited adipocyte differentiation via the peroxisome proliferator-activated receptor γ signaling pathway (Shan et al., 2016). However, it is unknown whether RPM supply affects the mTOR pathway in bovine adipose tissue.

Despite Arg being a semi-essential AA for adult mammals, data highlight the significance of Arg in promoting milk protein synthesis (Ding et al., 2019) and alleviating inflammatory responses in lactating Holstein cows challenged with lipopolysaccharide (**LPS**) (Zhao et al., 2018). In vitro studies also reported that increased Arg concentration (Lys: Arg ratio at 1:1) led to downregulated mRNA abundance of solute carrier family 7 member 1 (***SLC7A1***), a

major Arg transporter, along with greater activation of p-mTOR (p-mTOR/total mTOR) in primary BMEC (Hu et al., 2020). However, enhanced Arg supply attenuated downregulation of *SLC7A1* in BMEC challenged with LPS (Dai et al., 2020). Collectively, data suggest that increased Arg supplementation could enhance lactation performance and help alleviate inflammation partly due to altered AA metabolism and mTOR activation. A recent in vitro study observed that 200 μmol L-Arg/L compared with 50 and 100 μmol/L upregulated p-mTOR in ovine adipocyte precursor cells (Ma et al., 2017), which underscored that L-Arg could stimulate mTOR in ruminant SAT. Whether these effects also might occur locally in bovine SAT is unknown.

Body Condition

Body condition is used to evaluate body energy reserves in dairy cows (Roche et al., 2013). However, direct measurement of body energy reserves on a large scale is not practical. Therefore, body condition score (**BCS**) is introduced to appraise apparent adiposity based on stored energy reserves of dairy cows (Wildman et al., 1982). The 5-point scale is widely used in North America. It is noteworthy that high BCS (**HBCS**) cows at calving have a greater risk of milk fever, ketosis, and fatty liver (Roche et al., 2013). Additionally, cows calving at HBCS are more sensitive to oxidative stress (Bernabucci et al., 2005) and are more likely to experience a greater extent of insulin resistance at the end of the dry period (De Koster et al., 2015). Subcutaneous adipose tissue of overconditioned cows (BCS $\geq$ 4.0) has lower mRNA and protein abundance of the insulin receptor (Zhang et al., 2019) and has greater pro-inflammatory response postpartum than cows calving at a “normal” BCS (Vailati-Riboni et al., 2016, Zhang et al., 2019). Thus, BCS management before calving on dairy farms has important implications for production performance, herd health, animal welfare, and overall farm profitability.

It is well-known that energy metabolism, especially for lipid metabolism, contributes to the different incidences of metabolic disorders between HBCS and low BCS (**LBCS**) cows (Roche et al., 2009, De Koster et al., 2016). Studies have verified that limiting AA, such as Met and Lys, supplementation plays a crucial role in regulating dairy cow production performance and immunometabolism in the last two decades (Schwab and Broderick, 2017). However, little is known about whether nitrogen metabolism (e.g., AA metabolism) differs between cows with HBCS or LBCS, especially in adipose tissue. At least cows with different BCS at calving have different strategies to meet their energy requirement during the periparturient period, for instance, HBCS (BCS ≥ 3.75) cows mobilize more body fat rather than muscle compared with LBCS (2.75 ≤ BCS) cows (Pires et al., 2013) which is likely to lead to differences in nitrogen metabolism. Human and rodent studies have demonstrated that adipose tissue is able to utilize AA (Feller and Feist, 1963, Badoud et al., 2014). A study on mice also verified that adipose tissue has a complete urea cycle (Arriarán et al., 2015). A recent metabolomics study observed that compared with normal BCS (**NBCS**) (BCS < 3.5) cows before calving, calving at HBCS (BCS > 3.75) led to greater abundance of BCAA catabolism-related molecules along with increased circulating concentrations of Leu, Ile, Val, His, Lys, and Orn (Ghaffari et al., 2019b). The mTOR, regulated by AA such as Leu, plays a crucial role in cellular growth, differentiation, and protein synthesis (Javed and Fairweather, 2019). Compared with NBCS cows, skeletal muscle of HBCS cows had greater mRNA abundance of *mTOR* and eukaryotic translation initiation factor 4E binding protein 1 without changes in ribosomal protein S6 kinase 1, suggesting that BCS is associated with unique mTOR signaling pathway profiles (Ghaffari et al., 2019a). Despite extensive research on the use of BCS as a management tool and its association

with important physiological aspects, molecular mechanisms of oxidative stress and nitrogen metabolism associated with BCS in adipose tissue are largely unknown.

Amino Acid Transporters

Amino acids are not only building blocks for protein synthesis but also participate in the TCA cycle and regulate cellular redox balance (Stipanuk, 2004, Wu, 2009). The TCA cycle is the hub of carbohydrate, lipid, and protein metabolism, which is essential for cell homeostasis. Furthermore, accumulating evidence suggests that intermediates of the TCA cycle (e.g., acetyl-CoA, citrate, and succinate) play important roles in regulating innate immunity and inflammation (Williams and O'Neill, 2018, Martínez-Reyes and Chandel, 2020). Therefore, some AA may modulate the immune responses via the alterations of TCA intermediates. Amino acids can be transported to intracellular space or some organelles via membrane-bound proteins called AA transporters (Kandasamy et al., 2018). Amino acid transporters can be classified into symporter, uniporter, and antiporter and each AA transporter is responsible for transporting specific AA (Bröer, 2002). Amino acid transporters can also be classified into systems A, N, ASC, L, T, x^-c, and y^+ according to transport function (Kandasamy et al., 2018). For example, the L-type AA transporter, SLC7A5, transports BCAA to the intracellular space in exchange for glutamine (Scalise et al., 2018). System A transporters, SLC38A1 and SLC38A2, are responsible for glutamine transport (Bröer, 2014). Branched-chain amino acids, particularly leucine, are potent modulators of the mTOR pathway (Lynch and Adams, 2014). Amino acids including glutamate, glycine, and cysteine are substrates for GSH synthesis (Lu, 2013). Glutamine can be deaminated to glutamate via glutaminase (Nissim, 1999), and subsequently, glutamate can be further utilized for GSH synthesis. Besides, glutamine is an important fuel for immune cells (Newsholme, 2001). Thus, AA transporters can regulate AA availability in intracellular space and subsequently affect

protein synthesis, TCA cycle, and redox balance in cells, which plays a pivotal role in controlling cell function homeostasis (Sundberg et al., 2008, Kandasamy et al., 2018).

In non-ruminants, AA transporters are widely expressed in different types of tissues such as the intestine, skeletal muscle, brain, and adipose tissue (Fotiadis et al., 2013, Li et al., 2016). Most dairy research related to AA transporters focuses on how they regulate milk protein synthesis in the bovine mammary gland (Dai et al., 2019, Dai et al., 2020, Hu et al., 2020). Previous in vitro studies indicate that greater essential AA (e.g., BCAA and Met) supply increased gene expression of AA transporters which may promote the activation of mTOR to stimulate protein synthesis in BMEC (Dong et al., 2018, Dai et al., 2019, Hu et al., 2020). Besides, in vivo studies also observed that greater RPM supply upregulates gene expression of AA transporters in both mammary gland and placenta in dairy cows (Batistel et al., 2017a, Ma et al., 2019a). Thus, available data support the idea that mRNA abundance of AA transporters is modulated by AA levels in the diet.

Dairy cow plasma NEFA are mainly composed of oleic acid (C18:1), palmitic acid (C16:0), and stearic acid (C18:0), and also include arachidonic acid (C20:4) and docosahexaenoic acid (C22:6) (Contreras et al., 2010). Oleic acid enhances system A AA uptake, without affecting system L AA activity in cultured human primary trophoblast cells, which is mediated via TLR4 (Lager et al., 2013). Besides TLR4, other cytokines such as cytokines interleukin (**IL**)-6 and tumor necrosis factor (**TNF α**) also stimulate the activity of AA transporter system A rather than system L (Jones et al., 2009). Although docosahexaenoic acid alone did not alter AA transport activity, the combination of oleic acid and docosahexaenoic acid increased system A AA activity in human primary trophoblast cells (Lager et al., 2014). In pigs, dietary n-6:n-3 polyunsaturated fatty acids (**PUFA**) ratios of 1:1–5:1 modulate AA profile and

AA transporters (e.g., large neutral AA transporter and *SLC38A2*) transcription level in skeletal muscle indicating that PUFA alters AA transport and metabolism (Li et al., 2015). Those results reveal that fatty acids play a role in regulating AA transport in different types of cells in non-ruminants. It is well established that lipolysis leads to inflammation in dairy cows during the transition period subsequently leading to increased mRNA abundance of pro-inflammatory cytokines such as *TNF α* and *IL-6* (Contreras et al., 2018). Over-conditioned cows have larger adipocytes in SAT, and larger adipocytes have greater basal lipolytic activity (De Koster et al., 2015), suggesting more NEFA are available in the adipose tissue of overconditioned cows. Negative energy balance also leads to increased gene expression of *TLR4* in bovines in blood polymorphonuclear cells (Moyes et al., 2010). Additionally, an in vitro study revealed that LPS challenge increased gene expression of *TLR 4* in bovine adipose tissue (Mukesh et al., 2010). Thus, fat mobilization may affect the gene expression of AA transporters in adipose tissue due to increased pro-inflammatory cytokines. However, limited research has been done on AA transporters in bovine adipose tissue. Both nutritional strategy and body condition affect oxidative stress and inflammation in peripartal cows (Bernabucci et al., 2005, Alharthi et al., 2018, Batistel et al., 2018). Therefore, it is of great interest to explore whether RPM supply and body condition help improve health status via the alterations of AA transporters in bovine adipose tissue.

SUMMARY

Peripartal cows experience systemic oxidative stress, inflammation, and insulin resistance. However, the exact molecular mechanisms on these responses are still unclear, particularly in adipose tissue. NFE2L2, a key transcription factor in regulating redox balance in mammal cells, promotes antioxidative responses under the condition of oxidative stress (Bataille

and Manautou, 2012, Kansanen et al., 2013, Ma, 2013). Glutathione is a major antioxidant and Met can be utilized for GSH synthesis via the transsulfuration pathway (Stipanuk, 2004, Aquilano et al., 2014). mTOR plays a critical role in regulating cell homeostasis and AA (e.g., Met, Arg, and Leu) are key regulators of the activation of mTOR (Howell and Manning, 2011). Amino acid availability in intracellular space is partly regulated by AA transporters. Thus the changes of AA transporters may influence antioxidant synthesis and the activation of mTOR in adipose tissue.

Our general hypothesis is that enhanced essential AA supply and BCS prepartum alter the protein abundance of AA transporters, NFE2L2 and mTOR pathways. The overall objective of this dissertation is to investigate whether AA supply (in vivo and in vitro) and body condition regulate the amino acid transporter, antioxidant, inflammation, and mTOR pathways in bovine SAT during the periparturient period or when challenged with stresses such as hydrogen peroxide and C2:0-ceramide.

REFERENCES

Abuelo, A., V. Alves-Nores, J. Hernandez, R. Muiño, J. Benedito, and C. Castillo. 2016a. Effect of parenteral antioxidant supplementation during the dry period on postpartum glucose tolerance in dairy cows. J. Vet. Intern. Med. 30:892-898.

Abuelo, A., J. Hernández, J. L. Benedito, and C. Castillo. 2019. Redox biology in transition periods of dairy cattle: Role in the health of periparturient and neonatal animals. Antioxidants 8:20.

Abuelo, Á., J. Hernández, J. L. Benedito, and C. Castillo. 2016b. Association of oxidative status and insulin sensitivity in periparturient dairy cattle: an observational study. J. Anim. Physiol. Anim. Nutr. 100:279-286.

Akter, S., S. Häussler, D. Germeroth, D. Von Soosten, S. Dänicke, K.-H. Südekum, and H. Sauerwein. 2012. Immunohistochemical characterization of phagocytic immune cell infiltration into different adipose tissue depots of dairy cows during early lactation. J. Dairy Sci. 95:3032-3044.

Aleksunes, L. M. and J. E. Manautou. 2007. Emerging role of Nrf2 in protecting against hepatic and gastrointestinal disease. Toxicol. Pathol. 35:459-473.

Alharthi, A., D. Coleman, Y. Liang, F. Batistel, A. Elolimy, R. Yambao, E. Abdel-Hamied, Y.-X. Pan, C. Parys, and I. Alhidary. 2019. Hepatic 1-carbon metabolism enzyme activity, intermediate metabolites, and growth in neonatal Holstein dairy calves are altered by maternal supply of methionine during late pregnancy. J. Dairy Sci. 102:10291-10303.

Alharthi, A., Z. Zhou, V. Lopreiato, E. Trevisi, and J. J. Loor. 2018. Body condition score prior to parturition is associated with plasma and adipose tissue biomarkers of lipid metabolism and inflammation in Holstein cows. J. Anim. Sci. Biotechnol. 9:12.

Appuhamy, J., J. Knapp, O. Becvar, J. Escobar, and M. Hanigan. 2011. Effects of jugular-infused lysine, methionine, and branched-chain amino acids on milk protein synthesis in high-producing dairy cows. J. Dairy Sci. 94:1952-1960.

Appuhamy, J. R. N., N. A. Knoebel, W. D. Nayananjalie, J. Escobar, and M. D. Hanigan. 2012. Isoleucine and leucine independently regulate mTOR signaling and protein synthesis in MAC-T cells and bovine mammary tissue slices. J. Nutr. 142:484-491.

Aquilano, K., S. Baldelli, and M. R. Ciriolo. 2014. Glutathione: new roles in redox signaling for an old antioxidant. Front. Pharmacol. 5:196.

Arriarán, S., S. Agnelli, X. Remesar, J.-A. Fernández-López, and M. Alemany. 2015. The urea cycle of rat white adipose tissue. RSC Advances 5:93403-93414.

Badoud, F., K. P. Lam, A. DiBattista, M. Perreault, M. A. Zulyniak, B. Cattrysse, S. Stephenson, P. Britz-McKibbin, and D. M. Mutch. 2014. Serum and adipose tissue amino acid homeostasis in the metabolically healthy obese. J. Proteome Res. 13:3455-3466.

Basiricò, L., P. Morera, D. Dipasquale, A. Tröscher, and U. Bernabucci. 2017. Comparison between conjugated linoleic acid and essential fatty acids in preventing oxidative stress in bovine mammary epithelial cells. J. Dairy Sci. 100:2299-2309.

Bataille, A. and J. Manautou. 2012. Nrf2: a potential target for new therapeutics in liver disease. CPT Pharmacometrics Syst. Pharmacol. 92:340-348.

Batistel, F., A. S. Alharthi, L. Wang, C. Parys, Y.-X. Pan, F. C. Cardoso, and J. J. Loor. 2017a. Placentome nutrient transporters and mammalian target of rapamycin signaling proteins are altered by the methionine supply during late gestation in dairy cows and are associated with newborn birth weight. J. Nutr. 147:1640-1647.

Batistel, F., J. Arroyo, A. Bellingeri, L. Wang, B. Saremi, C. Parys, E. Trevisi, F. Cardoso, and J. Loor. 2017b. Ethyl-cellulose rumen-protected methionine enhances performance during the periparturient period and early lactation in Holstein dairy cows. J. Dairy Sci. 100:7455-7467.

Batistel, F., J. Arroyo, C. Garces, E. Trevisi, C. Parys, M. Ballou, F. Cardoso, and J. Loor. 2018. Ethyl-cellulose rumen-protected methionine alleviates inflammation and oxidative stress and improves neutrophil function during the periparturient period and early lactation in Holstein dairy cows. J. Dairy Sci. 101:480-490.

Bell, A. W. and D. E. Bauman. 1997. Adaptations of glucose metabolism during pregnancy and lactation. J. Mammary Gland Biol. Neoplasia. 2:265-278.

Bernabucci, U., B. Ronchi, N. Lacetera, and A. Nardone. 2005. Influence of body condition score on relationships between metabolic status and oxidative stress in periparturient dairy cows. J. Dairy Sci. 88:2017-2026.

Bertoni, G., E. Trevisi, X. Han, and M. Bionaz. 2008. Effects of inflammatory conditions on liver activity in puerperium period and consequences for performance in dairy cows. J. Dairy Sci. 91:3300-3310.

Bionaz, M., E. Trevisi, L. Calamari, F. Librandi, A. Ferrari, and G. Bertoni. 2007. Plasma paraoxonase, health, inflammatory conditions, and liver function in transition dairy cows. J. Dairy Sci. 90:1740-1750.

Bradford, B., K. Yuan, J. Farney, L. Mamedova, and A. Carpenter. 2015. Invited review: Inflammation during the transition to lactation: New adventures with an old flame. J. Dairy Sci. 98:6631-6650.

Bröer, S. 2002. Adaptation of plasma membrane amino acid transport mechanisms to physiological demands. Pflugers Arch. 444:457-466.

Bröer, S. 2014. The SLC38 family of sodium–amino acid co-transporters. Pflugers Arch. 466:155-172.

Butler-Hogg, B., J. Wood, and J. Bines. 1985. Fat partitioning in British Friesian cows: the influence of physiological state on dissected body composition. J. Agric. Sci. 104:519-528.

Cai, H., L. Q. Dong, and F. Liu. 2016. Recent advances in adipose mTOR signaling and function: therapeutic prospects. Trends Pharmacol. Sci. 37:303-317.

Cannon, B. and J. Nedergaard. 2004. Brown adipose tissue: function and physiological significance. Physiol. Rev. 84:277-359.

Ceciliani, F., J. J. Ceron, P. D. Eckersall, and H. Sauerwein. 2012. Acute phase proteins in ruminants. J. Proteomics 75:4207-4231.

Celi, P. 2011. Biomarkers of oxidative stress in ruminant medicine. Immunopharmacol. Immunotoxicol. 33:233-240.

Chaurasia, B., V. A. Kaddai, G. I. Lancaster, D. C. Henstridge, S. Sriram, D. L. A. Galam, V. Gopalan, K. B. Prakash, S. S. Velan, and S. Bulchand. 2016. Adipocyte ceramides regulate subcutaneous adipose browning, inflammation, and metabolism. Cell Metab. 24:820-834.

Coleman, D. N., A. S. Alharthi, Y. Liang, M. G. Lopes, V. Lopreiato, M. Vailati-Riboni, and J. J. Loor. 2021. Multifaceted role of one-carbon metabolism on immunometabolic control and growth during pregnancy, lactation and the neonatal period in dairy cattle. J. Anim. Sci. Biotechnol. 12:1-28.

Contreras, G. A., N. J. O'Boyle, T. H. Herdt, and L. M. Sordillo. 2010. Lipomobilization in periparturient dairy cows influences the composition of plasma nonesterified fatty acids and leukocyte phospholipid fatty acids. J. Dairy Sci. 93:2508-2516.

Contreras, G. A., C. Strieder-Barboza, and J. De Koster. 2018. Symposium review: Modulating adipose tissue lipolysis and remodeling to improve immune function during the transition period and early lactation of dairy cows. J. Dairy Sci. 101:2737-2752.

Contreras, G. A., C. Strieder-Barboza, J. De Souza, J. Gandy, V. Mavangira, A. L. Lock, and L. M. Sordillo. 2017. Periparturient lipolysis and oxylipid biosynthesis in bovine adipose tissues. PLoS One 12:e0188621.

Dai, H., D. Coleman, L. Hu, I. Martinez-Cortés, M. Wang, C. Parys, X. Shen, and J. Loor. 2020. Methionine and arginine supplementation alter inflammatory and oxidative stress responses during lipopolysaccharide challenge in bovine mammary epithelial cells in vitro. J. Dairy Sci. 103:676-689.

Dai, W., F. Zhao, J. Liu, and H. Liu. 2019. ASCT2 is involved in SARS-mediated β-casein synthesis of bovine mammary epithelial cells with methionine supply. J. Agric. Food Chem. 68:13038-13045.

Dam, V., T. Sikder, and S. Santosa. 2016. From neutrophils to macrophages: differences in regional adipose tissue depots. Obes Rev. 17:1-17.

De Koster, J., M. Hostens, M. Van Eetvelde, K. Hermans, S. Moerman, H. Bogaert, E. Depreester, W. Van den Broeck, and G. Opsomer. 2015. Insulin response of the glucose and fatty acid metabolism in dry dairy cows across a range of body condition scores. J. Dairy Sci. 98:4580-4592.

De Koster, J., C. Strieder-Barboza, J. de Souza, A. L. Lock, and G. A. Contreras. 2018. Short communication: Effects of body fat mobilization on macrophage infiltration in adipose tissue of early lactation dairy cows. J. Dairy Sci. 101:7608-7613.

De Koster, J., W. Van den Broeck, L. Hulpio, E. Claeys, M. Van Eetvelde, K. Hermans, M. Hostens, V. Fievez, and G. Opsomer. 2016. Influence of adipocyte size and adipose depot on the in vitro lipolytic activity and insulin sensitivity of adipose tissue in dairy cows at the end of the dry period. J. Dairy Sci. 99:2319-2328.

De Koster, J. D. and G. Opsomer. 2013. Insulin resistance in dairy cows. Vet. Clin. North Am. Food Anim. Pract. 29:299-322.

Ding, L., Y. Shen, Y. Wang, G. Zhou, X. Zhang, M. Wang, J. J. Loor, L. Chen, and J. Zhang. 2019. Jugular arginine supplementation increases lactation performance and nitrogen utilization efficiency in lactating dairy cows. J. Anim. Sci. Biotechnol. 10:3.

Dludla, P. V., B. B. Nkambule, B. Jack, Z. Mkandla, T. Mutize, S. Silvestri, P. Orlando, L. Tiano, J. Louw, and S. E. Mazibuko-Mbeje. 2019. Inflammation and oxidative stress in an obese state and the protective effects of gallic acid. Nutrients 11:23.

Dong, X., Z. Zhou, L. Wang, B. Saremi, A. Helmbrecht, Z. Wang, and J. Loor. 2018. Increasing the availability of threonine, isoleucine, valine, and leucine relative to lysine while maintaining an ideal ratio of lysine: methionine alters mammary cellular metabolites, mammalian target of rapamycin signaling, and gene transcription. J. Dairy Sci. 101:5502-5514.

Drackley, J. K. 1999. Biology of dairy cows during the transition period: The final frontier? J. Dairy Sci. 82:2259-2273.

Du, X., T. Shen, H. Wang, X. Qin, D. Xing, Q. Ye, Z. Shi, Z. Fang, Y. Zhu, Y. Yang, Z. Peng, C. Zhao, B. Lv, X. Li, G. Liu, and X. Li. 2018. Adaptations of hepatic lipid metabolism and mitochondria in dairy cows with mild fatty liver. J. Dairy Sci. 101:9544-9558.

Feller, D. and E. Feist. 1963. Conversion of methionine and threonine to fatty acids by adipose tissue. Can. J. Biochem. 41:269-273.

Fernández-Sánchez, A., E. Madrigal-Santillán, M. Bautista, J. Esquivel-Soto, Á. Morales-González, C. Esquivel-Chirino, I. Durante-Montiel, G. Sánchez-Rivera, C. Valadez-Vega, and J. A. Morales-González. 2011. Inflammation, oxidative stress, and obesity. Int. J. Mol. Sci. 12:3117-3132.

Fotiadis, D., Y. Kanai, and M. Palacín. 2013. The SLC3 and SLC7 families of amino acid transporters. Mol. Aspects Med. 34:139-158.

Frayn, K., K. Khan, S. Coppack, and M. Elia. 1991. Amino acid metabolism in human subcutaneous adipose tissue in vivo. Clin. Sci. 80:471-474.

Galván-Peña, S. and L. A. O'Neill. 2014. Metabolic reprograming in macrophage polarization. Front. Immunol. 5:420.

Gessner, D., G. Schlegel, J. Keller, F. Schwarz, R. Ringseis, and K. Eder. 2013. Expression of target genes of nuclear factor E2-related factor 2 in the liver of dairy cows in the transition period and at different stages of lactation. J. Dairy Sci. 96:1038-1043.

Ghaffari, M., K. Schuh, G. Dusel, D. Frieten, C. Koch, C. Prehn, J. Adamski, H. Sauerwein, and H. Sadri. 2019a. Mammalian target of rapamycin signaling and ubiquitin-proteasome–related gene expression in skeletal muscle of dairy cows with high or normal body condition score around calving. J. Dairy Sci. 102:11544–11560.

Ghaffari, M. H., A. Jahanbekam, H. Sadri, K. Schuh, G. Dusel, C. Prehn, J. Adamski, C. Koch, and H. Sauerwein. 2019b. Metabolomics meets machine learning: Longitudinal metabolite profiling in serum of normal versus overconditioned cows and pathway analysis. J. Dairy Sci. 02:11561–11585.

Han, L., F. Batistel, Y. Ma, A. Alharthi, C. Parys, and J. Loor. 2018a. Methionine supply alters mammary gland antioxidant gene networks via phosphorylation of nuclear factor erythroid 2-like 2 (NFE2L2) protein in dairy cows during the periparturient period. J. Dairy Sci. 01:8505–8512.

Han, L., Z. Zhou, Y. Ma, F. Batistel, J. Osorio, and J. Loor. 2018b. Phosphorylation of nuclear factor erythroid 2-like 2 (NFE2L2) in mammary tissue of Holstein cows during the periparturient period is associated with mRNA abundance of antioxidant gene networks. J. Dairy Sci. 101:6511-6522.

Häussler, S., D. Germeroth, L. Laubenthal, L. Ruda, J. Rehage, S. Dänicke, and H. Sauerwein. 2017. Immunohistochemical localization of the immune cell marker CD68 in bovine adipose tissue: impact of tissue alterations and excessive fat accumulation in dairy cows. Vet. Immunol. Immunopathol. 183:45-48.

Heilbronn, L. K. and L. V. Campbell. 2008. Adipose tissue macrophages, low grade inflammation and insulin resistance in human obesity. Curr. Pharm. Des. 14:1225-1230.

Herman, M. A., P. She, O. D. Peroni, C. J. Lynch, and B. B. Kahn. 2010. Adipose tissue branched-chain amino acid (BCAA) metabolism modulates circulating BCAA levels. J. Biol. Chem. M109. 075184.

Howell, J. J. and B. D. Manning. 2011. mTOR couples cellular nutrient sensing to organismal metabolic homeostasis. Trends Endocrinol. Metab. 22:94-102.

Hu, L., Y. Chen, I. M. Cortes, D. N. Coleman, H. Dai, Y. Liang, C. Parys, C. Fernandez, M. Wang, and J. J. Loor. 2020. Supply of methionine and arginine alters phosphorylation of mechanistic target of rapamycin (mTOR), circadian clock proteins, and α-s1-casein abundance in bovine mammary epithelial cells. Food Funct. 11:883-894.

Jacometo, C., A. Alharthi, Z. Zhou, D. Luchini, and J. Loor. 2018. Maternal supply of methionine during late pregnancy is associated with changes in immune function and abundance of microRNA and mRNA in Holstein calf polymorphonuclear leukocytes. J. Dairy Sci. 101:8146-8158.

Jacometo, C., Z. Zhou, D. Luchini, M. Correa, and J. Loor. 2017. Maternal supplementation with rumen-protected methionine increases prepartal plasma methionine concentration and alters hepatic mRNA abundance of 1-carbon, methionine, and transsulfuration pathways in neonatal Holstein calves. J. Dairy Sci. 100:3209-3219.

Jacometo, C. B., J. S. Osorio, M. Socha, M. N. Corrêa, F. Piccioli-Cappelli, E. Trevisi, and J. J. Loor. 2015. Maternal consumption of organic trace minerals alters calf systemic and neutrophil mRNA and microRNA indicators of inflammation and oxidative stress. J. Dairy Sci. 98:7717-7729

Javed, K. and S. J. Fairweather. 2019. Amino acid transporters in the regulation of insulin secretion and signalling. Biochem. Soc. Trans. 47:571-590.

Ji, P., J. Osorio, J. Drackley, and J. Loor. 2012. Overfeeding a moderate energy diet prepartum does not impair bovine subcutaneous adipose tissue insulin signal transduction and induces marked changes in peripartal gene network expression1. J. Dairy Sci. 95:4333-4351.

Jin, X., K. Wang, H. Liu, F. Hu, F. Zhao, and J. Liu. 2016. Protection of bovine mammary epithelial cells from hydrogen peroxide-induced oxidative cell damage by resveratrol. Oxid. Med. Cell. Longev. 2016:2572175.

Jones, H. N., T. Jansson, and T. Powell. 2009. IL-6 stimulates system A amino acid transporter activity in trophoblast cells through STAT3 and increased expression of SNAT2. Am. J. Physiol. Cell Physiol. 297:C1228-C1235.

Kahn, C. R. 1978. Insulin resistance, insulin insensitivity, and insulin unresponsiveness: a necessary distinction. Metabolism 27:1893-1902.

Kajimura, S., B. M. Spiegelman, and P. Seale. 2015. Brown and beige fat: physiological roles beyond heat generation. Cell Metab. 22:546-559.

Kanda, H., S. Tateya, Y. Tamori, K. Kotani, K.-i. Hiasa, R. Kitazawa, S. Kitazawa, H. Miyachi, S. Maeda, and K. Egashira. 2006. MCP-1 contributes to macrophage infiltration into adipose tissue, insulin resistance, and hepatic steatosis in obesity. J. Clin. Invest. 116:1494-1505.

Kandasamy, P., G. Gyimesi, Y. Kanai, and M. A. Hediger. 2018. Amino acid transporters revisited: new views in health and disease. Trends Biochem. Sci. 43:752-789.

Kansanen, E., S. M. Kuosmanen, H. Leinonen, and A.-L. Levonen. 2013. The Keap1-Nrf2 pathway: mechanisms of activation and dysregulation in cancer. Redox Biol. 1:45-49.

Kenéz, Á., L. Ruda, S. Dänicke, and K. Huber. 2019. Insulin signaling and insulin response in subcutaneous and retroperitoneal adipose tissue in Holstein cows during the periparturient period. J. Dairy Sci. 102:11718-11729.

Khiaosa-ard, R., P. Pourazad, S. Aditya, E. Humer, and Q. Zebeli. 2018. Factors related to variation in the susceptibility to subacute ruminal acidosis in early lactating Simmental cows fed the same grain-rich diet. Anim. Feed. Sci. Technol. 238:111-122.

Kimball, S. R., P. A. Farrell, and L. S. Jefferson. 2002. Invited Review: Role of insulin in translational control of protein synthesis in skeletal muscle by amino acids or exercise. J. Appl. Physiol. 93:1168-1180.
Klasing, K. and V. Iseri. 2013. Recent advances in understanding the interactions between nutrients and immunity in farm animals. Energy and protein metabolism and nutrition in sustainable animal production 353-359.
Kleiner, S., N. Douris, E. C. Fox, R. J. Mepani, F. Verdeguer, J. Wu, A. Kharitonenkov, J. S. Flier, E. Maratos-Flier, and B. M. Spiegelman. 2012. FGF21 regulates PGC-1α and browning of white adipose tissues in adaptive thermogenesis. Genes Dev. 26:271-281.
Lager, S., F. Gaccioli, V. I. Ramirez, H. N. Jones, T. Jansson, and T. L. Powell. 2013. Oleic acid stimulates system A amino acid transport in primary human trophoblast cells mediated by toll-like receptor 4. J. Lipid Res. 54:725-733.
Lager, S., T. Jansson, and T. L. Powell. 2014. Differential regulation of placental amino acid transport by saturated and unsaturated fatty acids. Am. J. Physiol. Cell Physiol. 307:C738-C744.
Li, F., Y. Duan, Y. Li, Y. Tang, M. Geng, O. A. Oladele, S. W. Kim, and Y. Yin. 2015. Effects of dietary n-6: n-3 PUFA ratio on fatty acid composition, free amino acid profile and gene expression of transporters in finishing pigs. Br. J. Nutr. 113:739-748.
Li, Y., H. Ding, L. Liu, Y. Song, X. Du, S. Feng, X. Wang, X. Li, Z. Wang, and X. Li. 2020. Non-esterified fatty acid induce dairy cow hepatocytes apoptosis via the mitochondria-mediated ROS-JNK/ERK signaling pathway. Front. Cell Dev. Biol. 8:245.
Li, Y., H. Wei, F. Li, S. Chen, Y. Duan, Q. Guo, Y. Liu, and Y. Yin. 2016. Supplementation of branched-chain amino acids in protein-restricted diets modulates the expression levels of amino acid transporters and energy metabolism associated regulators in the adipose tissue of growing pigs. Anim. Nutr. 2:24-32.
Ling, T., M. Hernandez-Jover, L. M. Sordillo, and A. Abuelo. 2018. Maternal late-gestation metabolic stress is associated with changes in immune and metabolic responses of dairy calves. J. Dairy Sci. 101:6568-6580.
Loor, J. J., H. M. Dann, R. E. Everts, R. Oliveira, C. A. Green, N. A. J. Guretzky, S. L. Rodriguez-Zas, H. A. Lewin, and J. K. Drackley. 2005. Temporal gene expression profiling of liver from periparturient dairy cows reveals complex adaptive mechanisms in hepatic function. Physiol. Genomics 23:217-226.
Lu, J., G. Xie, W. Jia, and W. Jia. 2013. Insulin resistance and the metabolism of branched-chain amino acids. Front. Med. 7:53-59.
Lu, L., X. Gao, Q. Li, J. Huang, R. Liu, and H. Li. 2012. Comparative phosphoproteomics analysis of the effects of L-methionine on dairy cow mammary epithelial cells. Canadian J. Anim. Sci. 92:433-442.
Lu, S. C. 2013. Glutathione synthesis. Biochim. Biophys. Acta. Gen. Subj. 1830:3143-3153.
Lumeng, C. N., J. L. Bodzin, and A. R. Saltiel. 2007. Obesity induces a phenotypic switch in adipose tissue macrophage polarization. J. Clin. Invest. 117:175-184.
Lynch, C. J. and S. H. Adams. 2014. Branched-chain amino acids in metabolic signalling and insulin resistance. Nat. Rev. Endocrinol. 10:723.
Ma, Q. 2013. Role of nrf2 in oxidative stress and toxicity. Annu. Rev. Pharmacol. Toxicol. 53:401-426.

Ma, X., M. Han, D. Li, S. Hu, K. R. Gilbreath, F. W. Bazer, and G. Wu. 2017. L-Arginine promotes protein synthesis and cell growth in brown adipocyte precursor cells via the mTOR signal pathway. Amino Acids 49:957-964.
Ma, Y., F. Batistel, T. Xu, L. Han, R. Bucktrout, Y. Liang, D. Coleman, C. Parys, and J. Loor. 2019a. Phosphorylation of AKT serine/threonine kinase and abundance of milk protein synthesis gene networks in mammary tissue in response to supply of methionine in periparturient Holstein cows. J. Dairy Sci. 102:4264-4274.
Ma, Y., L. Zhao, D. Coleman, M. Gao, and J. Loor. 2019b. Tea polyphenols protect bovine mammary epithelial cells from hydrogen peroxide-induced oxidative damage in vitro by activating NFE2L2/HMOX1 pathways. J. Dairy Sci. 102:1658-1670.
Martínez-Reyes, I. and N. S. Chandel. 2020. Mitochondrial TCA cycle metabolites control physiology and disease. Nat. Commun. 11:1-11.
Maury, E. and S. Brichard. 2010. Adipokine dysregulation, adipose tissue inflammation and metabolic syndrome. Mol. Cell Endocrinol. 314:1-16.
McCormack, S. E., O. Shaham, M. A. McCarthy, A. A. Deik, T. J. Wang, R. E. Gerszten, C. B. Clish, V. K. Mootha, S. K. Grinspoon, and A. Fleischman. 2013. Circulating branched-chain amino acid concentrations are associated with obesity and future insulin resistance in children and adolescents. Pediatr. Obes. 8:52-61.
McFadden, J. and J. Rico. 2019. Invited review: Sphingolipid biology in the dairy cow: The emerging role of ceramide. J. Dairy Sci. 102:7619-7639.
Moyes, K. M., J. K. Drackley, D. E. Morin, and J. J. Loor. 2010. Greater expression of TLR2, TLR4, and IL6 due to negative energy balance is associated with lower expression of HLA-DRA and HLA-A in bovine blood neutrophils after intramammary mastitis challenge with Streptococcus uberis. Funct. Integr. Genomics. 10:53-61.
Mukesh, M., M. Bionaz, D. Graugnard, J. K. Drackley, and J. J. Loor. 2010. Adipose tissue depots of Holstein cows are immune responsive: inflammatory gene expression in vitro. Domest. Anim. Endocrinol. 38:168-178.
Nan, X., D. Bu, X. Li, J. Wang, H. Wei, H. Hu, L. Zhou, and J. J. Loor. 2014. Ratio of lysine to methionine alters expression of genes involved in milk protein transcription and translation and mTOR phosphorylation in bovine mammary cells. Physiol. Genomics. 46:268-275.
Newgard, C. B., J. An, J. R. Bain, M. J. Muehlbauer, R. D. Stevens, L. F. Lien, A. M. Haqq, S. H. Shah, M. Arlotto, and C. A. Slentz. 2009. A branched-chain amino acid-related metabolic signature that differentiates obese and lean humans and contributes to insulin resistance. Cell Metab. 9:311-326.
Newman, A. W., A. Miller, F. A. Leal Yepes, E. Bitsko, D. Nydam, and S. Mann. 2019. The effect of the transition period and postpartum body weight loss on macrophage infiltrates in bovine subcutaneous adipose tissue. J. Dairy Sci. 102:1693-1701.
Newsholme, P. 2001. Why is L-glutamine metabolism important to cells of the immune system in health, postinjury, surgery or infection? J. Nutr. 131:2515S-2522S.
Nichols, K., J. Kim, M. Carson, J. Metcalf, J. Cant, and J. Doelman. 2016. Glucose supplementation stimulates peripheral branched-chain amino acid catabolism in lactating dairy cows during essential amino acid infusions. J. Dairy Sci. 99:1145-1160.
Nissim, I. 1999. Newer aspects of glutamine/glutamate metabolism: the role of acute pH changes. Am. J. Physiol. Renal. Physiol. 277:F493-F497.

Osorio, J., P. Ji, J. Drackley, D. Luchini, and J. Loor. 2013. Supplemental Smartamine M or MetaSmart during the transition period benefits postpartal cow performance and blood neutrophil function. J. Dairy Sci. 96:6248-6263.
Osorio, J., P. Ji, J. Drackley, D. Luchini, and J. Loor. 2014a. Smartamine M and MetaSmart supplementation during the peripartal period alter hepatic expression of gene networks in 1-carbon metabolism, inflammation, oxidative stress, and the growth hormone–insulin-like growth factor 1 axis pathways. J. Dairy Sci. 97:7451-7464.
Osorio, J., E. Trevisi, P. Ji, J. Drackley, D. Luchini, G. Bertoni, and J. Loor. 2014b. Biomarkers of inflammation, metabolism, and oxidative stress in blood, liver, and milk reveal a better immunometabolic status in peripartal cows supplemented with Smartamine M or MetaSmart. J. Dairy Sci. 97:7437-7450.
Ott, M., V. Gogvadze, S. Orrenius, and B. Zhivotovsky. 2007. Mitochondria, oxidative stress and cell death. Apoptosis 12:913-922.
Pessin, J. E. and A. R. Saltiel. 2000. Signaling pathways in insulin action: molecular targets of insulin resistance. J. Clin. Invest. 106:165-169.
Pires, J., C. Delavaud, Y. Faulconnier, D. Pomies, and Y. Chilliard. 2013. Effects of body condition score at calving on indicators of fat and protein mobilization of periparturient Holstein-Friesian cows. J. Dairy Sci. 96:6423-6439.
Rico, J., W. Myers, D. Laub, A. Davis, Q. Zeng, and J. McFadden. 2018. Hot topic: Ceramide inhibits insulin sensitivity in primary bovine adipocytes. J. Dairy Sci. 101:3428-3432.
Rico, J. E., V. V. R. Bandaru, J. M. Dorskind, N. J. Haughey, and J. W. McFadden. 2015. Plasma ceramides are elevated in overweight Holstein dairy cows experiencing greater lipolysis and insulin resistance during the transition from late pregnancy to early lactation. J. Dairy Sci. 98:7757-7770.
Rico, J. E., S. S. Samii, A. T. Mathews, J. Lovett, N. J. Haughey, and J. W. McFadden. 2017. Temporal changes in sphingolipids and systemic insulin sensitivity during the transition from gestation to lactation. PLoS One 12:e0176787.
Roche, J. R., N. C. Friggens, J. K. Kay, M. W. Fisher, K. J. Stafford, and D. P. Berry. 2009. Invited review: Body condition score and its association with dairy cow productivity, health, and welfare. J. Dairy Sci. 92:5769-5801.
Roche, J. R., J. K. Kay, N. C. Friggens, J. J. Loor, and D. P. Berry. 2013. Assessing and managing body condition score for the prevention of metabolic disease in dairy cows. Vet. Clin. North Am. Food Anim. Pract. 29:323-336.
Sabedra, D. A. 2012. Serum haptoglobin as an indicator for calving difficulties and postpartal diseases in transition dairy cows. Undergraduate Thesis. 2012.
Salans, L. B., J. L. Knittle, and J. Hirsch. 1968. The role of adipose cell size and adipose tissue insulin sensitivity in the carbohydrate intolerance of human obesity. J. Clin. Invest. 47:153-165.
Saremi, B., A. Al-Dawood, S. Winand, U. Müller, J. Pappritz, D. Von Soosten, J. Rehage, S. Dänicke, S. Häussler, and M. Mielenz. 2012. Bovine haptoglobin as an adipokine: Serum concentrations and tissue expression in dairy cows receiving a conjugated linoleic acids supplement throughout lactation. Vet. Immunol. Immunopathol. 146:201-211.
Scalise, M., M. Galluccio, L. Console, L. Pochini, and C. Indiveri. 2018. The human SLC7A5 (LAT1): the intriguing histidine/large neutral amino acid transporter and its relevance to human health. Front. Chem. 6:243.

Schwab, C. G. and G. A. Broderick. 2017. A 100-Year Review: Protein and amino acid nutrition in dairy cows. J. Dairy Sci. 100:10094-10112.
Sechen, S. J., F. R. Dunshea, and D. E. Bauman. 1990. Somatotropinin lactating cows: effect on response to epinephrine and insulin. Am. J. Physiol. 258:E582–E588.
Shan, T., P. Zhang, Q. Jiang, Y. Xiong, Y. Wang, and S. Kuang. 2016. Adipocyte-specific deletion of mTOR inhibits adipose tissue development and causes insulin resistance in mice. Diabetologia 59:1995-2004.
Shimomura, Y., M. Obayashi, T. Murakami, and R. A. Harris. 2001. Regulation of branched-chain amino acid catabolism: nutritional and hormonal regulation of activity and expression of the branched-chain α-keto acid dehydrogenase kinase. Curr. Opin. Clin. Nutr. Metab. Care. 4:419-423.
Shulman, G. I. 2000. Cellular mechanisms of insulin resistance. J. Clin. Invest. 106:171-176.
Sidossis, L. and S. Kajimura. 2015. Brown and beige fat in humans: thermogenic adipocytes that control energy and glucose homeostasis. J. Clin. Invest. 125:478-486
Sies, H. 1997. Oxidative stress: oxidants and antioxidants. Exp. Physiol. 82:291-295.
Smith, K. L., J. Hogan, and W. Weiss. 1997. Dietary vitamin E and selenium affect mastitis and milk quality. J. Anim. Sci. 75:1659-1665.
Song, Y., N. Li, J. Gu, S. Fu, Z. Peng, C. Zhao, Y. Zhang, X. Li, Z. Wang, and X. Li. 2016. β-Hydroxybutyrate induces bovine hepatocyte apoptosis via an ROS-p38 signaling pathway. J. Dairy Sci. 99:9184-9198.
Song, Y., X. Li, Y. Li, N. Li, X. Shi, H. Ding, Y. Zhang, X. Li, G. Liu, and Z. Wang. 2014. Non-esterified fatty acids activate the ROS–p38–p53/Nrf2 signaling pathway to induce bovine hepatocyte apoptosis in vitro. Apoptosis 19:984-997.
Sordillo, L. and V. Mavangira. 2014. The nexus between nutrient metabolism, oxidative stress and inflammation in transition cows. Anim. Prod. Sci. 54:1204-1214.
Sordillo, L. M. and S. L. Aitken. 2009. Impact of oxidative stress on the health and immune function of dairy cattle. Vet. Immunol. Immunopathol. 128:104-109.
Sordillo, L. M., G. Contreras, and S. L. Aitken. 2009. Metabolic factors affecting the inflammatory response of periparturient dairy cows. Anim. Health. Res. Rev. 10:53-63.
Spears, J. W. and W. P. Weiss. 2008. Role of antioxidants and trace elements in health and immunity of transition dairy cows. Vet. J. 176:70-76.
Stipanuk, M. H. 2004. Sulfur amino acid metabolism: pathways for production and removal of homocysteine and cysteine. Annu. Rev. Nutr. 24:539-577.
Sun, F., Y. Cao, C. Cai, S. Li, C. Yu, and J. Yao. 2016. Regulation of nutritional metabolism in transition dairy cows: Energy homeostasis and health in response to post-ruminal choline and methionine. PLoS One 11:e0160659.
Sun, X., X. Li, H. Jia, J. J. Loor, R. Bucktrout, Q. Xu, Y. Wang, X. Shu, J. Dong, and R. Zuo. 2019. Effect of heat-shock protein B7 on oxidative stress in adipocytes from preruminant calves. J. Dairy Sci. 102:5673-5685.
Sundberg, B. E., E. Wååg, J. A. Jacobsson, O. Stephansson, J. Rumaks, S. Svirskis, J. Alsiö, E. Roman, T. Ebendal, and V. Klusa. 2008. The evolutionary history and tissue mapping of amino acid transporters belonging to solute carrier families SLC32, SLC36, and SLC38. J. Mol. Neurosci. 35:179-193.
Tothova, C., O. Nagy, and G. Kovac. 2014. Acute phase proteins and their use in the diagnosis of diseases in ruminants: a review. Vet Med (Praha). 59:4.

Trigona, W. L., I. K. Mullarky, Y. Cao, and L. M. Sordillo. 2006. Thioredoxin reductase regulates the induction of haem oxygenase-1 expression in aortic endothelial cells. Biochem. J. 394:207-216.

Vailati-Riboni, M., M. Kanwal, O. Bulgari, S. Meier, N. Priest, C. Burke, J. Kay, S. McDougall, M. Mitchell, and C. Walker. 2016. Body condition score and plane of nutrition prepartum affect adipose tissue transcriptome regulators of metabolism and inflammation in grazing dairy cows during the transition period. J. Dairy Sci. 99:758-770.

Vailati Riboni, M., S. Meier, N. Priest, C. Burke, J. Kay, S. McDougall, M. Mitchell, C. Walker, M. Crookenden, and A. Heiser. 2015. Adipose and liver gene expression profiles in response to treatment with a nonsteroidal antiinflammatory drug after calving in grazing dairy cows. J. Dairy Sci. 98:3079-3085.

Vázquez-Añón, M., J. Nocek, G. Bowman, T. Hampton, C. Atwell, P. Vazquez, and T. Jenkins. 2008. Effects of feeding a dietary antioxidant in diets with oxidized fat on lactation performance and antioxidant status of the cow. J. Dairy Sci. 91:3165-3172.

Webb, L., H. Sadri, K. Schuh, S. Egert, P. Stehle, I. Meyer, C. Koch, G. Dusel, and H. Sauerwein. 2020. Branched-chain amino acids: Abundance of their transporters and metabolizing enzymes in adipose tissue, skeletal muscle, and liver of dairy cows at high or normal body condition. J. Dairy Sci. 103:2847-2863.

Webb, L., H. Sadri, D. von Soosten, S. Dänicke, S. Egert, P. Stehle, and H. Sauerwein. 2019. Changes in tissue abundance and activity of enzymes related to branched-chain amino acid catabolism in dairy cows during early lactation. J. Dairy Sci. 102:3556-3568.

Wildman, E., G. Jones, P. Wagner, R. Boman, H. Troutt Jr, and T. Lesch. 1982. A dairy cow body condition scoring system and its relationship to selected production characteristics. J. Dairy Sci. 65:495-501.

Williams, N. C. and L. A. O'Neill. 2018. A role for the Krebs cycle intermediate citrate in metabolic reprogramming in innate immunity and inflammation. Front. Immunol. 9:141.

Wu, G. 2009. Amino acids: metabolism, functions, and nutrition. Amino acids 37:1-17.

Xu, T., A. Alharthi, F. Batistel, A. Helmbrecht, C. Parys, E. Trevisi, X. Shen, and J. Loor. 2018. Hepatic phosphorylation status of serine/threonine kinase 1, mammalian target of rapamycin signaling proteins, and growth rate in Holstein heifer calves in response to maternal supply of methionine. J. Dairy Sci. 101:8476-8491.

Yang, F. L. and X. S. Li. 2015. Role of antioxidant vitamins and trace elements in mastitis in dairy cows. J. Adv. Vet. Anim. Res. 2:1-9.

Yoneshiro, T., Q. Wang, K. Tajima, M. Matsushita, H. Maki, K. Igarashi, Z. Dai, P. J. White, R. W. McGarrah, and O. R. Ilkayeva. 2019. BCAA catabolism in brown fat controls energy homeostasis through SLC25A44. Nature 572:614-619.

Zachut, M. 2015. Defining the adipose tissue proteome of dairy cows to reveal biomarkers related to peripartum insulin resistance and metabolic status. J. Proteome Res. 14:2863-2871.

Zahrazadeh, M., A. Riasi, H. Farhangfar, and S. A. Mahyari. 2018. Effects of close-up body condition score and selenium-vitamin E injection on lactation performance, blood metabolites, and oxidative status in high-producing dairy cows. J. Dairy Sci. 101:10495-10504.

Zhang, F., D. Li, Q. Wu, J. Sun, W. Guan, Y. Hou, Y. Zhu, and J. Wang. 2019. Prepartum body conditions affect insulin signaling pathways in postpartum adipose tissues in transition dairy cows. J. Anim. Sci. Biotechnol. 10:38.

Zhao, F., T. Wu, H. Wang, L. Ding, G. Ahmed, H. Li, W. Tian, and Y. Shen. 2018. Jugular arginine infusion relieves lipopolysaccharide-triggered inflammatory stress and improves immunity status of lactating dairy cows. J. Dairy Sci. 101:5961-5970.

Zhou, Z., M. Vailati-Riboni, D. N. Luchini, and J. J. Loor. 2016a. Methionine and choline supply during the periparturient period alter plasma amino acid and one-carbon metabolism profiles to various extents: Potential role in hepatic metabolism and antioxidant status. Nutrients 9:10.

Zhou, Z., M. Vailati-Riboni, E. Trevisi, J. Drackley, D. Luchini, and J. Loor. 2016b. Better postpartal performance in dairy cows supplemented with rumen-protected methionine compared with choline during the peripartal period. J. Dairy Sci. 99:8716-8732.

CHAPTER 2: GLUTATHIONE METABOLISM AND NUCLEAR FACTOR ERYTHROID 2-LIKE 2 (NFE2L2)-RELATED PROTEINS IN ADIPOSE TISSUE ARE ALTERATED BY SUPPLY OF ETHYL-CELLULOSE RUMEN-PROTECTED METHIONINE IN PERIPARTAL HOLSTEIN COWS

-Journal of Dairy Science, 2019, 102 (6): 5530-5541.

ABSTRACT

Enhancing the supply of rumen-protected Met (RPM) during the peripartum alleviates inflammation and oxidative stress status in dairy cows. We tested the hypothesis that RPM could increase the abundance of genes and proteins related to glutathione (GSH) metabolism and the antioxidant transcription factor nuclear factor erythroid 2-like 2 (NFE2L2) in s.c. adipose tissue. Multiparous Holstein cows were fed a basal diet [control prepartum diet, 1.47 Mcal/kg of dry matter (DM) and 15.3% crude protein (CP); control postpartum diet, 1.67 Mcal/kg DM and 17.7% CP] or control plus ethyl-cellulose rumen-protected Met (RPM) at a rate of 0.09% and 0.10% of DMI before expected calving and after calving, respectively. Sixty cows were assigned to treatments based on parity, previous 305-d milk yield, and body condition score (BCS) at 28 d from parturition. Diets were fed from –28 to 30 d. Biopsies of s.c. adipose tissue collected on d -10, 10, and 30 relative to parturition from 7 cows in each group were used for measuring concentrations of GSH, reactive oxygen species (ROS), superoxide dismutase (SOD), malondialdehyde (MDA), and mRNA (RT-PCR) and protein abundance (Western blotting). A repeated-measures ANOVA was used for statistics, with $P \leq 0.05$ being the threshold for significance. The statistical model included the random effect of block and fixed effect of treatment, time, and its interaction. There was a diet × time effect for ROS due to lower concentrations in Met versus control cows specifically at d -10. Cows fed Met also had lower concentrations of MDA in s.c. adipose tissue. Compared with controls, overall mRNA abundance of the GSH metabolism-related genes cystathionine-beta-synthase (*CBS*), glutamate-

cysteine ligase modifier subunit (*GCLM*), glutathione reductase (*GSR*), and glutathione peroxidase 1 (*GPX1*) was greater in cows fed Met. Furthermore, supply of Met resulted in an overall upregulation of protein abundance of glutathione peroxidase 1 (GPX1), GPX3, glutathione S-transferase mu 1 (GSTM1), and glutathione S-transferase alpha 4 (GSTA4) all related to GSH metabolism. There was a diet × time effect for protein abundance of NFE2L2 and its repressor kelch like ECH associated protein 1 (KEAP1) due to lower values at 30 d in cows fed Met versus controls. The abundance of p-NFE2L2 was lower at 30 d in response to Met. Overall, the data suggest that exogenous Met may play a role in activating GSH metabolism and the anti-oxidant NFE2L2 pathways in s.c. adipose tissue.

Key words: amino acid, inflammation, lactation, oxidative stress

INTRODUCTION

During the peripartal period, dairy cows usually experience negative energy balance due to the increased nutrient requirements for fetal growth, milk synthesis, and decreased feed intake (Grummer, 1995, Drackley, 1999). Therefore, mobilization of body fat and skeletal muscle help cows satisfy their energy demands. Reactive oxygen species (**ROS**) concentrations in plasma increase during early lactation contributing to oxidative stress status (Bernabucci et al., 2005). ROS production due to the mobilization of fatty acids, lipotoxicity, and mitochondrial activity (Fernández-Sánchez et al., 2011) in the adipose tissue contributes to oxidative stress (Furukawa et al., 2004). A pronounced state of oxidative stress could lead to inflammation and immune dysfunction both of which contribute to metabolic disorders (Sordillo and Aitken, 2009, Zhu et al., 2018). For example, an inadequate supply of essential vitamins and trace minerals (e.g., vitamin E or Se) due to decreased DMI around parturition could impair antioxidant synthesis and lower the functionality of circulating leukocytes (Bendich, 1993, Spears, 2000). Oxidative stress

increases oxylipid production derived from cellular membrane omega-6 fatty acid metabolism and can contribute to inflammation (Sordillo and Mavangira, 2014, Mavangira and Sordillo, 2018). Therefore, oxidative stress has a negative effect on both production performance and welfare in dairy cows (Loor et al., 2013).

Glutathione (**GSH**) is a well-established antioxidant in cells and plays a critical role in the maintenance and regulation of the thiol-redox status (Aquilano et al., 2014). Methionine, which is one of the most-limiting AA for lactating dairy cattle, participates in one-carbon metabolism and synthesis of GSH both of which occur primarily in the liver (Martinov et al., 2010, Zhou et al., 2016a, Schwab and Broderick, 2017). When Lys was adequate, feeding RPM to achieve a Lys: Met ratio close to 2.8:1 in the MP during the periparturient period consistently alleviated oxidative stress status and inflammation in dairy cows and improved DMI and milk yield (Osorio et al., 2014b; Zhou et al., 2016a; Batistel et al., 2017). Previous data has provided some indication that adipose may play a role in the induction of oxidative stress (Bernabucci et al., 2005, Contreras et al., 2017). For instance, at least in non-ruminants, adipose tissue can secrete a number of adipokines that are associated with oxidative stress and inflammation (Shoelson et al., 2006, McGown et al., 2014, Murri et al., 2014). In non-ruminants, nuclear factor, erythroid-derived 2-like 2 (**NFE2L2**, formerly Nrf2) is a key transcription factor controlling cellular oxidative stress in part by increasing the mRNA abundance of antioxidant enzymes (Kaspar et al., 2009). In dairy cows, heat stress was associated with greater protein abundance of NFE2L2 in s.c. adipose in late-pregnancy indicating that stressors can elicit a tissue-specific antioxidant response (Zachut et al., 2017). Thus, NFE2L2 may play an important role in the s.c. adipose tissue during the periparturient period. The specific objectives of the current study were to use adipose tissue samples from control and

RPM-fed cows in the study of Batistel et al. (2017) to evaluate changes in mRNA and protein abundance of various components of the GSH synthesis pathway and the NFE2L2 signaling pathway.

MATERIALS AND METHODS

Experiment Design and Treatments

All procedures involving animals were conducted under protocols approved by the University of Illinois Institutional Animal Care and Use Committee (Urbana; protocol #14270). Details of the experimental design have been published previously (Batistel et al., 2017). Briefly, 60 multiparous Holstein cows (average lactation number 3.22 ± 1.11) were assigned to a basal diet (control, n = 30) without additional Met or the basal diet with ethyl-cellulose RPM (Met, n = 30; Mepron, Evonik Nutrition and Care Gmbh, Hanau-Wolfgang, Germany) in a randomized, complete block design. Mepron contains 85% DL-Met. The rumen bypass coefficient of Mepron is 80% (Overton et al., 1996). The RPM was topdressed from −28 to 60 d relative to parturition at a rate of 0.09% and 0.10% of DMI of the previous day before and after calving to achieve a Lys:Met ratio of 2.8:1. The basal diet had a Lys:Met of 3.71:1 (prepartum) to 3.78:1 (postpartum). A Lys:Met ratio of 2.8:1 to 2.9:1 has been proven beneficial for dairy cow production performance and health including greater DMI, milk yield, and better immune function, and lower incidence of ketosis postpartum (Osorio et al., 2013, Zhou et al., 2016b). From -45 to -29 d relative to calving date, all cows were fed the same diet without RPM. Diets were mixed daily using a TMR truck with horizontal rotors and fed once daily (1300 h). The cows were milked daily at 0600, 1400, and 2200 h. The ingredient and chemical composition of the diets were published previously (Batistel et al., 2017). Diets were formulated to meet predicted requirements for dairy cows according to NRC (2001).

Adipose Tissue Biopsies

A subset of 7 cows in the control or Met groups were used for adipose biopsies. These cows were selected based on actual days receiving diets prepartum (28 ± 3 d), absence of clinical disorders, and all had the full set of biopsies. These cows did not receive any veterinary treatment. Furthermore, they averaged 21,420 to 22,062 kg milk in the previous 305-d lactation and had a BCS of 3.5 to 3.7 at treatment assignment. Tissue was harvested from the tail head (alternating between the right and left tail head region) at −10 (±3 d), 10, and 30 d relative to parturition according to previous procedures from our laboratory (Ji et al., 2012). Upon collection, adipose tissue was immediately placed in screw-capped, microcentrifuge tubes, snap-frozen in liquid nitrogen, and preserved at −80 °C until further analysis. Health was monitored for 7 d after surgery. Surgical clips were removed after 7 d post-biopsy. Cows were the last to be milked and returned to their tie-stalls after the 0400 milking. They did not have access to feed before biopsy, all of which were completed at approximately 0800 h. No antibiotics were administered post-biopsy.

RNA isolation, cDNA Synthesis, and Quantitative PCR

Total RNA was isolated from 200 mg of adipose tissue using the miRNeasy kit (Qiagen, Hilden, Germany) according to the manufacturer's protocols. The RNA samples were digested with DNaseI and quantification was assessed using a NanoDrop ND-1000 spectrophotometer (Thermo Fisher Scientific, Waltham, MA). The quality of RNA samples was measured using an Agilent 2100 Bioanalyzer (Agilent Technologies, Santa Clara, CA). The quantitative PCR was performed as described previously (Osorio et al., 2014a). Previously validated internal controls for adipose tissue were ribosomal protein S9 (***RPS9***), ***GAPDH*** and actin beta (***ACTB***) (Vailati Riboni et al., 2015, Vailati-Riboni et al., 2016, Vailati-Riboni et al., 2017). A comprehensive

literature search was conducted to select *NFE2L2* and GSH metabolism target genes and regulators that play crucial roles in cellular antioxidant mechanisms (Motohashi and Yamamoto, 2004, Stipanuk, 2004, Lu, 2009). Gene symbols and names are presented in Supplemental Table A.1. Quantitative PCR performance and primer information are included in Supplemental Table A.1.

Western Blot Analysis

Total protein was extracted from 100 mg adipose tissue using a tissue protein extraction reagent (catalog no. 78510; Thermo Fisher Scientific) containing Halt protease and phosphatase inhibitor cocktail (100x, catalog no. 78442; Thermo Fisher Scientific). The concentration of total protein was determined using a NanoDrop ND-1000 (Thermo Fisher Scientific, Waltham, MA). Protein samples were denatured by heating at 100 °C for 5 min before loading 75 µg protein into each lane of a 4-20% SDS-PAGE gel (catalog no. 4561096; Bio-Rad). Reactions were run for 10 min at 180 V, then for 45 to 60 min at 110 V. After activating a polyvinyldene fluoride membrane (catalog number 1620261; Bio-Rad, Hercules, CA) with methanol for 1 min, the protein sample was transferred to the membrane in a Trans-Blot SD Semi-Dry Electrophoretic Transfer Cell (catalog no. 170-3940, Bio-Rad). Membranes were then blocked in 1x Tris-buffered saline (1xTBST) containing 5% nonfat milk for 2 h at room temperature. The membranes were then incubated in 1x TBST containing primary antibodies to HCAR2, GPX1, GPX3, GSTM1, GSTA4, KEAP1, HMOX1, ERK1, phospho-ERK1(Thr202), NFE2L2, and phospho-NFE2L2(Ser40) (catalog number and dilution ratio are included in Supplemental Table A.2) overnight at 4 °C. The membranes were then washed 6 times with 1x TBST and incubated with anti-rabbit HRP-conjugated secondary antibodies (catalog no. 7074S; Cell Signaling Technology, dilution 1:3000) for 1 h at room temperature. Subsequently, the membranes were

washed 6 times with 1x TBST and then incubated with ECL reagent (catalog no. 170-5060; Bio-Rad) for 3 min in the dark prior to image acquisition. Actin beta (catalog no. 4967S; Cell Signaling Technology) was used as the internal control. Images were acquired using the ChemiDOC MP Imaging System (Bio-Rad). The intensities of the bands were measured with Image-Pro Plus 6.0 software. Specific target protein band density values were normalized to β-actin density values. Representative blots are included in Supplemental Figure A.1.

Oxidative Stress Analysis in Subcutaneous Adipose Tissue

Superoxide dismutase (SOD) (catalog no.706002; Cayman), malondialdehyde (MDA) (catalog no. 10009055; Cayman), GSH (catalog no. NWK-GSH01; Northwest Life Science Specialties), and ROS (catalog no. STA-347, Cell Biolabs) were analyzed in s.c. adipose tissue using commercial kits. The concentration of total protein of the adipose samples was measured using the BCA assay kit (catalog no. 23227; Thermo Scientific).

Statistical Analysis

The data were analyzed using the MIXED procedure of SAS v.9.4 (SAS Institute Inc., Cary, NC) according to the following model with repeated measures:

$$Y_{jl} = \mu + M_j + T_l + MT_{jl} + e_{jl},$$

where Y_{jl} = dependent, continuous variable, μ = overall mean, M_j = fixed effect of diet (j = control vs. Met), T_l = fixed effect of day (-10, 10, and 30 d), MT_{jl} = interaction between diet and day, and e_{jl} = residual error. Cow, nested within treatment, was the random effect. The Kenward-Roger statement was used for computing the denominator degrees of freedom. The covariance structure of the repeated measurements was spatial power [SP(POW)]. When the interaction was significant, least squares means separation between and within time points was performed using the PDIFF statement with Tukey adjustment. Normality of the residuals was

checked with normal probability and box plots, and homogeneity of variances was checked with plots of residuals versus predicted values. Significance was determined at $P \leq 0.05$ and tendencies at $P \leq 0.10$.

RESULTS

NFE2L2 Target Gene Abundance

Main effects of diet, day, and interactions are reported in Figure 2.1-3. The diet × day effect was not significant ($P > 0.05$) for any gene measured. Abundance of *NFE2L2* ($P = 0.06$, Figure 2.1) and *CBS* ($P = 0.06$, Figure 2.2) tended to be greater in response to enhanced Met supply. In addition, enhanced Met supply led to greater overall mRNA abundance (Figure 2.3) of *GCLM* ($P = 0.03$), *GSR* ($P = 0.02$), *TALDO1* ($P = 0.04$), and *ME1* ($P = 0.04$).

Protein Abundance

Main effects of diet, day, and interactions are reported in Figure 2.4-6. The diet × day interaction was significant for protein abundance of NFE2L2 ($P = 0.05$) and KEAP1 ($P < 0.01$) namely due to lower abundance of NFE2L2 ($P < 0.01$) at 10 d and greater abundance of KEAP1 at 30 d in Met compared with control cows (Figure 2.4). Although abundance of p-NFE2L2 could not be detected at -10 and 10 d in both control and Met cows, at 30 d postpartum abundance of p-NFE2L2 ($P < 0.05$) was lower compared with controls (Figure 2.4). However, there was no difference in p- NFE2L2: NFE2L2 ratio between Met cows and the controls. Compared with controls, cows fed Met had lower abundance of the NFE2L2 target HMOX1 ($P < 0.05$).

Among the enzymes associated with GSH metabolism, enhancing the supply of Met resulted in an overall upregulation ($P < 0.05$) of GPX1, GPX3, GSTM1, and GSTA4 ($P < 0.05$) (Figure 2.5). The diet × day interaction tended to be significant ($P = 0.06$) for p-ERK1 due to

Met cows having greater ($P < 0.01$) abundance at 10 d compared with controls (Figure 2.6). In addition, p-ERK1 tended to be greater ($P = 0.06$) in Met compared with control cows at 30 d. Overall abundance of HCAR2 and ERK1 in response to enhancing Met supply was greater ($P < 0.05$) (Figure 2.6). The ratio of p-ERK1 to total ERK1 was greater ($P < 0.01$) in cows fed Met compared with controls due to greater ($P < 0.05$) values at d 10.

Oxidative Stress in s.c. Adipose Tissue

Main effects of diet, time, and interactions are reported in Figure 2.7. The diet × day interaction was significant for ROS ($P < 0.05$) namely due to lower concentration ($P < 0.05$) at -10 d in Met compared with control cows (Figure 2.7). The concentration of MDA was lower ($P < 0.05$) overall in Met cows.

DISCUSSION

At a mechanistic level, changes in mRNA abundance associated with GSH metabolism and the NFE2L2 pathway in the liver and mammary gland tissue contribute to the reduction in oxidative stress in dairy cows receiving enhanced post-ruminal supply of Met (Osorio et al., 2014a, Han et al., 2018). Furthermore, enhanced supply of Met increased the phosphorylation status of NFE2L2 in the mammary gland (Han et al., 2018). In the current study, the potential benefit of Met on the s.c. adipose tissue antioxidant response is likely part of the overall benefits observed on alleviation of inflammation and oxidative stress in the same group of cows.

Oxidative Stress Biomarkers and mRNA Abundance of Genes in the One-carbon and GSH Metabolism Pathways in Adipose Tissue

The concentration of ROS is a well-established biomarker for oxidative stress. The lower plasma ROS concentration detected in the entire cohort of cows (Batistel et al., 2017, Batistel et al., 2018) used in this study agreed with previous data indicating a lower oxidative stress status

(Osorio et al., 2014b; Zhou et al., 2016ab). Although we did not attempt to quantify Met content in s.c. adipose, the lower concentration of MDA (measure of peroxides derived from PUFA) in cows fed Met suggests a less pronounced state of oxidative stress which is consistent with plasma data from the bigger cohort of cows in this study (Batistel et al., 2018).

Glutathione is one of the major antioxidants in the cell and helps prevent damage caused by ROS (Yu, 1994). At least in non-ruminants, Cys availability limits GSH biosynthesis (Griffith, 1999). Methionine can be converted to Cys by the transsulfuration pathway, with the enzyme CBS being rate-limiting (Kane et al., 1990). The greater overall mRNA abundance of *CBS* coupled with greater DMI (Batistel et al., 2017) in Met-fed cows could be taken as an indication that adipocytes had greater biosynthesis of cystathionine, Cys, and eventually GSH. Besides greater availability of Met in response to greater DMI, cows fed Met also would have had increased intakes of trace minerals (e.g., Se) and vitamins with roles as antioxidants, e.g., concentrations of β-carotene and tocopherol were greater in plasma from Met-fed cows (Batistel et al., 2018). Further in vitro studies may help understand the role of Met in GSH metabolism more clearly.

Glutathione reductase is an essential enzyme that converts oxidized GSH to the reduced form (Couto et al., 2016). The enzymes GCLC and GCLM are rate-limiting for GSH metabolism. Malic enzyme 1, a multifunctional protein linking the glycolytic and citric acid cycles, is important for NADPH production (Wen et al., 2015, Nakashima et al., 2018). The enzyme TALDO1 participates in the pentose phosphate pathway and helps provide cells with NADPH, an important redox cofactor (Samland and Sprenger, 2009) known for its role in mitigating oxidative stress. Thus, the upregulation of GSH metabolism genes (*GCLM*, *GSR*, *ME1*, and *TALDO1*) in response to enhanced post-ruminal supply of Met indicates that this AA,

either directly or via its positive effect on DMI, plays a direct role in helping adipose tissue alleviate oxidative stress during the transition period.

Abundance of Proteins Associated with GSH Metabolism and NFE2L2

The enzymes GSTM1, GSTA4, GPX1, and GPX3 play key roles in inactivating pro-oxidant products such as H_2O_2 and oxygen radicals in various tissues including adipose (Lee et al., 2008; Curtis et al., 2010). For instance, GPX3 (a selenium-dependent enzyme (Yan et al., 2007)) and GSTA4 in non-ruminant adipose tissue are essential to prevent oxidative stress in conditions associated with excessive fat deposition (Lee et al., 2008). Downregulation of GSTA4 in murine adipocytes resulted in increased ROS production along with lipolysis and reduced glucose uptake (Curtis et al., 2010). The GPX enzymes are oxidized by H_2O_2 and reduced by GSH (Sena and Chandel, 2012). Both GSTM1 and GSTA4 belong to the glutathione-*S*-transferase (GST) enzymes that are generally considered to be important for detoxification of electrophiles via GSH conjugation (Strange et al., 2001). Overall, protein abundance of GSH-related protein targets was consistent with mRNA abundance data. The upregulation of protein abundance of GPX1, GPX3, GSTM1, and GSTA4 in response to enhanced Met supply underscores not only that adipose tissue has antioxidant mechanisms related to GSH but also that these are responsive to greater Met supply and/or DMI.

The transcription factor NFE2L2 represents a major mechanism for cells to defend against oxidative stress. Expression of the gene was first reported in the transition cow liver (Loor, 2010), and more recent research provided some evidence that it can play an important role during the transition period and late pregnancy (Gessner et al., 2013, Zachut et al., 2017). Therefore, it seems that NFE2L2 plays an important role in the adipose tissue adaptations to the onset of lactation in dairy cows. Most dairy cows mobilize body fat to aid in meeting energy

demands for milk synthesis during the transition period, and in that process oxidation of fatty acids also generates ROS (Drackley, 1999, Sordillo and Aitken, 2009). Both nutrients and ROS can activate the NFE2L2 pathway (Nguyen et al., 2009, Cardozo et al., 2013), which triggers adaptations in the abundance of KEAP1 (Ade et al., 2008). In the cytosol, KEAP1 binds to NFE2L2, which inhibits its release and promotes proteasomal degradation (Kensler et al., 2007).

The fact that p-NFE2L2 was only detectable at 30 d postpartum agrees with other data indicating that oxidative stress status increases gradually after calving (Abuelo et al., 2013). In the entire cohort of cows (Batistel et al., 2018) we detected not only a temporal increase in the concentration of ROS in plasma but also greater overall values in control compared with Met-fed cows. This may partly explain the fact that p-NFE2L2 was not detectable at -10 d and 10 d relative to parturition. Along with mammary tissue data demonstrating a marked upregulation in abundance of p-NFE2L2/total NFE2L2 at 30 versus -30 d around parturition (Han et al., 2018b), these temporal responses underscore the potential role of NFE2L2 signaling in the defense mechanisms of mammary gland and adipose tissue against oxidative stress.

Taking into account the lower p-NFE2L2 at 30 d in cows fed Met and the similar ratio of p-NFE2L2/total NFE2L2 in the present study along with previous data in which enhanced Met supply upregulated the phosphorylation status of NFE2L2 in the bovine mammary gland (Han et al. 2018), it seems plausible that this transcription factor is less responsive to Met or less susceptible to ROS in adipose than mammary. Although the greater abundance of KEAP1 at 30 d in cows fed Met may partly explain the lower p-NFE2L2, the lack of difference in ROS concentration between groups coupled with greater overall abundance of GSTM1, GPX1, GSTA4, and GPX3 in response to Met suggests this AA helps control tissue ROS independent of NFE2L2.

Protein Abundance of Targets Associated with Response to Inflammation

It has been proposed that uncontrolled adipose tissue inflammation could intensify lipolysis (Contreras et al., 2018). Hydroxycarboxylic acid receptor 2 (HCAR2) belongs to the G protein-coupled receptor family and in non-ruminants it can serve both an antilipolytic (Offermanns et al., 2011) and anti-inflammatory role (Graff et al., 2016). Previous work demonstrated wide expression of HCAR2 in bovine tissues including adipose (Titgemeyer et al., 2011). In addition, there is an indication that enhancing the post-ruminal supply of nicotinic acid (an agonist of HCAR2) can signal through this receptor and reduce plasma free fatty acid concentrations (Morey et al., 2011, Yuan et al., 2012). Thus, the greater abundance of HCAR2 in response to enhanced Met supply might have served a dual role as in non-ruminants, i.e. help control lipolysis and also inflammation.

Previous research has clearly demonstrated that bovine adipose tissue undergoes an inflammatory response around parturition, which likely impacts the antioxidant defense system of the tissue (Vailati Riboni et al., 2015, Vailati-Riboni et al., 2016, Vailati-Riboni et al., 2017). Oxidative stress is known to cause apoptosis in various cell types and oxidative damage-induced apoptosis is partly mediated by ERK1/2 phosphorylation (Lee et al., 2003, Du et al., 2017). Thus, the greater phosphorylation status of ERK1 in response to enhanced Met supply was indicative that adipocyte survival might have been sustained in those cows.

CONCLUSIONS

Several components of the GSH metabolism and NFE2L2 antioxidant signaling pathways are expressed in s.c. adipose tissue and respond to the change in physiological state from late pregnancy to early lactation. The gradual increase in protein abundance of key components of these pathways reflects the state of oxidative stress experienced by cows. Supplementation of

Met was associated with lower MDA and higher activity of the glutathione antioxidant enzymes. Further in vitro studies using adipocytes may help us better understand the role and mechanisms for these responses.

FIGURES

Figure 2.1. mRNA abundance (log-10 scale) of the antioxidant transcription factor *NFE2L2* (panel A) and the *NFE2L2* repressors *KEAP1* (panel B), and *CUL3* (panel C) in s.c. adipose tissue harvested at -10, 10, and 30 d relative to parturition. Data are LS means, n = 7 cows per diet, ± pooled SEMs. *NFE2L2*, nuclear factor, erythroid 2 like 2; *KEAP1*, kelch like ECH associated protein 1; *CUL3*, cullin 3.

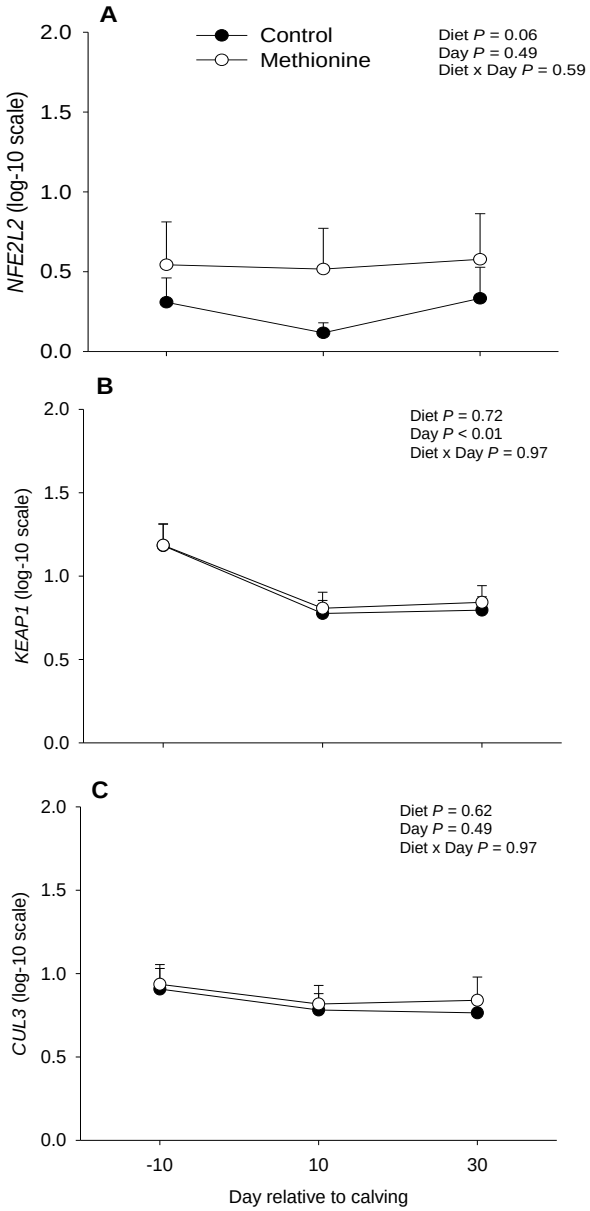

Figure 2.2. mRNA abundance (log-10 scale) of the one-carbon metabolism-related genes *MTR* (panel A), *BHMT* (panel B), *CBS* (panel C), and *CDO* (panel D) in s.c. adipose tissue harvested at -10, 10, and 30 d relative to parturition. Data are LS means, n = 7 cows per diet, ± pooled SEMs.

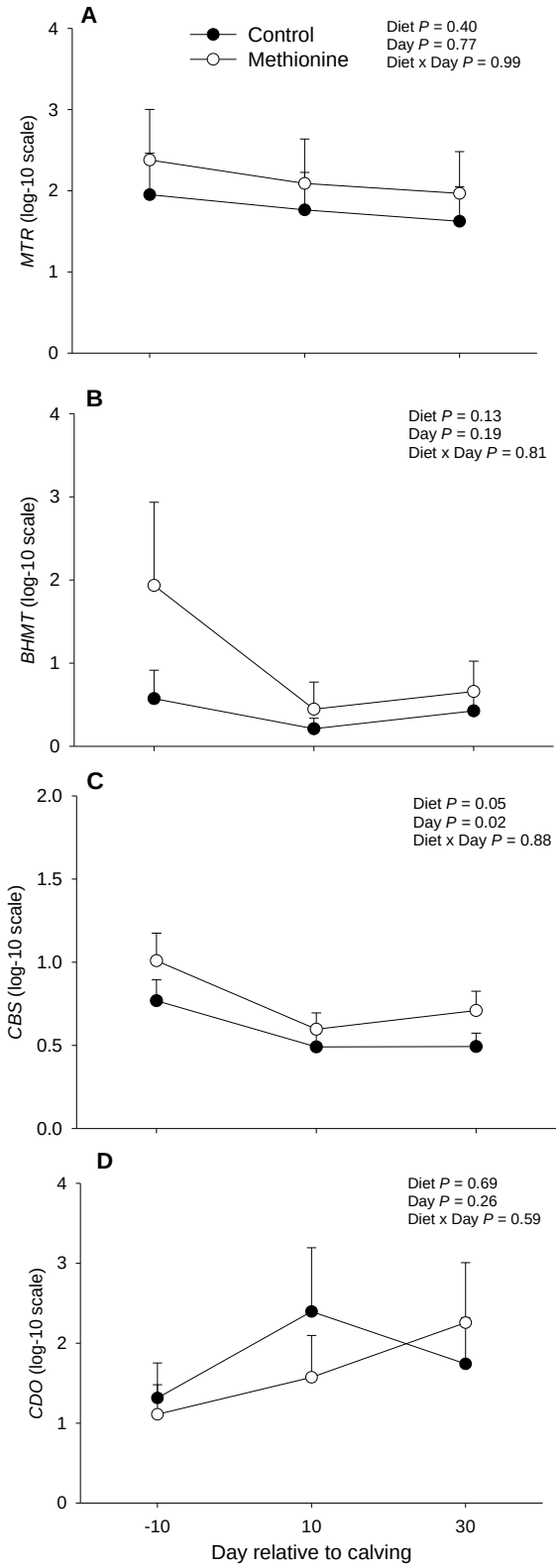

Figure 2.3. mRNA abundance (log-10 scale) of the glutathione metabolism-associated genes *GCLM* (panel A), *GPX1* (panel B), *GCLC* (panel C), *GSR* (panel D), *GSTM1* (panel E), *ME1* (panel F), and *TALDO1* (panel G) in s.c. adipose tissue harvested at -10, 10, and 30 d relative to parturitionData are LS means, n = 7 cows per diet, ± pooled SEMs.

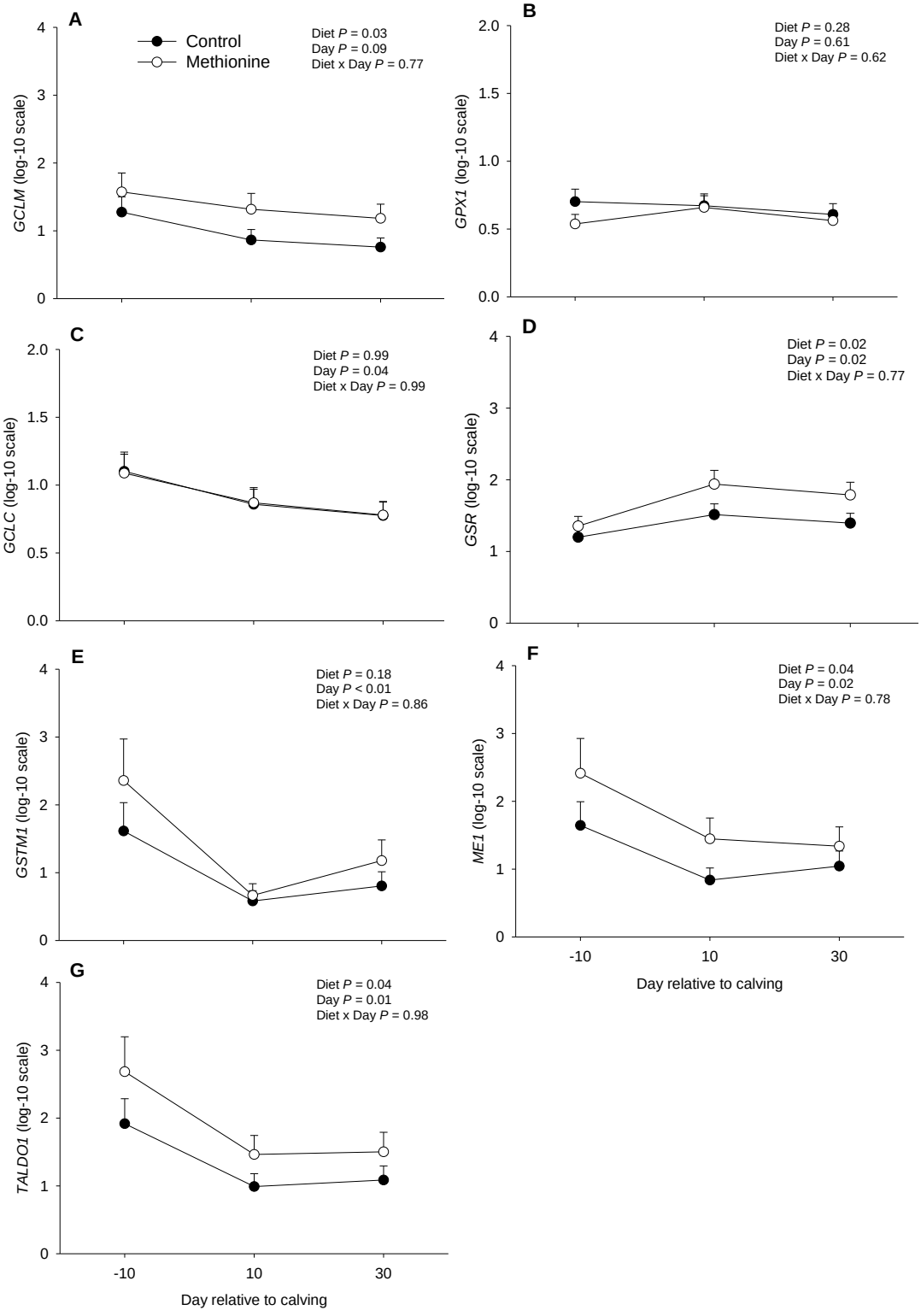

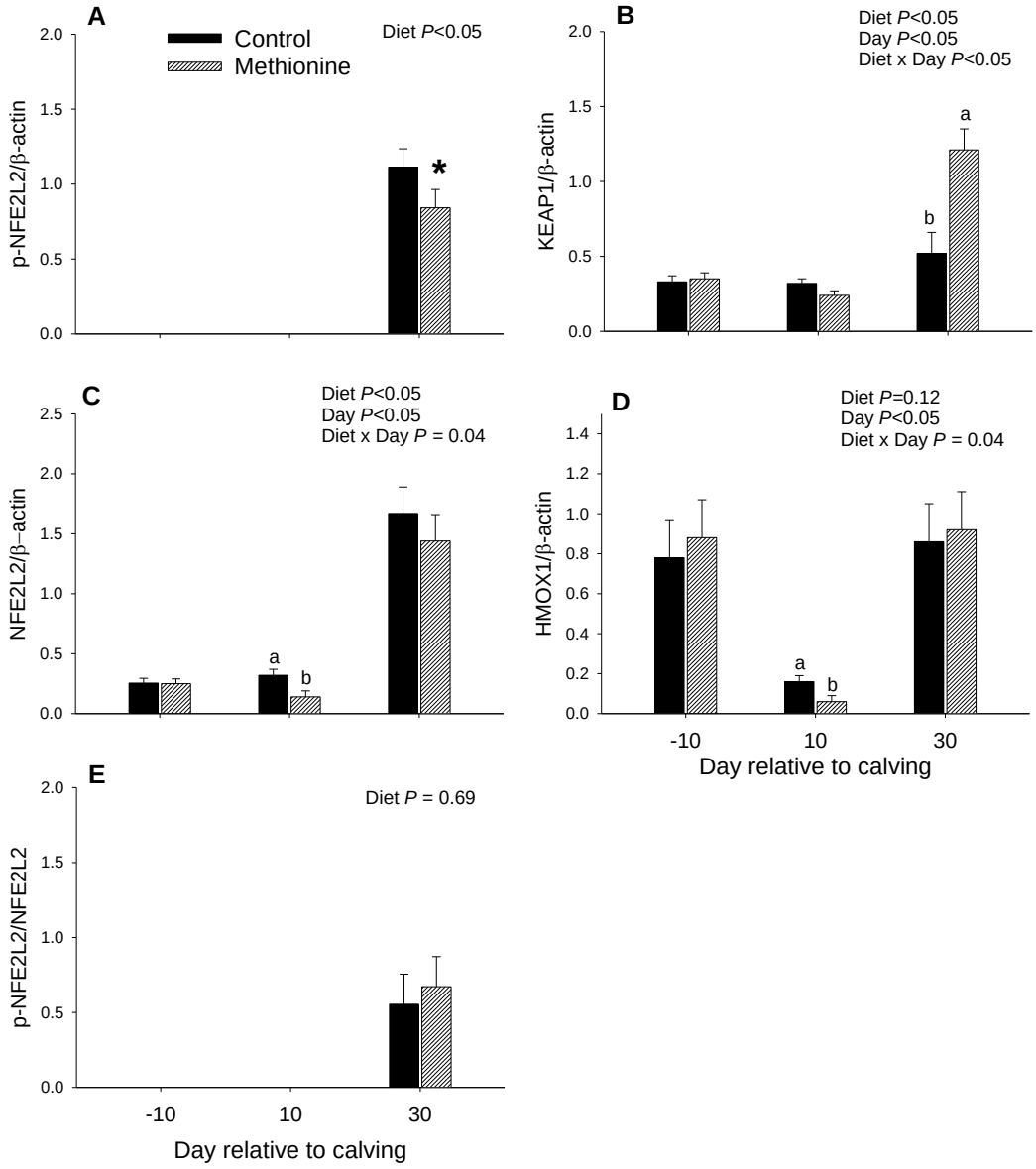

Figure 2.4. Protein abundance (relative to β-actin) of the antioxidant transcription factor p-NFE2L2 (active, panel A), NFE2L2 repressor KEAP1 (panel B), NFE2L2 (inactive, panel C), the NFE2L2 target HMOX1 (panel D), and the ratio of p-NFE2L2/NFE2L2 (panel E) in s.c. adipose tissue harvested at -10, 10, and 30 d relative to parturition. Data are LS means, n = 7 cows per diet, ± pooled SEMs. [ab]Means differ (Diet × Day, $P \leq 0.05$). *Means between Control and Met differ ($P \leq 0.05$).

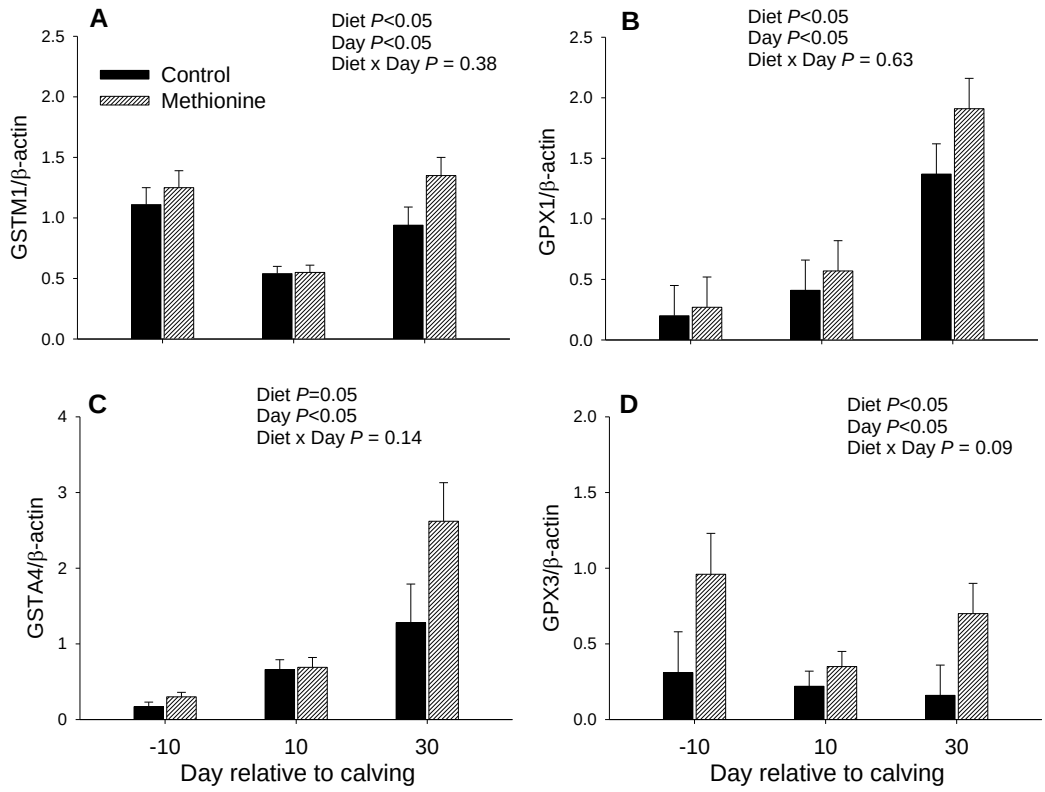

Figure 2.5. Protein abundance (relative to β-actin) of the glutathione metabolism-related enzymes GSTM1 (panel A), GPX1 (panel B), GSTA4 (panel C), and GPX3 (panel D) in s.c. adipose tissue harvested at -10, 10, and 30 d relative to parturition. Data are LS means, n = 7 cows per diet, ± pooled SEMs. GSTM1, glutathione S-transferase mu 1; GPX1, glutathione peroxidase 1; GPX3, glutathione peroxidase 3; GSTA4, glutathione S-transferase alpha 4.

Figure 2.6.

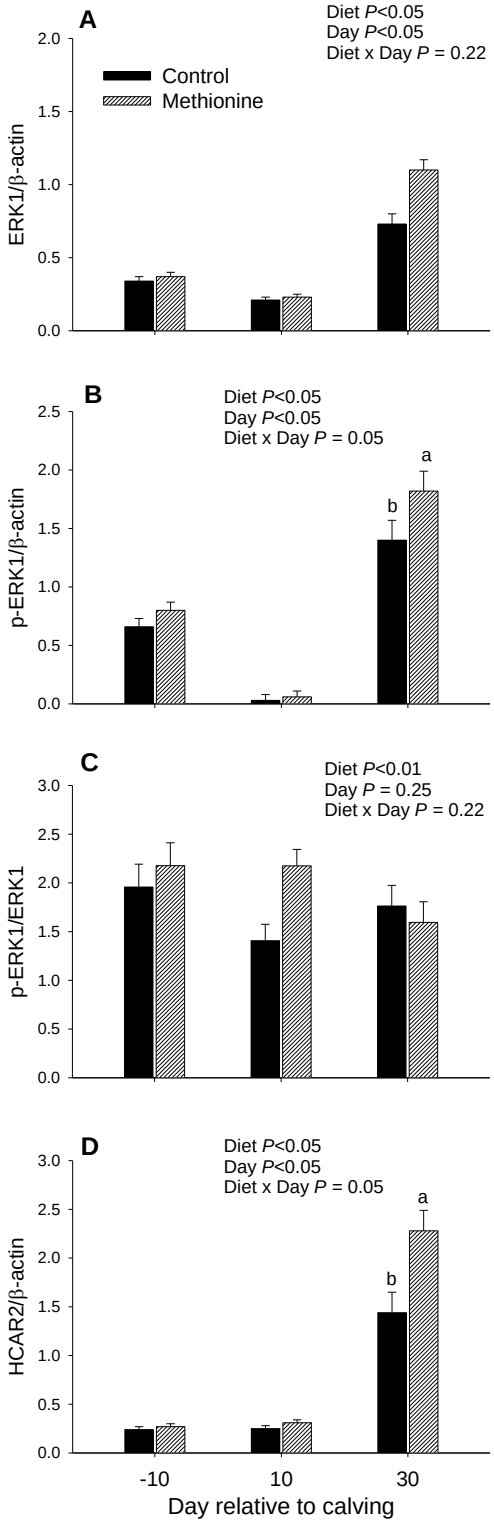

Figure 2.6. Protein abundance (relative to β-actin) of the oxidative stress-sensitive protein ERK1 (inactive, panel A), p-ERK1 (active, panel B), ratio of p-ERK1/ERK1 (panel C), and the

Figure 2.6. (cont.)
inflammation-related G-coupled protein receptor HCAR2 (panel D) in s.c. adipose tissue harvested at -10, 10, and 30 d relative to parturition. Holstein cows were fed a basal diet [control prepartum diet, 1.47 Mcal/kg of dry matter (DM) and 15.3% crude protein (CP); control postpartum diet, 1.67 Mcal/kg DM and 17.7% CP] or control plus ethyl-cellulose rumen-protected Met at a rate of 0.09% and 0.10% of DM intake from -28 to calving and from 1 through 30 d postcalving. Data are LS means, n = 7 cows per diet, ± pooled SEMs. ERK1, mitogen-activated protein kinase 3; HCAR2, hydroxycarboxylic acid receptor 2. [ab]Means differ (Diet × Day, $P \leq 0.05$).

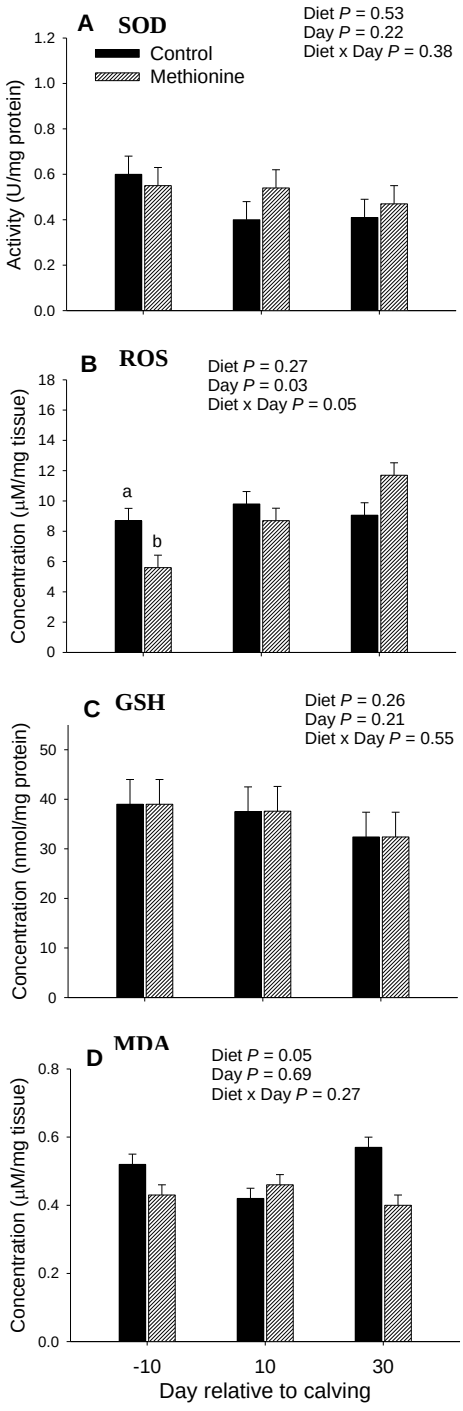

Figure 2.7. Activity of superoxide dismutase (SOD) (panel A), and concentrations of reactive oxygen species (ROS) (panel B), glutathione (GSH) (panel C), and malondialdehyde (MDA) (panel D) in s.c. adipose tissue harvested at -10, 10, and 30 d relative to parturition. Data are LS means, n = 7 cows per diet, ± pooled SEMs. [ab]Means differ (Diet × Day, $P \leq 0.05$).

REFERENCES

Abuelo, A., J. Hernandez, J. Benedito, and C. Castillo. 2013. Oxidative stress index (OSi) as a new tool to assess redox status in dairy cattle during the transition period. Animal 7:1374-1378.

Ade, N., F. Leon, M. Pallardy, J.-L. Peiffer, S. Kerdine-Romer, M.-H. Tissier, P.-A. Bonnet, I. Fabre, and J.-C. Ourlin. 2008. HMOX1 and NQO1 genes are upregulated in response to contact sensitizers in dendritic cells and THP-1 cell line: role of the Keap1/Nrf2 pathway. Toxicol. Sci. 107:451-460.

Aquilano, K., S. Baldelli, and M. R. Ciriolo. 2014. Glutathione: new roles in redox signaling for an old antioxidant. Front. Pharmacol. 5:196.

Batistel, F., J. Arroyo, A. Bellingeri, L. Wang, B. Saremi, C. Parys, E. Trevisi, F. Cardoso, and J. Loor. 2017. Ethyl-cellulose rumen-protected methionine enhances performance during the periparturient period and early lactation in Holstein dairy cows. J. Dairy Sci. 100:7455-7467.

Batistel, F., J. Arroyo, C. Garces, E. Trevisi, C. Parys, M. Ballou, F. Cardoso, and J. Loor. 2018. Ethyl-cellulose rumen-protected methionine alleviates inflammation and oxidative stress and improves neutrophil function during the periparturient period and early lactation in Holstein dairy cows. J. Dairy Sci. 101:480-490.

Bendich, A. 1993. Physiological role of antioxidants in the immune system. J. Dairy Sci. 76:2789-2794.

Bernabucci, U., B. Ronchi, N. Lacetera, and A. Nardone. 2005. Influence of body condition score on relationships between metabolic status and oxidative stress in periparturient dairy cows. J. Dairy Sci. 88:2017-2026.

Cardozo, L. F., L. M. Pedruzzi, P. Stenvinkel, M. B. Stockler-Pinto, J. B. Daleprane, M. Leite Jr, and D. Mafra. 2013. Nutritional strategies to modulate inflammation and oxidative stress pathways via activation of the master antioxidant switch Nrf2. Biochimie 95:1525-1533.

Contreras, G. A., C. Strieder-Barboza, and J. De Koster. 2018. Symposium review: Modulating adipose tissue lipolysis and remodeling to improve immune function during the transition period and early lactation of dairy cows. J. Dairy Sci. 101:2737-2752.

Contreras, G. A., C. Strieder-Barboza, J. De Souza, J. Gandy, V. Mavangira, A. L. Lock, and L. M. Sordillo. 2017. Periparturient lipolysis and oxylipid biosynthesis in bovine adipose tissues. PLoS One 12:e0188621.

Couto, N., J. Wood, and J. Barber. 2016. The role of glutathione reductase and related enzymes on cellular redox homoeostasis network. Free Radical Biol. Med. 95:27-42.

Curtis, J. M., P. A. Grimsrud, W. S. Wright, X. Xu, R. E. Foncea, D. W. Graham, J. R. Brestoff, B. M. Wiczer, O. Ilkayeva, and K. Cianflone. 2010. Downregulation of adipose glutathione S-transferase A4 leads to increased protein carbonylation, oxidative stress, and mitochondrial dysfunction. Diabetes 59:1132-1142.

Drackley, J. K. 1999. Biology of dairy cows during the transition period: The final frontier? J. Dairy Sci. 82:2259-2273.

Du, X., Z. Shi, Z. Peng, C. Zhao, Y. Zhang, Z. Wang, X. Li, G. Liu, and X. Li. 2017. Acetoacetate induces hepatocytes apoptosis by the ROS-mediated MAPKs pathway in ketotic cows. J. Cell. Physiol. 232:3296-3308.

Fernández-Sánchez, A., E. Madrigal-Santillán, M. Bautista, J. Esquivel-Soto, Á. Morales-González, C. Esquivel-Chirino, I. Durante-Montiel, G. Sánchez-Rivera, C. Valadez-

Vega, and J. A. Morales-González. 2011. Inflammation, oxidative stress, and obesity. Int. J. Mol. Sci. 12:3117-3132.
Furukawa, S., T. Fujita, M. Shimabukuro, M. Iwaki, Y. Yamada, Y. Nakajima, O. Nakayama, M. Makishima, M. Matsuda, and I. Shimomura. 2004. Increased oxidative stress in obesity and its impact on metabolic syndrome. J. Clin. Invest. 114:1752.
Gessner, D., G. Schlegel, J. Keller, F. Schwarz, R. Ringseis, and K. Eder. 2013. Expression of target genes of nuclear factor E2-related factor 2 in the liver of dairy cows in the transition period and at different stages of lactation. J. Dairy Sci. 96:1038-1043.
Graff, E. C., H. Fang, D. Wanders, and R. L. Judd. 2016. Anti-inflammatory effects of the hydroxycarboxylic acid receptor 2. Metabolism 65:102-113.
Griffith, O. W. 1999. Biologic and pharmacologic regulation of mammalian glutathione synthesis. Free Radical Biol. Med. 27:922-935.
Grummer, R. R. 1995. Impact of changes in organic nutrient metabolism on feeding the transition dairy cow. J. Anim. Sci. 73:2820-2833.
Han, L., F. Batistel, Y. Ma, A. Alharthi, C. Parys, and J. Loor. 2018a. Methionine supply alters mammary gland antioxidant gene networks via phosphorylation of nuclear factor erythroid 2-like 2 (NFE2L2) protein in dairy cows during the periparturient period. J. Dairy Sci. 101:6511-6522.
Han, L., Z. Zhou, Y. Ma, F. Batistel, J. Osorio, and J. J. Loor. 2018b. Phosphorylation of nuclear factor erythroid 2-like 2 (NFE2L2) in mammary tissue of Holstein cows during the periparturient period is associated with mRNA abundance of antioxidant gene networks. J. Dairy Sci. 101:6511-6522.
Ji, P., J. Osorio, J. Drackley, and J. Loor. 2012. Overfeeding a moderate energy diet prepartum does not impair bovine subcutaneous adipose tissue insulin signal transduction and induces marked changes in peripartal gene network expression1. J. Dairy Sci. 95:4333-4351.
Kane, R. E., J. Tector, J. J. Brems, A. P. Li, and D. L. Kaminski. 1990. Sulfation and glucuronidation of acetaminophen by cultured hepatocytes replicating in vivo metabolism. ASAIO Trans. 36:M607-610.
Kaspar, J. W., S. K. Niture, and A. K. Jaiswal. 2009. Nrf2: INrf2 (Keap1) signaling in oxidative stress. Free Radical Biol. Med. 47:1304-1309.
Kensler, T. W., N. Wakabayashi, and S. Biswal. 2007. Cell survival responses to environmental stresses via the Keap1-Nrf2-ARE pathway. Annu. Rev. Pharmacol. Toxicol. 47:89-116.
Lee, Y.-J., H.-N. Cho, J.-W. Soh, G. J. Jhon, C.-K. Cho, H.-Y. Chung, S. Bae, S.-J. Lee, and Y.-S. Lee. 2003. Oxidative stress-induced apoptosis is mediated by ERK1/2 phosphorylation. Exp. Cell Res. 291:251-266.
Lee, Y. S., A. Y. Kim, J. W. Choi, M. Kim, S. Yasue, H. J. Son, H. Masuzaki, K. S. Park, and J. B. Kim. 2008. Dysregulation of adipose glutathione peroxidase 3 in obesity contributes to local and systemic oxidative stress. Mol. Endo. 22:2176-2189.
Loor, J. 2010. Genomics of metabolic adaptations in the peripartal cow. Animal 4:1110-1139.
Loor, J., G. Bertoni, A. Hosseini, J. Roche, and E. Trevisi. 2013. Functional welfare–using biochemical and molecular technologies to understand better the welfare state of peripartal dairy cattle. Anim. Prod. Sci. 53:931-953.
Lu, S. C. 2009. Regulation of glutathione synthesis. Mol. Aspects Med. 30:42-59.
Martinov, M., V. Vitvitsky, R. Banerjee, and F. Ataullakhanov. 2010. The logic of the hepatic methionine metabolic cycle. Biochim. Biophys. Acta 1804:89-96.

Mavangira, V. and L. M. Sordillo. 2018. Role of lipid mediators in the regulation of oxidative stress and inflammatory responses in dairy cattle. Res. Vet. Sci. 116:4-14.
McGown, C., A. Birerdinc, and Z. M. Younossi. 2014. Adipose tissue as an endocrine organ. Clin. Liver Dis. 18:41-58.
Morey, S., L. Mamedova, D. Anderson, C. Armendariz, E. Titgemeyer, and B. Bradford. 2011. Effects of encapsulated niacin on metabolism and production of periparturient dairy cows. J. Dairy Sci. 94:5090-5104.
Motohashi, H. and M. Yamamoto. 2004. Nrf2–Keap1 defines a physiologically important stress response mechanism. Trends Mol. Med. 10:549-557.
Murri, M., M. Insenser, M. Luque, F. J. Tinahones, and H. F. Escobar-Morreale. 2014. Proteomic analysis of adipose tissue: informing diabetes research. Expert Rev. Proteomics 11:491-502.
Nakashima, C., K. Yamamoto, R. Fujiwara-Tani, Y. Luo, S. Matsushima, K. Fujii, H. Ohmori, T. Sasahira, T. Sasaki, and Y. Kitadai. 2018. Expression of cytosolic malic enzyme (ME1) is associated with disease progression in human oral squamous cell carcinoma. Cancer Sci. 109:2036.
Nguyen, T., P. Nioi, and C. B. Pickett. 2009. The Nrf2-antioxidant response element signaling pathway and its activation by oxidative stress. J. Biol. Chem. 284:13291-13295.
National Research Council. 2001. Nutrient requirements of dairy cattle. 7th rev. ed. Natl. Acad. Press, Washington, DC.
Offermanns, S., S. L. Colletti, T. W. Lovenberg, G. Semple, A. Wise, and A. P. IJzerman. 2011. International Union of Basic and Clinical Pharmacology. LXXXII: nomenclature and classification of hydroxy-carboxylic acid receptors (GPR81, GPR109A, and GPR109B). Pharmacol. Rev.pr. 110.003301.
Osorio, J., P. Ji, J. Drackley, D. Luchini, and J. Loor. 2013. Supplemental Smartamine M or MetaSmart during the transition period benefits postpartal cow performance and blood neutrophil function. J. Dairy Sci. 96:6248-6263.
Osorio, J., P. Ji, J. Drackley, D. Luchini, and J. Loor. 2014a. Smartamine M and MetaSmart supplementation during the peripartal period alter hepatic expression of gene networks in 1-carbon metabolism, inflammation, oxidative stress, and the growth hormone–insulin-like growth factor 1 axis pathways. J. Dairy Sci. 97:7451-7464.
Osorio, J., E. Trevisi, P. Ji, J. Drackley, D. Luchini, G. Bertoni, and J. Loor. 2014b. Biomarkers of inflammation, metabolism, and oxidative stress in blood, liver, and milk reveal a better immunometabolic status in peripartal cows supplemented with Smartamine M or MetaSmart. J. Dairy Sci. 97:7437-7450.
Overton, T. R., D. W. LaCount, T. M. Cicela, and J. Clark. 1996. Evaluation of a ruminally protected methionine product for lactating dairy cows1. J. Dairy Sci. 79:631-638.
Samland, A. K. and G. A. Sprenger. 2009. Transaldolase: from biochemistry to human disease. Int. J. Biochem. Cell Biol. 41:1482-1494.
Schwab, C. G. and G. A. Broderick. 2017. A 100-Year Review: Protein and amino acid nutrition in dairy cows. J. Dairy Sci. 100:10094-10112.
Sena, L. A. and N. S. Chandel. 2012. Physiological roles of mitochondrial reactive oxygen species. Mol. Cell 48:158-167.
Shoelson, S. E., J. Lee, and A. B. Goldfine. 2006. Inflammation and insulin resistance. The J. Clin. Invest. 116:1793-1801.

Sordillo, L. and V. Mavangira. 2014. The nexus between nutrient metabolism, oxidative stress and inflammation in transition cows. Anim. Prod. Sci. 54:1204-1214.
Sordillo, L. M. and S. L. Aitken. 2009. Impact of oxidative stress on the health and immune function of dairy cattle. Vet. Immunol. Immunopathol. 128:104-109.
Spears, J. W. 2000. Micronutrients and immune function in cattle. Proc. Nutr. Soc. 59:587-594.
Stipanuk, M. H. 2004. Sulfur amino acid metabolism: pathways for production and removal of homocysteine and cysteine. Annu. Rev. Nutr. 24:539-577.
Strange, R. C., M. A. Spiteri, S. Ramachandran, and A. A. Fryer. 2001. Glutathione-S-transferase family of enzymes. Mutat. Res. 482:21-26.
Titgemeyer, E., L. Mamedova, K. Spivey, J. Farney, and B. Bradford. 2011. An unusual distribution of the niacin receptor in cattle. J. Dairy Sci. 94:4962-4967.
Vailati-Riboni, M., G. Farina, F. Batistel, A. Heiser, M. Mitchell, M. Crookenden, C. Walker, J. Kay, S. Meier, and J. Roche. 2017. Far-off and close-up dry matter intake modulate indicators of immunometabolic adaptations to lactation in subcutaneous adipose tissue of pasture-based transition dairy cows. J. Dairy Sci. 100:2334-2350.
Vailati-Riboni, M., M. Kanwal, O. Bulgari, S. Meier, N. Priest, C. Burke, J. Kay, S. McDougall, M. Mitchell, and C. Walker. 2016. Body condition score and plane of nutrition prepartum affect adipose tissue transcriptome regulators of metabolism and inflammation in grazing dairy cows during the transition period. J. Dairy Sci. 99:758-770.
Vailati Riboni, M., S. Meier, N. Priest, C. Burke, J. Kay, S. McDougall, M. Mitchell, C. Walker, M. Crookenden, and A. Heiser. 2015. Adipose and liver gene expression profiles in response to treatment with a nonsteroidal antiinflammatory drug after calving in grazing dairy cows. J. Dairy Sci. 98:3079-3085.
Wen, D., D. Liu, J. Tang, L. Dong, Y. Liu, Z. Tao, J. Wan, D. Gao, L. Wang, and H. Sun. 2015. Malic enzyme 1 induces epithelial–mesenchymal transition and indicates poor prognosis in hepatocellular carcinoma. Tumor Biol. 36:6211-6221.
Yan, P. Y., G. Yu, G. Tseng, K. Cieply, J. Nelson, M. Defrances, R. Zarnegar, G. Michalopoulos, and J.-H. Luo. 2007. Glutathione peroxidase 3, deleted or methylated in prostate cancer, suppresses prostate cancer growth and metastasis. Cancer Res. 67:8043-8050.
Yu, B. P. 1994. Cellular defenses against damage from reactive oxygen species. Physiol. Rev. 74:139-162.
Yuan, K., R. Shaver, S. Bertics, M. Espineira, and R. Grummer. 2012. Effect of rumen-protected niacin on lipid metabolism, oxidative stress, and performance of transition dairy cows. J. Dairy Sci. 95:2673-2679.
Zachut, M., G. Kra, L. Livshitz, Y. Portnick, S. Yakoby, G. Friedlander, and Y. Levin. 2017. Seasonal heat stress affects adipose tissue proteome toward enrichment of the Nrf2-mediated oxidative stress response in late-pregnant dairy cows. J. Proteomics 158:52-61.
Zhou, Z., T. A. Garrow, X. Dong, D. N. Luchini, and J. J. Loor. 2016a. Hepatic activity and transcription of betaine-homocysteine methyltransferase, methionine synthase, and cystathionine synthase in periparturient dairy cows are altered to different extents by supply of methionine and choline. J. Nutr. 147:11-19.
Zhou, Z., M. Vailati-Riboni, E. Trevisi, J. Drackley, D. Luchini, and J. Loor. 2016b. Better postpartal performance in dairy cows supplemented with rumen-protected methionine compared with choline during the peripartal period. J. Dairy Sci. 99:8716-8732.

Zhu, Y., G. Liu, X. Du, Z. Shi, M. Jin, X. Sha, X. Li, Z. Wang, and X. Li. 2018. Expression patterns of hepatic genes involved in lipid metabolism in cows with subclinical or clinical ketosis. J. Dairy Sci. 102:1725-1735.

CHAPTER 3: METHIONINE SUPPLY DURING THE PERIPARTURIENT PERIOD ENHANCES INSULIN SIGNALING, AMINO ACID TRANSPORTERS, AND MECHANISTIC TARGET OF RAPAMYCIN PATHWAY PROTEINS IN ADIPOSE TISSUE OF HOLSTEIN COWS

-Journal of Dairy Science, 2019, 102 (5): 4403-4414.

ABSTRACT

Enhanced post-ruminal supply of methionine (Met) during the periparturient period increases dry matter intake (DMI) and milk yield. In non-ruminants, adipose tissue is responsive to AA supply, can utilize them as fuels, or for protein synthesis regulated in part via insulin and mechanistic target of rapamycin (mTOR) signaling. Whether enhancing supply of Met has an effect on insulin and mTOR pathways in adipose tissue in peripartal cows is unknown. Multiparous Holstein cows were assigned from –28 to 60 d relative to parturition to a basal diet (control; 1.47 Mcal/kg of DM and 15.3% CP prepartum; 1.67 Mcal/kg and 17.7% CP postpartum) or the control plus ethyl-cellulose rumen-protected Met (RPM). The RPM was fed individually at a rate of 0.09% of dry matter intake prepartum and 0.10% postpartum. Subcutaneous adipose tissue harvested at -10, 10, and 30 d (days in milk) relative to parturition was used for quantitative PCR and western blotting. A glucose tolerance test was performed at -12 and 12 DIM to evaluate insulin sensitivity. Area under the curve for glucose in the pre and postpartum tended to be smaller in cows fed Met. Enhanced Met supply led to greater overall mRNA abundance of Gln (*SLC38A1*), Glu (*SLC1A1*), L-type AA (Met, Leu, Val, Phe; *SLC3A2*), small zwitterionic α-AA (*SLC36A1*), and neutral AA (*SLC1A5*) transporters. Abundance of *AKT1*, *RPS6KB1*, and *EIF4EBP1* was also upregulated in response to Met. There was a diet × day interaction for protein abundance of INSR due to Met cows having lower values at 30 d postpartum compared with controls. The diet × day interaction was significant for hormone-sensitive lipase due to Met cows having greater abundance at 10 d postpartum compared with

controls. Enhanced Met supply upregulated protein abundance of insulin-responsive proteins p-AKT, peroxisome proliferator-activated receptor gamma, and fatty acid synthase. Overall abundance of SLC2A4 tended to be greater in cows fed Met. A diet × Day interaction was observed for mTOR protein abundance due to greater values for RPM cows at 30 d postpartum compared with controls. Enhanced RPM supply upregulated overall protein abundance of SLC1A3, p-mTOR, and RPS6. Overall, data indicate that mTOR and insulin signaling pathways in adipose tissue adapt to the change in physiologic state during the periparturient period. Further studies should be done to clarify whether the activation of p-AKT or increased availability of AA leads to the activation of mTOR.

Key words: amino acid transporter, mTOR, insulin response, transition period

INTRODUCTION

The periparturient or "transition" period is the most challenging of the production cycle of dairy cows. During this period cows undergo great immunometabolic changes and are more susceptible to a heightened state of oxidative stress and inflammation (Drackley, 1999, Sordillo and Raphael, 2013, Osorio et al., 2014b). A state of insulin resistance (Sordillo and Raphael, 2013, De Koster et al., 2018) designed to limit glucose utilization by tissues like adipose and muscle (Zhai et al., 2010) also characterizes the transition period. These endocrine and physiologic adaptations are now considered components of homeorhesis, allowing the mammary gland to have priority over nutrient utilization for milk synthesis (Bradford et al., 2015, Vailati Riboni et al., 2015). Despite the importance of insulin signaling in adipose tissue, few studies (e.g., Zachut et al., 2013) have addressed the concerted longitudinal adaptations of insulin-sensitive components including the insulin receptor (**INSR**), intracellular kinases (e.g., insulin receptor 1, **IRS1**; AKT serine/threonine kinase, **AKT**), glucose transporters (**SLC2A4),**

transcription regulators (e.g., PPARgamma, **PPARG**), and enzyme targets (e.g., fatty acid synthase, **FASN**).

Although it is well-established that adipose tissue is a major organ for glucose and lipid metabolism in mammalian species, hence responsive to insulin (De Koster and Opsomer, 2013), its role in systemic protein and AA metabolism in dairy cows is not well-known. For instance, feeding 20 g/d methionine hydroxyl analog to diets containing 11% or 14% crude protein between -14 through 60 d around parturition resulted in lower body protein loss (Phillips et al., 2003). Furthermore, crude protein alone enhanced fat and body protein gain between 60 to 120 d postpartum. Although the exact mechanisms for those responses were not studied, research in humans and rodents indicates that adipose tissue can utilize AA such as methionine (**Met**) and branched-chain amino acids (**BCAA**) (Feller and Feist, 1963, Badoud et al., 2014). Methionine is the first-limiting AA in dairy cows and feeding rumen-protected methionine (**RPM**) contributes to more efficient utilization of this and other AA for milk synthesis (Schwab and Broderick, 2017). Besides serving as backbone for protein synthesis, BCAA (leucine, isoleucine, and valine) are essential AA (Lu et al., 2013) with the capacity to regulate the activity of mechanistic target of rapamycin (**mTOR**) which controls protein synthesis and cell growth (Lynch and Adams, 2014).

Obesity research in monogastrics indicated a positive association between circulating BCAA and insulin resistance (Newgard et al., 2009, McCormack et al., 2013). Not only can adipose tissue catabolize BCAA in vivo, but also can help buffer circulating BCAA levels via the regulation of enzymes (Herman et al., 2010) such as branched-chain α-keto acid dehydrogenase kinase (**BCKDK**). This enzyme is key in controlling flux through the branched-chain α-keto acid dehydrogenase complex, which is the rate-liming step for BCAA catabolism (Shimomura et al.,

2001). Although mechanistic aspects of AA metabolism by adipose tissue in dairy cows is in its infancy, the concerted evaluation of AA transporters and key controls of AA signaling (e.g., mTOR pathway) could shed light on the relevance of nutritional management during the transition period in the context of adipose tissue function and remodeling.

The objective of this study was to use adipose tissue samples from control and RPM-fed cows in the study of Batistel et al. (2017b) to evaluate changes in mRNA and protein abundance of key AA transporters and various components of the mTOR and insulin signaling pathways during the transition period. Our general hypothesis was that enhanced RPM supply activates mTOR and dampens insulin resistance in s.c. adipose tissue.

MATERIALS AND METHODS

Experiment Design and Treatment

The University of Illinois Institutional Animal Care and Use Committee (Urbana; protocol #14270) approved all procedures involving animals for the current study. Details of the experimental design have been reported previously (Batistel et al., 2017b). Briefly, 60 multiparous Holstein cows per treatment were used in a randomized, complete, balanced block design experiment. Cows were fed a basal control (control) diet without additional Met or the control plus ethylcellulose RPM (Met; Mepron, Evonik Nutrition and Care Gmbh, Hanau-Wolfgang, Germany). The RPM was topdressed on the total mixed ration for each cow in the Met group from −28 to 60 d relative to parturition at a rate of 0.09% (prepartum) and 0.10% (postpartum) of the DMI of the previous day to achieve a Lys:Met ratio of 2.8:1. From −45 to −29 d relative to parturition, all cows were fed the same diet without Met. Diets were mixed daily using a tumble-mixer. The ingredient and chemical composition of the diets were reported

previously (Batistel et al., 2017b). Diets were formulated to meet cow predicted requirements according to the NRC (2001).

Glucose Tolerance Test

On d -12 and 12 relative to expected calving date, 10 cows in control and 10 in Met received a glucose tolerance test (**GTT**) while restrained in a squeeze chute, approximately 2 h after feeding. A solution of 50% glucose (Dextrose 50%, Agri Laboratories Ltd, St. Joseph, IL) was administrated at 0.25 g/kg of BW with an intravenous set (PBS Animal Health, Massillon, OH) and a disposable 14-gauge × 3.8 cm needle (Tyco Healthcare Group LP, Mansfield, MA) for jugular vein access. Cows were restrained in a squeeze chute and blood samples (20 mL) were obtained by puncture of the coccygeal vein or artery with 20-gauge × 2.5 cm needles (Becton Dickinson and Company, Franklin Lakes, NJ) at -15, -10, -5, 5, 10, 15, 30, 60, and 120 min relative to administration of glucose. Glucose concentration was measured using a glucose oxidase method (PGO Enzyme Product No. P7119; Sigma Chemical Co., St. Louis, MO). Intra- and interassay coefficients of variation were 5.1 and 8.5%, respectively.

Calculations of Plasma Biomarkers and GTT

Basal glucose and insulin concentrations (before GTT) were calculated averaging the concentrations at 15, 10, and 5 min before GTT. Peak, mean, and nadir concentrations for glucose and insulin were determined with the concentration values at 5, 10, 15, 30, 60, and 120 min after GTT. The areas under the curve of glucose (**AUC**) and insulin during the 120 min after GTT were calculated (after correcting for baseline) using the trapezoidal method and actual concentration values as described previously (Cardoso et al., 2011).

Daily Plasma Insulin Concentration

Blood samples from the same 7 cows in the control and Met groups used for biopsies was harvested via coccygeal venipuncture before feeding using evacuated tubes containing lithium heparin (Batistel et al., 2017b). Plasma was obtained by centrifugation at 2,000 × *g* for 30 min at 4°C and preserved at −80 °C until later analysis. Insulin concentration in plasma was determined using a bovine-specific commercial ELISA kit (catalog no. 10-1201-01; Mercodia, Uppsala, Sweden). Intra-and interassay coefficients of variation were 12.5 and 14.8%, respectively.

Adipose Tissue Biopsies

Seven cows from the Met group and 7 cows from the control were used for adipose biopsies. These cows were selected based on actual days receiving diets prepartum (28 ±3 d), absence of clinical disorders, and all had the full set of biopsies. Tissue was harvested from the tail head (alternating between the right and left tail head region) at −10 (±3 d), 10, and 30 d relative to parturition according to previous procedures from our laboratory (Ji et al., 2012). Upon collection, adipose tissue was immediately placed in screw-capped, microcentrifuge tubes, snap-frozen in liquid nitrogen, and preserved at −80 °C until further analysis. Health was monitored for 7 d after surgery. Surgical clips were removed after 7 d post-biopsy. All biopsies were harvested at approximately 0800 h.

RNA isolation, cDNA Synthesis, and Quantitative PCR

Total RNA was isolated from 200 mg of adipose tissue using the miRNeasy kit (Qiagen, Hilden, Germany) according to the manufacturer's protocols. The RNA samples were digested with DNaseI and quantification was assessed using a NanoDrop ND-1000 spectrophotometer (Thermo Scientific, Waltham, MA). The quality of RNA samples was measured using an Agilent 2100 Bioanalyzer (Agilent Technologies, Santa Clara, CA). The quantitative PCR was conducted

as described previously (Osorio et al., 2014a). Previously validated internal controls for adipose tissue were ribosomal protein S9 (***RPS9***), glyceraldehyde-3-phosphate dehydrogenase (***GAPDH***), and actin beta (***ACTB***) (Vailati Riboni et al., 2015, Vailati-Riboni et al., 2016, Vailati-Riboni et al., 2017). Gene symbols and names are presented in Table 3.1. Quantitative PCR performance and primer information are included in Supplemental Table B.1.

Western Blot Analysis

Total protein was extracted from 100 mg adipose tissue according to a published procedure from our laboratory (Batistel et al., 2017a). The concentration of total protein was determined using a NanoDrop ND-1000 (Thermo Fisher Scientific, Waltham, MA). Protein samples were denatured by heating at 100 °C for 5 min before loading 75 µg protein into each lane of a 4-20% SDS-PAGE gel (catalog no. 4561096; Bio-Rad, Hercules, CA). Reactions were run for 10 min at 180 V, and then for 45 to 60 min at 110 V. After activating a polyvinyldene fluoride membrane (catalog no. 1620261; Bio-Rad, Hercules, CA) with methanol for 1 min, the protein sample was transferred to the membrane in a Trans-Blot SD Semi-Dry Electrophoretic Transfer Cell (catalog no. 170-3940, Bio-Rad, Hercules, CA). Membranes were then blocked in 1×Tris-buffered saline (1×TBST) containing 5% nonfat milk for 2 h at room temperature. The membranes were then incubated in 1×TBST containing primary antibodies to mTOR, phospho-mTOR(Ser2448), AKT, phospho-AKT(Ser473), INSR, SLC2A4 (formerly GLUT4), phospho-4-EBP(Thr37/46), phospho-EEF2(Thr56), SLC3A1, SCL38A1, SLC1A5, BCKDK, RPS6, phospho-RPS6 (Ser235/236), FASN, LIPE (formerly HSL), phospho-LIPE (Ser563), PPARG, and IRS1 overnight at 4 °C. Additional information about dilution ratios and vendors is reported in Supplemental Table B.2. The membranes were washed 6 times with 1×TBST and incubated with anti-rabbit HRP-conjugated secondary antibodies (catalog no. ab6721; Abcam, Cambridge,

UK) for 1 h at room temperature. Subsequently, the membranes were then washed 6 times with 1×TBST and then incubated with ECL reagent (catalog no. 170-5060; Bio-Rad, Hercules, CA) for 3 min in the dark prior to image acquisition. Actin beta (catalog no. 4967S; Cell Signaling Technology, Danvers, MA) was used as the internal control. Images were acquired using the ChemiDOC MP Imaging System (Bio-Rad, Hercules, CA). The intensities of the bands were measured with Image-Pro Plus 6.0 software (Media Cybernetics, Inc., Rockville, MD). Relative abundance of target proteins was normalized using β-actin.

Statistical Analysis

The data were analyzed using the MIXED procedure of SAS v.9.4 (SAS Institute Inc., Cary, NC) according to the following model with repeated measures:

$$Y_{jl} = \mu + M_j + T_l + MT_{jl} + e_{jl},$$

where Y_{jl} = dependent, continuous variable, μ = overall mean, M_j = fixed effect of treatment (j = control vs. Met), T_l = fixed effect of time (day, -10, 10, and 30 d), MT_{jl} = interaction between treatment and time, and e_{jl} = residual error. Cow, nested within treatment, was the random effect. The Kenward-Roger statement was used for computing the denominator degrees of freedom. The covariance structure of the repeated measurements was spatial power [SP(POW)]. When the interaction was significant, least squares means separation between and within time points was performed using the PDIFF statement with Tukey adjustment. Normality of the residuals was checked with normal probability and box plots, and homogeneity of variances was checked with plots of residuals versus predicted values. The model to analyze area under the curve (**AUC**) of glucose and insulin contained the fixed effect of treatment, time, and their interaction (diet × day). Time (min) was specified as repeated with cow as subject. Concentrations before GTT were used as covariates when analyzing concentrations over time.

The spatial power (SP) covariance structure was used because of the unequally spaced data points. Significance was determined at $P \leq 0.05$ and tendencies at $P \leq 0.10$.

RESULTS

Glucose Tolerance Test and Plasma Insulin

In the prepartum, after the GTT Met cows had greater basal concentration and maximum concentration of glucose and insulin in plasma ($P < 0.05$) (Table 3.2). In addition, Met cows tended ($0.05 < P \leq 0.10$) to have smaller AUC for both glucose and insulin and shorter time to baseline for glucose. In the postpartum, the AUC for glucose after the GTT tended ($P = 0.09$) to be lower in Met cows. Although no effect of diet was detected, insulin concentration decreased ($P < 0.05$) significantly after parturition (Figure 3.1).

mRNA Abundance

Main effects of diet, time, and interactions are reported in Table 3.1. The diet × day interaction was not significant ($P > 0.05$) for any gene measured. Among the 7 AA transporters measured, enhanced Met supply led to greater mRNA abundance of Gln (***SLC38A1***), Glu (***SLC1A1***), L-type AA (Met, Leu, Val, Phe; ***SLC3A2***), small zwitterionic α-AA (***SLC36A1***), and neutral AA (***SLC1A5***) transporters ($P < 0.05$). Abundance of *AKT1* and the mTOR-related genes *RPS6KB1* and *EIF4EBP1* was also upregulated ($P < 0.05$) in Met cows compared with controls (Table 3.1).

Protein Abundance

Insulin signaling. Main effects of diet, time, and interactions are reported in Figures 3.2-4. There was a diet × day interaction ($P < 0.05$) for INSR in part due to Met cows having lower ($P < 0.05$) abundance at 30 d relative to parturition compared with controls (Figure 3.2). The

treatment × time interaction was also significant ($P < 0.05$) for LIPE due to Met cows having greater ($P < 0.05$) abundance at 10 d postpartum compared with controls (Figure 3.2). Enhanced RPM supply led to greater overall protein abundance of p-AKT, PPARG, SLC2A4, and FASN ($P < 0.05$; Figure 3.2). The abundance of p-LIPE and IRS1 could not be detected with the antibodies used.

Transporters of AA and mTOR pathway. The diet × day interaction was significant ($P < 0.05$) for mTOR due in part to Met cows having greater ($P < 0.05$) abundance at 30 d postpartum compared with controls (Figure 3.4). The diet × day interaction was significant for protein abundance of p-EEF2 ($P < 0.05$) due to a lower abundance ($P < 0.05$) at 10 d postpartum in Met cows compared with controls (Figure 3.4). Enhanced Met supply upregulated overall abundance of SLC1A3 (Figure 3.3), p-mTOR, and ribosomal protein S6 (**RPS6**; $P < 0.05$; Figure 3.4).

DISCUSSION

Recent studies feeding RPM to enhance Met supply during the periparturient period have underscored the importance of this AA for milk protein synthesis but also for synthesis of antioxidants such as glutathione (Osorio et al., 2014a, Zhou et al., 2018, Batistel et al., 2017b, Batistel et al., 2018). The decrease in plasma insulin after parturition is well documented (De Koster et al., 2018), and explains in part the typical surge in plasma fatty acids as detected in the cows used in this study (Batistel et al., 2018). Clearly, despite the greater rate of DMI in cows fed Met compared with controls (Batistel et al., 2017b), adipose tissue responded according to the homeorhetic theory (Bauman and Currie, 1980).

Insulin binding to the INSR triggers a cascade of events in which phosphorylation of AKT enhances INSR phosphorylation followed by activation of IRS1 with the end result of

enhancing the movement of SLC2A4 to the plasma membrane to allow for uptake of glucose (Pessin and Saltiel, 2000). Clearly, one of the key homeorhetic adaptations during the peripartal period is a decrease in insulin sensitivity of adipose and muscle to prioritize mammary utilization of insulin-sensitive nutrients such as glucose and AA (Bauman and Currie, 1980). A "side effect" of insulin insensitivity is the catabolism of fat depots and skeletal muscle, with the former often exacerbating the capacity of the liver to fully metabolize fatty acids and rendering cows more susceptible to fatty liver and ketosis (Bell and Bauman, 1997, Drackley, 1999).

In a previous study dealing with s.c. adipose tissue, the phosphorylation level of AKT under conditions of a GTT and BW loss after calving were used to classify periparturient cows into insulin resistant or insulin sensitive subgroups (Zachut et al., 2013). Data established an association between p-AKT status and degree of BW loss such that greater p-AKT after a glucose tolerance challenge was associated with a lower degree of BW loss, i.e. a response reflective of insulin sensitivity (Zachut et al., 2013). In a follow-up study with tissue from those subgroups, proteomics analysis revealed that out of a total of 586 proteins identified a subset of 18.9% (111) differed in insulin-resistant versus insulin-sensitive tissue and most were upregulated (Zachut, 2015). Bioinformatics analysis of those proteins identified as most-relevant pathways gluconeogenesis and glycolysis, 14-3-3 mediated signaling, tricarboxylic acid cycle, and extracellular signal–regulated kinase/mitogen-activated protein kinase signaling with accumulation of lipid, release of lipid, and lipolysis as the most-relevant lipid-related functions. It is also noteworthy that between late-prepartum and soon after calving, the vast majority of proteins identified had a decrease in abundance regardless of insulin sensitivity status (Zachut, 2015).

Although previous proteomics data demonstrated a clear change in the adipose tissue proteome and p-AKT status, the postpartum sample was harvested at 3-5 DIM which certainly would not have captured the physiological dynamics of the adipose tissue during the entire transition period (i.e. first ~30 DIM) (McNamara et al., 1995, Khan et al., 2013). The present study corroborates the decrease in abundance of plasma insulin along with INSR, AKT, p-AKT, and SLC2A4 soon after parturition, all of which are associated with insulin signaling in adipose. We also extend the work of Zachut et al. (2013) and Zachut (2015) to include data demonstrating the adipose response to supply of dietary Met across the periparturient period. The tendency for lower glucose AUC pre and postpartum along with the greater overall abundance of p-AKT, SLC2A4, PPARG, and FASN in Met cows provided evidence that enhanced Met supply partly alleviated insulin resistance during the transition period. As such, the data suggest that adipose tissue in Met cows not only readily utilized glucose but also had the ability to accrete lipid via lipogenesis (Chinetti et al., 2000) even during a time when cows still experienced negative energy balance (Batistel et al., 2017b). Recent data underscored that the ability of adipose tissue for lipogenesis at 7 and 28 d postpartum is intact and responds to supply of acetate (Khan et al., 2013). Thus, the fact that cows fed Met also had greater rates of DMI postpartum agrees with the protein abundance data related to glucose utilization and lipogenesis.

The greater overall abundance of LIPE in Met-fed cows particularly after calving is noteworthy and would suggest a more pronounced degree of lipolysis (Khan et al., 2013, Locher et al., 2015). Whether differences in abundance of LIPE are a reflection of insulin sensitivity status is unclear. For instance, the greater prepartum DMI in cows fed Met (Batistel et al., 2017b) agrees with the lower LIPE abundance in those cows. In addition, differences in overall abundance between -10 and 10 d postpartum regardless of diet appeared modest. The sole study

evaluating LIPE associations with loss of body mass early postpartum and insulin resistance detected no differences in abundance of this protein in spite of cows being classified as insulin resistant losing on average 89 kg BW in the first 30 d postpartum (Zachut, 2015).

From a mechanistic standpoint, active lipolysis also encompasses re-esterification of fatty acids within adipose tissue (Duncan et al., 2007, Nye et al., 2008) a process that would require phosphoenolpyruvate carboxykinase 1 (PCK1) activity to generate glycerol-3-phosphate via glyceroneogenesis. The mRNA abundance of *PCK1* in adipose tissue is greater in cows overfed energy prepartum and increases between the wk1 and 3 postpartum (Ji et al., 2012, Khan et al., 2013). Recent data indicated that in vitro basal lipolysis (measured via glycerol release) of tissue harvested at -7, 7, and 28 d around parturition is similar (Khan et al., 2013). Furthermore, adipose tissue harvested at those times responded to the same degree to lipolytic stimuli (isoprotenerol) in vitro. Thus, simultaneous lipogenesis and lipolysis clearly are normal responses to the onset of lactation and respond to level of nutrient intake, i.e. greater protein abundance helps accommodate the greater nutrient supply available to adipose tissue (Sumner and McNamara, 2007). We believe the existence of these seemingly contrasting processes is a normal aspect of the remodeling process that adipose tissue undergoes during early lactation (McNamara et al., 1995).

Previous data from studies in humans underscored a potentially important role of systemic AA availability on the overall metabolism of adipose tissue. Under fasting conditions, in vivo studies reported net uptake of Glu coupled with net release of Gln and Ala from human s.c. adipose tissue (Frayn et al., 1991). It was noteworthy that Ala uptake increased after a mixed meal when its concentrations in plasma rose. More recent data revealed that greater systemic AA availability in response to a meal increased AA transporter expression in human skeletal muscle

at least in the short-term (3 h post-feeding) (Drummond et al., 2010). Thus, it is likely that the systemic supply of AA could in part dictate their utilization by adipose.

Several transporters for AA across a wide array of cell types have been identified. For instance, solute carrier family 38 member 1 (**SLC38A1**) uses a Na^+ gradient to concentrate neutral AA within cells (Mackenzie and Erickson, 2004). Solute carrier family 1 member 5 (**SLC1A5**) is a high-affinity, Na^+-dependent transporter for Gln (Utsunomiya-Tate et al., 1996), and its inhibition blocks uptake of the AA and inhibits mTOR signaling (Nicklin et al., 2009). Solute carrier family 36 member 1 (**SLC36A1**) is a proton-coupled AA transporter localized specifically to lysosomes and exports AA from the lysosomal membrane to the cytosol where they can be utilized for protein synthesis (Zoncu et al., 2011). Solute carrier family 7 member 5 (**SLC7A5**) and SLC3A2 are bidirectional antiporters that regulate the exchange of intracellular Gln for extracellular Leu (Nicklin et al., 2009).

Because a previous study detected greater plasma concentrations of several essential and non-essential AA around parturition in response to feeding RPM (Zhou et al., 2016), we speculate that the upregulation (mRNA and protein) of AA transporters in adipose tissue would be reflective of a greater degree of uptake from plasma. Clearly, systemic concentrations of AA around parturition would be driven in part by DMI and utilization by the mammary gland at the onset of lactation. Although plasma insulin concentrations were not affected by feeding Met, those cows had greater rates of DMI (Batistel et al., 2017b), milk yield, and milk protein content, suggesting additional AA in the circulation could very well have been utilized by peripheral tissues including adipose.

The greater overall mRNA and protein abundance of the membrane AA transporter SLC1A3 in cows fed Met agrees with the greater DMI and suggests enhanced capacity for

utilization of AA. In fact, the gradual increase in abundance of SLC1A3 along with SLC1A5 (Na^+-independent) and SLC38A1 (Na-coupled and saturable) from late-pregnancy through 30 d postpartum regardless of diet underscores the ability of adipose tissue to utilize AA even during a period of negative energy balance. In addition, because the protein abundance of BCKDK [the rate-limiting enzyme for BCAA catabolism (Shimomura et al., 2001)] did not change between -10 and 10 d but increased at 30 d regardless of diet, we speculate that such response helps channel the utilization of BCAA from peripheral tissue to the mammary gland. Upregulation of *SLC1A1*, *SLC1A5*, *SLC3A2*, *SLC36A1*, and *SLC38A1* in cows fed Met support their role in allowing for AA use by adipose tissue. In fact, data from non-ruminant studies indicate that alterations in mRNA and protein abundance of AA transporters provide a link with intracellular activation of signaling pathways. For instance, mTOR activation is a powerful regulator of excitatory AA transporter 3 (**SLC1A1**) (Almilaji et al., 2012). Thus, both mRNA and protein abundance of AA transporters and mTOR could potentially provide a link between DMI, systemic AA availability, and peripheral tissue utilization.

Activation of mTOR by AA leads to phosphorylation and inactivation of the repressor of mRNA translation eukaryotic initiation factor 4E-binding protein (**EIF4EBP1**), the phosphorylation and activation of S6 kinase (**RPS6KB1**), and the activation of eukaryotic elongation factor 2 (**EEF2**), all of which increases rates of translation initiation and promotes the translocation step during elongation (Beugnet et al., 2003, Hay and Sonenberg, 2004, Wang and Proud, 2006, Kaul et al., 2011). Furthermore, activation of RPS6KB1 leads to phosphorylation of ribosomal protein S6 (**RPS6**) and consequently regulates protein synthesis (Wullschleger et al., 2006). The fact that overall protein abundance of p-EIF4EBP1 and p-RPS6 increased between 10 d prepartum and 30 d postpartum regardless of diet agrees with the pattern (mRNA and/or

protein) of most of the AA transporters measured. In part, this degree of concordance supports the idea that AA are readily utilized by adipose tissue during early lactation (despite negative energy balance). In addition, the marked upregulation of p-EIF4EBP1 (~4.5-fold) between -10 and 30 d also could be an indication that there is tight control of protein synthesis in adipose tissue in early lactation such that the priority for AA utilization still favors the mammary gland.

Based on the present and previous data, we could envision a situation in which the mammary gland has absolute priority over AA use in the early stages after calving, while over time and with the gradual increase in feed intake more AA become available for utilization by adipose tissue. Under such scenario, conditions that upregulate abundance of total mTOR and p-mTOR in adipose tissue might be the determining factor controlling AA use and the degree of protein synthesis. Although there is no evidence (to our knowledge), that an upregulation of AA transporters results in the activation of mTOR in adipose tissue, non-ruminant data indicate that upregulation of placental AA transporters contributes to fetal growth via the activation of mTOR signaling (Jansson et al., 2013, Batistel et al., 2017a). Thus, AA availability and utilization by adipose tissue after calving may not only help in the remodeling process (McNamara et al., 1995) but also may serve ancillary functions such as preventing localized inflammation and oxidative stress (Chimin et al., 2017).

A limitation of the present study is that we did not evaluate adipocyte diameter, number, or volume, all of which are known to change during the transition period and early lactation (McNamara et al., 1995). Although diameter and volume decrease after parturition and remain below prepartal levels until at least 60 d postpartum, the number of adipocytes per gram of tissue actually increases (McNamara et al., 1995). The reduction in insulin sensitivity during the transition period, especially early lactation, has been well-established (Bauman and Currie,

1980). Factors that cause this effect include the gradual reduction in DMI and the reduced sensitivity of the pancreas during lactation to insulinogenic signals (Lomax et al., 1979). Thus, such adaptations explain the decrease in lipid in adipose tissue especially during the first 30 d postpartum, and use of hyperinsulinemic-euglycemic clamps in early lactation have confirmed the potent antilipolytic effect of insulin (Corl et al., 2006).

In the present study, insulin concentration decreased after parturition which is consistent with previous reports (Rico et al., 2015, De Koster et al., 2018) indicating lipolysis was favored in the postpartum. Despite that, FASN and PPARG (key contributors to lipogenesis/adipogenesis) had the highest abundance at d 30, likely as a result of the gradual increase in DMI after parturition (Batistel et al., 2017b). During the transition period, a greater BW loss postpartum is associated with impaired insulin signaling in adipose tissue (Zachut et al., 2013). In mice, a deficiency of mTOR in adipocytes induces localized inflammation by promoting oxidative stress (Chimin et al., 2017). Thus, the fact that the lowest abundance of p-AKT and p-mTOR was detected at d 10 underscores the risk that cows face immediately postpartum for developing metabolic disorders related to adipose tissue function. Although not studied in ruminants, insulin can contribute to protein synthesis in adipose tissue of rodents (Krahl, 1964). Based on the present data, it is possible that the decrease in insulin after parturition also contributes to lower p-mTOR. Overall, the results indicate that mTOR and insulin signaling pathways in adipose tissue adapt to the change in physiologic state during the periparturient period.

CONCLUSIONS

Protein abundance of various components of insulin and mTOR signaling pathways in adipose tissue adjust to the onset of lactation. Upregulation of mRNA and protein abundance of

some amino acid transporters along with greater abundance of p-AKT and p-mTOR in response to supply of Met suggest a mechanistic link. Thus, at least from a transcription and translation level, insulin and mTOR signaling pathways seem responsive to DMI and the systemic availability of key nutrients including glucose, amino acids, and lipogenic substrates. Although the pattern of protein abundance of key proteins driving utilization of nutrients right after parturition seems to indicate a priority by the mammary gland, towards the end of the transition period the data indicate that adipose tissue is capable of readily utilizing nutrients without competing with the mammary gland. The exact molecular mechanisms linking nutrition of the periparturient cow with mTOR signaling and AA metabolism by adipose tissue merits further study.

TABLES AND FIGURES

Table 3.1. mRNA abundance (log-2 scale) of amino acid transporters and components of the mechanistic target of rapamycin (mTOR) pathway in subcutaneous adipose harvested at -10, 10, and 30 d relative to parturition. Holstein cows were fed a basal diet [control prepartum diet, 1.47 Mcal/kg of dry matter (DM) and 15.3% crude protein (CP); control postpartum diet, 1.67 Mcal/kg DM and 17.7% CP] or control plus ethyl-cellulose rumen-protected Met[3] at a rate of 0.09% and 0.10% of DM intake from -28 to calving and from 1 through 30 d postcalving. Data are LS means, n = 7 cows per diet, ± pooled SEMs.

		Diet				*P*-value		
Gene	Name	Control	Methionine	Difference[2]	SEM	Diet[1]	Day	Diet × Day
Amino acid transporters								
SLC7A1	High affinity cationic amino acid transporter	0.14	0.19	35.7	0.05	0.08	0.15	0.13
SCL7A5	Branched-chain and aromatic amino acid transporter	1.39	1.28	-7.91	0.08	0.76	0.66	0.73
SCL1A1	Glutamate transporter	1.08	1.89	75	0.07	0.02	0.03	0.95
SLC1A5	Neutral amino acid transporter	0.21	0.35	66.6	0.06	0.02	0.32	0.26
SCL3A2	Heavy-chain amino acid transporter	1.21	1.61	33.0	0.03	0.01	0.14	0.75
SCL36A1	Neutral and cationic amino acid transporter	1.66	2.04	22.8	0.02	0.02	0.07	0.65
SCL38A1	Neutral amino acid transporter	1.47	2.23	51.7	0.05	0.03	0.78	0.90
mTOR pathway								
AKT	Protein kinase B	1.97	2.58	30.9	0.02	0.01	0.31	0.72
RPS6KB1	Ribosomal protein S6 kinase B1	1.57	2.20	40.1	0.04	0.02	0.23	0.90
EIF4EBP1	Eukaryotic translation initiation factor 4E-binding protein	2.18	3.11	42.6	0.05	0.04	0.31	0.90

[1]Methionine effect.
[2]Difference in mRNA abundance = (methionine – control)/control × 100.
[3]Mepron® (Evonik Nutrition & Care GmbH, Germany).

Table 3.2. Plasma concentrations of insulin and glucose before (basal) and during a glucose tolerance test at -12 d prepartum and 12 d postpartum. Holstein cows were fed a basal diet [control prepartum diet, 1.47 Mcal/kg of dry matter (DM) and 15.3% crude protein (CP); control postpartum diet, 1.67 Mcal/kg DM and 17.7% CP] or control plus ethyl-cellulose rumen-protected Met[2] at a rate of 0.09% and 0.10% of DM intake from -28 to calving and from 1 through 30 d postcalving. Data are LS means, n = 10 cows per diet, ± pooled SEMs.

	Diet			
Item	Control	Methionine	SEM	*P*-value
Prepartum				
Glucose				
Basal concentration, mg/dL	43.1	46.9	1.85	0.02
Maximum concentration, mg/dL	161	172	4.38	0.03
Time to baseline, min	75.2	67.9	3.93	0.07
AUC[1], min × mg/dL	3,348	2,845	251	0.10
Postpartum				
Glucose				
Basal concentration, mg/dL	38.9	40.1	1.85	0.45
Maximum concentration, mg/dL	152	147	5.23	0.39
Time to baseline, min	59.3	55.4	3.54	0.29
AUC, mg/dL × min[1]	3,485	3,095	211	0.09

[1]AUC = area under the curve.

[2]Mepron® (Evonik Nutrition & Care GmbH, Germany).

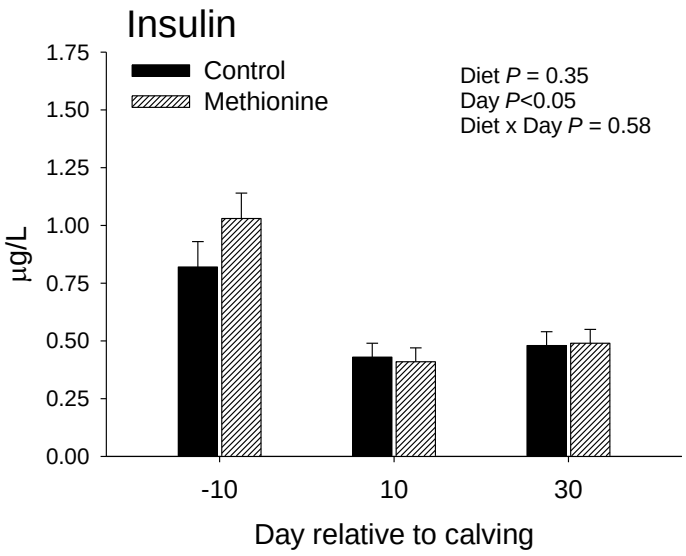

Figure 3.1. Insulin concentration in plasma from Holstein cows fed a basal diet [control prepartum diet, 1.47 Mcal/kg of dry matter (DM) and 15.3% crude protein (CP); control postpartum diet, 1.67 Mcal/kg DM and 17.7% CP] or control plus ethyl-cellulose rumen-protected Met at a rate of 0.09% and 0.10% of DM intake from -28 to calving and from 1 through 30 d postcalving. Data are LS means, n = 7 cows per diet, ± pooled SEMs.

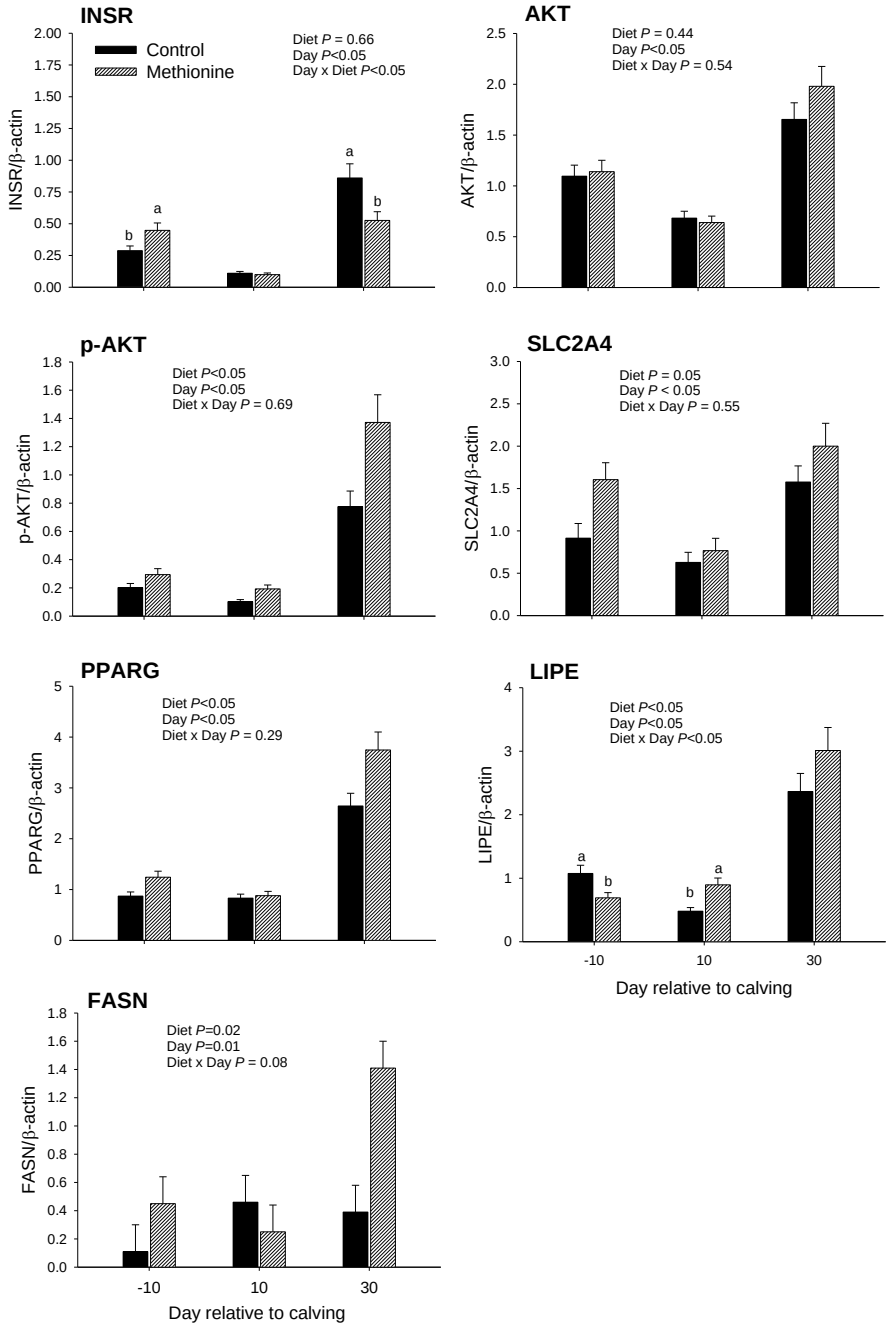

Figure 3.2. Protein abundance (relative to β-actin) of insulin signaling pathway components AKT, p-AKT, INSR, and SLC2A4, and lipid metabolism targets LIPE, FASN, and PPARG in s.c. adipose tissue harvested at -10, 10, and 30 d relative to parturition. Data are LS means, n = 7 cows per diet, ± pooled SEMs. [ab]Means differ (Diet × Day, $P \leq 0.05$).

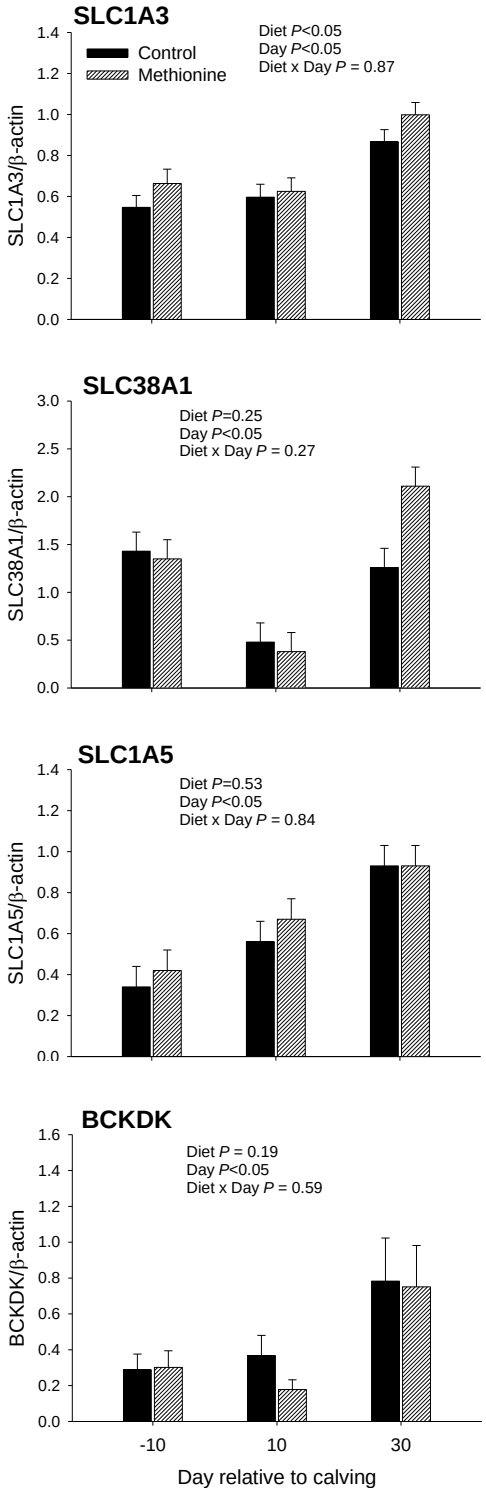

Figure 3.3. Protein abundance (relative to β-actin) of AA transporters SLC1A3, SLC38A1, and SLC1A5 and the rate-limiting enzyme for BCAA catabolism BCKDK in s.c. adipose tissue harvested at -10, 10, and 30 d relative to parturition. Data are LS means, n = 7 cows per diet, ± pooled SEMs.

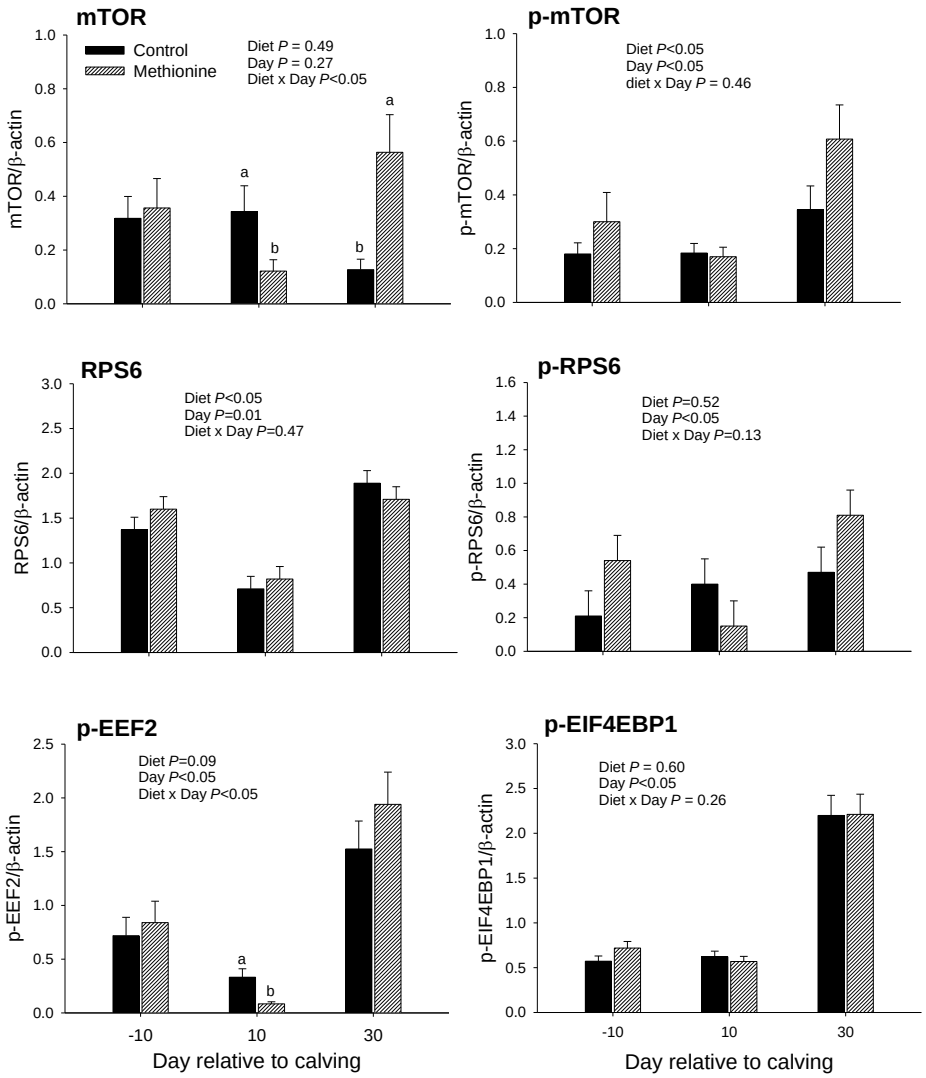

Figure 3.4. Protein abundance (relative to β-actin) of the mechanistic target of rapamycin (MTOR) pathway components mTOR, p-mTOR, p-EIF4EBP1, p-EEF2, RPS6, and p-RPS6 in s.c. adipose tissue harvested at -10, 10, and 30 d relative to parturition. Data are LS means, n = 7 cows per diet, ± pooled SEMs. [ab]Means differ (Diet × Day, $P \leq 0.05$).

REFERENCES

Almilaji, A., T. Pakladok, A. Guo, C. Munoz, M. Föller, and F. Lang. 2012. Regulation of the glutamate transporter EAAT3 by mammalian target of rapamycin mTOR. Biochem. Biophys. Res. Commun. 421:159-163.

Badoud, F., K. P. Lam, A. DiBattista, M. Perreault, M. A. Zulyniak, B. Cattrysse, S. Stephenson, P. Britz-McKibbin, and D. M. Mutch. 2014. Serum and adipose tissue amino acid homeostasis in the metabolically healthy obese. J. Proteome Res. 13:3455-3466.

Batistel, F., A. S. Alharthi, L. Wang, C. Parys, Y.-X. Pan, F. C. Cardoso, and J. J. Loor. 2017a. Placentome nutrient transporters and mammalian target of rapamycin signaling proteins are altered by the methionine supply during late gestation in dairy cows and are associated with newborn birth weight. J. Nutr. 147:1640-1647.

Batistel, F., J. Arroyo, A. Bellingeri, L. Wang, B. Saremi, C. Parys, E. Trevisi, F. Cardoso, and J. Loor. 2017b. Ethyl-cellulose rumen-protected methionine enhances performance during the periparturient period and early lactation in Holstein dairy cows. J. Dairy Sci. 100:7455-7467.

Batistel, F., J. Arroyo, C. Garces, E. Trevisi, C. Parys, M. Ballou, F. Cardoso, and J. Loor. 2018. Ethyl-cellulose rumen-protected methionine alleviates inflammation and oxidative stress and improves neutrophil function during the periparturient period and early lactation in Holstein dairy cows. J. Dairy Sci. 101:480-490.

Bauman, D. E. and W. B. Currie. 1980. Partitioning of nutrients during pregnancy and lactation: a review of mechanisms involving homeostasis and homeorhesis. J. Dairy Sci. 63:1514-1529.

Bell, A. W. and D. E. Bauman. 1997. Adaptations of glucose metabolism during pregnancy and lactation. J. Mammary Gland Biol. Neoplasia. 2:265-278.

Beugnet, A., A. R. Tee, P. M. Taylor, and C. G. Proud. 2003. Regulation of targets of mTOR (mammalian target of rapamycin) signalling by intracellular amino acid availability. Biochem. J. 372(Pt 2):555.

Bradford, B., K. Yuan, J. Farney, L. Mamedova, and A. Carpenter. 2015. Invited review: Inflammation during the transition to lactation: New adventures with an old flame. J. Dairy Sci. 98:6631-6650.

Chimin, P., M. L. Andrade, T. Belchior, V. A. Paschoal, J. Magdalon, A. S. Yamashita, É. Castro, A. Castoldi, A. B. Chaves-Filho, and M. Y. Yoshinaga. 2017. Adipocyte mTORC1 deficiency promotes adipose tissue inflammation and NLRP3 inflammasome activation via oxidative stress and de novo ceramide synthesis. J. Lipid Res. 58:1797-1807.

Chinetti, G., J.-C. Fruchart, and B. Staels. 2000. Peroxisome proliferator-activated receptors (PPARs): nuclear receptors at the crossroads between lipid metabolism and inflammation. Inflammation Res. 49:497-505.

Corl, B., S. Butler, W. Butler, and D. Bauman. 2006. Regulation of milk fat yield and fatty acid composition by insulin. J. Dairy Sci. 89:4172-4175.

De Koster, J., R. K. Nelli, C. Strieder-Barboza, J. de Souza, A. L. Lock, and G. A. Contreras. 2018. The contribution of hormone sensitive lipase to adipose tissue lipolysis and its regulation by insulin in periparturient dairy cows. Sci. Rep. 8:13378.

De Koster, J. D. and G. Opsomer. 2013. Insulin resistance in dairy cows. Vet. Clin. North Am. Food Anim. Pract. 29:299-322.

Drackley, J. K. 1999. Biology of dairy cows during the transition period: The final frontier? J. Dairy Sci. 82:2259-2273.
Drummond, M. J., E. L. Glynn, C. S. Fry, K. L. Timmerman, E. Volpi, and B. B. Rasmussen. 2010. An increase in essential amino acid availability upregulates amino acid transporter expression in human skeletal muscle. Am. J. Physiol. Endocrinol. Metab. 298:E1011-E1018.
Duncan, R. E., M. Ahmadian, K. Jaworski, E. Sarkadi-Nagy, and H. S. Sul. 2007. Regulation of lipolysis in adipocytes. Annu. Rev. Nutr. 27:79-101.
Feller, D. and E. Feist. 1963. Conversion of methionine and threonine to fatty acids by adipose tissue. Can. J. Biochem. Physiol. 41:269-273.
Frayn, K., K. Khan, S. Coppack, and M. Elia. 1991. Amino acid metabolism in human subcutaneous adipose tissue in vivo. Clin. Sci. 80:471-474.
Hay, N. and N. Sonenberg. 2004. Upstream and downstream of mTOR. Genes Dev. 18:1926-1945.
Herman, M. A., P. She, O. D. Peroni, C. J. Lynch, and B. B. Kahn. 2010. Adipose tissue branched-chain amino acid (BCAA) metabolism modulates circulating BCAA levels. J. Biol. Chem. 285:11348-11356.
Jansson, N., F. J. Rosario, F. Gaccioli, S. Lager, H. N. Jones, S. Roos, T. Jansson, and T. L. Powell. 2013. Activation of placental mTOR signaling and amino acid transporters in obese women giving birth to large babies. J. Clin. Endocrinol. Metab. 98:105-113.
Ji, P., J. Osorio, J. Drackley, and J. Loor. 2012. Overfeeding a moderate energy diet prepartum does not impair bovine subcutaneous adipose tissue insulin signal transduction and induces marked changes in peripartal gene network expression1. J. Dairy Sci. 95:4333-4351.
Kaul, G., G. Pattan, and T. Rafeequi. 2011. Eukaryotic elongation factor-2 (eEF2): its regulation and peptide chain elongation. Cell Biochem. Funct. 29:227-234.
Khan, M., A. Hosseini, S. Burrell, S. Rocco, J. McNamara, and J. Loor. 2013. Change in subcutaneous adipose tissue metabolism and gene network expression during the transition period in dairy cows, including differences due to sire genetic merit. J. Dairy Sci. 96:2171-2182.
Krahl, M. 1964. Stimulation of peptide synthesis in adipose tissue by insulin without glucose. Am. J. Physiol. 206:618-620.
Locher, L., S. Häussler, L. Laubenthal, S. Singh, J. Winkler, A. Kinoshita, Á. Kenéz, J. Rehage, K. Huber, and H. Sauerwein. 2015. Effect of increasing body condition on key regulators of fat metabolism in subcutaneous adipose tissue depot and circulation of nonlactating dairy cows. J. Dairy Sci. 98:1057-1068.
Lomax, M. A., G. D. Baird, C. B. Mallinson, and H. Symonds. 1979. Differences between lactating and non-lactating dairy cows in concentration and secretion rate of insulin. Biochem. J. 180:281-289.
Lu, J., G. Xie, W. Jia, and W. Jia. 2013. Insulin resistance and the metabolism of branched-chain amino acids. Front. Med. 7:53-59.
Lynch, C. J. and S. H. Adams. 2014. Branched-chain amino acids in metabolic signalling and insulin resistance. Nat. Rev. Endocrinol. 10:723.
Mackenzie, B. and J. D. Erickson. 2004. Sodium-coupled neutral amino acid (System N/A) transporters of the SLC38 gene family. Pflügers. Archiv. 447:784-795.

McCormack, S. E., O. Shaham, M. A. McCarthy, A. A. Deik, T. J. Wang, R. E. Gerszten, C. B. Clish, V. K. Mootha, S. K. Grinspoon, and A. Fleischman. 2013. Circulating branched-chain amino acid concentrations are associated with obesity and future insulin resistance in children and adolescents. Pediatr. Obes. 8:52-61.

McNamara, J., J. Harrison, R. Kincaid, and S. Waltner. 1995. Lipid metabolism in adipose tissue of cows fed high fat diets during lactation1. J. Dairy Sci. 78:2782-2796.

Newgard, C. B., J. An, J. R. Bain, M. J. Muehlbauer, R. D. Stevens, L. F. Lien, A. M. Haqq, S. H. Shah, M. Arlotto, and C. A. Slentz. 2009. A branched-chain amino acid-related metabolic signature that differentiates obese and lean humans and contributes to insulin resistance. Cell Metab. 9:311-326.

Nicklin, P., P. Bergman, B. Zhang, E. Triantafellow, H. Wang, B. Nyfeler, H. Yang, M. Hild, C. Kung, and C. Wilson. 2009. Bidirectional transport of amino acids regulates mTOR and autophagy. Cell 136:521-534.

National Research Council. 2001. Nutrient requirements of dairy cattle. 7th rev. ed. Natl. Acad. Press, Washington, DC.

Nye, C., J. Kim, S. C. Kalhan, and R. W. Hanson. 2008. Reassessing triglyceride synthesis in adipose tissue. Trends Endocrinol. Metab. 19:356-361.

Osorio, J., P. Ji, J. Drackley, D. Luchini, and J. Loor. 2014a. Smartamine M and MetaSmart supplementation during the peripartal period alter hepatic expression of gene networks in 1-carbon metabolism, inflammation, oxidative stress, and the growth hormone–insulin-like growth factor 1 axis pathways. J. Dairy Sci. 97:7451-7464.

Osorio, J., E. Trevisi, P. Ji, J. Drackley, D. Luchini, G. Bertoni, and J. Loor. 2014b. Biomarkers of inflammation, metabolism, and oxidative stress in blood, liver, and milk reveal a better immunometabolic status in peripartal cows supplemented with Smartamine M or MetaSmart. J. Dairy Sci. 97:7437-7450.

Pessin, J. E. and A. R. Saltiel. 2000. Signaling pathways in insulin action: molecular targets of insulin resistance. J. Clin Invest. 106:165-169.

Phillips, G., T. Citron, J. Sage, K. Cummins, M. Cecava, and J. McNamara. 2003. Adaptations in body muscle and fat in transition dairy cattle fed differing amounts of protein and methionine hydroxy analog. J. Dairy Sci. 86:3634-3647.

Rico, J., V. Bandaru, J. Dorskind, N. Haughey, and J. McFadden. 2015. Plasma ceramides are elevated in overweight Holstein dairy cows experiencing greater lipolysis and insulin resistance during the transition from late pregnancy to early lactation. J. Dairy Sci. 98:7757-7770.

Schwab, C. G. and G. A. Broderick. 2017. A 100-Year Review: Protein and amino acid nutrition in dairy cows. J. Dairy Sci. 100:10094-10112.

Shimomura, Y., M. Obayashi, T. Murakami, and R. A. Harris. 2001. Regulation of branched-chain amino acid catabolism: nutritional and hormonal regulation of activity and expression of the branched-chain α-keto acid dehydrogenase kinase. Curr. Opin. Clin. Nutr. Metab. Care 4:419-423.

Sordillo, L. M. and W. Raphael. 2013. Significance of metabolic stress, lipid mobilization, and inflammation on transition cow disorders. Vet. Clin. North Am. Food Anim. Pract. 29:267-278.

Sumner, J. and J. McNamara. 2007. Expression of lipolytic genes in the adipose tissue of pregnant and lactating Holstein dairy cattle1. J. Dairy Sci. 90:5237-5246.

Utsunomiya-Tate, N., H. Endou, and Y. Kanai. 1996. Cloning and functional characterization of a system ASC-like Na+-dependent neutral amino acid transporter. J. Biol. Chem. 271:14883-14890.
Vailati-Riboni, M., G. Farina, F. Batistel, A. Heiser, M. Mitchell, M. Crookenden, C. Walker, J. Kay, S. Meier, and J. Roche. 2017. Far-off and close-up dry matter intake modulate indicators of immunometabolic adaptations to lactation in subcutaneous adipose tissue of pasture-based transition dairy cows. J. Dairy Sci. 100:2334-2350.
Vailati-Riboni, M., M. Kanwal, O. Bulgari, S. Meier, N. Priest, C. Burke, J. Kay, S. McDougall, M. Mitchell, and C. Walker. 2016. Body condition score and plane of nutrition prepartum affect adipose tissue transcriptome regulators of metabolism and inflammation in grazing dairy cows during the transition period. J. Dairy Sci. 99:758-770.
Vailati Riboni, M., S. Meier, N. Priest, C. Burke, J. Kay, S. McDougall, M. Mitchell, C. Walker, M. Crookenden, and A. Heiser. 2015. Adipose and liver gene expression profiles in response to treatment with a nonsteroidal antiinflammatory drug after calving in grazing dairy cows. J. Dairy Sci. 98:3079-3085.
Wang, X. and C. G. Proud. 2006. The mTOR pathway in the control of protein synthesis. Physiology 21:362-369.
Wullschleger, S., R. Loewith, and M. N. Hall. 2006. TOR signaling in growth and metabolism. Cell 124:471-484.
Zachut, M. 2015. Defining the adipose tissue proteome of dairy cows to reveal biomarkers related to peripartum insulin resistance and metabolic status. J. Proteome Res. 14:2863-2871.
Zachut, M., H. Honig, S. Striem, Y. Zick, S. Boura-Halfon, and U. Moallem. 2013. Periparturient dairy cows do not exhibit hepatic insulin resistance, yet adipose-specific insulin resistance occurs in cows prone to high weight loss. J. Dairy Sci. 96:5656-5669.
Zhai, W., C. Xu, Y. Ling, S. Liu, J. Deng, Y. Qi, C. Londos, and G. Xu. 2010. Increased lipolysis in adipose tissues is associated with elevation of systemic free fatty acids and insulin resistance in perilipin null mice. Horm. Metab. Res. 42:247-253.
Zhou, Z., F. Ferdous, P. Montagner, D. Luchini, M. Corrêa, and J. Loor. 2018. Methionine and choline supply during the peripartal period alter polymorphonuclear leukocyte immune response and immunometabolic gene expression in Holstein cows. J. Dairy Sci. 101:10374-10382.
Zhou, Z., M. Vailati-Riboni, D. N. Luchini, and J. J. Loor. 2016. Methionine and choline supply during the periparturient period alter plasma amino acid and one-carbon metabolism profiles to various extents: Potential role in hepatic metabolism and antioxidant status. Nutrients 9:10.
Zoncu, R., L. Bar-Peled, A. Efeyan, S. Wang, Y. Sancak, and D. M. Sabatini. 2011. mTORC1 senses lysosomal amino acids through an inside-out mechanism that requires the vacuolar H+-ATPase. Science 334:678-683.

CHAPTER 4: BODY CONDITION ALTERS GLUTATHIONE AND NUCLEAR FACTOR ERYTHROID 2-LIKE 2 (NFE2L2)-RELATED ANTIOXIDANT NETWORK ABUNDANCE IN SUBCUTANEOUS ADIPOSE TISSUE OF PERIPARTURIENT HOLSTEIN COWS

-Journal of Dairy Science, 2020, 103, 6439-6453.

ABSTRACT

Dairy cows with high body condition score (BCS) in late-prepartum are more susceptible to oxidative stress (OS). Nuclear factor erythroid 2-like 2 (NFE2L2) is a major antioxidant transcription factor. We investigated the effect of pre-calving BCS on blood biomarkers associated with OS, inflammation, and liver function along with mRNA and protein abundance of targets related to NFE2L2 and glutathione (GSH) metabolism in s.c. adipose tissue (SAT) of periparturient dairy cows. Twenty-two multiparous Holstein cows were retrospectively classified into a high BCS (HBCS; n = 11, BCS ≥ 3.5) or normal BCS (NBCS; n = 11, BCS ≤ 3.17) on d 28 before parturition. Cows were fed a corn silage- and wheat straw-based total mixed ration (TMR) during late prepartum and a corn silage- and alfalfa hay-based TMR postpartum. Blood samples obtained at -10, 7, 15, and 30 d relative to parturition were used for analyses of biomarkers associated with inflammation including albumin, ceruloplasmin, haptoglobin, and myeloperoxidase, and oxidative stress including ferric reducing ability of plasma (FRAP), reactive oxygen species (ROS), and β-carotene. Adipose biopsies harvested at -15, 7, and 30 d relative to parturition were analyzed for mRNA (real-time quantitative PCR) and protein abundance (Western blotting) of targets associated with the antioxidant transcription regulator nuclear factor, erythroid 2 like 2 (NFE2L2) and GSH metabolism pathway. In addition, concentrations of GSH, ROS, and malondialdehyde were measured. HBCS cows had lower prepartum dry matter intake expressed as a percentage of body weight along with greater BCS loss between -4 to 4 wk relative to parturition. Plasma concentrations of ROS and FRAP

increased after parturition regardless of treatment. Compared with NBCS, HBCS cows had greater concentrations of FRAP at d 7 postpartum, which coincided with peak values in those cows. In addition, NBCS cows experienced a marked decrease in plasma ROS after d 7 postpartum, while HBCS cows maintained a constant concentration by d 30 postpartum. Overall ROS concentrations in SAT were greater in HBCS cows. However, overall mRNA abundance of *NFE2L2* was lower and cullin 3 (*CUL3*), a negative regulator of NFE2L2, was greater in HBCS cows. Although HBCS cows had greater overall total protein abundance of NFE2L2 in SAT, ratio of phosphorylated (p)-NFE2L2-to-total NFE2L2 was lower suggesting a decrease in the activity of this antioxidant system. Overall mRNA abundance of the GSH metabolism-related genes: glutathione reductase (*GSR*), glutathione peroxidase 1 (*GPX1*), and transaldolase 1 (*TALDO1*) along with protein abundance of glutathione S-transferase mu 1 (GSTM1) were greater in HBCS cows. Data suggest that HBCS cows might experience greater systemic OS after parturition, while increased abundance of mRNA and protein components of the GSH metabolism pathway in SAT might help alleviate tissue oxidant status. Data underscored the importance of antioxidant mechanisms at the tissue level. Thus, targeting these pathways in SAT during the periparturient period via nutrition might help control tissue remodeling while allowing optimal performance.

Key words: body condition score, oxidative stress, NFE2L2, adipose

INTRODUCTION

Body condition is used to evaluate the degree of apparent adiposity in dairy cows (Roche et al., 2013). High body condition (BCS $\geq$ 3.5) at calving is negatively associated with early lactation DMI and milk yield, and is positively related to the incidence of periparturient metabolic disorders (Roche et al., 2009). For instance, cows calving at a high BCS (**HBCS**) are

more likely to experience fatty liver, subclinical ketosis, and chronic oxidative stress (**OS**) during the transition period (Reid et al., 1986, Bernabucci et al., 2005, Schulz et al., 2014). Despite extensive research on the use of BCS as a management tool and its association with important physiological aspects such as lipid metabolism, insulin resistance, and inflammation (De Koster et al., 2015, Depreester et al., 2018, Newman et al., 2019), molecular mechanisms of oxidative stress associated with BCS in adipose tissue are not well-known.

Nuclear factor erythroid 2-like 2 (**NFE2L2**), considered a master antioxidant transcription factor, plays a critical role against OS damage via regulating a wide range of antioxidant response-dependent genes in mammals (Ma, 2013). Changes in transcription of *NFE2L2* in the liver during the transition period were suggested to play a role in regulating tissue antioxidant response (Gessner et al., 2013). More recent in vitro and in vivo data indicated that activation of NFE2L2 (and its target genes) could serve as a mechanism to maintain oxidant status in the mammary gland (Han et al., 2018a, Han et al., 2018b, Ma et al., 2018). Greater protein abundance of targets associated with the NFE2L2 pathway coupled with elevated plasma malondialdehyde (**MDA**) was reported in s.c. adipose tissue (**SAT**) in cows calving during the summer compared with winter, suggesting this pathway also might be important in coping with oxidative stress in SAT (Zachut et al., 2017). Indeed, an essential role of the NFE2L2 pathway in the antioxidant response in bovine adipose tissue was underscored by a recent in vitro study demonstrating that mild OS led to greater abundance of NFE2L2 at both transcription and translation levels, while severe OS resulted in lower abundance (Sun et al., 2019).

Glutathione (**GSH**) is a well-known antioxidant in cells and contributes to eliminating H_2O_2 within the cytosol, hence, preventing oxidative damage and regulating the thiol-redox status in tissues (Aquilano et al., 2014). A previous study from our group revealed that enhanced

post-ruminal supply of Met, the source of thiol-groups, led to alleviated oxidative stress along with greater mRNA abundance of glutamate-cysteine ligase modifier subunit (***GCLM***), glutathione reductase (***GSR***), and glutathione peroxidase 1 (***GPX1***). The greater activity of various GSH-related antioxidant enzymes in peripartal dairy cow SAT underscored the importance of GSH metabolism and its responsiveness to changes in physiologic state (Batistel et al., 2017, Liang et al., 2019).

Our general hypothesis was that low prepartal BCS leads to the activation of the NFE2L2 pathways ensuing greater GSH synthesis in SAT. The main objective of this study was to investigate changes in mRNA and protein abundance of major components related to the NFE2L2 and GSH pathways in SAT along with plasma and tissue biomarkers of OS in peripartal cows calving at a high or normal BCS.

MATERIALS AND METHODS

Experiment Design

All procedures were conducted under protocols approved by the University of Illinois Institutional Animal Care and Use Committee (Urbana; protocol #17168). BCS was monitored weekly by three individuals from -4 wk to 4 wk relative to expected parturition date, and mean values were used for classifying cows in the current study. Twenty-two clinically healthy multiparous Holstein cows were retrospectively classified into 2 groups: HBCS (3.75 ± 0.25, 3.5 to 4.0; mean ± SD; n = 11) and NBCS (3.07 ± 0.07, 3.0 to 3.17; mean ± SD; n = 11), at d 28 before parturition based on a 5-point scale (Edmonson et al., 1989). The average (mean ± SD) BW at -4 wk relative to parturition was 896 ± 51 kg and 786 ± 48 kg in HBCS and NBCS, respectively. The average for parity (mean ± SD) was 3.5 ± 1.6 in HBCS cows and 3.0 ± 1.1 for NBCS. Cows were fed a corn silage- and wheat straw-based TMR during the late-prepartum

period and a corn silage- and alfalfa hay-based TMR after parturition (Table 4.1). Cows were fed once daily (0600 h) with ad libitum access to the diet. Dry cows were housed in a free-stall barn with an individual Calan gate feeding system (American Calan, Northwood, NH, USA). After calving, cows were housed in a tie-stall barn and milked 3 times daily at approximately 0600, 1400, and 2200 h. Milk production and feed refusals were recorded daily for each cow. Diets were formulated to meet predicted requirements for dairy cows according to NRC (2001).

Feed Sample Collection

Individual ingredients and TMR samples were collected once a week to determine the DM and used to adjust the DM of the TMR accordingly. Weekly samples of ingredients and TMR were frozen at -20 °C and pooled monthly for nutrient composition analysis, as described previously (Batistel et al., 2017). The ingredient and nutrient compositions of the diets fed are reported in Table 4.1.

Blood Collection and Analyses

Blood was obtained from the coccygeal vein before morning feeding on d -10 (± 1 d), 7, 15, and 30 relative to parturition. Samples were collected into vacutainer tubes containing lithium heparin (BD Vacutainer, Becton, Dickinson and Co., Franklin Lakes, NJ) and were immediately placed on ice. Plasma was harvested by centrifugation at 2,000 × *g* for 15 min at 4°C and aliquots stored at −80°C until further analysis. Activities of aspartate aminotransferase (**AST**), γ-glutamyl transpeptidase (**GGT**), alkaline phosphatase, myeloperoxidase and paraoxonase (**PON**), and concentrations of albumin, total bilirubin, total plasma reactive oxygen species (**ROS**), ferric reducing ability of plasma (**FRAP**), haptoglobin, ceruloplasmin, nitric oxide, and nitric oxide metabolites, β-carotene, retinol, and tocopherol were analyzed as described by Lopreiato et al. (2019).

Adipose Tissue Biopsies

Cows in HBCS and NBCS averaged 28 ± 3 d in the close-up dry period. All (i.e., 11/group) were free of clinical disorders and had the full set of biopsies. Tissue was harvested from the tail-head (alternating between the right and left tail head region) at −15 (± 2 d), 7, and 30 d relative to parturition according to previous procedures from our laboratory (Ji et al., 2012). Upon collection, adipose tissue was immediately placed in screw-capped microcentrifuge tubes, snap-frozen in liquid nitrogen, and preserved at −80 °C until further analysis. Health was monitored for 7 d after surgery and surgical clips were removed after 7 d post-biopsy. No antibiotics were administered post-biopsy.

RNA isolation, cDNA Synthesis, and Quantitative PCR

Total RNA isolation was exactly as described in our previous study (Liang et al., 2019). Briefly, total RNA was isolated from 200 mg of adipose tissue using the miRNeasy kit (Qiagen, Hilden, Germany) according to the manufacturer's protocols. The RNA samples were digested with DNaseI and quantification was assessed using a NanoDrop ND-1000 spectrophotometer (Thermo Fisher Scientific, Waltham, MA). The quality of RNA samples was measured using an Agilent 2100 Bioanalyzer (Agilent Technologies, Santa Clara, CA). The quantitative PCR was performed as described previously (Osorio et al., 2014). The internal controls for adipose tissue were ribosomal protein S9 (***RPS9***), ***GAPDH*** and actin beta (***ACTB***). These internal control genes were previously confirmed as suitable for adipose tissue gene expression analysis (Vailati-Riboni et al., 2015, Vailati-Riboni et al., 2016, Vailati-Riboni et al., 2017). Gene symbols and names, quantitative PCR performance, and primer information are reported in Supplemental Table C.1.

Western Blot Analysis

Total protein was extracted from 100 mg adipose tissue using a tissue protein extraction

reagent (catalog no. 78510; Thermo Fisher Scientific) containing Halt protease and phosphatase inhibitor cocktail (100x, catalog no. 78442; Thermo Fisher Scientific). The concentration of total protein was determined using the Pierce BCA protein assay kit (catalog no. 23227; Thermo Fisher Scientific). Details of western blot were reported in a previous study from our group (Liang et al., 2019). Briefly, protein samples were denatured by heating at 95 °C for 5 min before loading 10 µL protein into each lane of a 4-20% SDS-PAGE gel (catalog no. 4561096; Bio-Rad). Reactions were run for 10 min at 180 V, and then for 45 to 60 min at 110 V. Then the protein sample was transferred to the membrane in a Trans-Blot SD Semi-Dry Electrophoretic Transfer Cell (catalog no. 170-3940, Bio-Rad). Membranes were then blocked in 1× Tris-buffered saline (1×TBST) containing 5% nonfat milk for 2 h at room temperature. The membranes were then incubated in TBST containing primary antibodies to glutathione S-transferase mu 1 (**GSTM1**), Kelch-like ECH associated protein 1 (**KEAP1**), extracellular signal-regulated protein kinases 1 and 2 (**ERK1/2**), phospho-ERK1/2(Thr202/Tyr204), NFE2L2, and phospho-NFE2L2(Ser40) (catalog # and dilution ratio are included in Supplemental Table C.2) overnight at 4 °C. The membranes were then washed with 1x TBST and incubated with anti-rabbit HRP-conjugated secondary antibodies (catalog no. 7074S; Cell Signaling Technology, dilution 1:1000). Subsequently, the membranes were washed with 1× TBST and then incubated with ECL reagent (catalog no. 170-5060; Bio-Rad) before image acquisition. Actin beta (catalog no. 4967S; Cell Signaling Technology) was used as the internal control. Images were acquired using the ChemiDOC MP Imaging System (Bio-Rad). The intensities of the bands were measured with Image-Pro Plus 6.0 software. Specific target protein band density values were normalized to β-actin density values. Representative blots are included in Supplemental Figure C.2.

Biomarker Analysis in Subcutaneous Adipose Tissue

As in our previous study (Liang et al., 2019), the following OS biomarkers in SAT were determined using commercial kits according to manufacturer's instructions: ROS (catalog no. STA-347, Cell Biolabs, San Diego, CA), malondialdehyde (**MDA**; catalog no. 10009055; Cayman Chemical), and GSH (catalog no. NWK-GSH01; Northwest Life Science Specialties, Vancouver, WA). Adipose tissue total protein concentration was measured using the Pierce BCA assay kit (catalog no. 23227; Thermo Scientific).

Statistical Analysis

The data were analyzed using the MIXED procedure of SAS v.9.4 (SAS Institute Inc., Cary, NC) according to the following model with repeated measures:

$$Y_{jl} = \mu + M_j + T_l + MT_{jl} + e_{jl},$$

where Y_{jl} = dependent, continuous variable, μ = overall mean, M_j = fixed effect of BCS (j = HBCS vs. NBCS), T_l = fixed effect of Day (for blood biomarkers, -10, 7, 15, and 30 d; for qPCR, western blot, and oxidative stress biomarker in SAT analysis, -15, 7, and 30 d), MT_{jl} = interaction between BCS and Day, and e_{jl} = residual error. Cow, nested within BCS, was the random effect. The Kenward-Roger statement was used for computing the denominator degrees of freedom. The covariance structure of the repeated measurements was spatial power [SP(POW)]. When the interaction was significant, least squares means separation between and within time points was performed using the PDIFF statement with Tukey adjustment. Normality of the residuals was checked with normal probability and box plots, and homogeneity of variances was checked with plots of residuals versus predicted values. Outliers were removed when the absolute value of studentized residual was greater than 2. Significance was declared at $P \leq 0.05$ and tendencies at $P \leq 0.10$.

RESULTS AND DISCUSSION

Body Condition and Animal Performance

HBCS cows had greater BCS compared with NBCS cows from -4 to 4 wk relative to calving date ($P < 0.01$; Figure 4.1). Additionally, HBCS cows had greater BCS loss in comparison with NBCS cows ($P < 0.05$; Figure 4.1). Both prepartum and postpartum DMI did not differ between HBCS and NBCS cows ($P = 0.77$ and $P = 0.89$; Figure 4.2A and C) which is in line with Alharthi et al. (2018) and Pires et al. (2013). However, when expressed as % of BW, NBCS cows had greater prepartum DMI ($P = 0.04$; Figure 4.2 B) and tended to have greater postpartum DMI ($P = 0.09$; Figure 4.2 D). Feed intake and milk yield might play a role in regulating BCS when cows are fed and managed under the same conditions (Rocco and McNamara, 2013). Due to the lack of difference in actual amounts of DMI and milk yield ($P = 0.77$; Figure 4.2 E), DMI as % of BW) seems to be a more reasonable indicator of BCS effects on performance.

Blood Parameters Associated with Inflammation and Oxidative Stress

Compared with the prepartum, plasma ceruloplasmin and haptoglobin concentrations increased after parturition in both HBCS and NBCS cows (Day, $P < 0.01$; Table 4.2, Figure 4.3A and B). However, ceruloplasmin tended to decrease from 7 to 30 d postpartum in NBCS cows, while HBCS cows had an opposite trend (BCS×Day, $P = 0.10$; Figure 4.3A). Overall, plasma myeloperoxidase activity increased between -10 and 15 d around parturition followed by a sudden decrease at 30 d after parturition irrespective of BCS (Day, $P = 0.01$; Figure 4.3C). Regardless of BCS, AST activity and bilirubin concentration (indicators of liver function) were greater after parturition and reached a peak at d 7 (Day, $P < 0.01$; Figure 4.5B and C). Similarly, GGT increased after parturition regardless of BCS (Day, $P < 0.01$; Figure 4.5A).

Acute-phase proteins (**APP**), a critical part of the acute-phase response, include positive APP (i.e. increase during inflammation) such as haptoglobin, ceruloplasmin, and serum amyloid-A and negative APP (i.e. decrease during inflammation) such as albumin, apolipoproteins, retinol-binding protein, and also PON (Ceciliani et al., 2012, Trevisi et al., 2013, Tothova et al., 2014). Through its antimicrobial activity, myeloperoxidase is a critical enzyme in regulating innate immunity (Depreester et al., 2017). Changes in the various APP along with markers of liver function are commonly used to study inflammation status of periparturient cows (Bionaz et al., 2007, Bertoni et al., 2008, Graugnard et al., 2013). Increased ceruloplasmin concentration is associated with inflammation (Cerón et al., 2005), thus, its sharp increase after parturition in HBCS and NBCS cows was suggestive of a greater chronic inflammatory response postpartum (Bionaz et al., 2007, Batistel et al., 2018). However, the subsequent decrease in ceruloplasmin in NBCS cows suggested they experienced a shorter inflammatory period (Figure 4.3A). Although the greater inflammatory status during transition is one adaptive mechanism for dairy cows to cope with acute metabolic changes that occur, a prolonged inflammatory response exacerbates the induction of metabolic disorders (Bradford et al., 2015). Thus, as reported previously (Treacher et al., 1986, Roche et al., 2009), a prolonged inflammatory response in HBCS cows might contribute to greater susceptibility to metabolic disorders.

The lower concentration of plasma ROS prepartum and the increase postpartum (Figure 4.4B) were in agreement with previous studies (Bernabucci et al., 2005, Batistel et al., 2018). The change in ROS between pre and postpartum might have been due to the well-known increases in metabolic rate (Reynolds et al., 2003) along with potential direct effects of free fatty acids (**FFA**) and β-hydroxybutyrate (**BHB**) on circulating immune cells (Lacetera et al., 2005) or the liver (Sun et al., 2019). Overproduction of ROS results in OS and an ensuing inflammatory

response both of which increase the incidence of metabolic disorders (Abuelo et al., 2015). Thus, we speculate that the relative stability of plasma ROS concentration in HBCS cows after d 7 postpartum (unlike the lower plasma ROS level in NBCS cows) denoted a more prolonged inflammatory state, which agrees with some of the plasma biomarkers analyzed.

β-carotene, an important cellular antioxidant, is mainly stored in the adipose tissue (Tourniaire et al., 2009), and not only is the major dietary precursor of vitamin A in dairy cattle but is also a precursor for the synthesis of retinoic acid, a metabolite of vitamin A (LeBlanc et al., 2004, Frey and Vogel, 2011). β-carotene supplementation contributes to reduced risk of mastitis and retained placenta, a response associated with its antioxidant properties (Spears and Weiss, 2008). In humans, obesity is associated with lower β-carotene concentrations in adipocytes (Östh et al., 2014). Although we are unaware if adipose tissue mobilization contributes to the circulating β-carotene level during the transition period, the fact that all-trans retinoic acid supplementation inhibited inflammation in bovine adipocytes challenged with lipopolysaccharide suggests a potentially important indirect effect of this vitamin (Xu et al., 2019). We speculate that maintaining higher concentrations of β-carotene in the circulation, either through supplementation or optimizing DMI, might directly or indirectly contribute to antioxidant status in SAT during the transition period.

Insulin supplementation in culture medium increased β-carotene content in bovine adipose explants while epinephrine decreased it, which suggested that hormones related to lipid metabolism influence β-carotene mobilization from adipose tissue (Arias, 2009). However, BCS does not necessarily impact plasma insulin concentrations (e.g., Alharthi et al., 2018). It is well-recognized that dairy cows experience increased lipolysis during the transition period especially after parturition (Contreras et al., 2018). Intense lipolysis is linked to oxidative stress and

uncontrolled inflammatory responses (Sordillo and Raphael, 2013). In the current study, the postpartal decrease in plasma concentration of β-carotene regardless of BCS was consistent with previous results (Osorio et al., 2014, Batistel et al., 2018). These responses suggest that increased lipolysis along with oxidative stress and enhanced inflammatory response might contribute to lower levels of circulating β-carotene. Thus, without differences in DMI, we speculate that HBCS cows are likely to utilize more circulating β-carotene due to their greater BCS loss. Taken together, the greater overall plasma β-carotene concentrations in NBCS cows might contribute to their reduced inflammatory response.

Similar to concentrations of ROS, FRAP increased after parturition regardless of BCS, and there was a BCS×Day effect ($P < 0.01$) due to a greater response in plasma FRAP on d 7 postpartum in HBCS cows followed by a decrease until 30 d postpartum (Figure 4.4A). These results are consistent with plasma ROS and β-carotene data and support the view that HBCS cows might have experienced greater OS status especially after parturition (Abuelo et al., 2013, Bernabucci et al., 2005). Whether the lipolysis rate in bovine adipose tissue affects β-carotene metabolism and utilization merits further study.

Oxidative Stress Biomarkers in Adipose Tissue

Main effects of BCS, Day, and their interaction on oxidative stress biomarkers are reported in Table 4.3, Figure 4.6, Figure 4.7, and Figure 4.8. HBCS cows had lower overall abundance of *NFE2L2* ($P = 0.03$; Table 4.3). In rodents, *NFE2L2* plays a critical role in the liver in regulating OS via increasing mRNA abundance of key antioxidant enzymes (Ma, 2013). In dairy cows, mRNA abundance of *NFE2L2* was first reported in the liver during the periparturient period (Loor, 2010) and recent studies revealed that *NFE2L2* is also expressed in the mammary gland and SAT (Zachut et al., 2017, Han et al., 2018b, Liang et al., 2019). In vitro, enhanced

activity of NFE2L2 and its target heme oxygenase-1 (**HMOX1**) contributed partly to controlling oxidant status in bovine mammary epithelial cells (**BMEC**) (Ma et al., 2019).

Overall, the concentration of ROS in SAT was greater in HBCS than NBCS cows ($P < 0.01$; Figure 4.6A). Free radicals are essential for normal cellular metabolism, but overproduction without sufficient antioxidant capacity often results in DNA and protein damage and apoptosis (Valko et al., 2007). Reactive oxygen species can activate *NFE2L2* to protect cells from OS damage (Ray et al., 2012). A recent in vitro study reported that an increase in H_2O_2 concentration from 0 to 100 μM upregulated mRNA abundance of *NFE2L2* in bovine adipocytes; however, mRNA abundance of *NFE2L2* decreased when the concentration of H_2O_2 reached 200 μM (Sun et al., 2019). We speculate that the lower overall abundance of *NFE2L2* in HBCS cows (Table 4.3) coupled with greater ROS in SAT were suggestive of diminished capacity of the tissue to mount an antioxidant response.

Studies in rodents have demonstrated that NFE2L2 function is not only important in regulating OS, but also for adipose development and insulin sensitivity (Schneider and Chan, 2013, Seo and Lee, 2013). The latter is particularly important because periparturient cows experience insulin resistance especially early postpartum (Bell and Bauman, 1997, Holtenius et al., 2003, De Koster et al., 2018a), while recent studies demonstrated that AT insulin resistance, especially in over-conditioned cows, develops prepartum (Jaakson et al., 2018). Over-conditioned cows have larger adipocytes in both SAT and omental AT; furthermore, larger adipocytes are more sensitive to lipolytic signals (De Koster et al., 2016). A recent study revealed that BCS loss is positively associated with macrophage infiltration in SAT during early-lactation (De Koster et al., 2018b). The fact that macrophage infiltration leads to overproduction of ROS and inflammatory cytokines in human and rodent AT (Surmi and Hasty, 2010). In the

present study, greater ROS concentration in SAT along with greater BCS loss in HBCS cows led us to speculate that macrophage infiltration might play a role in controlling oxidant status in cows calving at HBCS. The link between NFE2L2 and macrophage infiltration in regulating insulin resistance and adipocyte differentiation as it relates to calving BCS merits further study.

The decrease in plasma ROS after 7 and 15 d postpartum in NBCS and HBCS cows, respectively (Figure 4.4B), is noteworthy because ROS concentration in SAT was relatively steady from -15 d prepartum to 30 d postpartum regardless of BCS (Figure 4.6A). Thus, these data suggest that SAT might take a longer time to recover from OS. Compared with NBCS, HBCS cows had greater overall abundance of cullin 3 (***CUL3***; $P = 0.03$; Table 4.3). Both KEAP1 and CUL3 are inhibitors of NFE2L2 (Suzuki and Yamamoto, 2017), hence, greater abundance of *CUL3* explains at least in part the lower abundance of *NFE2L2* in HBCS cows.

In contrast to mRNA abundance, greater overall protein abundance of NFE2L2 and lower p-NFE2L2/NFE2L2 ratio was observed in HBCS cows ($P < 0.01$ and $P < 0.01$; Figure 4.7A and Figure 4.7C). The difference between mRNA and protein abundance of NFE2L2 suggests that the activity of NFE2L2 is not regulated at the transcription level. In the present study, there was a BCS×Day effect for p-NFE2L2 ($P < 0.01$) due to a decrease in abundance in HBCS cows and an increase in NBCS cows from 7 to 30 d after parturition (Figure 4.7B). These data provide additional support for the idea that OS status increases with time in HBCS cows during the transition period.

Glutathione Metabolism

Main effects of BCS, Day, and their interaction related to GSH metabolism are reported in Table 4.3 and Figure 4.8. The greater overall abundance of genes associated with GSH metabolism including *GXP1*, *GSR* and transaldolase 1 (***TALDO1***) in HBCS cows ($P = 0.02$; $P <$

0.01; P = 0.04; Table 4.3) was surprising in part because those cows had lower abundance of *NFE2L2* (P = 0.03; Table 4.3). Cows in HBCS also had greater overall protein abundance of GSTM1 (P = 0.03; Figure 4.8A). Despite these differences at the transcription and translation levels of GSH metabolism components, there was no difference in tissue GSH concentration (P > 0.05; Figure 4.6B).

Glutathione is a crucial antioxidant in mammalian cells (Aquilano et al., 2014), and the GSH metabolism pathway is one target regulated by NFE2L2 (Harvey et al., 2009). Although GSH metabolism is closely regulated by OS status in non-ruminants (Dickinson and Forman, 2002), other factors such as NF-kB activity (Buelna-Chontal and Zazueta, 2013) and availability of substrates such as Cys, Gly, and Ser impact the pathway (Wu et al., 2004, Lu, 2009). It could be that differences in the rate of mobilization of body protein and differences in DMI to satisfy energy needs determine the availability of AA and other intermediates of the GSH pathway in SAT (Pires et al., 2013, Batistel et al., 2018, Liang et al., 2019). If true, lower availability of AA would lead to decreased mRNA and protein abundance of targets in the GSH metabolism pathway. This idea is partly supported by data from cows fed rumen-protected Met in which a greater DMI was associated with greater mRNA abundance of *GCLM*, *GSR*, and *GPX1* in SAT (Liang et al., 2019). Due to the lack of difference in DMI, we speculate that in the present study GSH metabolism was partly regulated by protein mobilization.

Glutathione peroxidases play a crucial role in scavenging and inactivating hydrogen and lipid peroxides in mammalian cells (Cohen and Hochstein, 1963, Drevet, 2006), and also in controlling the inflammatory response (Bozinovski et al., 2012). Thus, it is commonly accepted that greater GPX activity is a positive indicator of health. However, a study in mice demonstrated that overexpression of *GPX* promotes inflammation in the lung (Bozinovski et al.,

2012). Additionally, decreased GPX activity in mouse adipocytes led to the accumulation of GSH and reduced insulin sensitivity (Kobayashi et al., 2009). Thus, the difference in gene expression of *GPX1* between HBCS and NBCS cows might be associated with inflammatory response and insulin resistance in SAT. Although there are no available data in bovine demonstrating a direct link between GSTM1 and oxidative stress in adipose tissue, dairy cows calving in summer exhibited signs of oxidative stress along with lower s.c. abundance of GSTM1 (Zachut et al., 2017). In human lymphocytes, the absence of *GSTM1* did not lead to abnormal susceptibility to an oxidant challenge in vitro (Onaran et al., 2001). We speculate that increased mRNA and protein abundance of targets associated with GSH metabolism in SAT were adaptive responses in HBCS cows to counteract the negative effect caused by increased ROS concentration. Overall, these data seem to underscore the need for further studies to better understand the mechanistic role of GSH metabolism in bovine adipose tissue.

CONCLUSIONS

Although both HBCS and NBCS cows experience OS and inflammation during the periparturient period, these events are likely more pronounced in cows with HBCS, e.g., they had lower overall plasma β-carotene and ROS concentrations in SAT especially after parturition. Activation of NFE2L2 in SAT might partly explain the reduced inflammatory response in dairy cows with NBCS. The role of GSH metabolism in bovine adipose tissue merits further study.

TABLES AND FIGURES

Table 4.1. Ingredient and nutrient composition of diets fed to Holsten cows with prepartum high (HBCS, BCS ≥ 3.5) or normal body condition score (NBCS, BCS ≤ 3.17) during the close-up (−28d to calving) dry period and early lactation (calving to 30d).

Item	Close-up	Lactation
Ingredient (% of DM)		
Corn silage	37.45	41.18
Ground shelled corn	11.10	23.40
Wheat straw	21.80	2.30
Canola meal	11.66	3.20
Soybean meal	6.30	13.00
Alfalfa hay	-	8.60
Soychlor[1]	3.37	-
Corn gluten	2.80	2.50
ProvAAL2 AADvantage[2]	0.47	0.72
Biotin[3]	0.10	0.08
Rumensin[4]	0.19	0.02
Calcium sulfate	0.53	0.12
Magnesium oxide	0.10	0.12
Ca	0.66	1.00
P	0.33	0.35
Salt	0.10	0.25
Na	0.12	0.45
Cl	0.78	0.68
Mg	0.45	0.38
K	1.36	1.45
S	0.33	0.20
Nutrient composition		
CP, % of DM	14.50	17.00
NDF, % of DM	43.30	21.50
ADF, % of DM	33.80	16.76
aNDFom, % of DM	49.21	27.01
NFC, % of DM	28.22	46.83
NE_L, Mcal/kg of DM	1.37	1.65
NE_L allowable milk, kg/d	-	25.85
MP allowable milk, kg/d	-	28.66
RDP, % of DM	8.45	11.00
RUP, % of DM	6.05	6.00
RDP required, g/d	1,165	1,873
RDP supplied, g/d	1,152	1,995
RDP balance, g/d	-18	122
RUP required, g/	158	1,510
RUP supplied, g/d	821	1,088
RUP balance, g/d	662	-421
MP required, g/d	821	2,404
MP supplied, g/d	1,360	2,041
MP balance, g/d	539	-362

[1]West Central Soy.
[2]Perdue AgriBusiness (Salisbury, MD).
[3]ADM Animal Nutrition (Quincy, IL).
[4]Rumensin, Elanco Animal Health (Greenfield, IN).

Table 4.2. Least square means (n = 11) ± pooled SEMs for plasma biomarkers of inflammation and oxidative stress in Holstein cows with prepartum high (HBCS, BCS ≥ 3.5) or normal body condition score (NBCS, BCS ≤ 3.17).

	Group			*P*-value		
Item	HBCS	NBCS	SEM	BCS	Day	BCS×Day
Inflammation						
Albumin, g/L	36.4	35.3	0.59	0.22	0.40	0.42
Ceruloplasmin, μmol/L	3.21	3.11	0.14	0.59	<0.01	0.10
Haptoglobin, g/L	0.35	0.35	0.03	0.92	<0.01	0.68
Myeloperoxidase, U/L	526	518	15.2	0.71	0.01	0.63
Oxidative stress						
FRAP[1], μmol/L	123	120	3.99	0.66	<0.01	0.02
ROS[2], H_2O_2/100 mL	16.0	15.2	0.50	0.28	<0.01	0.06
NO, μmol/L	26.3	26.4	0.33	0.74	<0.01	0.55
$NO2^-$, μmol/L	3.86	3.57	0.21	0.31	<0.01	0.26
$NO3^-$, μmol/L	21.9	22.5	0.35	0.23	<0.01	0.92
β-Carotene, mg/100 mL	0.17	0.23	0.02	0.08	<0.01	0.29
Retinol, μg/mL	24.9	26.5	2.01	0.58	<0.01	0.64
Tocopherol, μg/mL	2.85	3.18	0.18	0.21	<0.01	0.96
Liver function						
Alkaline phosphatase, U/L	43.9	52.8	4.42	0.13	0.22	0.04
AST[3] ,U/L	102	103	5.85	0.96	<0.01	0.20
GGT[4],U/L	23.5	20.6	1.58	0.18	<0.01	0.26
Paraoxonase, U/L	74.1	69.9	4.06	0.47	<0.01	0.44
Bilirubin, μmol/L	5.03	4.06	0.49	0.13	<0.01	0.22

[1] FRAP= Ferric-reducing ability of plasma.
[2] ROS= Reactive oxygen species.
[3] AST = Aspartate aminotransferase.
[4] GGT = γ-glutamyl transpeptidase.

Table 4.3. Least square means (n = 11) ± pooled SEMs for mRNA abundance related to NFE2L2 pathway and glutathione metabolism in Holstein cows with prepartum high (HBCS, BCS ≥ 3.5) or normal body condition score (NBCS, BCS ≤ 3.17).

	Group				*P*-value		
Gene[1]	HBCS	NBCS	% Difference[2]	SEM	BCS	Day	BCS×Day
NFE2L2 pathway							
NFE2L2	0.90	1.05	-13.5	0.04	0.03	<0.01	0.09
KEAP1	1.22	1.05	16.3	0.08	0.11	0.05	0.49
CUL3	1.54	1.25	22.7	0.10	0.03	<0.01	0.01
Glutathione metabolism							
ME1	0.84	0.75	12.3	0.09	0.45	<0.01	0.32
TALDO1	1.31	1.08	22.0	0.08	0.04	<0.01	0.27
GSR	0.20	0.14	41.1	0.01	<0.01	0.33	0.10
GCLM	0.51	0.51	-0.58	0.04	0.96	0.01	0.51
GPX1	0.79	0.64	22.4	0.05	0.02	0.05	0.23
GCLC	0.86	0.79	9.66	0.05	0.24	0.08	0.23

[1]*NFE2L2*=Nuclear factor, erythroid 2 like 2; *KEAP1*=Kelch-like ECH-associated protein1; *CUL3*=Cullin3; *ME1*= enzyme 1; *TALDO1*= Transaldolase 1; *GSR* =Glutathione reductase; *GCLM* =Glutamate-cysteine ligase modifier s *GPX1*=Glutathione peroxidase 1; *GCLC* =Glutamate-cysteine ligase catalytic subunit.
[2]Difference in mRNA abundance = (HBCS – NBCS)/NBCS × 100.

Figure 4.1. Change in body condition score (BCS) and BCS loss between −4 and 4 wk relative to parturition in Holstein cows with prepartum (28d before expected parturition) high (HBCS, BCS ≥ 3.5) or normal body condition score (NBCS, BCS ≤ 3.17). Data are LS means, n = 11 cows per group, ± pooled SEMs. [ab]Means groups differ ($P \leq 0.05$).

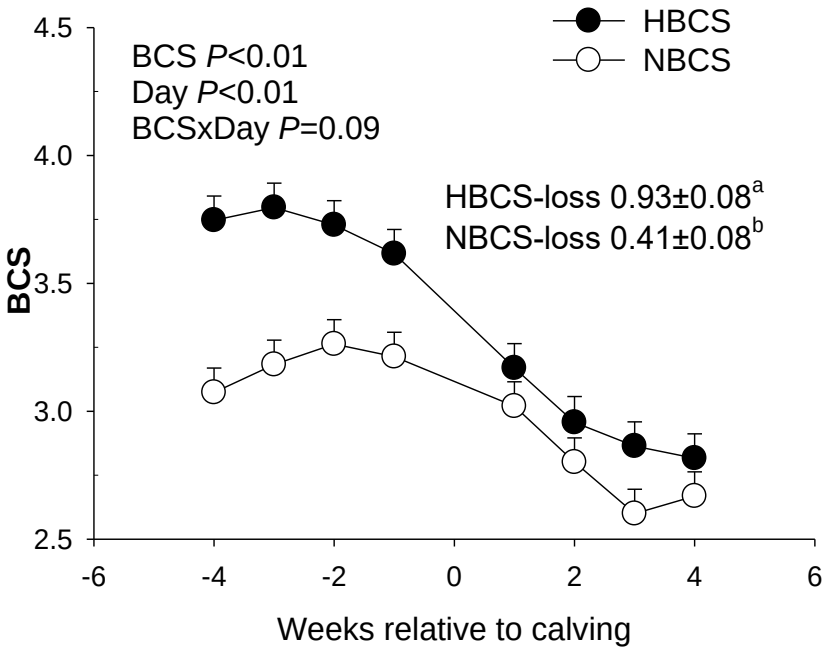

Figure 4.2. Prepartum and postpartum DMI, DMI as % of body weight and milk yield of Holstein cows with prepartum (28d before expected parturition) high (HBCS, BCS ≥3.5) or normal body condition score (NBCS, BCS≤ 3.17) through -30 to 30 d relative to parturition. Data are LS means, n = 11 cows per group, ± pooled SEMs.

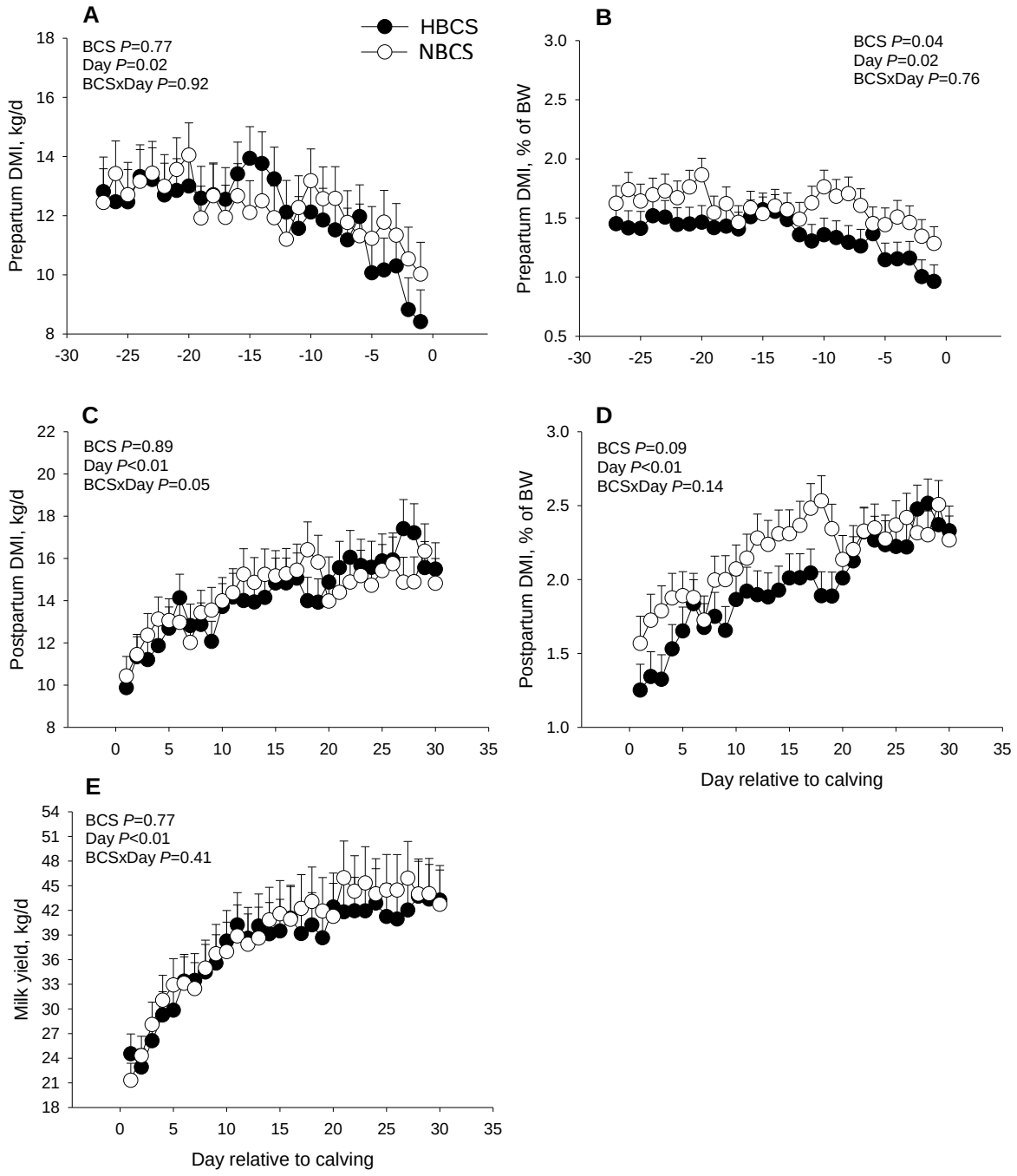

Figure 4.3. Plasma biomarkers of inflammation in Holstein cows with prepartum (28d before expected parturition) high (HBCS, BCS ≥ 3.5) or normal body condition score (NBCS, BCS ≤ 3.17) (panel A= Ceruloplasmin; panel B= Haptoglobin; panel C= Myeloperoxidase). Data are LS means, n = 11 cows per group, ± pooled SEMs. [ab]Means differ (BCS × Day, $P \leq 0.05$).

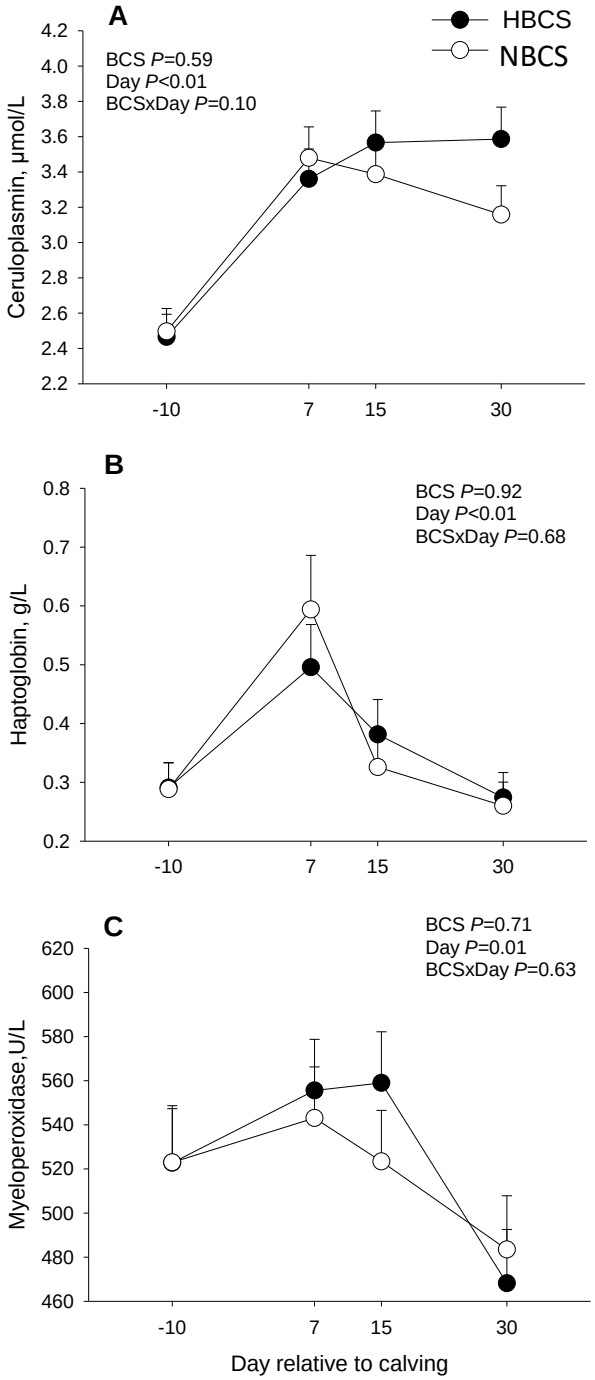

Figure 4.4. Plasma biomarkers of oxidative stress in Holstein cows with prepartum (28d before expected parturition) high (HBCS, BCS ≥ 3.5) or normal body condition score (NBCS, BCS ≤ 3.17) (panel A= FRAP; panel B= ROS; panel C= β-Carotene). FRAP= Ferric-reducing ability of plasma; ROS= Reactive oxygen species. Data are LS means, n = 11 cows per group, ± pooled SEMs. [ab]Means differ (BCS × Day, $P \leq 0.05$).

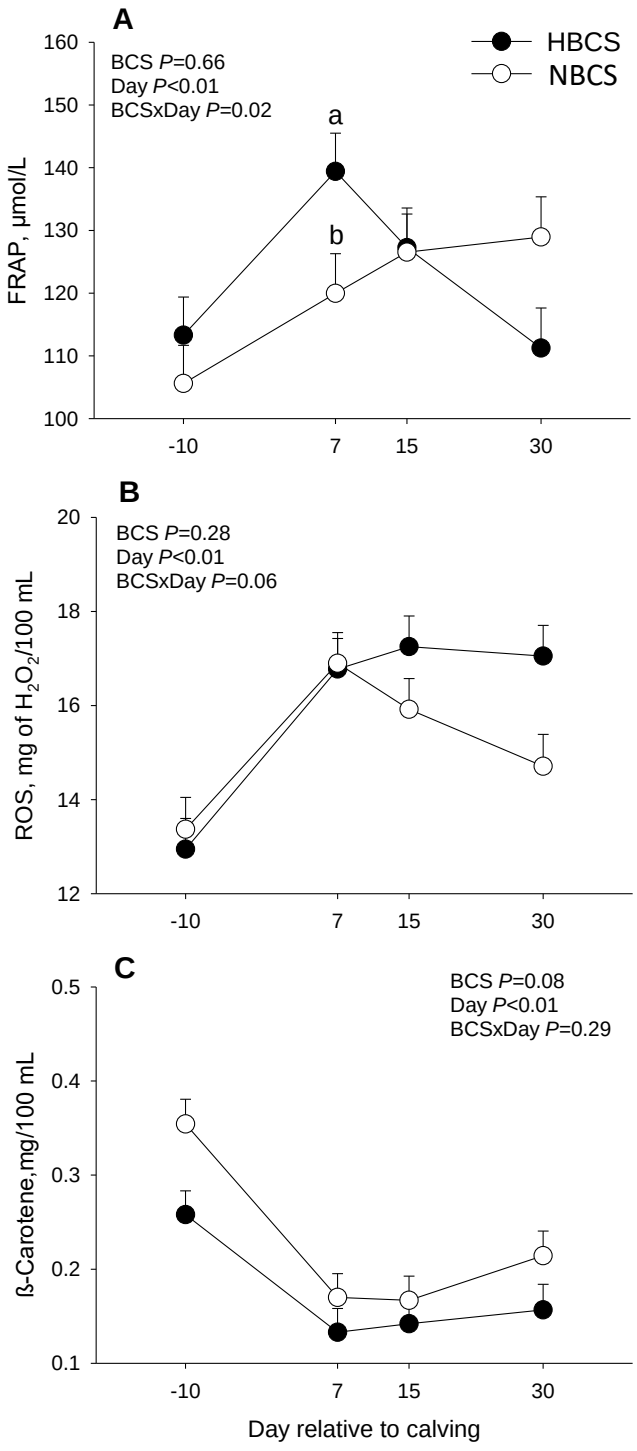

Figure 4.5. Plasma biomarkers of liver function in Holstein cows with prepartum (28d before expected parturition) high (HBCS, BCS ≥ 3.5) or normal body condition score (NBCS, BCS ≤ 3.17) (panel A= GGT; panel B= AST; panel C= Bilirubin). AST = Aspartate aminotransferase; GGT = γ-glutamyl transpeptidase. Data are LS means, n = 11 cows per group, ± pooled SEMs. [ab]Means differ (BCS × Day, $P \leq 0.05$).

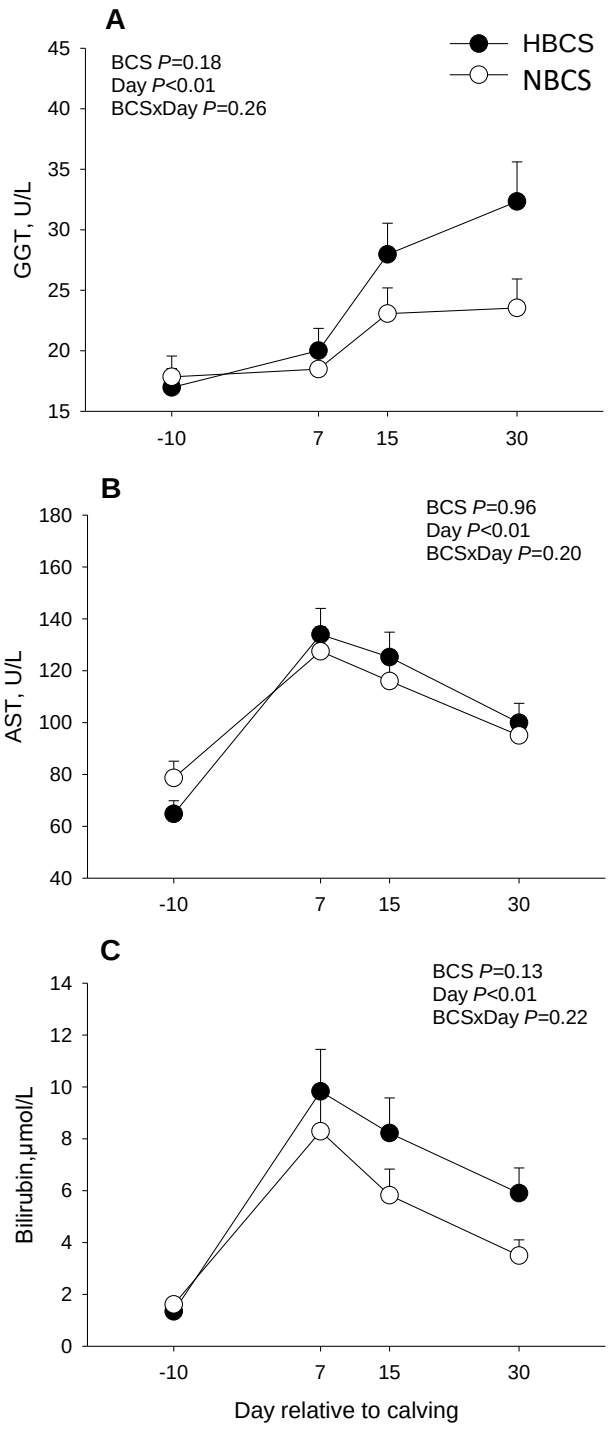

Figure 4.6. Concentrations of reactive oxygen species (ROS) (panel A), glutathione (GSH) (panel B), and malondialdehyde (MDA) (panel C) in SAT of Holstein cows with prepartum (28d before expected parturition) high (HBCS, BCS ≥ 3.5) or normal body condition score (NBCS, BCS ≤ 3.17). Data are LS means, n = 11 cows per group, ± pooled SEMs. [ab]Means differ (BCS × Day, $P \leq 0.05$).

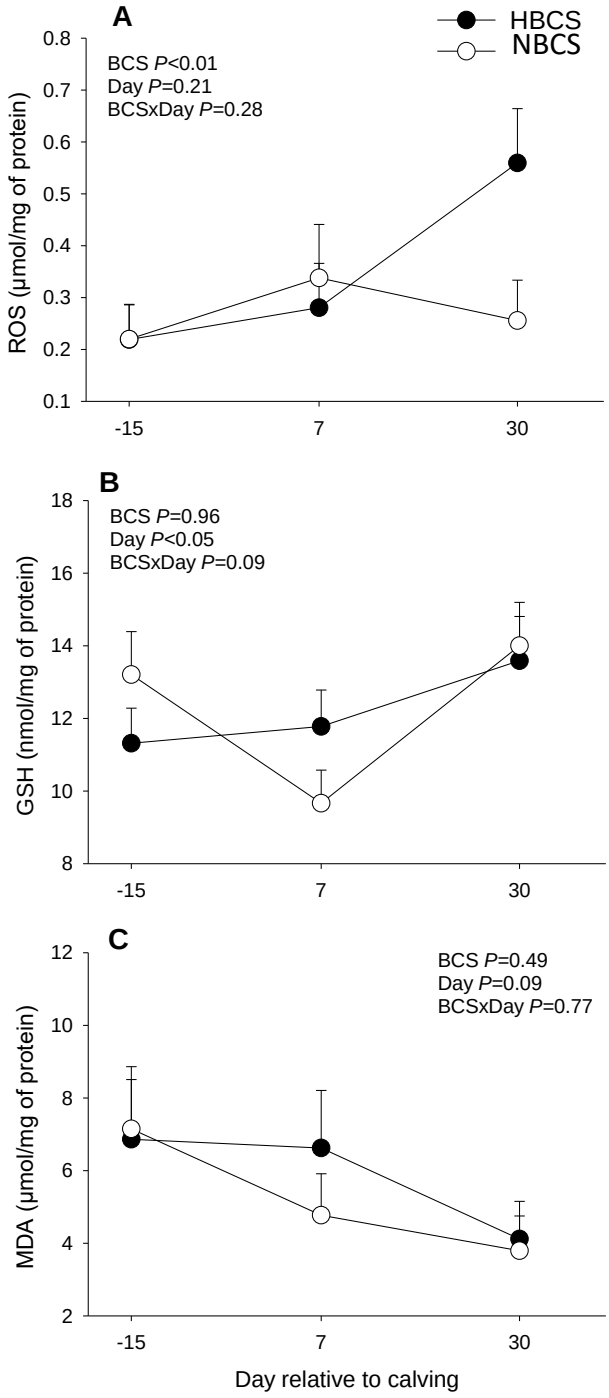

Figure 4.7. Protein abundance (relative to β-actin) of the NFE2L2 (inactive, panel A), p-NFE2L2 (active, panel B), ratio of p-NFE2L2/NFE2L2 (panel C), NFE2L2 repressor KEAP1 (panel D) in SAT of Holstein cows with prepartum (28d before expected parturition) high (HBCS, BCS ≥ 3.5) or normal body condition score (NBCS, BCS ≤ 3.17). Data are LS means, n = 11 cows per group, ± pooled SEMs. [ab]Means differ (BCS × Day, $P \leq 0.05$).

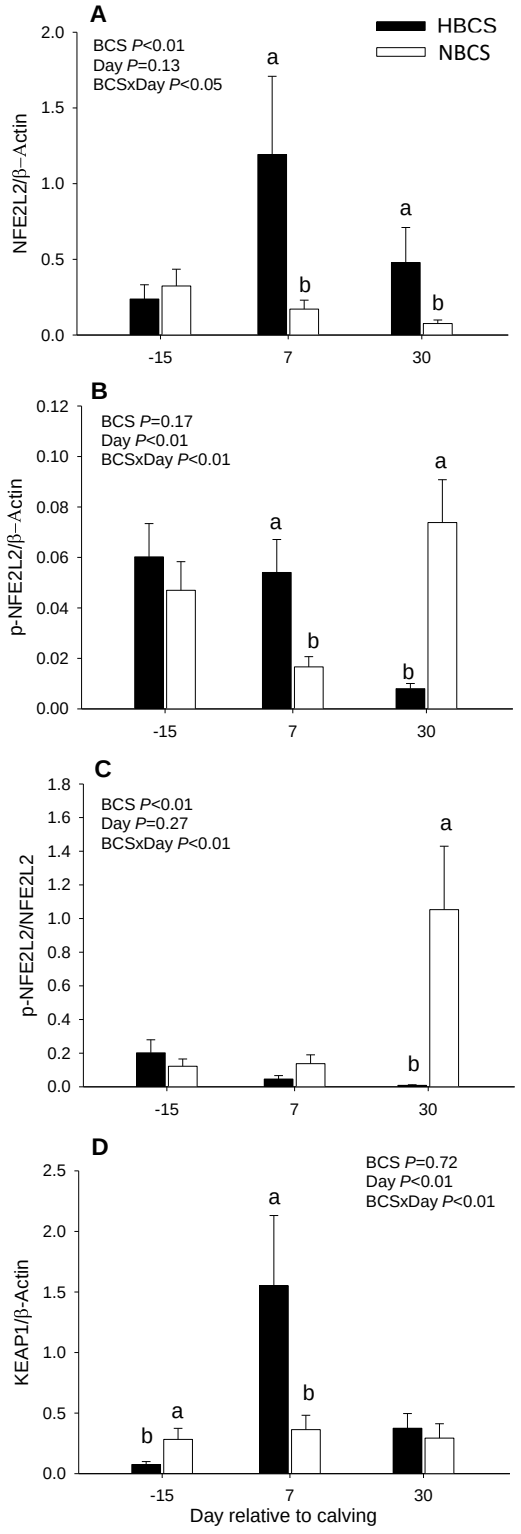

Figure 4.8. Protein abundance (relative to β-actin) of the GSTM1 (panel A), ERK1/2 (inactive, panel B), p-ERK1/2 (active, panel C), ratio of p-ERK1/ERK1/2 (panel D) in SAT of Holstein cows with prepartum (28d before expected parturition) high (HBCS, BCS ≥ 3.5) or normal body condition score (NBCS, BCS ≤ 3.17). Data are LS means, n = 11 cows per group, ± pooled SEMs. [ab]Means differ (BCS × Day, $P \leq 0.05$).

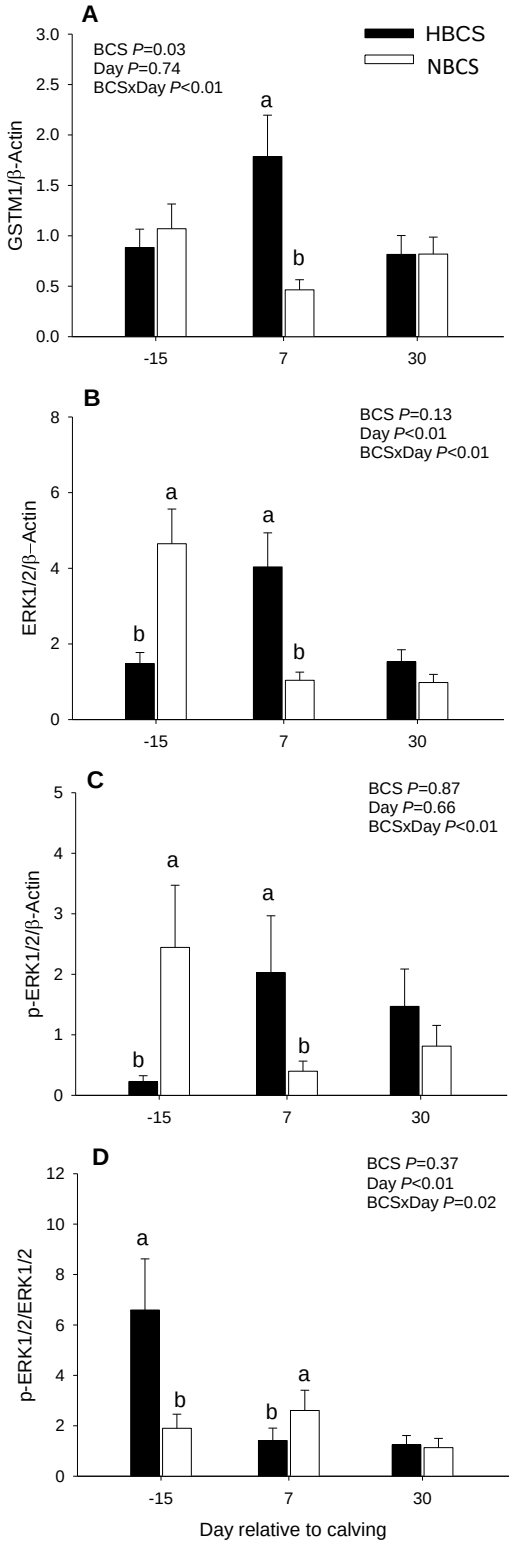

REFERENCES

Abuelo, A., J. Hernández, J. L. Benedito, and C. Castillo. 2013. Oxidative stress index (OSi) as a new tool to assess redox status in dairy cattle during the transition period. Animal 7:1374-1378.

Abuelo, A., J. Hernández, J. L. Benedito, and C. Castillo. 2015. The importance of the oxidative status of dairy cattle in the periparturient period: revisiting antioxidant supplementation. J. Anim. Physiol. Anim. Nutr. 99:1003-1016.

Alharthi, A., Z. Zhou, V. Lopreiato, E. Trevisi, and J. J. Loor. 2018. Body condition score prior to parturition is associated with plasma and adipose tissue biomarkers of lipid metabolism and inflammation in Holstein cows. J. Anim. Sci. Biotechnol. 9:12.

Aquilano, K., S. Baldelli, and M. R. Ciriolo. 2014. Glutathione: new roles in redox signaling for an old antioxidant. Front. Pharmacol. 5:196.

Arias, E., González, A, Shimada, A, Varela-Echavarria, A, Ruiz-López, F, During, A, and Mora, O. 2009. B-Carotene is incorporated or mobilized along with triglycerides in bovine adipose tissue in response to insulin or epinephrine. J. Anim. Physiol. Anim. Nutr. 93:83-93.

Batistel, F., J. Arroyo, A. Bellingeri, L. Wang, B. Saremi, C. Parys, E. Trevisi, F. Cardoso, and J. Loor. 2017. Ethyl-cellulose rumen-protected methionine enhances performance during the periparturient period and early lactation in Holstein dairy cows. J. Dairy Sci. 100:7455-7467.

Batistel, F., J. Arroyo, C. Garces, E. Trevisi, C. Parys, M. Ballou, F. Cardoso, and J. Loor. 2018. Ethyl-cellulose rumen-protected methionine alleviates inflammation and oxidative stress and improves neutrophil function during the periparturient period and early lactation in Holstein dairy cows. J. Dairy Sci. 101:480-490.

Bell, A. W. and D. E. Bauman. 1997. Adaptations of glucose metabolism during pregnancy and lactation. J. Mammary Gland Biol. Neoplasia.2:265-278.

Bernabucci, U., B. Ronchi, N. Lacetera, and A. Nardone. 2005. Influence of body condition score on relationships between metabolic status and oxidative stress in periparturient dairy cows. J. Dairy Sci. 88:2017-2026.

Bertoni, G., E. Trevisi, X. Han, and M. Bionaz. 2008. Effects of inflammatory conditions on liver activity in puerperium period and consequences for performance in dairy cows. J. Dairy Sci. 91:3300-3310.

Bionaz, M., E. Trevisi, L. Calamari, F. Librandi, A. Ferrari, and G. Bertoni. 2007. Plasma paraoxonase, health, inflammatory conditions, and liver function in transition dairy cows. J. Dairy Sci. 90:1740-1750.

Bozinovski, S., H. J. Seow, P. J. Crack, G. P. Anderson, and R. Vlahos. 2012. Glutathione peroxidase-1 primes pro-inflammatory cytokine production after LPS challenge in vivo. PLoS One 7:e33172.

Bradford, B., K. Yuan, J. Farney, L. Mamedova, and A. Carpenter. 2015. Invited review: Inflammation during the transition to lactation: New adventures with an old flame. J. Dairy Sci. 98:6631-6650.

Buelna-Chontal, M. and C. Zazueta. 2013. Redox activation of Nrf2 & NF-κB: A double end sword? Cell Signal. 25:2548-2557.

Ceciliani, F., J. J. Ceron, P. D. Eckersall, and H. Sauerwein. 2012. Acute phase proteins in ruminants. J. Proteomics 75:4207-4231.

Cerón, J. J., P. D. Eckersall, and S. Martínez-Subiela. 2005. Acute phase proteins in dogs and cats: current knowledge and future perspectives. Vet. Clin. Pathol. 34:85-99.
Cohen, G. and P. Hochstein. 1963. Glutathione peroxidase: the primary agent for the elimination of hydrogen peroxide in erythrocytes. Biochem. 2:1420-1428.
Contreras, G. A., C. Strieder-Barboza, and J. De Koster. 2018. Symposium review: Modulating adipose tissue lipolysis and remodeling to improve immune function during the transition period and early lactation of dairy cows. J. Dairy Sci. 101:2737–2752.
De Koster, J., M. Hostens, M. Van Eetvelde, K. Hermans, S. Moerman, H. Bogaert, E. Depreester, W. Van den Broeck, and G. Opsomer. 2015. Insulin response of the glucose and fatty acid metabolism in dry dairy cows across a range of body condition scores. J. Dairy Sci. 98:4580-4592.
De Koster, J., R. K. Nelli, C. Strieder-Barboza, J. de Souza, A. L. Lock, and G. A. Contreras. 2018a. The contribution of hormone sensitive lipase to adipose tissue lipolysis and its regulation by insulin in periparturient dairy cows. Sci. Rep. 8:13378.
De Koster, J., C. Strieder-Barboza, J. de Souza, A. L. Lock, and G. A. Contreras. 2018b. Short communication: Effects of body fat mobilization on macrophage infiltration in adipose tissue of early lactation dairy cows. J. Dairy Sci. 101:7608-7613.
De Koster, J., W. Van den Broeck, L. Hulpio, E. Claeys, M. Van Eetvelde, K. Hermans, M. Hostens, V. Fievez, and G. Opsomer. 2016. Influence of adipocyte size and adipose depot on the in vitro lipolytic activity and insulin sensitivity of adipose tissue in dairy cows at the end of the dry period. J. Dairy Sci. 99:2319-2328.
Depreester, E., E. Meyer, K. Demeyere, M. Van Eetvelde, M. Hostens, and G. Opsomer. 2017. Flow cytometric assessment of myeloperoxidase in bovine blood neutrophils and monocytes. J. Dairy Sci. 100:7638-7647.
Depreester, E., J. De Koster, M. Van Poucke, M. Hostens, W. Van den Broeck, L. Peelman, G. A. Contreras, and G. Opsomer. 2018. Influence of adipocyte size and adipose depot on the number of adipose tissue macrophages and the expression of adipokines in dairy cows at the end of pregnancy. J. Dairy Sci. 101:6542-6555.
Dickinson, D. A. and H. J. Forman. 2002. Cellular glutathione and thiols metabolism. Biochem. Pharmacol. 64:1019-1026.
Drackley, J. K. 1999. Biology of dairy cows during the transition period: The final frontier? J. Dairy Sci. 82:2259-2273.
Drevet, J. R. 2006. The antioxidant glutathione peroxidase family and spermatozoa: a complex story. Mol. Cell. Endocrinol. 250:70-79.
Edmonson, A. J., I. J. Lean, L. D. Weaver, T. Farver, and G. Webster. 1989. A body condition scoring chart for Holstein dairy cows. J. Dairy Sci. 72:68–78.
Frey, S. K. and S. Vogel. 2011. Vitamin A metabolism and adipose tissue biology. Nutrients 3:27-39.
Gessner, D., G. Schlegel, J. Keller, F. Schwarz, R. Ringseis, and K. Eder. 2013. Expression of target genes of nuclear factor E2-related factor 2 in the liver of dairy cows in the transition period and at different stages of lactation. J. Dairy Sci. 96:1038-1043.
Grummer, R. R. 1993. Etiology of lipid-related metabolic disorders in periparturient dairy cows. J. Dairy Sci. 76:3882-3896.
Han, L., F. Batistel, Y. Ma, A. Alharthi, C. Parys, and J. Loor. 2018a. Methionine supply alters mammary gland antioxidant gene networks via phosphorylation of nuclear factor

erythroid 2-like 2 (NFE2L2) protein in dairy cows during the periparturient period. J. Dairy Sci. 101: 8505-8512.
Han, L., Z. Zhou, Y. Ma, F. Batistel, J. Osorio, and J. J. Loor. 2018b. Phosphorylation of nuclear factor erythroid 2-like 2 (NFE2L2) in mammary tissue of Holstein cows during the periparturient period is associated with mRNA abundance of antioxidant gene networks. J. Dairy Sci. 101:6511-6522.
Harvey, C., R. Thimmulappa, A. Singh, D. Blake, G. Ling, N. Wakabayashi, J. Fujii, A. Myers, and S. Biswal. 2009. Nrf2-regulated glutathione recycling independent of biosynthesis is critical for cell survival during oxidative stress. Free Radical Biol. Med. 46:443-453.
Holtenius, K., S. Agenäs, C. Delavaud, and Y. Chilliard. 2003. Effects of feeding intensity during the dry period. 2. Metabolic and hormonal responses. J. Dairy Sci. 86:883-891.
Jaakson, H., P. Karis, K. Ling, A. Ilves-Luht, J. Samarütel, M. Henno, I. Jõudu, A. Waldmann, E. Reimann, and P. Pärn. 2018. Adipose tissue insulin receptor and glucose transporter 4 expression, and blood glucose and insulin responses during glucose tolerance tests in transition Holstein cows with different body condition. J. Dairy Sci.101:752-766..
Jamali Emam Gheise, N., A. Riasi, A. Zare Shahneh, P. Celi, and S. M. Ghoreishi. 2017. Effect of pre-calving body condition score and previous lactation on BCS change, blood metabolites, oxidative stress and milk production in Holstein dairy cows. Ital. J. Anim. Sci.16:474-483.
Ji, P., J. Osorio, J. Drackley, and J. Loor. 2012. Overfeeding a moderate energy diet prepartum does not impair bovine subcutaneous adipose tissue insulin signal transduction and induces marked changes in peripartal gene network expression1. J. Dairy Sci. 95:4333-4351.
Kobayashi, H., M. Matsuda, A. Fukuhara, R. Komuro, and I. Shimomura. 2009. Dysregulated glutathione metabolism links to impaired insulin action in adipocytes. Am. J. Physiol. Endocrinol. Metab. 296:E1326-E1334.
Lacetera, N., D. Scalia, U. Bernabucci, B. Ronchi, D. Pirazzi, and A. Nardone. 2005. Lymphocyte functions in overconditioned cows around parturition. J. Dairy Sci. 88:2010-2016.
LeBlanc, S. J., T. H. Herdt, W. M. Seymour, T. F. Duffield, and K. E. Leslie. 2004. Peripartum serum vitamin E, retinol, and betacarotene in dairy cattle and their associations with disease. J. Dairy Sci. 87:609–619.
Liang, Y., F. Batistel, C. Parys, and J. Loor. 2019. Glutathione metabolism and nuclear factor erythroid 2-like 2 (NFE2L2)-related proteins in adipose tissue are altered by supply of ethyl-cellulose rumen-protected methionine in peripartal Holstein cows. J. Dairy Sci. 102:5530-5541.
Loor, J. 2010. Genomics of metabolic adaptations in the peripartal cow. Animal 4:1110-1139.
Lopreiato, V., Minuti, A., Trimboli, F., Britti, D., Morittu, V.M., Cappelli, F.P., Loor, J.J. and Trevisi, E., 2019. Immunometabolic status and productive performance differences between periparturient Simmental and Holstein dairy cows in response to pegbovigrastim. J. Dairy Sci. 102:9312-9327.
Lu, S. C. 2009. Regulation of glutathione synthesis. Mol. Aspects Med. 30:42-59.
Ma, Q. 2013. Role of nrf2 in oxidative stress and toxicity. Annu. Rev. Pharmacol. Toxicol. 53:401-426.

Ma, Y., Z. Wu, M. Gao, and J. J. Loor. 2018. Nuclear factor erythroid 2-related factor 2 antioxidant response element pathways protect bovine mammary epithelial cells against H_2O_2-induced oxidative damage in vitro. J. Dairy Sci. 101:5329-5344.

Ma, Y. F., L. Zhao, D. N. Coleman, M. Gao, and J. J. Loor. 2019. Tea polyphenols protect bovine mammary epithelial cells from hydrogen peroxide-induced oxidative damage in vitro by activating NFE2L2/HMOX1 pathways. J. Dairy Sci. 102:1658-1670.

National Research Council. 2001. Nutrient requirements of dairy cattle. 7th rev. ed. Natl. Acad. Press, Washington, DC.

Newman, A. W., A. Miller, F. A. Leal Yepes, E. Bitsko, D. Nydam, and S. Mann. 2019. The effect of the transition period and postpartum body weight loss on macrophage infiltrates in bovine subcutaneous adipose tissue. J. Dairy Sci.102:1693-1701.

Onaran, İ., G. Güven, A. Ozaydin, and T. Ulutin. 2001. The influence of GSTM1 null genotype on susceptibility to in vitro oxidative stress. Toxicology 157:195-205.

Östh, M., A. Öst, P. Kjolhede, and P. Strålfors. 2014. The concentration of β-carotene in human adipocytes, but not the whole-body adipocyte stores, is reduced in obesity. PLoS One 9:e85610.

Osorio, J., P. Ji, J. Drackley, D. Luchini, and J. Loor. 2014. Smartamine M and MetaSmart supplementation during the peripartal period alter hepatic expression of gene networks in 1-carbon metabolism, inflammation, oxidative stress, and the growth hormone–insulin-like growth factor 1 axis pathways. J. Dairy Sci. 97:7451-7464.

Pires, J. A. A., C. Delavaud, Y. Faulconnier, D. Pomiès, and Y. Chilliard. 2013. Effects of body condition score at calving on indicators of fat and protein mobilization of periparturient Holstein-Friesian cows. J. Dairy Sci. 96:6423-6439.

Ray, P. D., B.-W. Huang, and Y. Tsuji. 2012. Reactive oxygen species (ROS) homeostasis and redox regulation in cellular signaling. Cell. Signal. 24:981-990.

Reid, I., C. Roberts, R. Treacher, and L. Williams. 1986. Effect of body condition at calving on tissue mobilization, development of fatty liver and blood chemistry of dairy cows. Animal Science 43:7-15.

Reynolds, C., P. Aikman, B. Lupoli, D. Humphries, and D. Beever. 2003. Splanchnic metabolism of dairy cows during the transition from late gestation through early lactation. J. Dairy Sci. 86:1201-1217.

Roche, J. R., N. C. Friggens, J. K. Kay, M. W. Fisher, K. J. Stafford, and D. P. Berry. 2009. Invited review: Body condition score and its association with dairy cow productivity, health, and welfare. J. Dairy Sci. 92:5769-5801.

Roche, J. R., J. K. Kay, N. C. Friggens, J. J. Loor, and D. P. Berry. 2013. Assessing and managing body condition score for the prevention of metabolic disease in dairy cows. Vet. Clin. North Am. Food Anim. Pract. 29:323–336.

Rocco, S. and J. McNamara. 2013. Regulation of bovine adipose tissue metabolism during lactation. 7. Metabolism and gene expression as a function of genetic merit and dietary energy intake. J. Dairy Sci. 96:3108-3119.

Schneider, K. S. and J. Y. Chan. 2013. Emerging role of Nrf2 in adipocytes and adipose biology. Adv. Nutr. 4:62-66.

Schulz, K., J. Frahm, U. Meyer, S. Kersten, D. Reiche, J. Rehage, and S. Dänicke. 2014. Effects of prepartal body condition score and peripartal energy supply of dairy cows on postpartal lipolysis, energy balance and ketogenesis: an animal model to investigate subclinical ketosis. J. Dairy Res. 81:257-266.

Seo, H. and I.-K. Lee. 2013. The role of Nrf2: adipocyte differentiation, obesity, and insulin resistance. Oxid. Med. Cell. Longev. 2013: 184598-184598.
Spears, J. W., and W. P. Weiss. 2008. Role of antioxidants and trace elements in health and immunity of transition dairy cows. Vet. J. 176:70–76.
Sordillo, L. M. and W. Raphael. 2013. Significance of metabolic stress, lipid mobilization, and inflammation on transition cow disorders. Vet. Clin. North Am. Food Anim. Pract. 29:267-278.
Sun, X., X. Li, H. Jia, J. J. Loor, R. Bucktrout, Q. Xu, Y. Wang, X. Shu, J. Dong, and R. Zuo. 2019. Effect of heat-shock protein B7 on oxidative stress in adipocytes from preruminant calves. J. Dairy Sci. 102:5673-5685.
Surmi, B. K. and A. H. Hasty. 2010. The role of chemokines in recruitment of immune cells to the artery wall and adipose tissue. Vascul. Pharmacol. 52:27-36.
Suzuki, T., J. Gao, Y. Ishigaki, K. Kondo, S. Sawada, T. Izumi, K. Uno, K. Kaneko, S. Tsukita, and K. Takahashi. 2017. ER stress protein CHOP mediates insulin resistance by modulating adipose tissue macrophage polarity. Cell reports 18:2045-2057.
Suzuki, T. and M. Yamamoto. 2017. Stress-sensing mechanisms and the physiological roles of the Keap1–Nrf2 system during cellular stress. J. Biol. Chem. 292:16817-16824.
Tothova, C., O. Nagy, and G. Kovac. 2014. Acute phase proteins and their use in the diagnosis of diseases in ruminants: a review. Vet. Med. (Praha) 59:163-80.
Tourniaire, F., E. Gouranton, J. Von Lintig, J. Keijer, M. L. Bonet, J. Amengual, G. Lietz, and J.-F. Landrier. 2009. β-Carotene conversion products and their effects on adipose tissue. Genes Nutr. 4:179.
Treacher, R., I. Reid, and C. Roberts. 1986. Effect of body condition at calving on the health and performance of dairy cows. Animal Science 43:1-6.
Trevisi, E., G. Bertoni, R. Lombardelli, and A. Minuti. 2013. Relation of inflammation and liver function with the plasma cortisol response to adrenocorticotropin in early lactating dairy cows. J. Dairy Sci. 96:5712-5722.
Vailati-Riboni, M., G. Farina, F. Batistel, A. Heiser, M. Mitchell, M. Crookenden, C. Walker, J. Kay, S. Meier, and J. Roche. 2017. Far-off and close-up dry matter intake modulate indicators of immunometabolic adaptations to lactation in subcutaneous adipose tissue of pasture-based transition dairy cows. J. Dairy Sci. 100:2334-2350.
Vailati-Riboni, M., M. Kanwal, O. Bulgari, S. Meier, N. Priest, C. Burke, J. Kay, S. McDougall, M. Mitchell, and C. Walker. 2016. Body condition score and plane of nutrition prepartum affect adipose tissue transcriptome regulators of metabolism and inflammation in grazing dairy cows during the transition period. J. Dairy Sci. 99:758-770.
Vailati Riboni, M., S. Meier, N. Priest, C. Burke, J. Kay, S. McDougall, M. Mitchell, C. Walker, M. Crookenden, and A. Heiser. 2015. Adipose and liver gene expression profiles in response to treatment with a nonsteroidal antiinflammatory drug after calving in grazing dairy cows. J. Dairy Sci. 98:3079-3085.
Valko, M., D. Leibfritz, J. Moncol, M. T. D. Cronin, M. Mazur, and J. Telser. 2007. Free radicals and antioxidants in normal physiological functions and human disease. Int. J. Biochem. Cell Biol. 39:44-84.
Wu, G., Y.-Z. Fang, S. Yang, J. R. Lupton, and N. D. Turner. 2004. Glutathione metabolism and its implications for health. J. Nutr. 134:489-492.

Xu, Q., H. Jia, L. Ma, G. Liu, C. Xu, Y. Li, X. Li, and X. Li. 2019. All-trans retinoic acid inhibits lipopolysaccharide-induced inflammatory responses in bovine adipocytes via TGFβ1/Smad3 signaling pathway. BMC Vet. Res. 15:48.

Zachut, M., G. Kra, L. Livshitz, Y. Portnick, S. Yakoby, G. Friedlander, and Y. Levin. 2017. Seasonal heat stress affects adipose tissue proteome toward enrichment of the Nrf2-mediated oxidative stress response in late-pregnant dairy cows. J. Proteomics 158:52-61.

CHAPTER 5: MOLECULAR NETWORKS OF INSULIN SIGNALING AND AMINO ACID METABOLISM IN SUBCUTANEOUS ADIPOSE TISSUE ARE ALTERED BY BODY CONDITION IN PERIPARTURIENT HOLSTEIN COWS

-Journal of Dairy Science, 2020, 103 (11): 10459-10476.

ABSTRACT

Peripartal cows not only mobilize body fat, but also body protein to satisfy their energy requirements. The objective of this study was to determine the effect of prepartum BCS on blood biomarkers related to energy and nitrogen metabolism, and mRNA and protein abundance associated with AA metabolism and insulin signaling in s.c. adipose tissue (SAT) in peripartal cows. Twenty-two multiparous Holstein cows were retrospectively classified into a high BCS (HBCS; n = 11, BCS ≥ 3.5) or normal BCS (NBCS; n = 11, BCS ≤ 3.17) group at d 28 before expected parturition. Cows were fed the same diet as a total mixed ration (TMR) before parturition and were fed the same lactation diet postpartum. Blood samples collected at -10, 7, 15, and 30 d relative to parturition were used for analyses of biomarkers associated with energy and nitrogen metabolism. SAT biopsies harvested at -15, 7, and 30 d relative to parturition were used for mRNA (RT-PCR) and protein abundance (Western blotting) assays. Data were subjected to ANOVA using the MIXED procedure of SAS, with $P \leq 0.05$ being the threshold for significance. Cows in HBCS had greater overall plasma non-esterified fatty acid (NEFA) concentrations due to marked increases at 7 and 15 d postpartum. This response was similar (BCS × Day effect) to protein abundance of phosphorylated (p) protein kinase B (p-AKT), the insulin-induced glucose transporter (SLC2A4), and the sodium-coupled neutral AA transporter (SLC38A1). Abundance of these proteins was lower at -15 d compared with NBCS cows and either increased (SLC2A4, SLC38A1) or did not change (p-AKT) at 7 d postpartum in HBCS. Unlike protein abundance, however, overall mRNA abundance of the high-affinity cationic (*SLC7A1*), proton-coupled (*SLC36A1*), and sodium-coupled amino acid transporters (*SLC38A2*)

was greater in HBCS than NBCS cows namely due to upregulation in the postpartum phase. Those responses were similar to protein abundance of p-mTOR, which increased (BCS × Day effect) at 7 d in HBCS compared with NBCS cows. mRNA abundance of argininosuccinate lyase (*ASL*) and arginase 1 (*ARG1*) also was greater overall in HBCS cows. Together, these responses suggested impaired insulin signaling coupled with greater postpartum AA transport rate and urea cycle activity in SAT of HBCS cows. An in vitro study using adipocyte and macrophage co-cultures stimulated with various concentrations of fatty acids could provide some insights into the role of immune cells in modulating AT immunometabolic status including insulin resistance and amino acid metabolism.

Key words: body condition, amino acid transporter, urea cycle, insulin resistance, s.c. adipose tissue

INTRODUCTION

Body condition, a subjective assessment of body energy reserves, has important implications for dairy cow management (Bewley and Schutz, 2008; Roche et al., 2013). Compared with cows calving at a normal body condition score (**NBCS**), s.c. adipose tissue (**SAT**) of over-conditioned cows (**HBCS**) has lower mRNA and protein abundance of the insulin receptor along with more pronounced pro-inflammatory responses postpartum (Vailati-Riboni et al., 2016; Zhang et al., 2019). In contrast, mRNA abundance of AA transporters and phosphorylated (**p**) protein kinase B (**AKT**), a key regulator of the insulin signaling pathway, in SAT were greater in response to rumen-protected Met supplementation during the periparturient period (Liang et al., 2019). Thus, available data indicate that enhanced supply of certain AA during the periparturient period could help alleviate insulin resistance in SAT.

Human and rodent studies revealed that insulin resistance and obesity are accompanied by increased circulating levels of branched-chain amino acids (**BCAA**) (Newgard et al., 2009). Compared with muscle, liver, and mammary gland, AT (visceral and s.c.) had the highest mRNA abundance of BCAA transaminase 2, suggesting that dairy cow AT might play a critical role in regulating BCAA catabolism in early lactation (Webb et al., 2019). Furthermore, compared with NBCS (BCS < 3.5) cows before calving, calving at HBCS (BCS >3.75) led to greater abundance of BCAA catabolism-related molecules along with increased circulating concentrations of Leu, Ile, Val, His, Lys, and Orn (Ghaffari et al., 2019a). Altogether, these data suggest a potential relationship among body fatness, i.e. degree of BCS, insulin signaling, and AA metabolism during the peripartal period.

The mechanistic target of rapamycin (**mTOR**), regulated by AA such as Leu, plays a crucial role in cellular growth, differentiation, and protein synthesis (Javed and Fairweather, 2019). Compared with NBCS cows, skeletal muscle of HBCS cows had greater mRNA abundance of *mTOR* and eukaryotic translation initiation factor 4E binding protein 1 (***EIF4EBP1***) without changes in ribosomal protein S6 kinase 1 (***RPS6KB1***) suggesting that BCS is associated with unique mTOR signaling pathway profiles (Ghaffari et al., 2019b). Our previous work indicated that enhanced post-ruminal supply of Met in peripartal cows resulted in greater concentrations of phosphorylated (activated) mTOR (p-mTOR) along with greater protein abundance of the Glu transporter SLC1A3 in SAT (Liang et al., 2019). Although solute carrier family 38 member 1 (**SLC38A1**), a neutral AA transporter, is responsible for Gln transport into cells (Mackenzie and Erickson, 2004), metabolism of Glu also can lead to synthesis of Gln via Gln synthetase (Palmieri et al., 2014). Beyond utilization for synthesis of cellular proteins, a recent study in rat white AT underscored the importance of a functional urea

cycle (Arriarán et al., 2015) in the context of whole-body nitrogen metabolism. For instance, Gln is not only a critical oxidative fuel in cells (e.g., macrophages and neutrophils) but also a precursor for Orn, an important component of the urea cycle (Newsholme et al., 2003). Thus, changes in mRNA and protein abundance of mTOR components and AA transporters in AT might offers clues regarding novel aspects of nitrogen metabolism.

Our general hypothesis was that HBCS is associated with altered abundance of SAT and plasma biomarkers of energy and nitrogen metabolism during the periparturient period. Thus, the main objective of this study was to evaluate changes in mRNA and protein abundance of major components related to insulin signaling, AA transport, and urea cycle in SAT of peripartal cows with high or normal BCS in the late prepartum period.

MATERIALS AND METHODS

Experiment Design

All procedures involving animals were approved by the University of Illinois Institutional Animal Care and Use Committee (Urbana; protocol #17168). Details of the experiment design were reported previously (Liang et al., 2020). Briefly, BCS was determined by three individuals weekly from -4 wk to 4 wk relative to expected calving date, and mean values of BCS were used for classifying cows in the present study. Twenty-two clinically healthy, multiparous Holstein cows were retrospectively classified into HBCS (3.75 ± 0.25, 3.5 to 4.0; mean ± SD; n = 11) and NBCS (3.07 ± 0.07, 3.0 to 3.17; mean ± SD; n = 11) on d 28 before expected parturition date based on a 5-point scale (Edmonson et al., 1989). Dry cows were housed in a free-stall barn with an individual Calan gate feeding system (American Calan, Northwood, NH, USA). After calving, cows were housed in a tie-stall barn. All cows had ad libitum access to a corn silage- and wheat straw-based TMR during the late prepartum period and a corn silage- and alfalfa hay-

based TMR after parturition with free access to water during the entire study. Diets were formulated to meet predicted requirements for dairy cows according to NRC (2001).

Blood Collection and Analyses

Blood obtained from the coccygeal vein before morning feeding, on d -10, 7, 15, and 30 relative to parturition were collected into vacutainer tubes containing lithium heparin (BD Vacutainer, Becton, Dickinson and Co., Franklin Lakes, NJ) and immediately placed on ice. Plasma was harvested by centrifugation at 2,000 × *g* for 15 min at 4 °C, and aliquots were stored at −80 °C until further analysis. Plasma concentrations of glucose, β-hydroxybutyrate (**BHB**), non-esterified fatty acid (**NEFA**), urea, and creatinine were determined following procedures described previously (Bionaz et al., 2007; Trevisi et al., 2012).

Adipose Tissue Biopsies

Cows in HBCS and NBCS averaged 28 ± 3 d in the close-up dry period. All (i.e., 11/group) were free of clinical disorders and had the full set of biopsies. Tissue was harvested from the tail-head (alternating between the right and left tail head region) at −15 (±2 d), 7, and 30 d relative to parturition according to previous procedures from our laboratory (Ji et al., 2012). Briefly, the biopsy site was shaved, disinfected using iodine scrub and 70% alcohol, and anesthetized with 10 mL of 2% lidocaine HCl (VetOne, Boise, ID) prior to blunt dissection with sterile forceps and a scalpel. The incision was then closed with surgical staples (Henry Schein, Melville, NY) and iodine ointment (First Priority, Elgin, IL) was applied to the wound. Upon collection, AT was immediately placed in screw-capped, microcentrifuge tubes, snap-frozen in liquid nitrogen, and preserved at −80 °C until further analysis. Health was monitored for 7 d after surgery and surgical clips were removed after 7 d post-biopsy. No antibiotics were administered post-biopsy.

RNA isolation, cDNA Synthesis, and Quantitative PCR

Total RNA isolation was as reported previously by our laboratory (Liang et al., 2020). Briefly, total RNA was isolated from 200 mg of SAT using the miRNeasy kit (Qiagen, Hilden, Germany) according to the manufacturer's protocols. RNA samples were digested with DNaseI and quantified using a NanoDrop ND-1000 spectrophotometer (Thermo Fisher Scientific, Waltham, MA). Quality of RNA was measured using an Agilent 2100 Bioanalyzer (Agilent Technologies, Santa Clara, CA). Quantitative PCR was as described previously (Osorio et al., 2014). Validated internal controls were ribosomal protein S9 (***RPS9***), ***GAPDH*** and actin beta (***ACTB***) (Vailati-Riboni et al., 2015; Vailati-Riboni et al., 2016; Vailati-Riboni et al., 2017). Target genes and regulators associated with the insulin signaling pathway and nitrogen metabolism were based on previous studies (Takagi et al., 2008; Liang et al., 2019). Gene symbols, names, quantitative PCR performance, and primer information are included in Supplemental Table D.1.

Western Blot Analysis

Approximately 100 mg of frozen SAT were homogenized with a MiniBeadBeater-16 (BioSpec Products, Bartlesville, OK) in 800 µL T-PER reagent (catalog no. 78510; Thermo Fisher Scientific) containing Halt protease and phosphatase inhibitor cocktail (100x, catalog no. 78442; Thermo Fisher Scientific) for 60 s with 1 stainless steel bead (5 mm diameter; catalog no. 69989; Qiagen) and centrifuged at 10,000 × *g* for 15 min at 4 °C. The fat layer was removed and the supernatant was then carefully transferred into 1.5-mL tubes. Total proteins were extracted within 10 mo after sampling. The concentration of total protein was determined using the Pierce BCA protein assay kit (catalog no. 23227; Thermo Fisher Scientific). Details of the Western blot protocol were reported in our previous study (Liang et al., 2019). Briefly, protein samples were

denatured by heating at 95 °C for 5 min before loading 10 µL protein into each lane of a 4-20% SDS-PAGE gel (catalog no. 4561096; Bio-Rad). Reactions were run for 10 min at 180 V, and then run for 45 to 60 min at 110 V. Then protein samples were transferred to a membrane in a Trans-Blot SD Semi-Dry Electrophoretic Transfer Cell (catalog no. 170-3940, Bio-Rad). Membranes were then blocked in 1× Tris-buffered saline (1×TBST) containing 5% nonfat milk for 2 h at room temperature. Membranes were then incubated in TBST containing primary antibodies to mTOR, p-mTOR (Ser2448), AKT, p-AKT(Ser473), solute carrier family 2 member 4 (**SLC2A4**) (formerly GLUT4), solute carrier family 38 member 1 (**SLC38A1**), branched-chain α-keto acid dehydrogenase kinase (**BCKDK**) (Catalog no and dilution ratio were included in Supplemental Table D.2) overnight at 4 °C. Antibodies for mTOR, p-mTOR (Ser2448), AKT, and p-AKT (Ser473) have been used previously in bovine tissues (Appuhamy et al., 2011; Zachut et al., 2013; Mann et al., 2016). SLC2A4, SLC38A1, and BCKDK are predicted to work with cows and their predicted homology in bovine species is 100, 86, and 97%, respectively (https://blast.ncbi.nlm.nih.gov/Blast.cgi). Furthermore, these antibodies were used successfully in our previous work with SAT (Liang et al., 2019). The dilution ratio of each antibody used in the current study was determined from 5 consecutive dilution ratios based on manufacturer's recommendations. Membranes were then washed with 1×TBST and incubated with anti-rabbit HRP-conjugated secondary antibodies (catalog no. 7074S; Cell Signaling Technology, dilution 1:1000). Subsequently, membranes were washed with 1×TBST and then incubated with ECL reagent (catalog no. 170-5060; Bio-Rad) before image acquisition.

Visualized immunoblots were stripped and reprobed for target proteins and β-actin. β-actin is a well-established internal control for bovine AT (Locher et al., 2011; Zachut et al., 2013; Mann et al., 2016), hence, it was chosen (catalog no. 4967S; Cell Signaling Technology)

for our previous (Liang et al., 2019, 2020) and current studies. Images were acquired using the ChemiDOC MP Imaging System (Bio-Rad). The intensities of the bands were measured with Image-Pro Plus 6.0 software. Chemiluminescence signals were determined with at least 5 consecutive exposure times to ascertain the linear range of signal intensity of each antibody to guarantee that quantitative data were obtained. Specific target protein band density values were normalized to β-actin density values. Representative blots are included in Supplemental Figure D.1.

Statistical Analysis

The data were analyzed using the MIXED procedure of SAS v.9.4 (SAS Institute Inc., Cary, NC) according to the following model with repeated measures:

$$Y_{jl} = \mu + M_j + T_l + MT_{jl} + e_{jl},$$

where Y_{jl} = dependent, continuous variable, μ = overall mean, M_j = fixed effect of BCS (j = H-BCS vs. NBCS), T_l = fixed effect of Day (for blood parameter analysis, -10, 7, 15, and 30 d; for q-PCR and Western blot in SAT analysis, -15, 7, and 30 d), MT_{jl} = interaction between BCS and Day, and e_{jl} = residual error. Cow, nested within BCS, was the random effect. The Kenward-Roger statement was used for computing the denominator degrees of freedom. The covariance structure of the repeated measurements was spatial power [SP(POW)]. When the interaction was significant, least squares means separation between and within time points was performed using the PDIFF statement with Tukey adjustment. Normality of the residuals was checked with normal probability and box plots, and homogeneity of variances was checked with plots of residuals versus predicted values. Significance was declared at $P \leq 0.05$ and tendencies at $P \leq 0.10$.

RESULTS AND DISCUSSION

Performance Responses

Production performance was reported previously (Liang et al., 2020). Briefly, both prepartum (12.0 vs. 12.3 kg/d) and postpartum (14.1 vs. 14.2 kg/d) dry matter intake (**DMI**) did not differ between HBCS and NBCS cows ($P > 0.05$); however, when expressed as percentage of BW, HBCS cows had lower prepartum DMI than NBCS (1.36 vs. 1.59; $P < 0.05$). Furthermore, there was no difference in milk yield between HBCS (37.2 kg/d) and NBCS cows (38.2 kg/d) ($P > 0.05$). Additionally, BCS or BCS × Day did not affect milk composition and milk component yields (all $P > 0.05$; Table 5.1) which might partly be attributed to similar actual postpartum DMI between HBCS and NBCS cows.

Body Condition and Metabolic Status

Main effects of BCS, Day, and their interaction on BW changes, and energy and nitrogen metabolism biomarkers in plasma are reported in Figure 5.1 and Figure 5.2. Although there was no effect of BCS or BCS × Day on plasma concentrations of glucose, BHB, cholesterol, and urea (all $P > 0.05$; Figure 5.2A, C, D, and E) which is similar to previous findings (Busato et al., 2002; Zhang et al., 2019), those metabolites exhibited a sharp decrease or increase after parturition (Day, all $P < 0.01$; Figure 5.2A, C, D, and E) which was at least partly caused by decreased DMI and increased milk production. HBCS cows had greater overall plasma NEFA concentration ($P < 0.01$; Figure 5.2B) which agrees with the results of Rico et al. (2015) and Jamali Emam Gheise et al. (2017). NEFA is one of the major indicators of lipomobilization in dairy cows (González et al., 2011). Thus, greater plasma NEFA concentrations in HBCS cows underscored their noticeable fat mobilization during the periparturient period, which is in line with greater BW loss ($P < 0.01$; Figure 5.1). Despite the fact that we did not determine plasma

insulin concentrations in the current study, previous research consistently reported that HBCS cows have similar or greater plasma insulin levels compared with NBCS cows (Dann et al., 2005; Janovick et al., 2011; Pires et al., 2013; Alharthi et al., 2018; Schuh et al., 2019). Additionally, HBCS cows usually experience greater BW losses along with decreased insulin sensitivity in SAT during the periparturient period (Zachut et al., 2013; Rico et al. 2015). Thus, plasma insulin alone is clearly not a "bullet-proof" biomarker for the assessment of insulin sensitivity in SAT.

Plasma creatinine is an index of muscle mobilization and its excretion is proportional to body muscle mass (Ghaffari et al., 2019c; Megahed et al., 2019). Plasma creatinine concentration decreased after parturition irrespective of BCS (Day, $P < 0.01$; Figure 5.2F), which is consistent with the results reported by Ghaffari et al. (2019c) and Pires et al. (2013) indicating that dairy cows mobilize more body protein after parturition to compensate for decreased DMI and increased production energy requirements. Taken together, HBCS cows exhibited greater BW loss and mobilized more body fat to meet energy demands during the transition period. Although no effects due to body condition were detected, dairy cows appeared to mobilize muscle mass postpartum to meet energy requirements for milk production.

Insulin Signaling Components in Subcutaneous Adipose Tissue

Main effects of BCS, Day, and their interaction for components of the insulin signaling pathway are reported in Figure 5.3 and Figure 5.4. Compared with HBCS, NBCS cows had lower overall mRNA abundance of *AKT1* ($P = 0.04$; Figure 5.3A) and greater overall mRNA abundance of insulin receptor substrate 1 (***IRS1***) ($P = 0.02$; Figure 5.3B). In NBCS cows, protein abundance of AKT decreased markedly from -15 to 7 d relative to calving, whereas during the same period, it increased slightly in HBCS cows (BCS × Day, $P < 0.01$; Figure 5.4A). There was

a BCS × Day interaction for protein abundance of SLC2A4 due to decreased protein abundance in NBCS cows and increased protein abundance in HBCS cows from -15 to 7 d relative to parturition ($P < 0.01$; Figure 5.4D). A murine study revealed that silencing peroxisome proliferator-activated receptor-γ (***PPARG***), a key regulator of lipid metabolism and glucose homeostasis, led to reduced SLC2A4 translocation in 3T3-L1 adipocytes (Liao et al., 2007) suggesting that *PPARG* activation contributes to the greater abundance of SLC2A4 in AT. We determined in a previous study that HBCS cows have greater mRNA abundance of *PPARG* in SAT (Vailati-Riboni et al., 2016), a response partly attributed to greater NEFA availability due to more pronounced lipolysis (Bionaz et al., 2013). Thus, we speculate that greater plasma concentrations of NEFA might promote PPARG activation in HBCS cows, subsequently influencing changes in SLC2A4 protein around parturition. Further research is warranted to illustrate the role of *PPARG* in regulating glucose homeostasis in bovine SAT.

Insulin resistance, a key biological adaptation in peripartal cows, channels glucose to the placenta and lactating mammary gland, but if excessive it can lead to greater incidence of metabolic disorders (De Koster and Opsomer, 2013). It is noteworthy that insulin resistance is more severe in SAT than liver during the periparturient period (Zachut et al., 2013), a response underscoring the essential role of SAT as insulin-sensitive tissue in mammals. In AT, insulin binding to the INSR triggers a cascade of events including activation of IRS1 and phosphorylation of AKT (Saltiel and Kahn, 2001). There was a BCS × Day interaction for *INSR* due to greater mRNA abundance in NBCS cows at d 7 postpartum ($P = 0.03$; Figure 5.3C) which is in line with the findings of Zhang et al. (2019). Such response might have been partly responsible for greater activation of AKT (p-AKT/total AKT) at 7 d postpartum ($P < 0.01$; Figure 5.4C). A downregulation of *IRS1* mRNA abundance was observed in murine adipocytes

experiencing insulin resistance (Jager et al., 2007). Thus, the greater mRNA abundance of *IRS1* in NBCS compared with HBCS cows suggests they were more sensitive to insulin.

Although a murine study demonstrated that AKT1 is mainly responsible for protein synthesis and cell survival, and AKT2 is involved in glucose homeostasis (Whiteman et al., 2002), the role of AKT isoforms in bovine is not well-documented (Ji et al., 2012). At least in vitro, both AKT1 and AKT2 can be activated by insulin (Gonzalez and McGraw, 2009) suggesting these 2 isoforms are sensitive to insulin. Furthermore, both in vivo and in vitro studies have verified that cows with greater insulin sensitivity display greater activation of AKT (i.e., p-AKT/total AKT) in SAT (Zachut et al., 2013; Rico et al., 2018). Thus, greater p-AKT/total AKT in NBCS compared with HBCS cows ($P < 0.01$; Figure 5.4C) agrees with both greater mRNA abundance of *IRS1* and lower plasma NEFA and suggests better insulin sensitivity in SAT. These data also agree with the fact that over-conditioned cows exhibit decreased insulin sensitivity and reduced insulin responsiveness during late pregnancy (De Koster et al., 2015). Additionally, overconditioned cows experience a greater degree of lipolysis between late pregnancy and early lactation (Rico et al., 2015), a response partly reflected by the greater BW loss they experience (Zachut et al., 2013). Thus, greater BW loss in HBCS cows after calving corresponds with other markers of insulin sensitivity and lipolysis.

In the context of AT function in the periparturient period, the fact that visceral and SAT have structural and functional differences (Ibrahim, 2010) underscores the need for additional mechanistic data in bovine. For instance, in obese humans and rodents, it is well-established that macrophage infiltration in SAT leads to impaired insulin sensitivity (Kanda et al., 2006). Molecular data at the mRNA and protein level have revealed some differences in metabolism and immune responsiveness among bovine SAT and visceral depots (Ji et al., 2014a; Contreras et

al., 2015; Kenéz et al., 2019). Although there are conflicting reports (Akter et al., 2012; Häussler et al., 2017), recent data indicated that macrophage infiltration occurs in dairy cow SAT during the transition period and is positively associated with body fat mobilization (De Koster et al., 2018; Newman et al., 2019). Thus, HBCS cows might be more prone to macrophage infiltration in SAT contributing to alterations in insulin sensitivity. These data underscore the need for further research, for instance, an in vitro study using adipocyte and macrophage co-cultures challenged with increasing levels of NEFA could expand our understanding of the role of macrophages in modulating tissue insulin sensitivity.

Main effects of BCS, Day, and their interaction of AA transporters and mTOR are reported in Figures 5.5 and 5.6. Compared with NBCS, HBCS cows had greater overall mRNA abundance of sodium-coupled AA transporter (***SLC38A2***), proton-coupled AA transporter (***SLC36A1***) and high-affinity cationic transporter (***SLC7A1***) mainly due to the upregulation postpartum ($P = 0.02$; $P < 0.01$; $P < 0.01$; Figure 5.5 A, B and D). There was a BCS × Day interaction for protein abundance of SLC38A1 due to decreased protein abundance in NBCS cows and increased protein abundance in HBCS cows from -15 to 7 d relative to parturition ($P < 0.01$; Figure 5.6A). This effect was similar to the pattern of SLC2A4. Furthermore, a BCS × Day interaction was observed for protein abundance of p-mTOR due to greater values at 7 d postpartum ($P < 0.01$; Figure 5.6D) in HBCS cows.

Amino acid transporters control uptake and flow across plasma membranes (Closs et al., 2006; Sundberg et al., 2008). For instance, SLC38A2 belonging to AA transport system A transports Asn, His, Ser, Cys, Met, and Gln (Mackenzie and Erickson, 2004; Menchini and Chaudhry, 2019). SLC7A1 plays a key role in Arg metabolism (Wang et al., 2014). SLC36A1 is an efficient carrier of Gly, Pro and Ala (Broer, 2008). An in vivo study in humans demonstrated

that SAT contributes to net Ala and Gln production and Glu uptake during fasting (Frayn et al., 1991). Thus, available data suggest that AA transporters in SAT play an important role during normal tissue metabolism or in response to changes in nutrient supply.

Despite the fact that research related to AA metabolism in bovine SAT is still in its infancy, our recent studies established an association between enhanced post-ruminal supply of Met, greater DMI (Batistel et al., 2017) and plasma Met (Vailati-Riboni et al., 2019), and upregulated mRNA abundance of the AA transporters *SLC38A1*, Glu (***SLC1A1***) and *SLC1A5* in SAT (Liang et al., 2019). Thus, enhanced post-ruminal supply of AA might increase SAT utilization of AA partly through adaptations at the molecular level. Our previous work also confirmed that neutral AA (***SLC1A5***), BCAA (***SLC7A5***), and *SLC38A1* transporters are expressed in bovine SAT (Liang et al., 2019). In addition, compared with liver and skeletal muscle, bovine SAT has the greatest mRNA abundance of the BCAA transporters *SLC1A5* and *SLC7A5*, and branched-chain aminotransferase 2 (Webb et al., 2020). Thus, available data suggest that AA uptake and metabolism in SAT are important aspects of tissue metabolism.

Overall mRNA abundance of *SLC7A5, SLC1A1,* and *SLC1A5* was not affected by BCS ($P = 0.11$, $P = 0.94$, $P = 0.12$; Figure 5.5C, E and F) which is similar to the results reported by Webb et al. (2020), indicating that BCAA uptake in SAT might not be affected by BCS. This is partly supported by the lack of differences in overall plasma BCAA and Glu concentrations (Ghaffari et al., 2019b; Webb et al., 2020). Furthermore, given the fact that SAT might be a major site for BCAA uptake and catabolism (Webb et al., 2019; Webb et al., 2020), the similar overall protein abundance of BCKDK in SAT between HBCS and NBCS cows ($P = 0.09$; Figure 5.6B) coincided with the finding that overall plasma BCAA concentrations are independent of BCS (Webb et al., 2020). Of particular interest, HBCS cows had greater serum/plasma

concentrations of Ile or Leu than NBCS cows on d +21 relative to calving (Ghaffari et al., 2019a; Ghaffari et al., 2019b; Webb et al., 2020).

The fact that HBCS had greater protein abundance of BCKDK at d 7 postpartum, along with plasma data from Ghaffari et al. (2019), provides further support for the notion that SAT might play a critical role in regulating BCAA metabolism. However, we make this conclusion cautiously due to the fact that ruminal microbiota are important contributors of circulating BCAA (Xue et al., 2020). In that context, it is noteworthy that human and rodent studies revealed that gut microbiota associated with BCAA de novo synthesis are enriched in obese individuals and are associated with the development of insulin resistance in mice (Newgard, 2017). Thus, it is plausible that altered circulating BCAA levels in cows with different BCS might be modulated by the gut microbiome. The association between the gut microbiome and plasma BCAA concentrations in peripartal dairy cows merits further study, as it might help elucidate the role of the gut in regulating insulin resistance.

Non-ruminant studies indicate that restriction or underfeeding of dietary protein or AA can also control mRNA abundance of AA transporters in different tissues. For instance, reduced dietary protein supply increased mRNA abundance of *SLC7A1* and *SLC38A2* in the longissimus dorsi of pigs (Wang et al., 2017). Similarly, a low protein diet led to increased mRNA abundance in pig SAT of the AA transporters *SLC7A5* and *SLC38A2* (Li et al., 2016). Challenges to the immune system also alter tissue AA utilization, e.g., the acute-phase response channels AA towards synthesis of acute-phase proteins (**APP**) (Le Floc'h et al., 2004). Although the liver is the key organ where APP are synthesized there is evidence that cow adipose (Saremi et al., 2012) also produces some of the APP. Thus, undersupply of AA or immune challenges associated with parturition can signal upregulation of certain AA transporters. The only difference in

performance we detected was lower prepartal DMI as % BW in HBCS cows, thus, DMI per se cannot explain changes in AA transporters which occurred primarily in the postpartum. It is possible that the greater inflammatory status we detected in HBCS cows (Liang et al., 2020) had an indirect effect on upregulation of AA transporter mRNA abundance in HBCS cows. Further in vitro research using an inflammatory challenge such as hydrogen peroxide (Ma et al., 2019) or lipopolysaccharide (Mukesh et al., 2010) could provide additional information in this regard.

Human studies have demonstrated that hypoxia contributes to insulin resistance and inflammation partly due to dysregulated adipokine production in SAT of obese individuals (Hosogai et al., 2007; Trayhurn, 2013). Adiponectin (**ADIPOQ**), an important adipokine with anti-inflammatory and insulin-sensitizing functions, is primarily derived from white AT, and decreased ADIPOQ concentration in humans leads to tissue inflammation via enhancing lipolysis (Ruan and Dong, 2016). Serum ADIPOQ concentrations in dairy cows are positively related to insulin responsiveness and negatively associated with BCS prepartum (De Koster et al., 2017), indicating that greater BCS mitigates ADIPOQ secretion and potentially impairs insulin resistance. Although we did not measure ADIPOQ, a recent study from our laboratory reported that HBCS (BCS $\geq$ 3.75) compared with NBCS cows (BCS $\leq$ 3.25) had greater overall mRNA abundance of *ADIPOQ* in SAT from -10 to 20 d relative to calving (Alharthi et al., 2018). Thus, it could be possible that HBCS cows in the present study experienced hypoxia and alterations in ADIPOQ production and function. Support for this idea is the fact that feeding a high concentrate diet leading to HBCS was accompanied by greater protein abundance of hypoxia inducible factor 1 α in SAT (Laubenthal et al., 2017). If HBCS cows experienced a state of hypoxia in SAT it could partly explain the postpartal upregulation of *SLC38A1* as reported in murine adipocytes (Horie et al., 2018).

The SLC38A1 protein is one of the major transporters of Gln (Mackenzie and Erickson, 2004). This AA not only serves as crucial oxidative fuel for immune cells such as macrophages and neutrophils (Newsholme et al., 2003) but attenuates inflammation in SAT caused by excessive fat deposition (Petrus et al., 2020). Obese individuals typically have lower Gln concentrations in SAT, which partly explains their susceptibility to macrophage infiltration and pro-inflammatory response (Petrus et al., 2020). It is well-established that dairy cows experience an acute-phase response during early lactation (Bradford et al., 2015), which might be essential for normal immunometabolic functions. The fact that jugular Gln infusion (106 or 212 g/d) in peripartal cows without clinical signs of infectious or inflammatory diseases increased plasma concentrations of serum amyloid A and lipopolysaccharide-binding protein at d 7 after parturition and decreased concentrations of haptoglobin at d 14 and 21 postpartum (Jafari et al., 2006) suggested that post-ruminal Gln supply might contribute to improved immunometabolic status during early lactation; furthermore, lactating cows fed rumen-protected Gln (116 g/d) had greater plasma concentrations of interleukin (***IL***)-10, an anti-inflammatory cytokine (Caroprese et al., 2012), which underscored the role of this AA in the immune response.

As noted above, an increase in macrophage infiltration in SAT during the periparturient period might exacerbate insulin resistance. Thus, along with lower activation of AKT (p-AKT/total AKT) at 7 d postpartum the fact that HBCS compared with NBCS cows experienced a more pronounced inflammatory response particularly after parturition (Liang et al., 2020) suggests that increased protein abundance of SLC38A1 in HBCS cows might have been associated with immune cell infiltration. Thus, we speculate that increased protein abundance of SLC38A1 is an adaptive response to counterbalance prolonged inflammatory status induced during periods of negative energy balance or as a result of excessive fat deposition prepartum.

mTOR Signaling

Differences in BCS had no effect on overall mRNA abundance of *EIF4EBP1* and *RPS6KB1* ($P = 0.92$, $P = 0.95$; Figure 5.3D and E), but a BCS × Day interaction was observed for *EIF4EBP1* due to its greater expression in HBCS cows at d 30 postpartum ($P = 0.04$; Figure 5.3D). This was similar to results observed in bovine skeletal muscle (Gaffari et al., 2019b). Additionally, Gaffari et al. (2019b) reported that mRNA abundance of proteins associated with protein degradation such as ubiquitin-like modifier activating enzyme 1, ubiquitin-conjugating enzyme E2 G1 and atrogin-1 along with *mTOR* was greater on d 21 postpartum in HBCS cows. Thus, those data support the idea that HBCS cows undergo a greater extent of body protein turnover during early lactation.

Amino acids are essential components of the protein synthesis cascade triggered by activation of the mTOR pathway (Laplante and Sabatini, 2009). Besides the well-established role for Leu, Gln and Arg could activate mTOR (Bauchart-Thevret et al., 2010; van der Vos and Coffer, 2012). Beyond protein synthesis, data also indicate that deregulation of the mTOR signaling pathway in non-ruminants is associated with obesity and metabolic disorders (Cai et al., 2016). Although in vivo and in vitro studies in bovine have provided evidence that AA supplementation regulates milk protein synthesis through activation of mTOR (Burgos et al., 2010; Rius et al., 2010; Appuhamy et al., 2012) less is known for adipose tissue. A previous study from our group revealed that enhanced post-ruminal supply of Met during the periparturient period enhanced mRNA abundance of AA transporters and protein abundance of p-mTOR in SAT (Liang et al., 2019), a response that correlated with lower oxidative stress and inflammation status (Batistel et al., 2018). Thus, we speculate that the greater mRNA abundance of *SLC7A1* and *SLC38A2* in HBCS cows might have contributed to the increased protein

abundance of p-mTOR. Overall, data suggest that enhanced mRNA abundance of AA transporters and upregulated p-mTOR are part of an adaptive mechanism in HBCS cows to cope with peripartal oxidative stress and inflammation. Research with adipose tissue or cells exposed to oxidants could help shed light on this idea.

Amino Acid Metabolism, the Urea Cycle, and Inflammation

Main effects of BCS, Day, and their interaction on mRNA abundance of key enzymes of the urea cycle are reported in Figure 5.7. Abundance of arginase 1 (***ARG1***) and argininosuccinate lyase (***ASL***) was greater overall in HBCS cows ($P = 0.05$; $P = 0.03$; Figure 5.7A and C), suggesting a greater degree of urea cycle activity in those cows. Although it is well-established that the urea cycle in mammals is confined to the liver (Cynober et al., 1995), a previous study demonstrated that rat SAT contains a complete set of urea cycle enzymes: argininosuccinate synthase (***ASS1***), ASL, and ARG1 (Arriarán et al., 2015). Thus, available data suggest that AT plays a role in regulating Arg metabolism (Cynober et al., 1995), potentially via Cit synthesis (Arriarán et al., 2015). Greater overall mRNA abundance of *ARG1* and *ASL* in HBCS cows did not accompany greater plasma urea concentrations. Additionally, except for increased *ASS1* postpartum (Day, $P < 0.01$; Figure 5.7B), day relative to calving did not have an effect on mRNA abundance of *ARG1* and *ASL* ($P = 0.22$, $P = 0.18$; Figure 5.7A and C), which is inconsistent with decreased plasma urea concentrations after parturition (Day, $P < 0.01$; Figure 5.2E). Thus, results suggest that the urea cycle in SAT might not make a great contribution to the circulating levels of urea.

Arginase not only hydrolyzes Arg to Orn and urea but also regulates nitric oxide (**NO**) synthesis through competition with endothelial NO synthase for Arg (Durante, 2013). Activation of ARG and the reduction in NO synthesis can increase inflammation in non-ruminants (Durante,

2013). In contrast, both in vivo and in vitro data from rats indicated that ARG inhibition reduced macrophage infiltration and pro-inflammatory cytokine production (Hu et al., 2015). Although speculative, the upregulation of the Arg transporter *SLC7A1* in HBCS cows might partly explain the increased mRNA abundance of *ASL* and *ARG1*, but also macrophage infiltration that could trigger a local inflammatory response. Thus, we speculate that an important role for a functional urea cycle in SAT is to control inflammation, especially in overconditioned cows. This idea is supported in part by the greater mRNA abundance of toll-like receptor 4 (***TLR4***) and *TLR9* in SAT of peripartal HBCS (BCS ≥ 3.75) cows reported by Alharthi et al. (2018).

Our group was the first to report the immune-responsiveness of dairy cow SAT (Mukesh et al., 2010) and subsequently catalog differences in mRNA abundance of immune-related genes in various fat depots in response to control or higher-energy diets (Ji et al., 2014b; Moisa et al., 2017; Minuti et al., 2020). More recently, a positive association between mRNA abundance of leptin, *IL-6*, and tumor necrosis factor in SAT with adipocyte size was reported (Depreester et al., 2018). In the context of inflammatory responsiveness of AT, such a relationship was particularly important because adipocyte size increases with BCS (De Koster et al., 2016). Thus, the greater macrophage counts in SAT from cows losing more body mass postpartum (Newman et al., 2019) along with the greater loss of BW and BCS we detected in HBCS cows underscore the greater susceptibility to a chronic state of inflammation (Contreras et al., 2015). The exact molecular mechanisms whereby AA metabolism and urea cycle activity regulate SAT immune responsiveness remains to be established.

CONCLUSIONS

Overconditioning during late-prepartum leads to lower activation of AKT (p-AKT/total AKT) and more pronounced lipolysis postpartum; however, adipose tissue in overconditioned

cows might trigger compensatory mechanisms leading to upregulation of AA transport and activation of mTOR signaling. Thus, beyond use of AA for protein synthesis, adipose tissue of overconditioned cows seems to utilize AA to alleviate negative effects caused by a prolonged inflammatory response. Urea cycle activity, in particular, seems to be important in the context of inflammation in overconditioned cows. Further research is warranted to ascertain the potential roles of AA such as Met, Arg, Gln, and Glu in SAT in the context of physiological challenges that lead to inflammation and oxidative stress.

TABLE AND FIGURES

Table 5.1. Milk composition and milk component yields in Holstein cows with prepartum (28 d before expected parturition) high (HBCS, BCS ≥ 3.5) or normal body condition score (NBCS, BCS ≤ 3.17) during the first 4 wk postpartum. Data are LS means, n = 11 cows per group, ± pooled SEMs.

Milk composition	BCS group		SEM	*P*-value		
	HBCS	NBCS		BCS	Day	BCS×Day
Protein, %	2.95	3.08	0.08	0.23	<0.01	0.34
Protein, kg/d	1.19	1.22	0.13	0.90	0.39	0.61
Fat, %	3.25	3.35	0.40	0.87	0.36	0.10
Fat, kg/d	1.15	1.31	0.12	0.34	0.15	0.08
Lactose, %	4.78	4.85	0.05	0.24	0.02	0.11
Lactose, kg/d	1.96	1.99	0.17	0.90	<0.01	0.95

Figure 5.1. Change in body weight (BW) and BW loss (kg) between −4 and 4 wk relative to parturition in Holstein cows with prepartum (28 d before expected parturition) high (HBCS, BCS ≥ 3.5) or normal body condition score (NBCS, BCS ≤ 3.17). Data are LS means, n = 11 cows per group, ± pooled SEMs. Asterisk indicates that means differ (BCS × Day, $P \leq 0.05$) between groups (HBCS and NBCS). [ab]Means groups differ ($P \leq 0.05$).

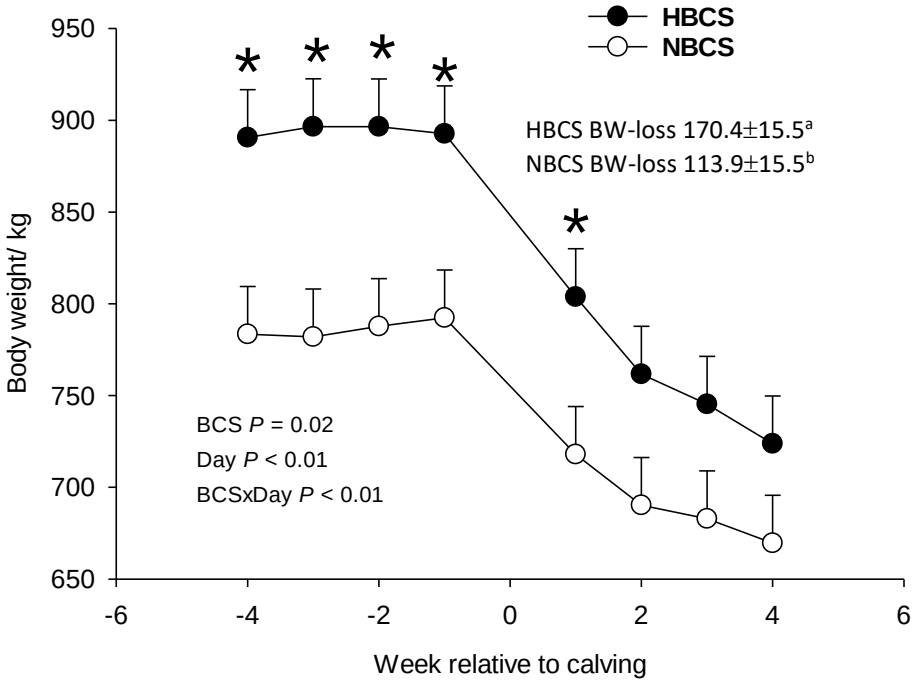

Figure 5.2. Plasma biomarkers of energy and nitrogen metabolism at -10, 7, 15 and 30 d relative to calving in Holstein cows with prepartum (28 d before expected parturition) high (HBCS, BCS ≥ 3.5) or normal body condition score (NBCS, BCS ≤ 3.17). Data are LS means, n = 11 cows per group, ± pooled SEMs.

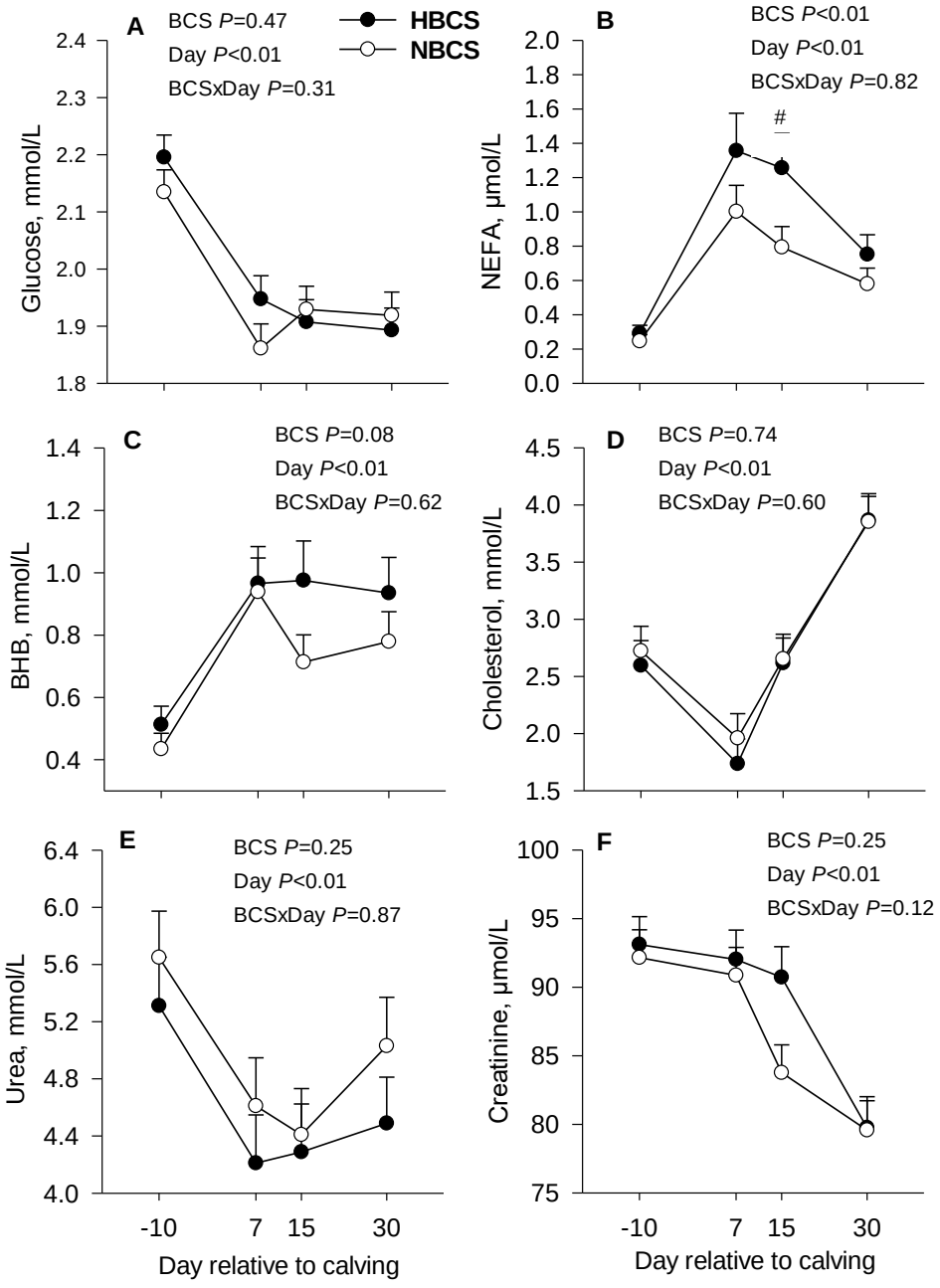

Figure 5.3. mRNA abundance of genes related to the mammalian target of rapamycin (mTOR) and insulin signaling pathways in s.c. adipose tissue of Holstein cows with prepartum (28 d before expected parturition) high body condition score (HBCS, BCS ≥3.5) and normal body condition score (NBCS, BCS ≤ 3.17) at -15, 7 and 30 d relative to calving. Data are LS means, n = 11 cows per group, ± pooled SEMs. * Means differ (BCS × Day, $P \leq 0.05$) between groups (HBCS and NBCS).

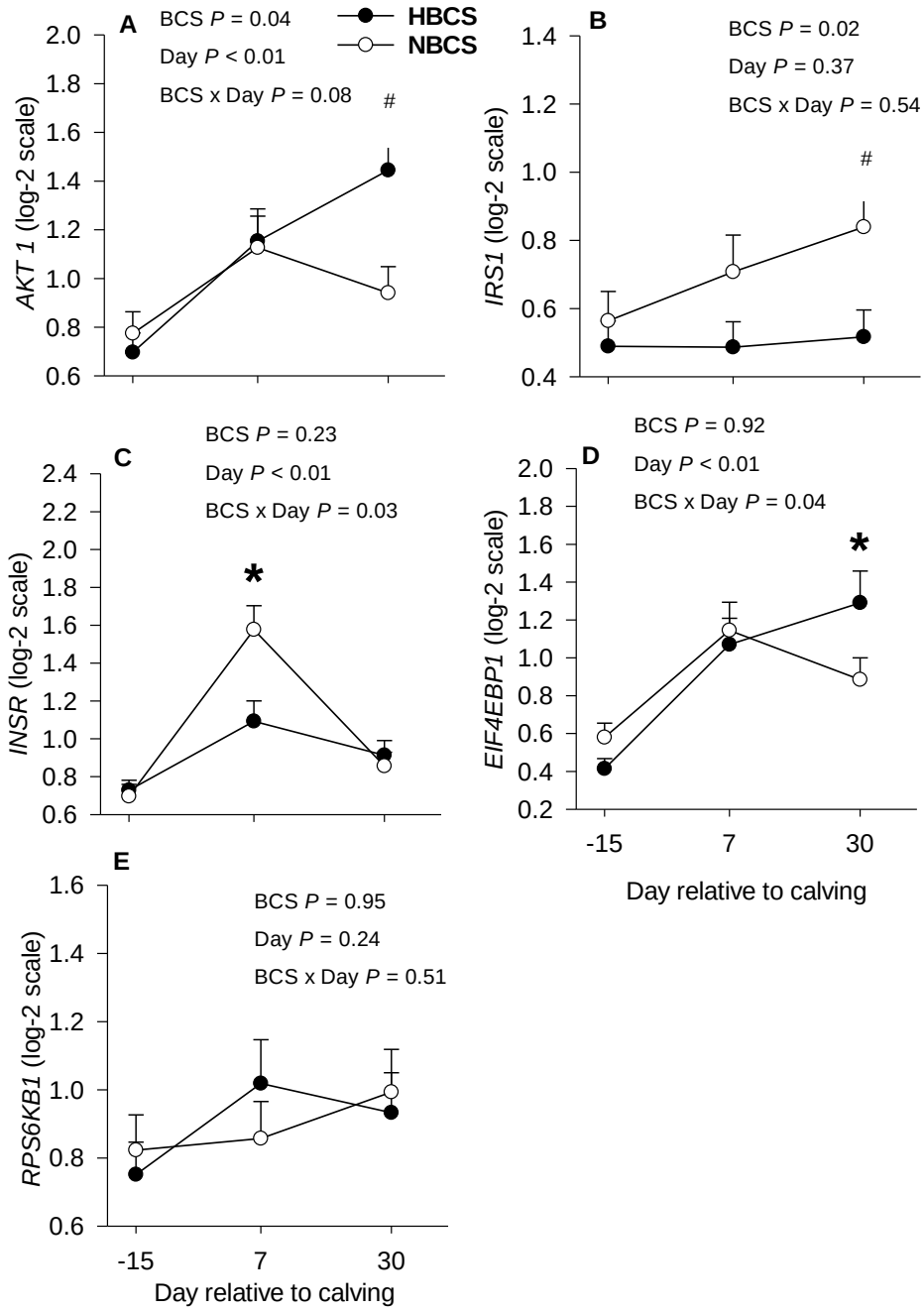

Figure 5.4. Protein abundance (relative to β-actin) of the AKT (total, panel A), p-AKT (active, panel B), ratio of p-AKT/AKT (panel C) and SLC2A4 (panel D) in s.c. adipose tissue of Holstein cows with prepartum (28 d before expected parturition) high (HBCS, BCS ≥ 3.5) or normal body condition score (NBCS, BCS ≤ 3.17) at -15, 7 and 30 d relative to calving. AKT = protein kinase B; SLC2A4 = Glucose transporter 4. Data are LS means, n = 11 cows per group, ± pooled SEMs. [ab]Means differ (BCS × Day, $P \leq 0.05$).

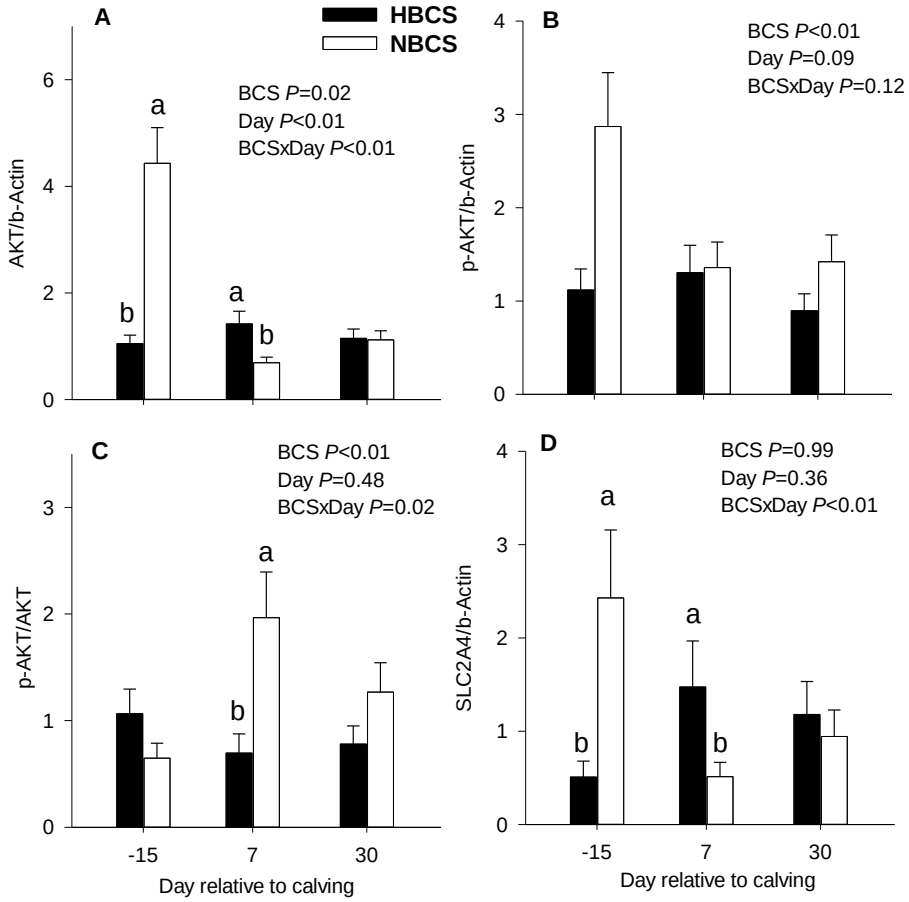

Figure 5.5. mRNA abundance of genes related to AA transport in s.c. adipose tissue of Holstein cows with prepartum (28 d before expected parturition) high body condition score (HBCS, BCS ≥ 3.5) and normal body condition score (NBCS, BCS ≤ 3.17) at -15, 7 and 30 d relative to calving. Data are LS means, n = 11 cows per group, ± pooled SEMs.

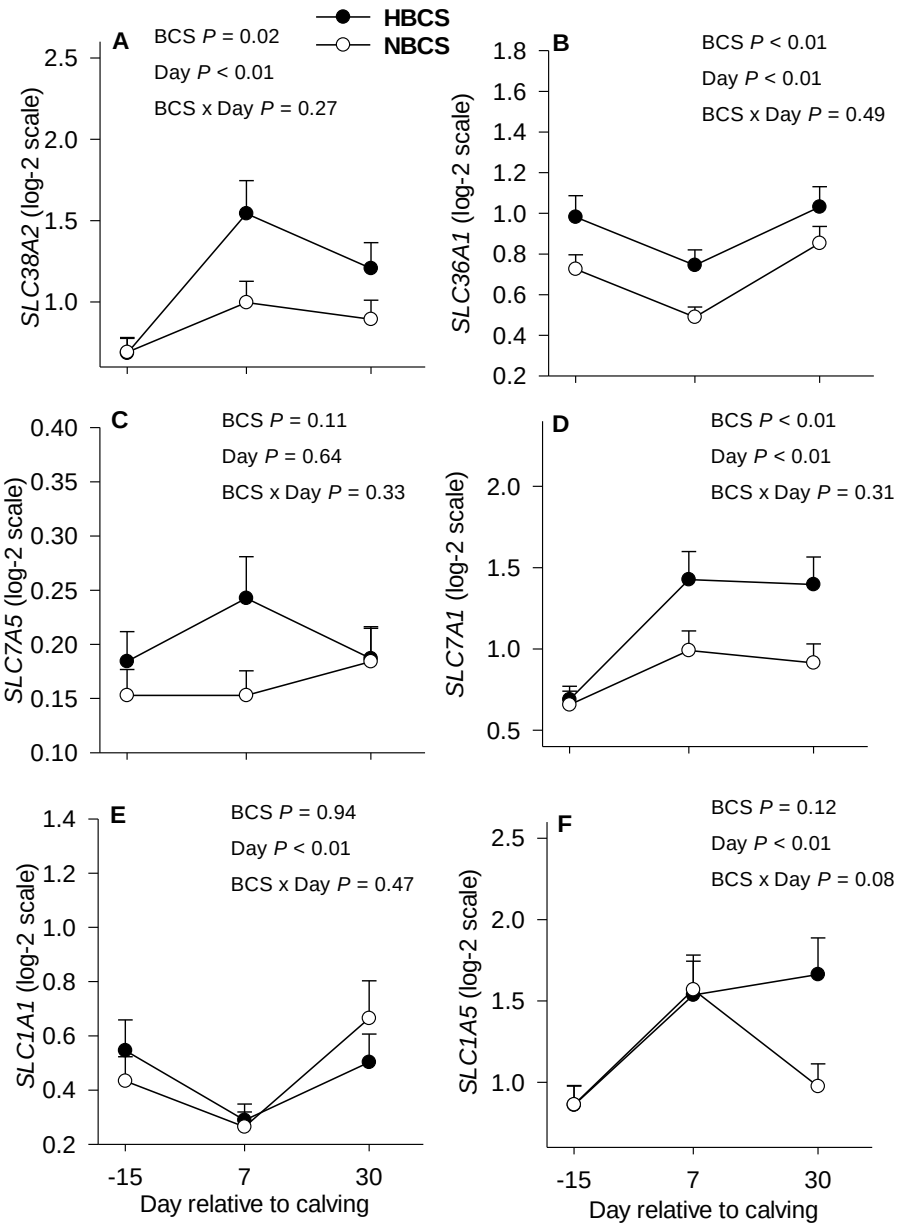

Figure 5.6. Protein abundance (relative to β-actin) of SLC38A1 (panel A), BCKDK (panel B), mTOR (total, panel C), p-mTOR (active, panel D) and ratio of p-mTOR/mTOR (panel E) in s.c. adipose tissue of Holstein cows with prepartum (28 d before expected parturition) high (HBCS, BCS ≥ 3.5) or normal body condition score (NBCS, BCS ≤ 3.17) at -15, 7 and 30 d relative to calving. Data are LS means, n = 11 cows per group, ± pooled SEMs. [ab]Means differ (BCS × Day, $P \leq 0.05$).[#]Means tend to differ (BCS × Day, $P = 0.08$).

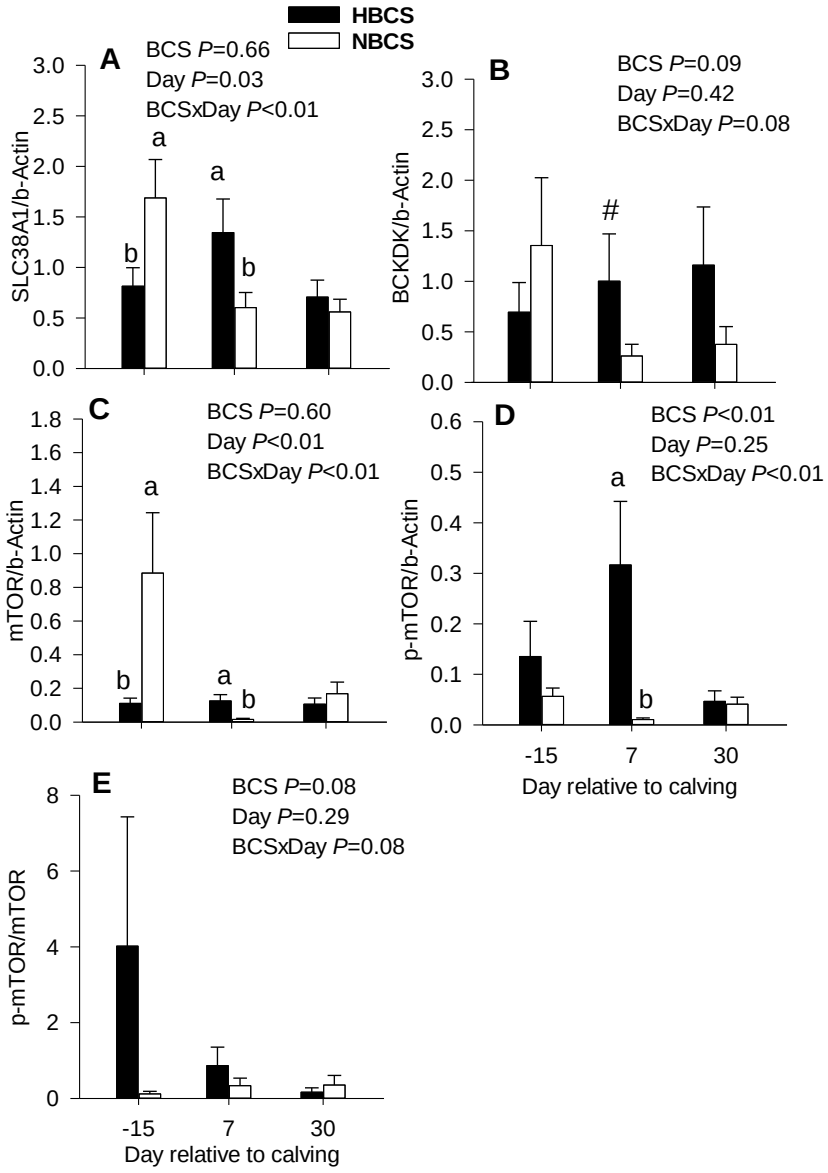

Figure 5.7. mRNA abundance of genes related to the urea cycle in s.c. adipose tissue of Holstein cows with prepartum (28 d before expected parturition) high body condition score (HBCS, BCS ≥ 3.5) and normal body condition score (NBCS, BCS ≤ 3.17) at -15, 7 and 30 d relative to calving. Data are LS means, n = 11 cows per group, ± pooled SEMs. *ASL* = Arginino-succinate lyase; *ARG1*= Arginase 1; *ASS1* = Arginino-succinate synthase.

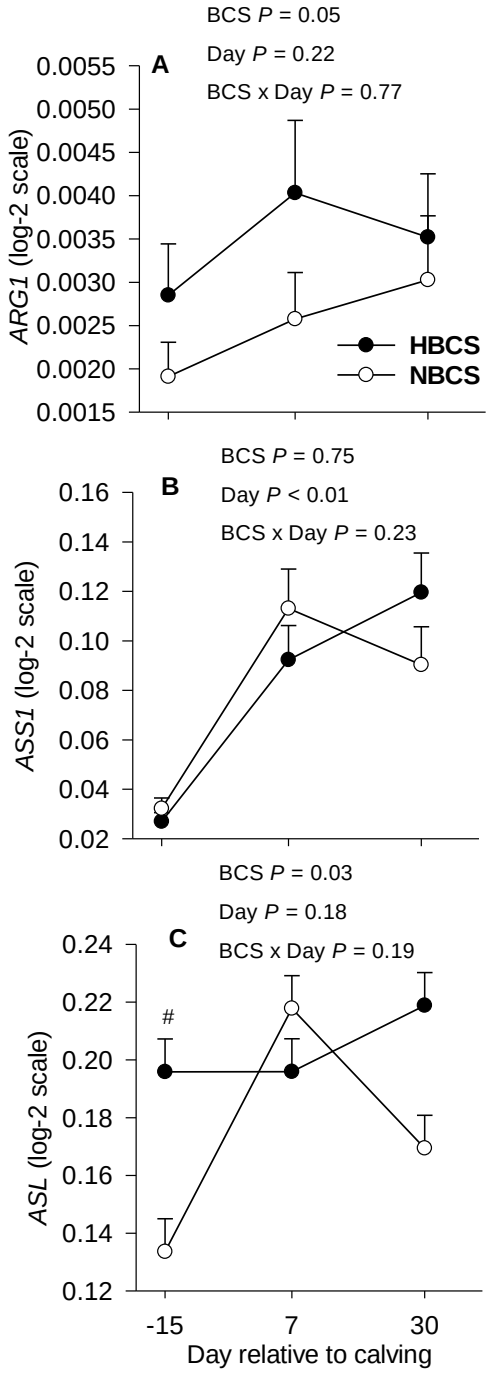

REFERENCES

Akter, S., S. Häussler, D. Germeroth, D. Von Soosten, S. Dänicke, K.-H. Südekum, and H. Sauerwein. 2012. Immunohistochemical characterization of phagocytic immune cell infiltration into different adipose tissue depots of dairy cows during early lactation. J. Dairy Sci. 95:3032-3044.

Alharthi, A., Z. Zhou, V. Lopreiato, E. Trevisi, and J. J. Loor. 2018. Body condition score prior to parturition is associated with plasma and adipose tissue biomarkers of lipid metabolism and inflammation in Holstein cows. J. Anim. Sci. Biotechnol. 9:12.

Appuhamy, J. R. N., N. A. Knoebel, W. D. Nayananjalie, J. Escobar, and M. D. Hanigan. 2012. Isoleucine and leucine independently regulate mTOR signaling and protein synthesis in MAC-T cells and bovine mammary tissue slices. J. Nutr.142:484-491.

Arriarán, S., S. Agnelli, X. Remesar, J.-A. Fernández-López, and M. Alemany. 2015. The urea cycle of rat white adipose tissue. RSC. Adv. 5:93403-93414.

Batistel, F., J. Arroyo, A. Bellingeri, L. Wang, B. Saremi, C. Parys, E. Trevisi, F. Cardoso, and J. Loor. 2017. Ethyl-cellulose rumen-protected methionine enhances performance during the periparturient period and early lactation in Holstein dairy cows. J. Dairy Sci. 100:7455-7467.

Batistel, F., J. Arroyo, C. Garces, E. Trevisi, C. Parys, M. Ballou, F. Cardoso, and J. Loor. 2018. Ethyl-cellulose rumen-protected methionine alleviates inflammation and oxidative stress and improves neutrophil function during the periparturient period and early lactation in Holstein dairy cows. J. Dairy Sci. 101:480-490.

Bauchart-Thevret, C., L. Cui, G. Wu, and D. G. Burrin. 2010. Arginine-induced stimulation of protein synthesis and survival in IPEC-J2 cells is mediated by mTOR but not nitric oxide. Am. J. Physiol. Endocrinol. Metab. 299:E899-E909.

Bewley, J. and M. Schutz. 2008. An interdisciplinary review of body condition scoring for dairy cattle. Prof. Anim. Sci. 24:507-529.

Bionaz, M., E. Trevisi, L. Calamari, F. Librandi, A. Ferrari, and G. Bertoni. 2007. Plasma paraoxonase, health, inflammatory conditions, and liver function in transition dairy cows. J. Dairy Sci. 90:1740-1750.

Bionaz, M., S. Chen, M. J. Khan, and J. J. Loor. 2013. Functional role of PPARs in ruminants: Potential targets for fine-tuning metabolism during growth and lactation. PPAR Res. 2013:684159.

Bradford, B. J., K. Yuan, J. K. Farney, L. K. Mamedova, and A. J. Carpenter. 2015. Invited review: Inflammation during the transition to lactation: New adventures with an old flame J. Dairy Sci. 98:6631-6650.

Broer, S. 2008. Apical transporters for neutral amino acids: physiology and pathophysiology. Physiology 23:95-103.

Burgos, S., M. Dai, and J. Cant. 2010. Nutrient availability and lactogenic hormones regulate mammary protein synthesis through the mammalian target of rapamycin signaling pathway. J. Dairy Sci. 93:153-161.

Busato, A., D. Faissler, U. Küpfer, and J. W. Blum. 2002. Body condition scores in dairy cows: Associations with metabolic and endocrine changes in healthy dairy cows. J. Vet. Med. A Physiol. Pathol. Clin. Med. 49:455-460.

Cai, H., L. Q. Dong, and F. Liu. 2016. Recent advances in adipose mTOR signaling and function: therapeutic prospects. Trends Pharmacol. Sci. 37:303-317.

Caroprese, M., M. Albenzio, R. Marino, A. Santillo, and A. Sevi. 2012. Immune response and milk production of dairy cows fed graded levels of rumen-protected glutamine. Res. Vet. Sci. 93:202-209.
Closs, E., J.-P. Boissel, A. Habermeier, and A. Rotmann. 2006. Structure and function of cationic amino acid transporters (CATs). J. Membr. Biol. 213:67-77.
Contreras, G. A., E. Kabara, J. Brester, L. Neuder, and M. Kiupel. 2015. Macrophage infiltration in the omental and subcutaneous adipose tissues of dairy cows with displaced abomasum. J. Dairy Sci. 98:6176-6187.
Cynober, L., J. Le Boucher, and M.-P. Vasson. 1995. Arginine metabolism in mammals. J. Nutr. Biochem. 6:402-413.
Dann, H. M., D. E. Morin, G. A. Bollero, M. R. Murphy, and J. K. Drackley. 2005. Prepartum intake, postpartum induction of ketosis, and periparturient disorders affect the metabolic status of dairy cows. J. Dairy Sci. 88:3249-3264.
De Koster, J., C. Urh, M. Hostens, W. Van den Broeck, H. Sauerwein, and G. Opsomer. 2017. Relationship between serum adiponectin concentration, body condition score, and peripheral tissue insulin response of dairy cows during the dry period. Domest. Anim. Endocrinol. 59:100-104.
De Koster, J., M. Hostens, M. Van Eetvelde, K. Hermans, S. Moerman, H. Bogaert, E. Depreester, W. Van den Broeck, and G. Opsomer. 2015. Insulin response of the glucose and fatty acid metabolism in dry dairy cows across a range of body condition scores. J. Dairy Sci. 98:4580-4592.
De Koster, J., C. Strieder-Barboza, J. de Souza, A. L. Lock, and G. A. Contreras. 2018. Short communication: Effects of body fat mobilization on macrophage infiltration in adipose tissue of early lactation dairy cows. J. Dairy Sci. 101:7608-7613.
De Koster, J., W. Van den Broeck, L. Hulpio, E. Claeys, M. Van Eetvelde, K. Hermans, M. Hostens, V. Fievez, and G. Opsomer. 2016. Influence of adipocyte size and adipose depot on the in vitro lipolytic activity and insulin sensitivity of adipose tissue in dairy cows at the end of the dry period. J. Dairy Sci. 99:2319-2328.
De Koster, J. D. and G. Opsomer. 2013. Insulin resistance in dairy cows. Vet. Clin. North Am. Food Anim. Pract. 29:299-322.
Depreester, E., J. De Koster, M. Van Poucke, M. Hostens, W. Van den Broeck, L. Peelman, G. A. Contreras, and G. Opsomer. 2018. Influence of adipocyte size and adipose depot on the number of adipose tissue macrophages and the expression of adipokines in dairy cows at the end of pregnancy. J. Dairy Sci.101:6542-6555.
Durante, W. 2013. Role of arginase in vessel wall remodeling. Front. Immunol. 4:111.
Edmonson, A. J., I. J. Lean, L. D. Weaver, T. Farver, and G. Webster. 1989. A body condition scoring chart for Holstein dairy cows. J. Dairy Sci. 72:68–78.
Frayn, K., K. Khan, S. Coppack, and M. Elia. 1991. Amino acid metabolism in human subcutaneous adipose tissue in vivo. Clin. Sci. 80:471-474.
Ghaffari, M. H., A. Jahanbekam, H. Sadri, K. Schuh, G. Dusel, C. Prehn, J. Adamski, C. Koch, and H. Sauerwein. 2019a. Metabolomics meets machine learning: Longitudinal metabolite profiling in serum of normal versus overconditioned cows and pathway analysis. J. Dairy Sci. 102:11561-11585.
Ghaffari, M., K. Schuh, G. Dusel, D. Frieten, C. Koch, C. Prehn, J. Adamski, H. Sauerwein, and H. Sadri. 2019b. Mammalian target of rapamycin signaling and ubiquitin-proteasome–

related gene expression in skeletal muscle of dairy cows with high or normal body condition score around calving. J. Dairy Sci. 102:11544-11560.
Ghaffari, M., H. Sadri, K. Schuh, G. Dusel, D. Frieten, C. Koch, C. Prehn, J. Adamski, and H. Sauerwein. 2019c. Biogenic amines: Concentrations in serum and skeletal muscle from late pregnancy until early lactation in dairy cows with high versus normal body condition score. J. Dairy Sci.102: 6571-6586.
González, F. D., R. Muiño, V. Pereira, R. Campos, and J. L. Benedito. 2011. Relationship among blood indicators of lipomobilization and hepatic function during early lactation in high-yielding dairy cows. J. Vet. Sci. 12:251-255.
Gonzalez, E. and T. E. McGraw. 2009. Insulin-modulated Akt subcellular localization determines Akt isoform-specific signaling. Proc. Natl. Acad. Sci. U. S. A. 106:7004-7009.
Häussler, S., D. Germeroth, L. Laubenthal, L. Ruda, J. Rehage, S. Dänicke, and H. Sauerwein. 2017. Immunohistochemical localization of the immune cell marker CD68 in bovine adipose tissue: impact of tissue alterations and excessive fat accumulation in dairy cows. Vet. Immunol. Immunopathol.183:45-48.
Horie, T., K. Fukasawa, T. Iezaki, G. Park, Y. Onishi, K. Ozaki, T. Kanayama, M. Hiraiwa, Y. Kitaguchi, and K. Kaneda. 2018. Hypoxic stress upregulates the expression of Slc38a1 in brown adipocytes via hypoxia-inducible factor-1α. Pharmacology 101:64-71.
Hosogai, N., A. Fukuhara, K. Oshima, Y. Miyata, S. Tanaka, K. Segawa, S. Furukawa, Y. Tochino, R. Komuro, and M. Matsuda. 2007. Adipose tissue hypoxia in obesity and its impact on adipocytokine dysregulation. Diabetes 56:901-911.
Hu, H., J. Moon, J. H. Chung, O. Y. Kim, R. Yu, and M.-J. Shin. 2015. Arginase inhibition ameliorates adipose tissue inflammation in mice with diet-induced obesity. Biochem. Biophys. Res. Commun. 464:840-847.
Ibrahim, M. M. 2010. Subcutaneous and visceral adipose tissue: structural and functional differences. Obes. Rev. 11:11-18.
Jafari, A., D. Emmanuel, R. Christopherson, J. Thompson, G. Murdoch, J. Woodward, C. Field, and B. Ametaj. 2006. Parenteral administration of glutamine modulates acute phase response in postparturient dairy cows. J. Dairy Sci. 89:4660-4668.
Jager, J., T. Grémeaux, M. Cormont, Y. Le Marchand-Brustel, and J.-F. Tanti. 2007. Interleukin-1β-induced insulin resistance in adipocytes through down-regulation of insulin receptor substrate-1 expression. Endocrinol. 148:241-251.
Janovick, N. A., Y. R. Boisclair, and J. K. Drackley. 2011. Prepartum dietary energy intake affects metabolism and health during the periparturient period in primiparous and multiparous Holstein cows1. J. Dairy Sci. 94:1385-1400.
Jamali Emam Gheise, N., A. Riasi, A. Zare Shahneh, P. Celi, and S. M. Ghoreishi. 2017. Effect of pre-calving body condition score and previous lactation on BCS change, blood metabolites, oxidative stress and milk production in Holstein dairy cows. Ital. J. Anim. Sci. 16:474-483.
Javed, K. and S. J. Fairweather. 2019. Amino acid transporters in the regulation of insulin secretion and signalling. Biochem. Soc. Trans. 47:571-590.
Ji, P., J. K. Drackley, M. J. Khan, and J. J. Loor. 2014a. Inflammation- and lipid metabolism-related gene network expression in visceral and subcutaneous adipose depots of Holstein cows. J. Dairy Sci. 97:3441-3448.

Ji, P., J. K. Drackley, M. J. Khan, and J. J. Loor. 2014b. Overfeeding energy upregulates peroxisome proliferator-activated receptor (PPAR)γ-controlled adipogenic and lipolytic gene networks but does not affect proinflammatory markers in visceral and subcutaneous adipose depots of Holstein cows. J. Dairy Sci. 97:3431-3440.

Ji, P., J. Osorio, J. Drackley, and J.J. Loor. 2012. Overfeeding a moderate energy diet prepartum does not impair bovine subcutaneous adipose tissue insulin signal transduction and induces marked changes in peripartal gene network expression1. J. Dairy Sci. 95:4333-4351.

Kanda, H., S. Tateya, Y. Tamori, K. Kotani, K.-i. Hiasa, R. Kitazawa, S. Kitazawa, H. Miyachi, S. Maeda, and K. Egashira. 2006. MCP-1 contributes to macrophage infiltration into adipose tissue, insulin resistance, and hepatic steatosis in obesity. J. Clin. Invest. 116:1494-1505.

Kenéz, Á., L. Ruda, S. Dänicke, and K. Huber. 2019. Insulin signaling and insulin response in subcutaneous and retroperitoneal adipose tissue in Holstein cows during the periparturient period. J. Dairy Sci. 102:11718-11729.

Laplante, M. and D. M. Sabatini. 2009. mTOR signaling at a glance. J. Cell Sci. 122:3589-3594.

Laubenthal, L., L. Ruda, N. Sultana, J. Winkler, J. Rehage, U. Meyer, S. Dänicke, H. Sauerwein, and S. Häussler. 2017. Effect of increasing body condition on oxidative stress and mitochondrial biogenesis in subcutaneous adipose tissue depot of nonlactating dairy cows. J. Dairy Sci. 100:4976-4986.

Le Floc'h, N., D. Melchior, and C. Obled. 2004. Modifications of protein and amino acid metabolism during inflammation and immune system activation. Livest. Prod. Sci. 87:37-45.

Li, Y., H. Wei, F. Li, S. Chen, Y. Duan, Q. Guo, Y. Liu, and Y. Yin. 2016. Supplementation of branched-chain amino acids in protein-restricted diets modulates the expression levels of amino acid transporters and energy metabolism associated regulators in the adipose tissue of growing pigs. Anim. Nutr. 2:24-32.

Liang, Y., A. S. Alharthi, R. Bucktrout, A. A. Elolimy, V. Lopreiato, I. Martinez-Cortés, C. Xu, C. Fernandez, E. Trevisi, and J. J. Loor . 2020. Body condition alters glutathione and nuclear factor erythroid 2-like 2 (NFE2L2)-related antioxidant network abundance in subcutaneous adipose tissue of periparturient Holstein cows. J. Dairy Sci. 103:6439-6453.

Liang, Y., F. Batistel, C. Parys, and J. J. Loor. 2019. Methionine supply during the periparturient period enhances insulin signaling, amino acid transporters, and mechanistic target of rapamycin pathway proteins in adipose tissue of Holstein cows. J. Dairy Sci.102:4403-4414.

Liao, W., M. T. A. Nguyen, T. Yoshizaki, S. Favelyukis, D. Patsouris, T. Imamura, I. M. Verma, and J. M. Olefsky. 2007. Suppression of PPAR-γ attenuates insulin-stimulated glucose uptake by affecting both GLUT1 and GLUT4 in 3T3-L1 adipocytes. Am. J. Physiol. Endocrinol. Metab. 293:E219-E227.

Locher, L. F., N. Meyer, E. M. Weber, J. Rehage, U. Meyer, S. Dänicke, and K. Huber. 2011. Hormone-sensitive lipase protein expression and extent of phosphorylation in subcutaneous and retroperitoneal adipose tissues in the periparturient dairy cow. J. Dairy Sci. 94:4514-4523.

Ma, Y. F., L. Zhao, D. N. Coleman, M. Gao, and J. J. Loor. 2019. Tea polyphenols protect bovine mammary epithelial cells from hydrogen peroxide-induced oxidative damage in vitro by activating NFE2L2/HMOX1 pathways. J. Dairy Sci. 102:1658-1670.

Mackenzie, B. and J. D. Erickson. 2004. Sodium-coupled neutral amino acid (System N/A) transporters of the SLC38 gene family. Pflugers Arch. 447:784-795.
Mann, S., D. V. Nydam, A. Abuelo, F. A. Leal Yepes, T. R. Overton, and J. J. Wakshlag. 2016. Insulin signaling, inflammation, and lipolysis in subcutaneous adipose tissue of transition dairy cows either overfed energy during the prepartum period or fed a controlled-energy diet. J. Dairy Sci. 99:6737-6752.
Megahed, A., M. Hiew, D. Ragland, and P. D. Constable. 2019. Changes in skeletal muscle thickness and echogenicity and plasma creatinine concentration as indicators of protein and intramuscular fat mobilization in periparturient dairy cows. J. Dairy Sci. 102:5550-5565.
Menchini, R. J. and F. A. Chaudhry. 2019. Multifaceted regulation of the system A transporter Slc38a2 suggests nanoscale regulation of amino acid metabolism and cellular signaling. Neuropharmacology 161:107789.
Minuti, A., M. Bionaz, V. Lopreiato, N. A. Janovick, S. L. Rodriguez-Zas, J. K. Drackley, and J. J. Loor. 2020. Prepartum dietary energy intake alters adipose tissue transcriptome profiles during the periparturient period in Holstein dairy cows. J. Anim. Sci. Biotechnol. 11:1-14.
Moisá, S. J., P. Ji, J. K. Drackley, S. L. Rodriguez-Zas, and J. J. Loor. 2017. Transcriptional changes in mesenteric and subcutaneous adipose tissue from Holstein cows in response to plane of dietary energy. J. Anim. Sci. Biotechnol. 8:85.
Mukesh, M., M. Bionaz, D. Graugnard, J. K. Drackley, and J. J. Loor. 2010. Adipose tissue depots of Holstein cows are immune responsive: inflammatory gene expression in vitro. Domest. Anim. Endocrinol. 38:168-178.
National Research Council. 2001. Nutrient requirements of dairy cattle. 7th rev. ed. Natl. Acad. Press, Washington, DC.
Newgard, C. B. 2017. Metabolomics and metabolic diseases: Where do we stand? Cell Metab. 25:43-56.
Newgard, C. B., J. An, J. R. Bain, M. J. Muehlbauer, R. D. Stevens, L. F. Lien, A. M. Haqq, S. H. Shah, M. Arlotto, and C. A. Slentz. 2009. A branched-chain amino acid-related metabolic signature that differentiates obese and lean humans and contributes to insulin resistance. Cell Metab. 9:311-326.
Newman, A. W., A. Miller, F. A. Leal Yepes, E. Bitsko, D. Nydam, and S. Mann. 2019. The effect of the transition period and postpartum body weight loss on macrophage infiltrates in bovine subcutaneous adipose tissue. J. Dairy Sci. 102:1693-1701.
Newsholme, P., J. Procopio, M. M. R. Lima, T. C. Pithon‐Curi, and R. Curi. 2003. Glutamine and glutamate—their central role in cell metabolism and function. Cell Biochem. Funct. 21:1-9.
Osorio, J., P. Ji, J. Drackley, D. Luchini, and J. Loor. 2014. Smartamine M and MetaSmart supplementation during the peripartal period alter hepatic expression of gene networks in 1-carbon metabolism, inflammation, oxidative stress, and the growth hormone–insulin-like growth factor 1 axis pathways. J. Dairy Sci. 97:7451-7464.
Palmieri, E. M., I. Spera, A. Menga, V. Infantino, V. Iacobazzi, and A. Castegna. 2014. Glutamine synthetase desensitizes differentiated adipocytes to proinflammatory stimuli by raising intracellular glutamine levels. FEBS letters 588:4807-4814.

Petrus, P., S. Lecoutre, L. Dollet, C. Wiel, A. Sulen, H. Gao, B. Tavira, J. Laurencikiene, O. Rooyackers, and A. Checa. 2020. Glutamine links obesity to inflammation in human white adipose tissue. Cell Metab. 31:375-390. e311.

Pires, J., C. Delavaud, Y. Faulconnier, D. Pomies, and Y. Chilliard. 2013. Effects of body condition score at calving on indicators of fat and protein mobilization of periparturient Holstein-Friesian cows. J. Dairy Sci. 96:6423-6439.

Rico, J., W. Myers, D. Laub, A. Davis, Q. Zeng, and J. McFadden. 2018. Hot topic: Ceramide inhibits insulin sensitivity in primary bovine adipocytes. J. Dairy Sci. 101:3428-3432.

Rico, J. E., V. V. R. Bandaru, J. M. Dorskind, N. J. Haughey, and J. W. McFadden. 2015. Plasma ceramides are elevated in overweight Holstein dairy cows experiencing greater lipolysis and insulin resistance during the transition from late pregnancy to early lactation. J. Dairy Sci. 98:7757-7770.

Rius, A., J. Appuhamy, J. Cyriac, D. Kirovski, O. Becvar, J. Escobar, M. McGilliard, B. Bequette, R. Akers, and M. Hanigan. 2010. Regulation of protein synthesis in mammary glands of lactating dairy cows by starch and amino acids. J. Dairy Sci. 93:3114-3127.

Roche, J. R., J. K. Kay, N. C. Friggens, J. J. Loor, and D. P. Berry. 2013. Assessing and managing body condition score for the prevention of metabolic disease in dairy cows. Vet. Clin. North Am. Food Anim. Pract. 29:323-336.

Ruan, H. and L. Q. Dong. 2016. Adiponectin signaling and function in insulin target tissues. J Mol. Cell Biol. 8:101-109.

Saltiel, A. R. and C. R. Kahn. 2001. Insulin signalling and the regulation of glucose and lipid metabolism. Nature 414:799-806.

Saremi, B., A. Al-Dawood, S. Winand, U. Müller, J. Pappritz, D. von Soosten, J. Rehage, S. Dänicke, S. Häussler, M. Mielenz, and H. Sauerwein. 2012. Bovine haptoglobin as an adipokine: Serum concentrations and tissue expression in dairy cows receiving a conjugated linoleic acids supplement throughout lactation. Vet. Immunol. Immunopathol. 146:201-211.

Schuh, K., H. Sadri, S. Häussler, L. A. Webb, C. Urh, M. Wagner, C. Koch, J. Frahm, S. Dänicke, G. Dusel, and H. Sauerwein. 2019. Comparison of performance and metabolism from late pregnancy to early lactation in dairy cows with elevated v. normal body condition at dry-off. Animal 13:1478-1488.

Sundberg, B. E., E. Wååg, J. A. Jacobsson, O. Stephansson, J. Rumaks, S. Svirskis, J. Alsiö, E. Roman, T. Ebendal, and V. Klusa. 2008. The evolutionary history and tissue mapping of amino acid transporters belonging to solute carrier families SLC32, SLC36, and SLC38. J. Mol. Neurosci. 35:179-193.

Takagi, M., T. Yonezawa, S. Haga, H. Shingu, Y. Kobayashi, T. Takahashi, Y. Ohtani, Y. Obara, and K. Katoh. 2008. Changes of activity and mRNA expression of urea cycle enzymes in the liver of developing Holstein calves. J. Anim. Sci. 86:1526-1532.

Trayhurn, P. 2013. Hypoxia and adipose tissue function and dysfunction in obesity. Physiol. Rev. 93:1-21.

Trevisi, E., M. Amadori, S. Cogrossi, E. Razzuoli, and G. Bertoni. 2012. Metabolic stress and inflammatory response in high-yielding, periparturient dairy cows. Res. Vet. Sci. 93:695-704.

Vailati-Riboni, M., F. Batistel, R. R. C. S. Yambao, C. Parys, Y.-X. Pan, and J. J. Loor. 2019. Hepatic cystathionine β-Synthase activity is increased by greater postruminal supply of Met during the periparturient period in dairy cows. Cur. Dev. Nutr. 3.

Vailati-Riboni, M., G. Farina, F. Batistel, A. Heiser, M. Mitchell, M. Crookenden, C. Walker, J. Kay, S. Meier, and J. Roche. 2017. Far-off and close-up dry matter intake modulate indicators of immunometabolic adaptations to lactation in subcutaneous adipose tissue of pasture-based transition dairy cows. J. Dairy Sci. 100:2334-2350.

Vailati-Riboni, M., M. Kanwal, O. Bulgari, S. Meier, N. Priest, C. Burke, J. Kay, S. McDougall, M. Mitchell, and C. Walker. 2016. Body condition score and plane of nutrition prepartum affect adipose tissue transcriptome regulators of metabolism and inflammation in grazing dairy cows during the transition period. J. Dairy Sci. 99:758-770.

Vailati-Riboni, M., S. Meier, N. Priest, C. Burke, J. Kay, S. McDougall, M. Mitchell, C. Walker, M. Crookenden, and A. Heiser. 2015. Adipose and liver gene expression profiles in response to treatment with a nonsteroidal antiinflammatory drug after calving in grazing dairy cows. J. Dairy Sci. 98:3079-3085.

Van der Vos, K. E. and P. J. Coffer. 2012. Glutamine metabolism links growth factor signaling to the regulation of autophagy. Autophagy 8:1862-1864.

Wang, D., X. Wan, J. Peng, Q. Xiong, H. Niu, H. Li, J. Chai, and S. Jiang. 2017. The effects of reduced dietary protein level on amino acid transporters and mTOR signaling pathway in pigs. Biochem. Biophys. Res. Commun. 485:319-327.

Wang, X., J. W. Frank, D. R. Little, K. A. Dunlap, M. C. Satterfield, R. C. Burghardt, T. R. Hansen, G. Wu, and F. W. Bazer. 2014. Functional role of arginine during the peri-implantation period of pregnancy. I. Consequences of loss of function of arginine transporter SLC7A1 mRNA in ovine conceptus trophectoderm. FASEB J. 28:2852-2863.

Webb, L., H. Sadri, D. von Soosten, S. Dänicke, S. Egert, P. Stehle, and H. Sauerwein. 2019. Changes in tissue abundance and activity of enzymes related to branched-chain amino acid catabolism in dairy cows during early lactation. J. Dairy Sci. 102:3556-3568.

Webb, L., H. Sadri, K. Schuh, S. Egert, P. Stehle, I. Meyer, C. Koch, G. Dusel, and H. Sauerwein. 2020. Branched-chain amino acids: Abundance of their transporters and metabolizing enzymes in adipose tissue, skeletal muscle, and liver of dairy cows at high or normal body condition. J. Dairy Sci. 103:2847-2863.

Whiteman, E. L., H. Cho, and M. J. Birnbaum. 2002. Role of Akt/protein kinase B in metabolism. Trends Endocrinol. Metab. 13:444-451.

Xue, M.-Y., H.-Z. Sun, X.-H. Wu, J.-X. Liu, and L. L. Guan. 2020. Multi-omics reveals that the rumen microbiome and its metabolome together with the host metabolome contribute to individualized dairy cow performance. Microbiome 8:64.

Zachut, M., H. Honig, S. Striem, Y. Zick, S. Boura-Halfon, and U. Moallem. 2013. Periparturient dairy cows do not exhibit hepatic insulin resistance, yet adipose-specific insulin resistance occurs in cows prone to high weight loss. J. Dairy Sci. 96:5656-5669.

Zhang, F., D. Li, Q. Wu, J. Sun, W. Guan, Y. Hou, Y. Zhu, and J. Wang. 2019. Prepartum body conditions affect insulin signaling pathways in postpartum adipose tissues in transition dairy cows. J. Anim. Sci. Biotechnol. 10:38.

CHAPTER 6: METHIONINE AND ARGININE SUPPLEMENTATION ALTERS ABUNDANCE OF AMINO ACID, INSULIN SIGNALING, AND GLUTATHIONE METABOLISM-RELATED PROTEINS IN BOVINE SUBCUTANEOUS ADIPOSE EXPLANTS CHALLENGED WITH N-ACETYL-D-SPHINGOSINE

INTRODUCTION

Insulin resistance, a homeorhetic adaptation mechanism, is a well-known feature of dairy cows during the periparturient period (De Koster and Opsomer, 2013). Increased insulin resistance goes along with excessive body fat mobilization and increased circulating ceramides, especially in overconditioned cows (Rico et al. 2015), which may potentially contribute to the development of metabolic disorders (Oikawa and Oetzel, 2006; Bossaert et al., 2008; McFadden and Rico, 2019). Recent evidence suggests that ceramides are potential mediators in the regulation of insulin resistance in peripartal cows (McFadden and Rico, 2019). For instance, ceramides accumulate in the plasma and liver of dairy cows during the periparturient period and systemic insulin sensitivity is inversely related to plasma ceramide concentrations (Rico et al., 2017). A recent in vitro study demonstrated that exogenous C2:0-ceramide (100 μ*M*) led to reduced activation of protein kinase B [**AKT**; phosphorylated (**p**)-AKT/total AKT] along with reduced 2-deoxy-D-[^{3}H]-glucose uptake in primary bovine adipocytes (Rico et al., 2018), underscoring its negative effect on insulin sensitivity in subcutaneous adipose tissue (**SAT**). Taken together, available data indicate that C2:0-ceramide could impact negatively insulin sensitivity in bovine SAT through inhibition of AKT (p-AKT/total AKT) signaling.

Besides its profound effect on insulin sensitivity in mammalian cells, downregulation of amino acid (**AA**) transporters by ceramides could lead to cell death (Bikman and Summers, 2011). A lower protein abundance of sodium-dependent neutral amino acid transporter 2 (**SLC38A2**) along with decreased total intracellular AA concentrations were observed in rat L6 myotubes after C2:0-ceramide (100 μ*M*) treatment for 2 h (Hyde et al., 2004). In mouse

hepatocytes, C2:0-ceramide-induced cell death partly by inducing intracellular nutrient deprivation as a response to downregulation of the branched-chain amino acid (**BCAA**) transporter SLC3A2 (Guenther et al., 2008). In addition to being an insulin-sensitive tissue (Zachut et al., 2013), bovine SAT is a potentially important site for AA metabolism (Liang et al., 2019b; Webb et al., 2020). However, the role of ceramide in regulating AA uptake and intracellular AA metabolism in SAT is not well known.

Mechanistic target of rapamycin (**mTOR)**, a key regulator of protein synthesis and cell growth and proliferation in mammals (Ma and Blenis, 2009), is regulated by AA availability and plays multiple roles in adipose tissue (Lee et al., 2017). For example, specific depletion of *mTOR* in adipose tissue results in insulin resistance in mice (Shan et al., 2016). Enhanced rumen-protected limiting AA supplementation, particularly Met, improves dry matter intake (**DMI**), milk yield, and milk protein yield around parturition (Schwab and Broderick, 2017). Thus, enhanced essential AA (**EAA**) supply could be a practical strategy to improve metabolic status in peripartal cows (Osorio et al., 2013; Zhou et al., 2016; Batistel et al., 2017). Enhanced post-ruminal supply of Met by feeding rumen-protected Met (**RPM**) to achieve a dietary Lys:Met ratio of 2.9:1 alleviates systemic oxidative stress and potentially ameliorates insulin resistance (Osorio et al., 2013; Batistel et al., 2017; Liang et al., 2019b). The latter is supported, at least in part, by the upregulation of p-AKT in SAT of cows fed RPM (Liang et al., 2019b). Reduced oxidative stress in cows fed RPM is partly explained by increased protein abundance glutathione peroxidase and glutathione S-transferase mu 1 (**GSTM1**) in SAT, and enhanced RMP supply also resulted in greater protein abundance of p-mTOR (Liang et al., 2019b). Due to the concurrent increase in DMI, whether those responses were induced directly by increased circulating Met is unclear.

Despite Arg being a semi-essential AA for adult mammals, data highlight the significance of Arg in promoting milk protein synthesis (Ding et al., 2019) and alleviating inflammatory responses in lactating Holstein cows challenged with lipopolysaccharide (**LPS**) (Zhao et al., 2018). Jugular Arg infusion prevented the decrease of plasma AA such as Ile, Leu, and Arg in plasma of cows with LPS challenge (Zhao et al., 2018). In vitro studies also reported that increased Arg concentration (Lys:Arg ratio at 1:1) led to downregulated mRNA abundance of solute carrier family 7 member 1 (***SLC7A1***), a major Arg transporter, along with greater activation of mTOR (p-mTOR/total mTOR) in primary bovine mammary epithelial cells (**BMEC**) (Hu et al., 2020). However, enhanced Arg supply attenuated downregulation of *SLC7A1* in BMEC challenged with LPS (Dai et al., 2020). Furthermore, Arg supplementation led to greater activation of mTOR (p-mTOR/total mTOR) in BMEC stimulated with LPS (Wu et al., 2016). Thus, available data suggest that increased Arg supplementation could enhance lactation performance and help alleviate inflammation partly due to altered AA metabolism and mTOR activation. Of particular interest, a recent in vitro study observed that 200 μmol/L L-Arg compared with 50 and 100 μmol/L upregulated p-mTOR in ovine adipocyte precursor cells (Ma et al., 2017), which underscored that L-Arg could stimulate mTOR in ruminant SAT. Whether Arg promotes mTOR activation via altering AA transporters in bovine SAT during a ceramide challenge is unknown.

Because the role of Arg in modulating mTOR in bovine SAT is largely unknown, and there is evidence to support that Met potentially affects SAT signaling, our general hypothesis was that Met and/or Arg supply could relieve impaired insulin signaling via increased AA transport and mTOR activation in bovine SAT stimulated with ceramide. Thus, the main objective of this study was to investigate the effects of Met and Arg supply, alone or in

combination, on protein abundance of AA transporter, mTOR, and insulin signaling markers in bovine SAT explants challenged with C2:0-ceramide.

MATERIALS AND METHODS

Cows

All procedures were conducted under protocols approved by the University of Illinois Institutional Animal Care and Use Committee (Urbana; protocol # 19036). Four healthy multiparous lactating Holstein cows from the University of Illinois dairy herd were used. Average parity, DIM, and milk yield before slaughter were 4 ± 1.4, 248 ± 38, and 27.0 ± 13.5 (kg/d) (mean ± SD), respectively. Cows were fed the same diet formulated according to NRC (2001) once daily at 1400. Ingredients and nutrient composition of the diet are reported in Supplemental Table E.1 and E.2. Cows were milked twice daily, housed in a free-stall barn, and had free access to water.

Tissue Collection, Processing, and Cell Culture

Cows were euthanized by captive bolt at the College of Veterinary Medicine diagnostic facilities (University of Illinois). SAT samples from the tail-head were obtained immediately post-slaughter and brought to the laboratory in Dulbecco's Modified Eagle's Medium and Ham's F-12 nutrient mixture (DMEM:F-12; Sigma-Aldrich, St. Louis, MO) containing 1% penicillin/streptomycin (Pen/Streptomycin; Sigma-Aldrich) within 30 min of collection. Subsequently, the tissue was trimmed into pieces using a sterile scalpel blade in a sterile petri dish (catalog no. 101VR20, Thermo Fisher Scientific), and then 800 mg tissue was incubated in duplicate in 5 mL of medium in 6-well plates. Culture media were: ideal profile of EAA as the control (**IPAA**; Lys:Met 2.9:1, Lys:Arg 2:1), increased Met (**incMet**; Lys:Met 2.5:1), increased Arg (**incArg**; Lys:Arg 1:1), or incMet plus incArg (Lys:Met 2.5:1 Lys:Arg 1:1) with or without

100 μ*M* exogenous cell-permeable C2:0-ceramide (catalog no. A7191, Sigma-Aldrich). The dose of C2:0-ceramide was based on a previous adipose tissue in vitro study (Rico et al., 2018).

The 10 EAA (L-isomer, Sigma-Aldrich, St Louis, MO) were added into the custom high-glucose serum-free DMEM (devoid of these 10 EAA, custom made from Gibco, Carlsbad, CA) (Table 6.1). Briefly, the formulation of the EAA was as follows: control medium with the ideal AA ratio (IPAA; Lys:Met 2.9:1; Lys: Arg 2:1; Thr:Phe 1.05:1; Lys:Thr 1.8:1; Lys:His 2.38:1; Lys:Val 1.23:1), incMet (Lys:Met 2.5:1), incArg (Lys:Arg 1:1), and incMetArg (Lys:Met 2.5:1; Lys:Arg 1:1). Media were prepared by increasing only Met, only Arg, or both, while keeping other AA ratios the same as in IPAA. Incubations were carried out in a humidified incubator at 37 °C for 4 h with 5% CO_2. After 4 h incubation, SAT explants were transferred from 6-well plates to screw-capped microcentrifuge tubes, snap-frozen in liquid nitrogen, and preserved at −80 °C until further analysis.

Western Blotting

Total protein was extracted from 200 mg SAT using RIPA Lysis and Extraction Buffer (catalog no. 89900, Thermo Fisher Scientific) containing Halt protease and phosphatase inhibitor cocktail (100×, catalog no. 78442; Thermo Fisher Scientific) following the manufacturer's instructions. The protein concentration was measured using the Pierce BCA protein assay kit (catalog no. 23227; Thermo Fisher Scientific). Details of the western blot procedure were reported previously (Liang et al., 2019b). Briefly, protein samples were denatured by heating at 95 °C for 5 min before loading 20 μL protein into each lane of a 4-20% SDS-PAGE gel (catalog no. 4561094; Bio-Rad). Reactions were run for 10 min at 180 V, and then for 45 to 60 min at 110 V. After activating a polyvinylidene fluoride membrane (catalog no. 1620261; Bio-Rad) with methanol for 1 min, the protein sample was transferred to the membrane in a Trans-Blot SD

Semi-Dry Electrophoretic Transfer Cell (catalog no. 170-3940; Bio-Rad). Membranes were then blocked in 1× Tris-buffered saline (**TBST**) containing 5% nonfat milk for 2 h at room temperature. The whole membrane was cut into small bands based on the molecular weight of target proteins. Membranes were then incubated in 1× TBST containing primary antibodies to mTOR, p-mTOR (Ser2448), AKT, p-AKT (Ser473), eukaryotic elongation factor 2 (**eEF2**), p-eEF2 (Thr56), sodium-coupled neutral amino acid transporter 1 (**SLC38A1**), branched-chain α-keto acid dehydrogenase kinase (**BCKDK**), and GSTM1 overnight at 4 °C; catalog number and dilution ratios are included in Supplemental Table E.3. The protein GSTM1 catalyzes the conjugation of electrophilic compounds with glutathione (**GSH**) to facilitate their degradation or excretion (Strange et al., 2001) and eEF2, a downstream target of mTOR, regulates the translation elongation process (Kaul et al., 2011). Antibodies for mTOR, p-mTOR (Ser2448), eEF2, p-eEF2 (Thr56) (Appuhamy et al., 2011), AKT, p-AKT (Ser473) (Zachut et al., 2013), GSTM1 (Zachut et al., 2017), SLC38A1 and BCKDK (Liang et al., 2019b) have been used previously in bovine samples. Membranes were then washed 6 times with 1× TBST and incubated with anti-rabbit horseradish peroxidase-conjugated secondary antibodies (catalog no. 7074S; dilution 1:800; Cell Signaling Technology, Danvers, MA) for 1 h at room temperature. Subsequently, membranes were washed 6 times with 1× TBST and then incubated with enhanced chemiluminescence reagent (catalog no. 170-5060; Bio-Rad) for 3 min in the dark before image acquisition. Stripping and reprobing a Western blot was used for target proteins and β-actin which has the same or similar molecular weight. β-actin (catalog no. 4967S; Cell Signaling Technology) was used as the internal control. Images were acquired using the ChemiDOC MP Imaging System (Bio-Rad). The intensities of the bands were measured with Image-Pro Plus 6.0 software (Media Cybernetics, Rockville, MD). Specific target protein band density values were

normalized to β-actin density values. Representative blots are included in Supplemental Figure E.1.

Statistical Analysis

All data were analyzed as a 2 × 2 × 2 factorial arrangement of treatments using the MIXED procedure of SAS 9.4 (SAS Institute Inc., Cary, NC). The 3 factors were Met, Arg, and C2:0-ceramide, each including 2 levels: basal or increased levels of Met or Arg and with or without C2:0-ceramide, leading to 8 treatments. The model contained the main effects of Met, Arg, and C2:0-ceramide, as well as the following interactions: Met × Arg × C2:0-ceramide, Met × C2:0-ceramide, Arg × C2:0-ceramide, and Met × Arg. The random effect was individual cow. Variables were assessed for normality of distribution using the Shapiro-Wilk test. Non-normally distributed data were $\log_2$-scale transformed to fit normal distribution of residuals. Least squares means and standard errors were determined using the LSMEANS statement of SAS (SAS Institute Inc.) and were compared using Tukey's test when significant interactions were observed. Significance was determined at $P \leq 0.05$.

RESULTS

There was a Met×Arg×Ceramide interaction for p-AKT, p-mTOR and p-eEF2 ($P<0.01$; $P<0.01$; $P<0.01$; Figure 6.1B and Figure 6.2B and 6.2E). Ceramide stimulation downregulated overall abundance of p-AKT, p-mTOR and p-eEF2 ($P<0.01$; $P<0.01$; $P<0.01$; Table 6.2). Without ceramide stimulation, enhanced Met and Arg alone or in combination led to lower p-mTOR ($P<0.01$; $P<0.01$; $P<0.01$; Figure 6.2B). However, compared with IPAA challenged with ceramide, enhanced Met or Arg supply alone or in combination resulted in greater activation of AKT (p-AKT/total AKT) and mTOR (p-mTOR/total mTOR) ($P<0.01$; $P<0.01$; Figure 6.1C and

Figure 6.2C), with a more pronounced response due to Arg (P<0.01; Figure 6.1C and Figure 6.2C). In contrast, compared with IPAA challenged with ceramide, enhanced Met or Arg supply alone or in combination led to lower activation of eEF2 (p-eEF2/total eEF2) (P<0.01; P<0.01; P<0.01; Figure 6.2F). A Met×Arg×Ceramide interaction was observed for GSTM1 (P<0.01; Figure 6.1D). Ceramide stimulation downregulated overall abundance of GSTM1 (P<0.01; Table 6.2). It is noteworthy that greater Met supply during ceramide stimulation led to the greatest abundance of GSTM1 (P<0.01; Figure 6.1D).

A triple interaction between Met, Arg, and ceramide was observed for the protein abundance of SLC38A1 and BCKDK (P<0.01; P<0.01; Figure 6.3). Ceramide challenge reduced overall protein abundance of SLC38A1 and BCKDK (P<0.01; P<0.01; Table 6.2). With ceramide stimulation, compared with IPAA, greater supply of Met or Arg attenuated the downregulation of BCKDK (P<0.01; P<0.01; Figure 6.3B).

DISCUSSION

An observational study concluded that there is a potentially negative association between oxidative stress and insulin sensitivity in peripartal cows (Abuelo et al., 2016). Furthermore, rodent studies demonstrated that SAT oxidative stress contributes to the development of insulin resistance (Ruskovska and Bernlohr, 2013). Our previous studies consistently demonstrated that achieving a Lys:Met ratio of 2.8:1-2.9:1 by feeding RPM during the periparturient period could ameliorate oxidative stress and inflammation status (Osorio et al., 2013; Zhou et al., 2016; Batistel et al., 2017). A component of those responses is the greater and more consistent DMI and its effect on the synthesis of GSH and taurine, both of which are sulfur-containing antioxidants (Schwab and Broderick, 2017). Compared with cows without RPM supply, peripartal cows fed RPM had greater protein abundance of p-AKT (a key regulator of insulin

signaling) and GSTM1 in SAT, implying that those proteins might be crucial during this challenging physiological stage (Liang et al., 2019a,b). Dairy cows with greater oxidative stress status exhibited reduced protein abundance of GSTM1 in SAT (Zachut et al., 2017, Liang et al., 2019a), suggesting GSTM1 might play a role in alleviating oxidative stress in bovine SAT. In the current study, decreased GSTM1 coupled with lower activation of p-AKT in SAT stimulated with C2:0-ceramide suggested that ceramide not only impairs insulin signaling but may also disrupt redox balance in SAT. Although increased Met had no overall effect on the activation of AKT, it is noteworthy that the greatest protein abundance of GSTM1 in response to enhanced Met supply was observed in SAT challenged with ceramide, suggesting enhanced Met itself might play a positive role under stressful periods.

In non-ruminants, it is well-established that the mTOR signaling pathway is a key regulator of protein synthesis, cell growth, and proliferation (Javed and Fairweather, 2019). Amino acids such as Gln, Arg, and BCAA (particularly Leu) could activate mTOR (Bauchart-Thevret et al., 2010; van der Vos and Coffer, 2012). Despite the fact that greater Met and Arg supply alone or in combination did not reverse the reduction of SLC38A1 under ceramide stimulation, compared with IPAA, greater Met and Arg supply alone led to greater protein abundance of BCKDK. In non-ruminant cells, BCKDK is a rate-limiting enzyme regulating BCAA catabolism via inactivation and phosphorylation of the BCKD complex (Shimomura et al., 2001). Thus, greater protein abundance of BCKDK contributes to decreasing intracellular BCAA catabolism, which might partly explain the greater activation of mTOR (p-mTOR/total mTOR) and lower activation of eEF2 (p-eEF2/total eEF2) in SAT cultured with greater supply of Met or Arg alone and challenged with ceramide. Taken together, our results underscored that ceramide inhibits SLC38A1 abundance in bovine SAT which is likely to cause an intracellular

deficiency of AA. Enhanced supply of AA such as Met and Arg might, to some extent, counteract the negative effect of ceramide on intracellular AA deprivation. Thus, enhanced post-ruminal supply of AA might help maintain SAT homeostasis via enhancing AA availability during the periparturient period.

L-Arg not only acts as a potent regulator of mTOR in ovine adipocyte precursor cells (Ma et al., 2017) but also plays an important role in regulating cellular inflammatory responses in rat and murine macrophages (Rath et al., 2014). These effects might explain the more pronounced response induced by enhanced Arg supply during ceramide stimulation, i.e. attenuation of the activation of mTOR (p-mTOR/mTOR) in spite of lower SLC38A1 and a lack of effect on BCKDK abundance. Data from non-ruminants underscored how mTOR deficiency and ceramides can promote inflammation in SAT by increasing macrophage infiltration (Chimin et al., 2017) and reducing numbers of anti-inflammatory M2 macrophages (Chaurasia et al., 2016). Thus, increases in ceramide concentrations coupled with decreased activation of mTOR are likely to result in a localized inflammatory response within SAT. In bovine cells, enhanced Arg supply alleviated the downregulation of *SLC36A1* and *SLC7A1* mRNA abundance induced by LPS (Dai et al., 2020), underscoring its beneficial effect on immune function (Rath et al., 2014). We speculate that greater Arg supply to SAT could help alleviate inflammation.

Some limitations of the present study should be acknowledged. First, this study only determined the role of Met and Arg in regulating insulin signaling and the mTOR pathway with C2:0-ceramide stimulation under basal conditions without clarifying the effect of insulin. Second, C2:0-ceramide is not found naturally in vivo and therefore may not adequately reflect the ability of naturally occurring, longer-chain ceramides to modify insulin signaling in SAT. Lastly, adipose explants were obtained from late lactation cows; thus, the present data

might not sufficiently demonstrate a beneficial role of Arg and/or Met in regulating insulin signaling during the peripartal period due to obvious physiological differences across stages of lactation. Thus, future in vivo work is warranted to investigate how AA modulate the effect of longer-chain ceramides on insulin signaling in dairy cows, especially during the peripartal period.

Overall, data suggested that stimulation with C2:0-ceramide could inhibit AA uptake by adipose tissue and decrease insulin signaling. Under those conditions, enhancing the supply of Arg or Met contributed to altering AA metabolism by increasing the protein abundance of BCKDK and mTOR pathway activity (Figure 6.4). Unique responses to Arg and Met supply during ceramide stimulation included greater activation of mTOR by Arg, while Met increased the antioxidant response through upregulation of GSTM1. Future in vivo work is warranted to investigate how AA modulate the effect of longer-chain ceramides on insulin signaling in dairy cows, especially during the peripartal period. Focus should be placed not only on SAT but also on immune cell activation.

TABLES AND FIGURES

Table 6.1. Amino acid (AA) composition[1] of the culture media with an ideal AA profile (IPAA) and treatment media supplemented with greater amounts of Arg (incArg), Met (incMet), or both (incMet + incArg) to alter the ratio of Lys:Met and Lys:Arg relative to IPAA.

Amino acid	IPAA[1]	incMet[2]	incArg[3]	incMet+incArg[4]
L-Lys (µg/mL)	175	175	175	175
Lys:Met	2.9:1	2.5:1	2.9:1	2.5:1
Lys: Arg	2:1	2:1	1:1	1:1
L-Met (µg/mL)	60	70	60	70
L-Arg (µg/mL)	84	84	175	175
L-His (µg/mL)	74	74	74	74
L-Ile (µg/mL)	121	121	121	121
L-Leu (µg/mL)	206	206	206	206
L-Phe (µg/mL)	93	93	93	93
L-Thr (µg/mL)	97	97	97	97
L-Trp (µg/mL)	16	16	16	16
L-Val (µg/mL)	142	142	142	142

[1]IPAA = ideal AA profile, used as control medium. Ratios of essential AA are as follows: Lys:Met = 2.9, Lys:Thr = 1.8, Lys:His = 2.38, Lys:Val = 1.23, and Thr:Phe = 1.05, and were based on NRC (2001), Haque et al. (2012), and our previous studies [Li et al. (2016); Dong et al. (2018); Salama et al. (2019); Dai et al. (2019)].

[2]Composition of AA in the medium was prepared as described in our previous study [Dong et al. (2018)].

[3]Level of Met was based on previous in vitro studies from our laboratory (Dong et al. (2018); Dai et al. (2020)].

[4]Level of Arg was based on previous in vitro studies from our laboratory [Salama et al. (2019); Dai et al. (2020)].

Table 6.2. Abundance of proteins (relative to β-actin) related to the mechanistic target of rapamycin (mTOR) and insulin signaling pathways in subcutaneous adipose tissue cultured with different levels of Met or Arg and challenged with ceramide[1].

	Met			Arg			Cer			*P*-value					
Item[2]	-	+	SEM	-	+	SEM	-	+	SEM	Met	Arg	Cer	Met×Arg	Met×Cer	Arg×Cer
Insulin signaling															
AKT/β-actin	1.86	1.36	0.02	1.55	1.63	0.02	2.24	1.13	0.02	<0.01	<0.01	<0.01	<0.01	<0.01	<0.01
p-AKT/β-actin	0.80	0.57	0.02	0.39	1.16	0.03	1.48	0.30	0.04	<0.01	<0.01	<0.01	<0.01	<0.01	0.63
p-AKT/AKT	0.43	0.41	0.01	0.25	0.72	0.02	0.65	0.27	0.02	0.12	<0.01	<0.01	<0.01	<0.01	<0.01
Glutathione metabolism															
GSTM1/β-actin	1.40	2.10	0.02	1.62	1.88	0.02	2.66	0.84	0.02	<0.01	<0.01	<0.01	<0.01	<0.01	<0.01
Amino acid metabolism															
BCKDK/β-actin	1.19	0.88	0.01	0.76	1.37	0.01	1.97	0.53	0.02	<0.01	<0.01	<0.01	<0.01	<0.01	<0.01
SLC38A1/β-actin	0.51	0.60	0.01	0.67	0.46	0.01	1.66	0.19	0.03	<0.01	<0.01	<0.01	<0.01	<0.01	<0.01
mTOR pathway															
mTOR/β-actin	0.71	0.67	0.01	0.81	0.59	0.01	1.10	0.43	0.01	<0.01	<0.01	<0.01	<0.01	<0.01	<0.01
p-mTOR/β-actin	0.82	0.81	0.01	1.01	0.61	0.01	1.12	0.51	0.01	0.41	<0.01	<0.01	0.02	<0.01	<0.01
p-mTOR/mTOR	1.01	0.83	0.01	1.12	0.75	0.02	0.95	0.88	0.01	<0.01	<0.01	<0.01	<0.01	<0.01	<0.01
eEF2/β-actin	1.05	1.08	0.01	0.92	1.21	0.01	1.58	0.55	0.01	0.25	<0.01	<0.01	<0.01	<0.01	<0.01
p-eEF2/β-actin	1.23	1.85	0.01	1.17	1.91	0.01	2.28	0.79	0.01	<0.01	<0.01	<0.01	<0.01	<0.01	<0.01
p-eEF2/eEF2	1.58	1.31	0.02	1.72	1.17	0.02	1.37	1.52	0.02	<0.01	<0.01	<0.01	<0.01	<0.01	<0.01

[1]−Arg, −Met = cultures without increased supply of Arg or Met; +Arg, +Met = cultures with increased supply of Arg or Met; −/+ C2:0-ceramide (Cer), cultures without or with Cer stimulation. Control media contained an ideal AA profile with ratios of Lys:Met 2.9:1 and Lys:Arg 2:1. Treatment media was supplemented with greater amounts of Met or Arg to achieve ratios of Lys:Met 2.5:1 and Lys:Arg 2:1 (incMet), Lys:Met 2.9:1 and Lys:Arg 1:1 (incArg), or Lys:Met 2.5:1 and Lys:Arg 1:1 (incMetArg). Each treatment was challenge with or without 100 μM Cer. Data are LS means, n = 4 cows per group, ± pooled SEMs. Three-way interactions are depicted in Figure 6.1-3.

[2]AKT = protein kinase B; GSTM1 = glutathione S-transferase mu 1; BCKDK = branched-chain α-keto acid dehydrogenase kinase; SLC38A1= solute carrier family 38 member 1; mTOR = mechanistic target of rapamycin; eEF2 = eukaryotic elongation factor 2.

Figure 6.1. Protein abundance (relative to β-actin) of AKT (total, panel A), p-AKT (active, panel B), ratio of p-AKT/AKT (panel C) and GSTM1 (panel D) in subcutaneous adipose tissue cultured with different levels of Met or Arg and challenged with ceramide. Control media contained an ideal AA profile (IPAA) with ratios of Lys:Met 2.9:1 and Lys:Arg 2:1. Treatment media was supplemented with greater amounts of Met or Arg to achieve ratios of Lys:Met 2.5:1 and Lys:Arg 2:1 (incMet), Lys:Met 2.9:1 and Lys:Arg 1:1 (incArg), or Lys:Met 2.5:1 and Lys:Arg 1:1 (incMetArg). Different letters indicate differences between treatments (Met × Arg × Ceramide P <0.05). AKT = protein kinase B; GSTM1 = glutathione S-transferase mu 1. Data are LS means, n = 4 cows per group, ± pooled SEMs.

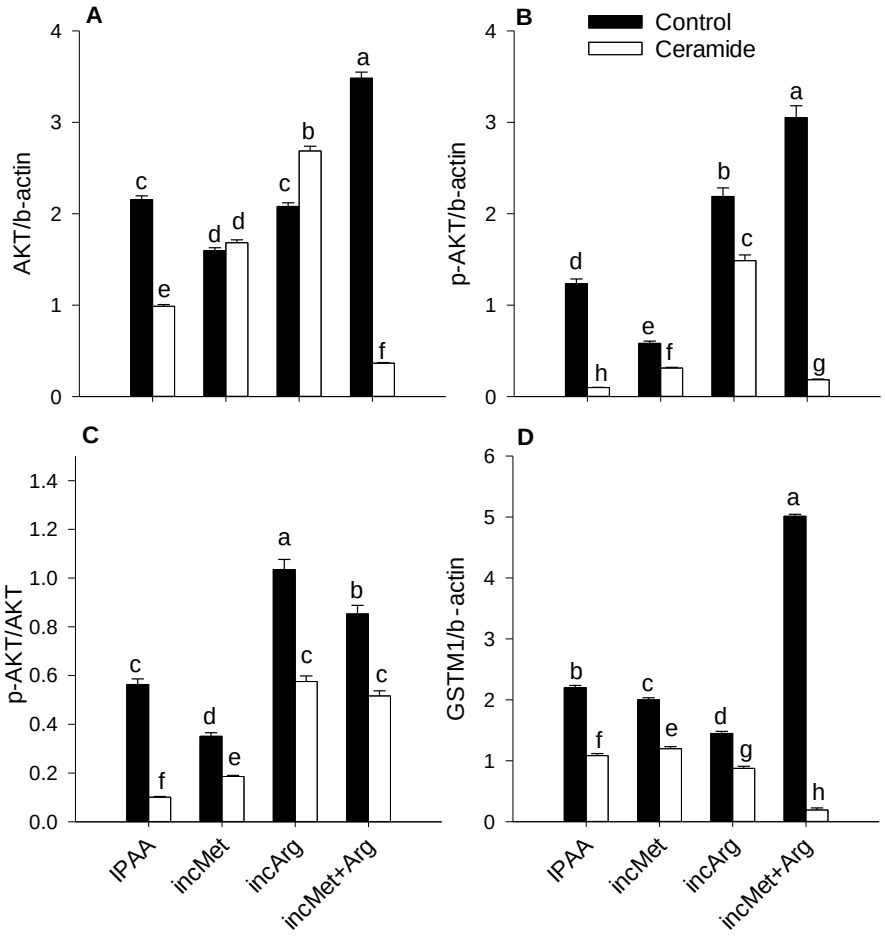

Figure 6.2. Protein abundance (relative to β-actin) of mTOR (total, panel A), p-mTOR (active, panel B), ratio of p-mTOR/mTOR (panel C) eEF2 (total, panel D), p-eEF2 (active, panel E), and ratio of p-eEF2/eEF2 (panel F) in subcutaneous adipose tissue cultured with different levels of Met or Arg and challenged with ceramide. Control media contained an ideal AA profile (IPAA) with ratios of Lys:Met 2.9:1 and Lys:Arg 2:1. Treatment media was supplemented with greater amounts of Met or Arg to achieve ratios of Lys:Met 2.5:1 and Lys:Arg 2:1 (incMet), Lys:Met 2.9:1 and Lys:Arg 1:1 (incArg), or Lys:Met 2.5:1 and Lys:Arg 1:1 (incMetArg). Different lowercase letters indicate differences between treatments (Met × Arg × Ceramide P <0.05). mTOR = mechanistic target of rapamycin; eEF2 = eukaryotic elongation factor 2. Data are LS means, n = 4 cows per group, ± pooled SEMs.

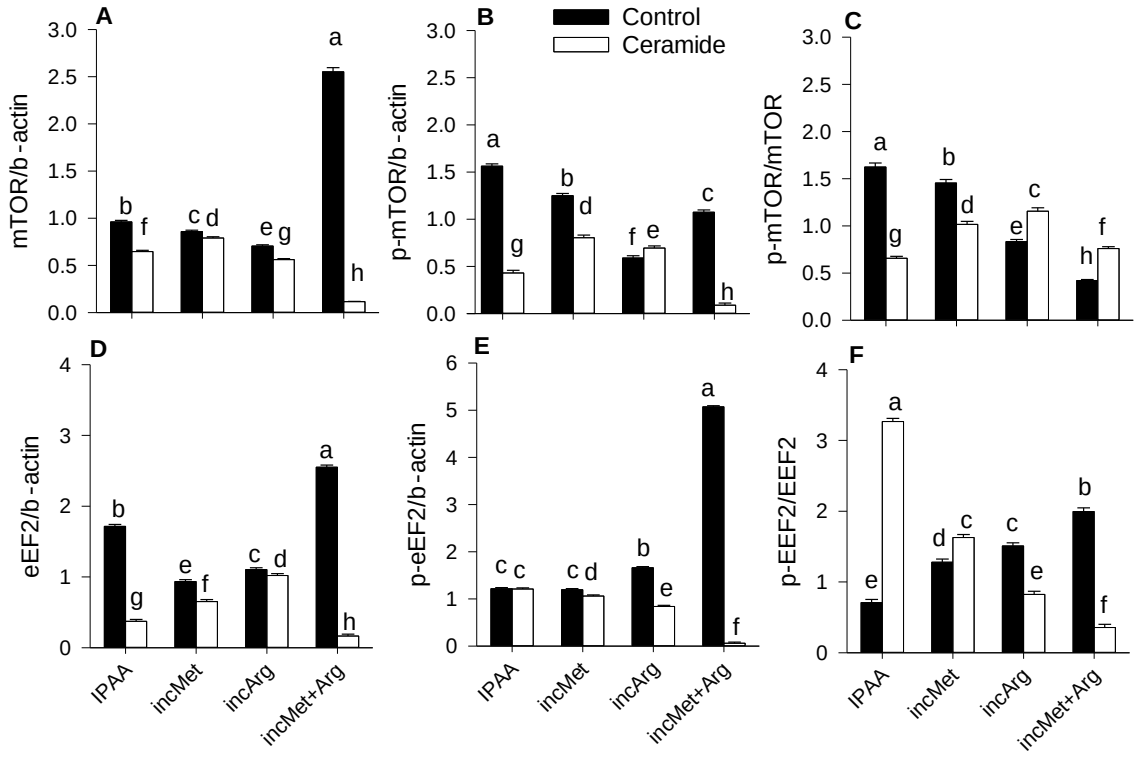

Figure 6.3. Protein abundance (relative to β-actin) of SLC38A1 (panel A) and BCKDK (panel B) in subcutaneous adipose tissue cultured with different levels of Met or Arg and challenged with ceramide. Control media contained an ideal AA profile (IPAA) with ratios of Lys:Met 2.9:1 and Lys:Arg 2:1. Treatment media was supplemented with greater amounts of Met or Arg to achieve ratios of Lys:Met 2.5:1 and Lys:Arg 2:1 (incMet), Lys:Met 2.9:1 and Lys:Arg 1:1 (incArg), or Lys:Met 2.5:1 and Lys:Arg 1:1 (incMetArg). Different letters indicate differences between treatments (Met × Arg × Ceramide $P < 0.05$). SLC38A1= solute carrier family 38 member 1; BCKDK = branched-chain α-keto acid dehydrogenase kinase. Data are LS means, n = 4 cows per group, ± pooled SEMs.

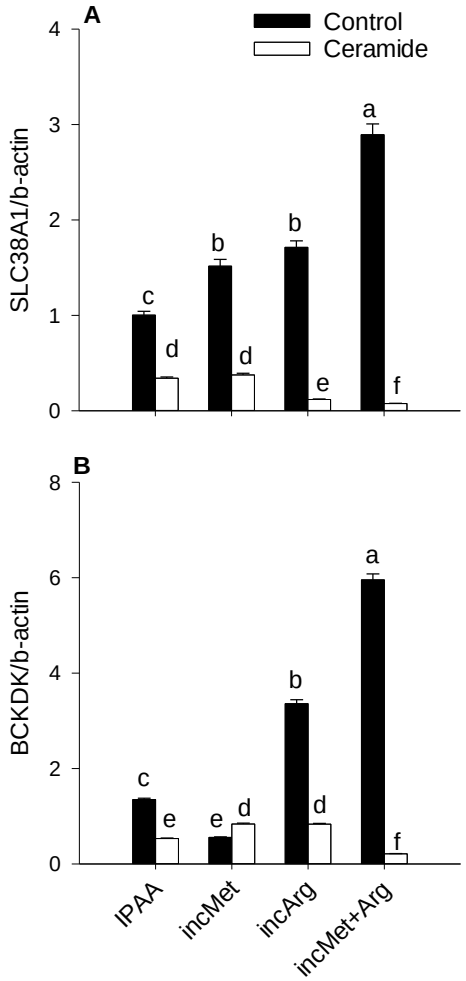

Figure 6.4. Putative model based on available data of protective effects of Met or Arg on adipose tissue challenged with C2:0-ceramide. AKT = protein kinase B; BCAA= branched-chain amino acids; BCKDK = branched-chain α-keto acid dehydrogenase kinase; mTOR = mechanistic target of rapamycin; SLC38A1= solute carrier family 38 member 1; ROS = reactive oxygen species; + = increase; - = decrease.

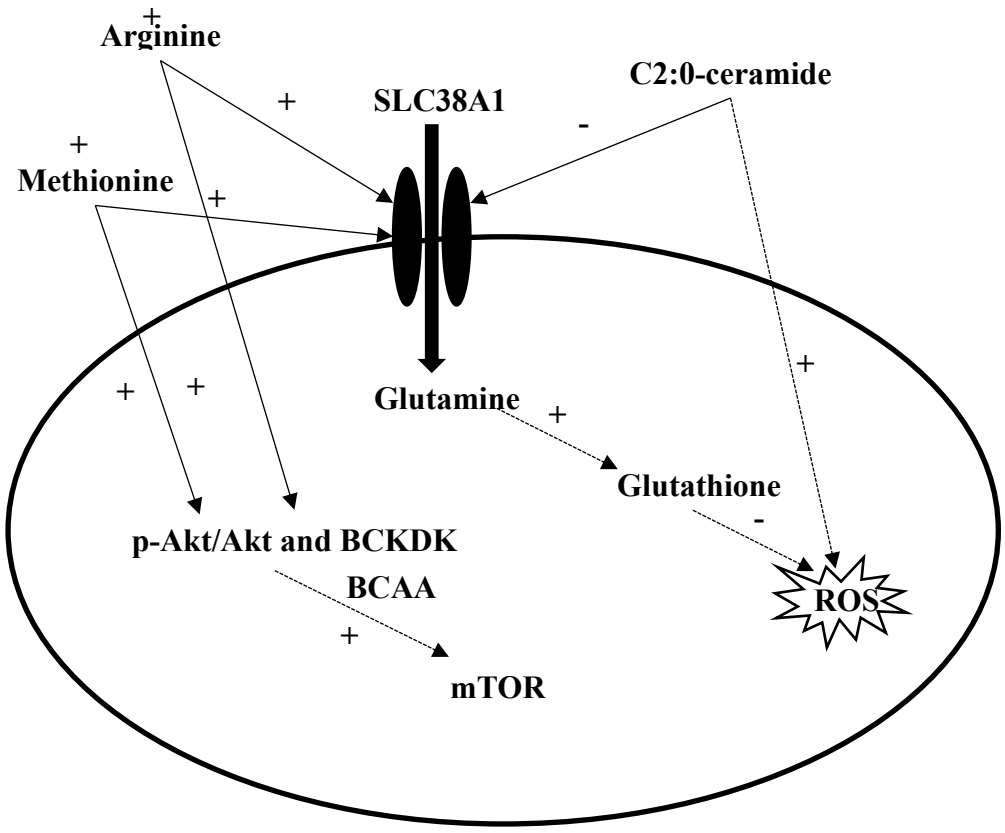

REFERENCES

Abuelo, A., J. Hernández, J. L. Benedito, and C. Castillo. 2016. Association of oxidative status and insulin sensitivity in periparturient dairy cattle: an observational study. J. Anim. Physiol. Anim. Nutr.100:279-286.

Appuhamy, J. R. N., N. A. Knoebel, W. D. Nayananjalie, J. Escobar, and M. D. Hanigan. 2012. Isoleucine and leucine independently regulate mTOR signaling and protein synthesis in MAC-T cells and bovine mammary tissue slices. J. Nutr.142:484-491.

Batistel, F., J. M. Arroyo, A. Bellingeri, L. Wang, B. Saremi, C. Parys, E. Trevisi, F. C. Cardoso, and J. J. Loor. 2017. Ethyl-cellulose rumen-protected methionine enhances performance during the periparturient period and early lactation in Holstein dairy cows. J. Dairy Sci. 100:7455-7467.

Bauchart-Thevret, C., L. Cui, G. Wu, and D. G. Burrin. 2010. Arginine-induced stimulation of protein synthesis and survival in IPEC-J2 cells is mediated by mTOR but not nitric oxide. Am. J. Physiol. Endocrinol. Metab. 299:E899-E909.

Bikman, B. T. and S. A. Summers. 2011. Ceramides as modulators of cellular and whole-body metabolism. J. Clin. Invest. 121:4222-4230.

Bossaert, P., J. L. M. R. Leroy, S. De Vliegher, and G. Opsomer. 2008. Interrelations between glucose-induced insulin response, metabolic indicators, and time of first ovulation in high-yielding dairy cows. J. Dairy Sci. 91:3363-3371.

Chaurasia, B., V. A. Kaddai, G. I. Lancaster, D. C. Henstridge, S. Sriram, D. L. A. Galam, V. Gopalan, K. N. B. Prakash, S. S. Velan, S. Bulchand, T. J. Tsong, M. Wang, M. M. Siddique, G. Yuguang, K. Sigmundsson, N. A. Mellet, J. M. Weir, P. J. Meikle, M. S. Bin M. Yassin, A. Shabbir, J. A. Shayman, Y. Hirabayashi, S.-A. T. E. Shiow, S. Sugii, and S. A. Summers. 2016. Adipocyte ceramides regulate subcutaneous adipose browning, Inflammation, and metabolism. Cell Metab. 24:820-834.

Chimin, P., M. L. Andrade, T. Belchior, V. A. Paschoal, J. Magdalon, A. S. Yamashita, É. Castro, A. Castoldi, A. B. Chaves-Filho, and M. Y. Yoshinaga. 2017. Adipocyte mTORC1 deficiency promotes adipose tissue inflammation and NLRP3 inflammasome activation via oxidative stress and de novo ceramide synthesis. J. Lipid Res. 58:1797-1807.

Dai, H., D. N. Coleman, L. Hu, I. Martinez-Cortés, M. Wang, C. Parys, X. Shen, and J. J. Loor. 2020. Methionine and arginine supplementation alter inflammatory and oxidative stress responses during lipopolysaccharide challenge in bovine mammary epithelial cells in vitro. J. Dairy Sci. 103:676-689.

De Koster, J. D. and G. Opsomer. 2013. Insulin resistance in dairy cows. Vet. Clin. North Am. Food Anim. Pract. 29:299-322.

Ding, L., Y. Shen, Y. Wang, G. Zhou, X. Zhang, M. Wang, J. J. Loor, L. Chen, and J. Zhang. 2019. Jugular arginine supplementation increases lactation performance and nitrogen utilization efficiency in lactating dairy cows. J. Anim. Sci. Biotechnol. 10:3.

Dong, X., Z. Zhou, B. Saremi, A. Helmbrecht, Z. Wang, and J. J. Loor. 2018. Varying the ratio of Lys: Met while maintaining the ratios of Thr: Phe, Lys: Thr, Lys: His, and Lys: Val alters mammary cellular metabolites, mammalian target of rapamycin signaling, and gene transcription. J. Dairy Sci. 101:1708–1718.

Guenther, G. G., E. R. Peralta, K. R. Rosales, S. Y. Wong, L. J. Siskind, and A. L. Edinger. 2008. Ceramide starves cells to death by downregulating nutrient transporter proteins. Proc. Natl. Acad. Sci. U S A.105:17402.

Haque, M. N., H. Rulquin, A. Andrade, P. Faverdin, J. L. Peyraud, and S. Lemosquet. 2012. Milk protein synthesis in response to the provision of an "ideal" amino acid profile at 2 levels of metabolizable protein supply in dairy cows. J. Dairy Sci. 95:5876–5887.

Hu, L., Y. Chen, I. M. Cortes, D. N. Coleman, H. Dai, Y. Liang, C. Parys, C. Fernandez, M. Wang, and J. J. Loor. 2020. Supply of methionine and arginine alters phosphorylation of mechanistic target of rapamycin (mTOR), circadian clock proteins, and α-s1-casein abundance in bovine mammary epithelial cells. Food Funct. 11:883-894.

Hyde, R., E. Hajduch, D. J. Powell, P. M. Taylor, and H. S. Hundal. 2004. Ceramide down-regulates System A amino acid transport and protein synthesis in rat skeletal muscle cells. FASEB J. 19:461-463.

Javed, K. and S. J. Fairweather. 2019. Amino acid transporters in the regulation of insulin secretion and signalling. Biochem Soc Trans. 47:571-590.

Kaul, G., G. Pattan, and T. Rafeequi. 2011. Eukaryotic elongation factor-2 (eEF2): its regulation and peptide chain elongation. Biochem. Funct. 29:227-234.

Lee, P. L., S. M. Jung, and D. A. Guertin. 2017. The complex roles of mechanistic target of rapamycin in adipocytes and beyond. Trends Endocrinol. Metab. 28:319-339.

Li, S., A. Hosseini, M. Danes, C. Jacometo, J. Liu, and J. J. Loor. 2016. Essential amino acid ratios and mTOR affect lipogenic gene networks and miRNA expression in bovine mammary epithelial cells. J. Anim. Sci. Biotechnol. 7:44.

Liang, Y., F. Batistel, C. Parys, and J. J. Loor. 2019a. Glutathione metabolism and nuclear factor erythroid 2-like 2 (NFE2L2)-related proteins in adipose tissue are altered by supply of ethyl-cellulose rumen-protected methionine in peripartal Holstein cows. J. Dairy Sci. 102:5530-5541.

Liang, Y., F. Batistel, C. Parys, and J. J. Loor. 2019b. Methionine supply during the periparturient period enhances insulin signaling, amino acid transporters, and mechanistic target of rapamycin pathway proteins in adipose tissue of Holstein cows. J. Dairy Sci. 102:4403-4414.

Ma, X., M. Han, D. Li, S. Hu, K. R. Gilbreath, F. W. Bazer, and G. Wu. 2017. L-Arginine promotes protein synthesis and cell growth in brown adipocyte precursor cells via the mTOR signal pathway. Amino Acids 49:957-964.

Ma, X. M. and J. Blenis. 2009. Molecular mechanisms of mTOR-mediated translational control. Nat. Rev. Mol. Cell Biol. 10:307-318.

McFadden, J. W. and J. E. Rico. 2019. Invited review: Sphingolipid biology in the dairy cow: The emerging role of ceramide. J. Dairy Sci. 102:7619-7639.

National Research Council. 2001. Nutrient requirements of dairy cattle. 7th rev. ed. Natl. Acad. Press, Washington, DC.

Oikawa, S. and G. R. Oetzel. 2006. Decreased insulin response in dairy cows following a four-day fast to induce hepatic lipidosis. J. Dairy Sci. 89:2999-3005.

Osorio, J. S., P. Ji, J. K. Drackley, D. Luchini, and J. J. Loor. 2013. Supplemental Smartamine M or MetaSmart during the transition period benefits postpartal cow performance and blood neutrophil function. J. Dairy Sci. 96:6248-6263.

Rath, M., I. Müller, P. Kropf, E. I. Closs, and M. Munder. 2014. Metabolism via arginase or nitric oxide synthase: Two competing arginine pathways in macrophages. Front. Immunol. 5:532.
Rico, J. E., V. V. R. Bandaru, J. M. Dorskind, N. J. Haughey, and J. W. McFadden. 2015. Plasma ceramides are elevated in overweight Holstein dairy cows experiencing greater lipolysis and insulin resistance during the transition from late pregnancy to early lactation. J. Dairy Sci. 98:7757-7770.
Rico, J. E., W. A. Myers, D. J. Laub, A. N. Davis, Q. Zeng, and J. W. McFadden. 2018. Hot topic: Ceramide inhibits insulin sensitivity in primary bovine adipocytes. J. Dairy Sci. 101:3428-3432.
Rico, J. E., S. Saed Samii, A. T. Mathews, J. Lovett, N. J. Haughey, and J. W. McFadden. 2017. Temporal changes in sphingolipids and systemic insulin sensitivity during the transition from gestation to lactation. PLoS One 12:e0176787-e0176787.
Ruskovska, T. and D. A. Bernlohr. 2013. Oxidative stress and protein carbonylation in adipose tissue — Implications for insulin resistance and diabetes mellitus. J. Proteomics 92:323-334.
Salama, A. A. K., M. Duque, L. Wang, K. Shahzad, M. Olivera, and J. J. Loor. 2019. Enhanced supply of methionine or arginine alters mechanistic target of rapamycin signaling proteins, messenger RNA, and microRNA abundance in heat-stressed bovine mammary epithelial cells in vitro. J. Dairy Sci. 102:2469–2480.
Schwab, C. G. and G. A. Broderick. 2017. A 100-Year Review: Protein and amino acid nutrition in dairy cows. J. Dairy Sci.100:10094-10112.
Shan, T., P. Zhang, Q. Jiang, Y. Xiong, Y. Wang, and S. Kuang. 2016. Adipocyte-specific deletion of mTOR inhibits adipose tissue development and causes insulin resistance in mice. Diabetologia 59:1995-2004.
Shimomura, Y., M. Obayashi, T. Murakami, and R. A. Harris. 2001. Regulation of branched-chain amino acid catabolism: nutritional and hormonal regulation of activity and expression of the branched-chain α-keto acid dehydrogenase kinase. Opin. Clin. Nutr. Metab. Care 4:419-423.
Strange, R. C., M. A. Spiteri, S. Ramachandran, and A. A. Fryer. 2001. Glutathione-S-transferase family of enzymes. Mutat. Res. 482:21-26.
van der Vos, K. E. and P. J. Coffer. 2012. Glutamine metabolism links growth factor signaling to the regulation of autophagy. Autophagy 8:1862-1864.
Webb, L. A., H. Sadri, K. Schuh, S. Egert, P. Stehle, I. Meyer, C. Koch, G. Dusel, and H. Sauerwein. 2020. Branched-chain amino acids: Abundance of their transporters and metabolizing enzymes in adipose tissue, skeletal muscle, and liver of dairy cows at high or normal body condition. J. Dairy Sci. 103:2847-2863.
Wu, T., C. Wang, L. Ding, Y. Shen, H. Cui, M. Wang, and H. Wang. 2016. Arginine relieves the inflammatory response and enhances the casein expression in bovine mammary epithelial cells induced by lipopolysaccharide. Mediators Inflamm. 2016:9618795.
Zachut, M., H. Honig, S. Striem, Y. Zick, S. Boura-Halfon, and U. Moallem. 2013. Periparturient dairy cows do not exhibit hepatic insulin resistance, yet adipose-specific insulin resistance occurs in cows prone to high weight loss. J. Dairy Sci. 96:5656-5669.
Zachut, M., G. Kra, L. Livshitz, Y. Portnick, S. Yakoby, G. Friedlander, and Y. Levin. 2017. Seasonal heat stress affects adipose tissue proteome toward enrichment of the Nrf2-mediated oxidative stress response in late-pregnant dairy cows. J. Proteomics 158:52-61.

Zhao, F. F., T. Y. Wu, H. R. Wang, L. Y. Ding, G. Ahmed, H. W. Li, W. Tian, and Y. Z. Shen. 2018. Jugular arginine infusion relieves lipopolysaccharide-triggered inflammatory stress and improves immunity status of lactating dairy cows. J. Dairy Sci. 101:5961-5970.
Zhou, Z., M. Vailati-Riboni, E. Trevisi, J. K. Drackley, D. N. Luchini, and J. J. Loor. 2016. Better postpartal performance in dairy cows supplemented with rumen-protected methionine compared with choline during the peripartal period. J. Dairy Sci. 99:8716-8732.

CHAPTER 7: HYDROGEN PEROXIDE AND METHIONINE SUPPLEMENTATION ALTER COMPONENTS OF INSULIN AND ANTIOXIDANT PROTEIN NETWORKS IN SUBCUTANEOUS BOVINE ADIPOSE EXPLANTS TO DIFFERENT EXTENTS

INTRODUCTION

Dairy cows experience negative energy balance (**NEB**) along with systemic inflammation and oxidative stress during the periparturient period (Sordillo and Aitken, 2009, Sordillo and Raphael, 2013, Bradford et al., 2015). Body fat mobilization during NEB helps fill the deficit between intake and requirements in peripartal cows (Loor et al., 2013), but excessive lipolysis could deplete the tissue's antioxidant reserves (Contreras et al., 2017b). Together, lipolysis, inflammation, and oxidative stress appear closely associated with insulin resistance and could delay the recovery of fat depots in dairy cows (McNamara and Huber, 2018). In non-ruminants, oxidative stress is considered a major contributing factor of insulin resistance, negatively affecting the control of glucose uptake, protein synthesis, lipogenesis, and aggravating lipolysis (Hurrle and Hsu, 2017; Curtis et al., 2010). Whether oxidative stress regulates insulin signaling or some of its components in bovine adipose tissue is still unclear.

Methionine (**Met**), an indispensable amino acid in lactating cows, not only improves milk protein production (Sun et al., 2016) but enhances innate immune response at the functional and transcriptional level (Zhou et al., 2016, Batistel et al., 2018, Lopreiato et al., 2019). Glutathione (**GSH**) is a major antioxidant in mammalian cells synthesized from the metabolism of Met via the transsulfuration pathway (Martinov et al., 2010). It helps remove reactive oxygen species via GSH-dependent glutathione peroxidase (**GPX**)-catalyzed reactions within the cytosol (Lushchak,

2012). Recently, our group reported that feeding rumen-protected Met at a rate of approximately 0.09% of dry matter intake to periparturient cows led to greater mRNA (cystathionine-β-synthase, glutamate-cysteine ligase modifier subunit, glutathione reductase, and *GPX1*) and protein abundance [GPX1, GPX3, glutathione S-transferase mu 1 (**GSTM1**), and glutathione S-transferase α 4] of targets associated with GSH metabolism in s.c. adipose tissue (**SAT**) (Liang et al., 2019). Whether Met supply was directly responsible for those molecular alterations is unknown.

The main objective of the current study was to generate investigate the effect of Met on insulin, amino acid, inflammation, and antioxidant signaling-related molecular networks in explants of SAT from Holstein cows. Because hydrogen peroxide (**H_2O_2**) is a typical "redox switch" that could lead to vicious cycles of redox stimulation (Hurrle and Hsu, 2017), it was chosen to challenge the SAT.

MATERIALS AND METHODS

Adipose Explant Culture and Treatments

All procedures were conducted under protocols approved by the University of Illinois Institutional Animal Care and Use Committee (Urbana; protocol # 19036). Four healthy multiparous lactating Holstein cows from the University of Illinois dairy herd were used. Average parity, DIM, and milk yield before slaughter were 4, 248 d, and 27.0 kg/d, respectively. Cows were euthanized by captive bolt at the College of Veterinary Medicine diagnostic facilities

(University of Illinois). Samples of SAT from the tail-head of each cow were obtained immediately post-slaughter and brought to the laboratory in Dulbecco's Modified Eagle's Medium and Ham's F-12 nutrient mixture (DMEM: F-12; Sigma-Aldrich, St. Louis, MO) containing 1% penicillin/streptomycin (Pen/Streptomycin; Sigma-Aldrich) within 30 min of collection. Subsequently, tissue was trimmed into pieces using a sterile scalpel blade in a sterile petri dish (catalog no. 101VR20, Thermo Fisher Scientific), and then 800 mg of tissue was incubated in duplicate in 5 mL of medium in 6-well plates. Culture media were (Dong et al., 2018; Vailati-Riboni et al., 2019; Dai et al., 2020): control media with an "ideal" profile of essential amino acids (**CTR**; Lys:Met 2.9:1), CTR plus 100 μM H_2O_2 (**HP**), CTR with enhanced Met supply plus 100 μM H_2O_2 (**HPMET**; Lys:Met 2.5:1) (Table 7.1). Incubations were carried out in a humidified incubator with 5% CO_2 at 37 °C. After 4 h incubation, SAT explants were transferred from 6-well plates to screw-capped microcentrifuge tubes, snap-frozen in liquid nitrogen, and preserved at −80 °C until further analysis.

RNA Isolation, cDNA synthesis, and Quantitative PCR

Detailed procedures for measuring target mRNA abundance have been reported in several of our previous publications (Han et al., 2018b, Dai et al., 2020). Briefly, total RNA was isolated from SAT using a miRNeasy kit (catalog no. 217004; Qiagen, Hilden, Germany) following the manufacturer's instruction. The concentration of RNA was measured with a NanoDrop ND-1000 spectrophotometer (Thermo Fisher Scientific, Waltham, MA). Quality of

RNA samples was ascertained further with the Agilent 2100 Bioanalyzer (Agilent Technologies, Santa Clara, CA). Total RNA (100 ng/µL RNAse-free water) was reverse transcribed to cDNA. After 1:4 dilution, the cDNA was used for qPCR. The qPCR system included SYBR Green Fast Mix ROX (catalog no. 101414-280; Quanta Biosciences, Gaithersburg, MD), forward and reverse primers and nuclease-free water. The qPCR was operated in an ABI Prism 7900 HT SDS instrument (Applied Biosystems). Ribosomal protein S9, *GAPDH*, and *ACTB* were chosen as internal control genes to normalize mRNA data by their geometric mean. For each gene, normalized qPCR data are presented as fold-change relative to CTR. To estimate standard errors for CTR data and prevent biases in statistical analysis, normalized data were transformed to obtain a perfect mean of 1.0, leaving the proportional difference between the biological replicate. The same proportional change was calculated for the treatment groups to obtain a fold-change relative to CTR. All reactions were run in triplicate. Gene symbols, primer information, and qPCR performance are included in Supplemental Table F.1 and F.2.

Western Blotting

Details of the western blot procedure were reported previously (Batistel et al., 2017). Briefly, approximately 100 mg adipose tissue was homogenized in 1 mL RIPA Lysis and Extraction Buffer (catalog no. 89900, Thermo Fisher) containing Halt protease and phosphatase inhibitor cocktail (100x, catalog no. 78442; Thermo Fisher Scientific) for 60 s and then place on ice for 20 min. The lysate was centrifuged at 14,000 × *g* for 15 min at 4 °C. The protein

concentration of the supernatant was determined using the Pierce bicinchoninic acid protein assay kit (catalog no. 23227, Thermo Scientific). Protein samples were denatured by heating at 95 °C for 5 min before loading 20 μL protein into each lane of 4% to 20% Mini-Protean TGX precast gels (catalog no. 4561093, Bio-Rad) and transferred onto a polyvinylidene difluoride (PVDF) membrane (catalog no. 1620261, Bio-Rad) in a Trans-Blot SD Semi-Dry Electrophoretic Transfer Cell (catalog no. 170-3940, Bio-Rad). After blocking with 5% nonfat milk in 1× Tris-buffered saline (1×TBST) at room temperature for 2 h, the membrane was incubated with primary antibodies overnight at 4 °C. The membrane was washed with 1×TBST, and incubated with HRP goat anti-rabbit IgG as the secondary antibody (catalog no. 7074S; Cell Signaling Technology, diluted to 1:1000) for 1 h. Visualization of target proteins was performed using the Clarity Western ECL Substrate (catalog no. 170-5060, Bio-Rad). Each protein was normalized against the expression of GAPDH, and data reported as a relative expression. The ECL signals were acquired using an imaging system (ChemiDoc MP, Bio-Rad), and the intensities of the bands were analyzed using Image-Pro Plus 6.0 software (Bio-Rad). All information for primary antibodies is listed in Supplemental Table F.3.

Statistical Analysis

Data were analyzed using the MIXED procedure of SAS 9.4 (SAS Institute Inc., Cary, NC) according to the following model with repeated measures:

$$Yj = \mu + Mj + ej,$$

where Yj = dependent, continuous variable, μ = overall mean, Mj = fixed effect of treatment (j = control, HP, or HPMET) and ej = residual error. Cow was the random effect. When treatment was significant, least squares means separation between groups was performed using the PDIFF statement with Tukey adjustment. Normality of the residuals was checked with normal probability and box plots, and homogeneity of variances was checked with plots of residuals versus predicted values. Significance was set at $P \leq 0.05$.

RESULTS

Abundance of Insulin and Amino Acid Metabolism-Related Proteins.

Treatment had a significant effect (Table 7.2) on the protein abundance of p-AKT ($P = 0.05$), p-mTOR ($P < 0.01$), phosphorylated 5'-prime-AMP-activated protein kinase (**p-AMPK**; $P = 0.05$) and fatty acid synthase (**FASN**; $P = 0.05$). Compared with CTR, abundance of p-AKT ($P = 0.05$) and p-mTOR ($P < 0.01$) was downregulated by H_2O_2 treatment. Compared with HP, enhanced Met supply resulted in greater protein abundance of p-AMPK and FASN. Additionally, treatment tended to influence the protein abundance of S-adenosylmethionine sensor upstream of TORC1 (**SAMTOR**; $P = 0.08$) and hormone-sensitive lipase (**LIPE**; $P = 0.10$). This occurs due to downregulation of SAMTOR and LIPE caused by H_2O_2 challenge along with upregulation of LIPE in response to enhanced Met supply. Treatment had a significant effect on the insulin-induced glucose transport carrier, solute carrier family 2 member 4 (**SLC2A4**) ($P = 0.05$; Table

7.2). Compared with CTR, HP led to downregulation of SLC2A4, and supply of Met restored protein abundance to the levels detected with CTR.

Abundance of Immune Response Proteins and Genes.

Protein abundance of nuclear factor-kappa B subunit p65 (a.k.a. **RELA**) ($P = 0.02$; Table 7.3) was significantly affected by treatment. Although HP did not affect protein abundance of RELA, the protein abundance of RELA was greater in response to HPMET. At the mRNA level, abundance of the cytokines *IL6, TNF*, *Il10,* and *IL1B* was not affected by treatment (All $P > 0.10$; Table 7.4).

Abundance of Antioxidant Signaling and Met Metabolism-related Proteins.

Treatment affected the protein abundance of GPX1, the antioxidant transcription regulator nuclear factor, erythroid 2 like 2 (**NFE2L2**), and the cytosolic oxidant product detoxification enzyme GSTM1 (Table 7.3). Compared with the HP cultures, enhanced supply of Met led to greater NFE2L2 ($P = 0.03$) and GPX1 ($P = 0.05$), but lower GSTM1 ($P = 0.02$) protein abundance.

DISCUSSION

Work from our laboratory using transcriptomics and bioinformatics on adipose tissue from peripartal or dry cows (Minuti et al., 2020; Moisa et al., 2017) has uncovered several biologically relevant pathways, of which AA signaling via mTOR seems particularly important given its role in coordinating aspects of tissue protein synthesis as a function of AA availability.

In non-ruminants, the mechanistic target of rapamycin C1 (**mTORC1**) silencing contributes to the manifestation of some stress-related phenotypes, suggesting that signaling through this kinase could regulate aspects of adipose tissue function (Cai et al., 2016). For instance, adipocyte mTORC1 deficiency in mice markedly decreased adipose tissue storage along with insulin resistance (Chimin et al., 2017). Activation of mTOR affects oxidative stress by regulating mitochondrial biogenesis and oxidative metabolism (Cunningham et al., 2007), while ROS production contributes to the inhibition of mTOR signaling (Zhao et al., 2017). Thus, a decrease in protein abundance of AKT and mTOR in adipose explants challenged with H_2O_2 suggested that intracellular oxidants might impair some aspects of normal bovine adipose function.

At least in non-ruminants, insulin signaling controls glucose absorption, lipogenesis, lipolysis, and protein synthesis (Kenez et al., 2019), all of which play vital roles in adipose tissue metabolism. A transient state of insulin resistance around parturition prevents peripheral tissues from using glucose to guarantee glucose supply for the mammary gland (Contreras et al., 2017a); however, prolonged insulin resistance contributes to the development of metabolic diseases such as ketosis and fatty liver. The fact that downregulation of SLC2A4 caused by oxidative stress dampened the sensitivity of adipose tissue to insulin (Hurrle and Hsu, 2017) led us to speculate that the H_2O_2 challenge resulted in oxidative stress and a subsequent decrease in protein abundance of SLC2A4.

The AMP-activated protein kinase plays an important role in controlling cellular energy homeostasis, partly through its role in altering glucose uptake via enhancing the translocation of intracellular storage vesicles of SLC2A4 to the plasma membrane (Hardie et al., 2012). Thus, upregulation of p-AMPK in response to enhanced Met supply partly explained the increase in protein abundance of SLC2A4. Activation of AMPK reduced de novo fatty acid synthesis by downregulating ACACA and *FASN* mRNA in bovine mammary epithelial cells (McFadden and Corl, 2009). Thus, the upregulation of p-AMPK and FASN in response to Met supply suggested this AA might contribute to de novo fatty acid synthesis independent of the AMPK pathway. Whether other AA in the culture medium induced a "lipogenic effect", e.g., by feeding the TCA cycle, cannot be discerned. Future research is warranted to investigate the mechanisms whereby Met and other AA may participate in the regulation of lipid synthesis in bovine adipose tissue.

At least in non-ruminants, nuclear factor, erythroid 2 like 2, a master regulator of cellular redox homeostasis, controls the transcription of many anti-oxidant enzymes such as superoxide dismutase (**SOD**), glutathione peroxidase, *CAT*, NAD(P)H dehydrogenase 1, and GSH metabolism-related enzymes (e.g., *GSR*, *GPX1*, *GPX2*, and *GPX3*) (Lushchak, 2012). Kelch-like ECH-associated protein 1 (**KEAP1**), a negative regulator of NFE2L2, prevents movement of the NFE2L2 protein into the nucleus of the cell, hence, inhibiting its activity. Greater rumen-protected Met (**RPM**) supplementation upregulated NFE2L2 and downregulated KEAP1 in bovine mammary tissue during the periparturient period (Han et al., 2018a). In addition,

compared with controls, RPM led to greater abundance of p-NFE2L2 in SAT at 30 d after parturition (Liang et al., 2019). Thus, available data suggested that increased post-ruminal Met supply might alter the interactions between NFE2L2 and KEAP1 with a net result of enhancing the antioxidant activity of the tissue.

Glutathione S-transferase mu 1, one of the GSH S-transferases, catalyzes the conjugation of GSH to electrophilic compounds (Han et al., 2018b), which led us to speculate that greater protein abundance of GSTM1 in bovine SAT from cows fed RPM was indicative of a reduction in oxidant status within the tissue (Liang et al., 2019). As such, the observed downregulation of GSTM1 in explants receiving added Met was somewhat unexpected. It could be possible that inherent differences in the responsiveness of SAT around parturition than later in lactation (Contreras et al., 2017b) account for some of these differences.

The complex formed by NF-κB and RELA mediates the transcription of pro-inflammatory cytokines such as *IL1B*, *IL6*, and *TNF* (Vallabhapurapu and Karin, 2009). In a previous in vitro study, we demonstrated that greater supply of Met reduced pro-inflammatory responses in bovine mammary epithelial cells exposed to a short-term challenge with lipopolysaccharide (Dai et al., 2020). Although the upregulation of RELA in response to Met supply in explants challenged with H_2O_2 appears paradoxical given the positive effect of this AA on NFE2L2 and GPX1, it could be possible that activation of the immune response under the conditions of the study represented a homeostatic response (Contreras et al., 2017b). Our

previous work and others have clearly demonstrated that immune responsiveness of SAT is an inherent feature of the tissue, which serves key functions such as allowing proper remodeling (Vailati-Riboni et al., 2016; Lopreiato et al., 2018; Moisa et al., 2017).

CONCLUSIONS AND PERSPECTIVES

Although direct measures of oxidant and antioxidant molecules were not performed, the responses observed indicated that exogenous H_2O_2 was able to alter tissue oxidant status. The short-term stimulation of adipose tissue with H_2O_2 had a negative effect on some of the components of insulin signaling. Overall, increasing the supply of Met attenuated the decrease in abundance of insulin signaling-related proteins and seemed to enhance NFE2L2 and GSH-related anti-oxidant responses (Figure 7.1). Further in vivo research is warranted to investigate the role of Met and other AA in regulating immune, antioxidant, and metabolic systems in bovine adipose tissue. Such work should encompass not only molecular tools, but also mass spectrometry, isotopic tracing technologies, and enzyme activity for key enzymes in those pathways.

TABLES AND FIGURE

Table 7.1. Amino acid (AA) composition of control media with an "ideal" profile of essential AA (CTR; Lys: Met 2.9:1), CTR plus 100 μM H_2O_2 (HP), and CTR with added Met plus 100 μM H_2O_2 (HPMET; Lys:Met 2.5:1).

	Treaments		
Item	CTR[1]	HP	HPMET
L-lysine (μg/mL)	175	175	175
Lys:Met	2.9:1	2.9:1	2.5:1
L-methionine (μg/mL)	60	60	70
L-arginine (μg/mL)	84	84	84
L-histidine (μg/mL)	74	74	74
L-isoleucine (μg/mL)	121	121	121
L-leucine (μg/mL)	206	206	206
L-phenylalanine (μg/mL)	93	93	93
L-threonine (μg/mL)	97	97	97
L-tryptophan (μg/mL)	16	16	16
L-valine (μg/mL)	142	142	142

[1]CTR: control media with an "ideal" profile of essential amino acids (AA) (ratio of EAA as follows: Lys:Met = 2.9, Lys:Thr = 1.8, Lys:His = 2.38, Lys:Val = 1.23, and Thr:Phe = 1.05) according to published recommendations (National Research Council, 2001, Haque et al., 2012) and our previous studies (Li et al., 2016, Vailati-Riboni et al., 2019). The level of added Met in the HPMET treatment was according to our previous work (Dong et al., 2018).

Table 7.2. Abundance of proteins associated with insulin and amino acid signaling, transsulfuration, and nutrient transporters in subcutaneous adipose tissue (SAT; n = 4/treatment) cultured in media with an "ideal" profile of essential amino acids (CTR; Lys: Met 2.9:1), SAT incubated with CTR plus 100 μM H_2O_2 (HP), or SAT incubated with CTR plus enhanced Met supply plus 100 μM H_2O_2 (HPMET; Lys:Met 2.5:1).

Item[1]	Treatments			SEM	*P* - value
	CTR	HP	HPMET		
Insulin signaling					
p-AKT	1.00[a]	0.26[b]	0.27[b]	0.21	0.05
PPARG	1.00	0.56	0.87	0.16	0.25
p-ACACA	1.00	1.24	0.71	0.21	0.24
FASN	1.00[b]	0.93[b]	1.78[a]	0.21	0.05
p-AMPK	1.00[b]	0.81[b]	2.76[a]	0.47	0.05
LIPE	1.00	0.54	1.02	0.15	0.10
Amino acid signaling					
p-mTOR	1.00[a]	0.40[b]	0.20[b]	0.08	<0.01
SAMTOR	1.00	0.48	0.41	0.17	0.08
Transsulfuration					
CBS	1.00	0.50	0.76	0.32	0.59
Glucose and amino acid transport					
SLC1A3	1.00	0.70	0.90	0.30	0.87
SLC2A4	1.00[ab]	0.48[b]	1.23[a]	0.19	0.05

[1]CBS= Cystathionine β-synthase; FASN= Fatty acid synthase; LIPE= Hormone-sensitive lipase; p-ACACA= Phosphorylated acetyl-CoA carboxylase alpha; p-AKT= Phosphorylated AKT serine/threonine kinase; p-AMPK= Phosphorylated 5'-prime-AMP-activated protein kinase; p-mTOR= Phosphorylated mechanistic target of rapamycin; PPARG= Peroxisome proliferator activated receptor gamma; SAMTOR= S-adenosylmethionine sensor upstream of TORC1; SLC1A3= Solute carrier family 1 member 3; SLC2A4= Solute carrier family 2 member 4(GLUT4).
[a-c]Means between treatment with different lowercase superscripts differ ($P \leq 0.05$).

Table 7.3. Abundance of proteins involved in inflammation and anti-oxidation in subcutaneous adipose tissue (SAT; n = 4/treatment) cultured in media with an "ideal" profile of essential amino acids (CTR; Lys: Met 2.9:1), SAT incubated with CTR plus 100 μM H_2O_2 (HP), or SAT incubated with CTR plus enhanced Met supply plus 100 μM H_2O_2 (HPMET; Lys:Met 2.5:1).

	Treatments				
Item[1]	CTR	HP	HPMET	SEM	*P*-value
Inflammation					
RELA	1.00[b]	0.64[b]	1.83[a]	0.25	0.02
Antioxidant signaling					
NFE2L2	1.00[b]	0.99[b]	3.82[a]	0.65	0.03
KEAP1	1.00	1.61	2.01	0.35	0.27
Glutathione metabolism					
GPX1	1.00[b]	0.60[b]	1.95[a]	0.28	0.05
GSTM1	0.98[a]	0.79[a]	0.43[b]	0.11	0.02

[1]GPX1= Glutathione peroxidase 1; GSTM1= Glutathione S-transferase mu 1; KEAP1= Kelch-like ECH-associated protein 1; NFE2L2= Nuclear factor, erythroid 2 like 2; RELA= Nuclear factor kappa B subunit p65.

[a-c]Means between treatment with different lowercase superscripts differ ($P \leq 0.05$).

Table 7.4. mRNA abundance of inflammation, antioxidant, and glutathione metabolism-related genes in subcutaneous adipose tissue (SAT; n = 4/treatment) cultured in media with an "ideal" profile of essential amino acids (CTR; Lys: Met 2.9:1), SAT incubated with CTR plus 100 μM H_2O_2 (HP), or SAT incubated with CTR plus enhanced Met supply plus 100 μM H_2O_2 (HPMET; Lys:Met 2.5:1).

	Treatments				
Item[1]	CTR	HP	HPMET	SEM	*P*-value
Inflammation					
IL6	1.00	0.90	0.76	0.11	0.34
TNF	1.00	0.44	0.51	0.27	0.33
IL10	1.00	0.53	0.57	0.16	0.15
IL1B	1.00	0.52	0.48	0.27	0.37
Antioxidant enzymes					
SOD1	1.00	1.04	0.85	0.06	0.14
SOD2	1.00	0.71	0.68	0.19	0.47
CAT	1.00	1.40	1.16	0.10	0.07

[1]*CAT* = Catalase; *IL6* = Interleukin 6; *IL10* = Interleukin 10; *IL1B* = Interleukin 1β; *SOD1* = Superoxide dismutase 1; *SOD2* = Superoxide dismutase 2, mitochondrial; *TNF* = Tumor necrosis factor.

Figure 7.1. Putative model based on available data of protective effects of Methionine on adipose tissue challenged with hydrogen peroxide. GPX1 = glutathione peroxidase 1; NFE2L2 = nuclear factor, erythroid 2 like 2; FASN = fatty acid synthase; ROS = reactive oxygen species; SLC2A4 = solute carrier family 2 member 4 (GLUT4); + = increase; - = decrease.

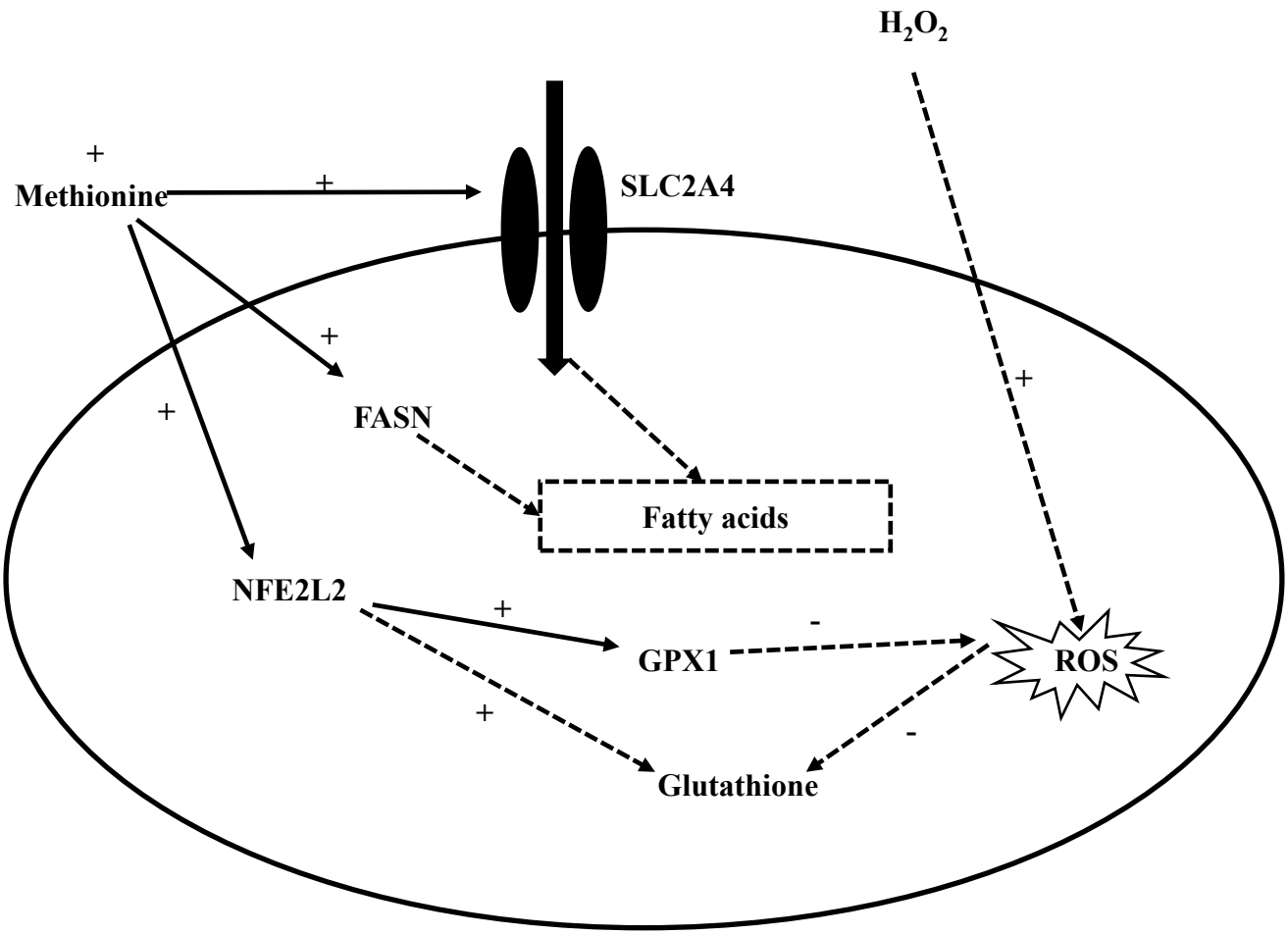

REFERENCES

Batistel, F., A. S. Alharthi, L. Wang, C. Parys, Y. X. Pan, F. C. Cardoso, and J. J. Loor. 2017. Placentome nutrient transporters and mammalian target of rapamycin signaling proteins are altered by the methionine supply during late gestation in dairy cows and are associated with newborn birth weight. J. Nutr. 147:1640-1647.

Batistel, F., J. M. Arroyo, C. I. M. Garces, E. Trevisi, C. Parys, M. A. Ballou, F. C. Cardoso, and J. J. Loor. 2018. Ethyl-cellulose rumen-protected methionine alleviates inflammation and oxidative stress and improves neutrophil function during the periparturient period and early lactation in Holstein dairy cows. J. Dairy Sci. 101:480-490.

Bradford, B. J., K. Yuan, J. K. Farney, L. K. Mamedova, and A. J. Carpenter. 2015. Invited review: Inflammation during the transition to lactation: New adventures with an old flame. J. Dairy Sci. 98:6631-6650.

Cai, H., L. Q. Dong, and F. Liu. 2016. Recent advances in adipose mTOR signaling and function: therapeutic prospects. Trends Pharmacol. Sci. 37:303-317.

Chimin, P., M. L. Andrade, T. Belchior, V. A. Paschoal, J. Magdalon, A. S. Yamashita, E. Castro, A. Castoldi, A. B. Chaves-Filho, M. Y. Yoshinaga, S. Miyamoto, N. O. Camara, and W. T. Festuccia. 2017. Adipocyte mTORC1 deficiency promotes adipose tissue inflammation and NLRP3 inflammasome activation via oxidative stress and de novo ceramide synthesis. J. Lipid Res. 58:1797-1807.

Contreras, G. A., C. Strieder-Barboza, J. de Souza, J. Gandy, V. Mavangira, A. L. Lock, and L. M. Sordillo. 2017a. Periparturient lipolysis and oxylipid biosynthesis in bovine adipose tissues. PLoS One 12:e0188621.

Contreras, G. A., C. Strieder-Barboza, and W. Raphael. 2017b. Adipose tissue lipolysis and remodeling during the transition period of dairy cows. J. Anim. Sci. Biotechnol. 8:41.

National Research Council. 2001. Nutrient requirements of dairy cattle. 7th rev. ed. Natl. Acad. Press, Washington, DC.

Cunningham, J. T., J. T. Rodgers, D. H. Arlow, F. Vazquez, V. K. Mootha, and P. Puigserver. 2007. mTOR controls mitochondrial oxidative function through a YY1-PGC-1alpha transcriptional complex. Nature 450:736-740.

Curtis, J. M., P. A. Grimsrud, W. S. Wright, X. Xu, R. E. Foncea, D. W. Graham, J. R. Brestoff, B. M. Wiczer, O. Ilkayeva, K. Cianflone, D. E. Muoio, E. A. Arriaga, and D. A. Bernlohr. 2010. Downregulation of adipose glutathione s-transferase A4 leads to increased protein carbonylation, oxidative stress, and mitochondrial dysfunction. Diabetes 59:1132-1142.

Dai, H., D. N. Coleman, L. Hu, I. Martinez-Cortes, M. Wang, C. Parys, X. Shen, and J. J. Loor. 2020. Methionine and arginine supplementation alter inflammatory and oxidative stress responses during lipopolysaccharide challenge in bovine mammary epithelial cells in vitro. J. Dairy Sci. 103:676-689.

Dong, X., Z. Zhou, B. Saremi, A. Helmbrecht, Z. Wang, and J. J. Loor. 2018. Varying the ratio of Lys:Met while maintaining the ratios of Thr:Phe, Lys:Thr, Lys:His, and Lys:Val alters mammary cellular metabolites, mammalian target of rapamycin signaling, and gene transcription. J. Dairy Sci. 101:1708-1718.

Han, L., F. Batistel, Y. Ma, A. S. M. Alharthi, C. Parys, and J. J. Loor. 2018a. Methionine supply alters mammary gland antioxidant gene networks via phosphorylation of nuclear factor

erythroid 2-like 2 (NFE2L2) protein in dairy cows during the periparturient period. J. Dairy Sci. 101:8505-8512.
Han, L. Q., Z. Zhou, Y. Ma, F. Batistel, J. S. Osorio, and J. J. Loor. 2018b. Phosphorylation of nuclear factor erythroid 2-like 2 (NFE2L2) in mammary tissue of Holstein cows during the periparturient period is associated with mRNA abundance of antioxidant gene networks. J. Dairy Sci. 101:6511-6522.
Haque, M. N., H. Rulquin, A. Andrade, P. Faverdin, J. L. Peyraud, and S. Lemosquet. 2012. Milk protein synthesis in response to the provision of an "ideal" amino acid profile at 2 levels of metabolizable protein supply in dairy cows. J. Dairy Sci. 95:5876-5887.
Hardie, D. G., F. A. Ross, and S. A. Hawley. 2012. AMPK: a nutrient and energy sensor that maintains energy homeostasis. Nat. Rev. Mol. Cell Biol. 13:251-262.
Hurrle, S. and W. H. Hsu. 2017. The etiology of oxidative stress in insulin resistance. Biomed. J. 40:257-262.
Kenez, A., L. Ruda, S. Danicke, and K. Huber. 2019. Insulin signaling and insulin response in subcutaneous and retroperitoneal adipose tissue in Holstein cows during the periparturient period. J. Dairy Sci. 102:11718-11729.
Li, S., A. Hosseini, M. Danes, C. Jacometo, J. Liu, and J. J. Loor. 2016. Essential amino acid ratios and mTOR affect lipogenic gene networks and miRNA expression in bovine mammary epithelial cells. J. Anim. Sci. Biotechnol. 7:44.
Liang, Y., F. Batistel, C. Parys, and J. J. Loor. 2019. Glutathione metabolism and nuclear factor erythroid 2-like 2 (NFE2L2)-related proteins in adipose tissue are altered by supply of ethyl-cellulose rumen-protected methionine in peripartal Holstein cows. J. Dairy Sci. 102:5530-5541.
Loor, J. J., M. Bionaz, and J. K. Drackley. 2013. Systems physiology in dairy cattle: nutritional genomics and beyond. Annual review of animal biosciences 1:365-392.
Lopreiato, V., A. Hosseini, F. Rosa, Z. Zhou, A. Alharthi, E. Trevisi, and J. J. Loor. 2018. Dietary energy level affects adipose depot mass but does not impair in vitro subcutaneous adipose tissue response to short-term insulin and tumor necrosis factor-α challenge in nonlactating, nonpregnant Holstein cows. J. Dairy Sci. 101:10206-10219.
Lopreiato, V., M. Vailati-Riboni, A. Bellingeri, I. Khan, G. Farina, C. Parys, and J. J. Loor. 2019. Inflammation and oxidative stress transcription profiles due to in vitro supply of methionine with or without choline in unstimulated blood polymorphonuclear leukocytes from lactating Holstein cows. J. Dairy Sci. 102:10395-10410.
Lushchak, V. I. 2012. Glutathione homeostasis and functions: potential targets for medical interventions. J. Amino Acids 2012:736837.
Martinov, M. V., V. M. Vitvitsky, R. Banerjee, and F. I. Ataullakhanov. 2010. The logic of the hepatic methionine metabolic cycle. Biochim. Biophys. Acta 1804:89-96.
McFadden, J. W. and B. A. Corl. 2009. Activation of AMP-activated protein kinase (AMPK) inhibits fatty acid synthesis in bovine mammary epithelial cells. Biochem. Biophys. Res. Commun. 390:388-393.
McNamara, J. P. and K. Huber. 2018. Metabolic and endocrine role of adipose tissue during lactation. Annu. Rev. Anim. Biosci. 6:177-195.
Minuti, A., M. Bionaz, V. Lopreiato, N.A. Janovick, S.L. Rodriguez-Zas, J.K. Drackley, and J. J. Loor. 2020. Prepartum dietary energy intake alters adipose tissue transcriptome profiles during the periparturient period in Holstein dairy cows. J. Anim. Sci. Biotechnol. 11:1.

Moisá, S.J., P. Ji, J. K. Drackley, S.L. Rodriguez-Zas, and J. J. Loor. 2017. Transcriptional changes in mesenteric and subcutaneous adipose tissue from Holstein cows in response to plane of dietary energy. J. Anim. Sci. Biotechnol. 8:85.

Sordillo, L. M. and S. L. Aitken. 2009. Impact of oxidative stress on the health and immune function of dairy cattle. Vet. Immunol. Immunopathol. 128:104-109.

Sordillo, L. M. and W. Raphael. 2013. Significance of metabolic stress, lipid mobilization, and inflammation on transition cow disorders. Vet. Clin. North Am. Food Anim. Pract. 29:267-278.

Sun, F., Y. Cao, C. Cai, S. Li, C. Yu, and J. Yao. 2016. Regulation of nutritional metabolism in transition dairy cows: Energy homeostasis and health in response to post-ruminal choline and methionine. PLoS One 11:e0160659.

Vailati-Riboni, M., M. Kanwal, O. Bulgari, S. Meier, N.V. Priest, C.R. Burke, J.K. Kay, S. McDougall, M.D. Mitchell, C.G. Walker, M. Crookenden, A. Heiser, J.R. Roche, and J. J. Loor. 2016. Body condition score and plane of nutrition prepartum affect adipose tissue transcriptome regulators of metabolism and inflammation in grazing dairy cows during the transition period. J. Dairy Sci. 99:758-70.

Vailati-Riboni, M., T. Xu, B. Qadir, R. Bucktrout, C. Parys, and J. J. Loor. 2019. In vitro methionine supplementation during lipopolysaccharide stimulation modulates immunometabolic gene network expression in isolated polymorphonuclear cells from lactating Holstein cows. J. Dairy Sci. 102:8343-8351.

Vallabhapurapu, S. and M. Karin. 2009. Regulation and function of NF-kappaB transcription factors in the immune system. Annu. Rev. Immunol. 27:693-733.

Zhao, D., J. Yang, and L. Yang. 2017. Insights for oxidative stress and mTOR signaling in myocardial ischemia/reperfusion injury under diabetes. Oxid. Med. Cell. Longev. 2017:6437467.

Zhou, Z., O. Bulgari, M. Vailati-Riboni, E. Trevisi, M. A. Ballou, F. C. Cardoso, D. N. Luchini, and J. J. Loor. 2016. Rumen-protected methionine compared with rumen-protected choline improves immunometabolic status in dairy cows during the peripartal period. J. Dairy Sci. 99:8956-8969.

CHAPTER 8: BRANCHED-CHAIN AMINO ACID SUPPLEMENTATION ALTERS ABUNDANCE OF MECHANISTIC TARGET OF RAPAMYCIN AND INSULIN SIGNALING PROTEINS IN BOVINE SUNCUTANEOUS ADIPOSE EXPLANTS

INTRODUCTION

It is well-recognized in a number of mammalian species that mechanistic target of rapamycin (**mTOR**) including two distinct protein complexes: mTOR complex 2 (**mTORC1**) and mTOR complex 2 (**mTORC2**), controlled by nutrients such as branched-chain amino acids (**BCAA**; Leu, Ile, and Val), regulates protein synthesis, cell growth and proliferation (Yang et al., 2008, Laplante and Sabatini, 2009, Burgos et al., 2010). Supplementation of Val, Leu, and Ile individually to immortalized bovine mammary epithelial cells (**MAC-T**) or bovine mammary tissue slices in vitro promoted protein synthesis via upregulating phosphorylation status of mTOR (Appuhamy et al., 2012, Dong et al., 2018). In an in vivo study, compared with post-ruminal Met and Lys supply, Met and Lys supply plus BCAA supplementation did not improve protein yield or protein content in high-producing cows; however, enhanced BCAA supply reduced milk urea nitrogen content (Appuhamy et al., 2011), suggesting that BCAA might affect proteins synthesis or degradation in peripheral tissues.

In humans, insulin resistance in obese subjects is positively related to greater concentrations of plasma BCAA (Adeva et al., 2012). The recent demonstration via metabolomics analysis that high body condition score is associated with greater BCAA degradation before calving (Ghaffari et al., 2019) suggested there is a potential relationship between body fat and BCAA metabolism in dairy cows. Although bovine adipose tissue has not been generally considered responsive to AA supply, recent research indicated that compared with liver and muscle s.c. adipose tissue (**SAT**) in dairy cows has the greatest mRNA abundance of mitochondrial branched-chain aminotransferase (***BCAT2***) (Webb et al., 2020); furthermore,

BCAA, Gln, and neutral AA transporters are expressed in bovine SAT (Liang et al., 2019, Webb et al., 2020). Hence, available data support the notion that bovine SAT is a potential site for BCAA uptake and metabolism.

Periparturient cows experience dramatic physiological changes in adipose tissue including localized inflammation and reduced insulin sensitivity, both of which are associated with lipolysis (Zachut et al., 2013, Contreras et al., 2018). Recent transcriptome analysis of peripartal SAT revealed that the BCAA catabolism pathway and upstream regulators of cytokines were both inhibited after parturition, underscoring the physiologic relevance of BCAA metabolism in regulating adipose function (Minuti et al., 2020). Whether BCAA contribute to the activation of mTOR and the occurrence of insulin resistance in bovine SAT is unclear. Therefore, the primary objective of this study was to determine the in vitro effects of enhanced BCAA supply on protein abundance of key components of the mTOR and insulin signaling pathway in bovine SAT explants.

MATERIALS AND METHODS

Animals

All procedures were approved by the University of Illinois Institutional Animal Care and Use Committee (Urbana; protocol # 19036). Four healthy multiparous lactating Holstein cows from the University of Illinois dairy herd were used. Average parity, DIM, and milk yield prior to slaughter were 4 ± 1.4, 248 ± 38, and 27.0 ± 13.5 (kg/d) (mean ± SD), respectively. Cows were fed the same diet formulated according to NRC (2001) once daily. Ingredient and nutrient composition of the diet are reported in Supplemental Table G.1 and G.2. All cows were milked twice daily, housed in a free-stall barn, and had free access to water.

Tissue Collection

Cows were euthanized by captive bolt at the College of Veterinary Medicine diagnostic facilities (University of Illinois). Subcutaneous adipose tissue samples from the tail-head were obtained immediately post-slaughter and brought to the laboratory using Dulbecco's Modified Eagle's Medium and Ham's F-12 nutrient mixture (DMEM:F-12; Sigma-Aldrich, St. Louis, MO) containing 1% penicillin/streptomycin (Pen/Streptomycin; Sigma-Aldrich) within 30 min of collection. Subsequently, the tissue was trimmed into pieces using a sterile scalpel blade in a sterile petri dish (catalog no. 101VR20, Thermo Fisher Scientific), and then 800 mg tissue was incubated in duplicate in 5 mL of medium in 6-well plates. Culture media were: ideal profile of essential AA (**EAA**) as the control (**IPAA**), increased Leu (**incLeu**; Lys:Leu 0.78:1), increased Ile (**incIle**; Lys: Ile 1.29:1), or increased Val (**incVal;** Lys:Val 1.12:1) (Table 8.1).

The 10 EAA (L-isomer, Sigma-Aldrich, St Louis, MO) were added into the custom high-glucose serum-free DMEM (devoid of these 10 EAA, custom made from Gibco, Carlsbad, CA). Media were prepared according to our previous study (Dong et al., 2018). Briefly, the formulation of the essential AA was as follows: control medium with the ideal AA ratio (IPAA, Lys:Met 2.9:1; Lys:Thr 1.8:1; Lys:His 2.38:1; Lys:Val 1.23:1; Lys:Ile 1.45:1; Lys:Leu 0.85:1; Lys:Arg 2.08:1), incLeu (Lys:Leu 0.78:1), incIle (Lys:Ile 1.29:1), and incVal (Lys:Val 1.12:1). Media were prepared by increasing Leu, Ile, or Val, individually, while maintaining other AA ratios the same as in IPAA. Subcutaneous adipose explants were incubated in a humidified incubator at 37 °C with 5% CO_2. After 4 h incubation, SAT explants were transferred from 6-well plates to screw-capped microcentrifuge tubes, snap-frozen in liquid nitrogen, and stored at −80 °C until further analysis.

Western Blotting

Total protein was extracted from 200 mg SAT using RIPA Lysis and Extraction Buffer (catalog no. 89900, Thermo Fisher Scientific) following the manufacturer's protocols. Protein concentration was determined using the Pierce BCA protein assay kit (catalog no. 23227; Thermo Fisher Scientific). Details of the western blot procedure were reported previously by our group (Liang et al., 2019). Briefly, protein samples were denatured by heating at 95 °C for 5 min before loading 20 µL protein into each lane of a 4-20% SDS-PAGE gel (catalog no. 4561094; Bio-Rad). Reactions were run for 10 min at 180 V, and then for 45 to 60 min at 110 V. After activating a polyvinylidene fluoride membrane (catalog no. 1620261; Bio-Rad) with methanol for 1 min, the protein sample was transferred to the membrane in a Trans-Blot SD Semi-Dry Electrophoretic Transfer Cell (catalog no. 170-3940; Bio-Rad). Membranes were then blocked in 1× Tris-buffered saline (**TBST**) containing 5% nonfat milk for 2 h at room temperature. Membranes were then incubated in 1× TBST containing primary antibodies to total mTOR (mTORC1 and mTORC2), phospho-mTOR (Ser2448), AKT, phospho-AKT (Ser473), eukaryotic elongation factor 2 (**eEF2**), phospho-eEF2 (Thr56), solute carrier family 38 member 1 (**SLC38A1**), and BCKDK overnight at 4 °C; catalog number and dilution ratios are included in Supplemental Table G.3. Membranes were then washed 6 times with 1× TBST and incubated with anti-rabbit horseradish peroxidase-conjugated secondary antibodies (catalog no. 7074S; dilution 1:800; Cell Signaling Technology, Danvers, MA) for 1 h at room temperature. Subsequently, membranes were washed 6 times with 1× TBST and then incubated with enhanced chemiluminescence reagent (catalog no. 170-5060; Bio-Rad) for 3 min in the dark prior to image acquisition. β-actin (catalog no. 4967S; Cell Signaling Technology) was used as the internal control. Images were acquired using the ChemiDOC MP Imaging System (Bio-Rad). The

intensities of the bands were measured with Image-Pro Plus 6.0 software (Media Cybernetics, Rockville, MD). Specific target protein band density values were normalized to β-actin density values.

Statistical Analysis

Statistical analysis was performed using the MIXED model in SAS (SAS Institute Inc., Cary, NC) with fixed effect of Lys:Ile, Lys:Val and Lys:Leu ratios and cow was used as a covariant. Variables were assessed for normality of distribution using the Shapiro-Wilk test. Least squares means and standard errors were determined using the LSMEANS statement of SAS (SAS Institute Inc.) and were compared using Tukey's test when significant interactions were observed. Significance was determined at $P \leq 0.05$ and tendencies at $P \leq 0.10$.

RESULTS

Compared with IPAA, enhanced Leu and Ile supplementation led to greater activation of AKT (p-AKT/total AKT) and mTOR (p-mTOR/total mTOR) with a more pronounced response due to incLeu ($P < 0.05$; $P < 0.05$, Figure 8.1C and Figure 8.2C). However, enhanced Val resulted in lower activation of mTOR (p-mTOR/total mTOR) compared with IPAA ($P < 0.05$, Figure 8.2C).

Despite protein abundance of SLC38A1 and BCKDK being greater compared with IPAA, supplementation of BCAA also led to greater activation of eEF2 **(**p-eEF2/total eEF2) ($P < 0.05$; $P < 0.05$; $P < 0.05$, Figure 8.3A, B and Figure 8.2C). In addition, compared with incVal or incIle, incLeu resulted in lower abundance of SLC38A1 and BCKDK ($P < 0.05$; $P < 0.05$, Figure 8.3A and B). It is noteworthy that SLC38A1 and BCKDK had similar changes in protein abundance in response to treatments.

DISCUSSION

Peripartal cows experience insulin resistance and excessive lipolysis, both of which contribute to increased incidence of metabolic disorders (De Koster and Opsomer, 2013). It is well-established that SAT is an important insulin-sensitive site in peripartal cows, e.g., phosphorylation of protein kinase B (**AKT**) responds to greater circulating glucose concentrations (Zachut et al., 2013). In addition, overfeeding a high-starch/high-energy diet prepartum upregulated lipogenic and insulin-responsive genes in SAT before calving (Ji et al., 2012), linking dietary energy to SAT sensitivity to insulin in the prepartum period. Besides these well-established physiologic adaptations, dairy cow SAT is immune-responsive (Mukesh et al., 2010) and immune-responsive genes are expressed not only in SAT but other depots of the cow (Ji et al., 2014). Thus, the recent recognition that peripartal SAT experiences a state of inflammation-driven in part by the sustained availability of long-chain fatty acids due to lipolysis (Contreras et al., 2018) underscores the complexity of mechanisms potentially controlling SAT function around calving.

In non-ruminants, it is well-established that BCAA are not only building blocks for protein synthesis but also key regulators of the mTOR signaling pathway (Zhang et al., 2017). Besides skeletal muscle, liver, and mammary cells, rodent studies have revealed that adipose tissue might play a role in modulating BCAA metabolism partly via changes in the activity of BCAA catabolic enzymes such as BCAT2 and branched-chain α-keto acid dehydrogenase kinase (**BCKDK**) (Herman et al., 2010, Blanchard et al., 2018, Yoneshiro et al., 2019). Alterations in the abundance of plasma membrane AA transporters and extracellular sensors of AA availability also can control BCAA metabolism, including signaling via mTORC1 (Zhou et al., 2016). Emerging evidence also indicates that adipose tissue might be a target organ for BCAA

metabolism in dairy cows (Webb et al., 2020), particularly during periods of glucose sufficiency (Nichols et al., 2016).

To the best of our knowledge, research on the effects of BCAA supply on dairy cows has mainly focused on the regulation of protein synthesis in the mammary gland or isolated mammary cells (Appuhamy et al., 2011, Appuhamy et al., 2012, Dong et al., 2018). Indeed, in vitro studies revealed that BCAA could promote protein synthesis via activation of the mTOR pathway (Appuhamy et al., 2012, Dong et al., 2018). It is noteworthy that human and rodent studies have provided evidence that increased circulating BCAA might be a potential biomarker to predict metabolic disorders such as insulin resistance and diabetes (McCormack et al., 2013). Dairy cows are prone to metabolic disorders during the periparturient period, hence, exploring the effects of BCAA on mTOR and insulin signaling in SAT will provide new perspectives on the nutritional management of peripartal cows.

The mechanistic target of rapamycin is composed of two distinct complexes, mTORC1 and mTORC2 (Wullschleger et al., 2006). The former stimulates protein synthesis prior to contributing to cell growth and proliferation, and the latter mediates cell survival and proliferation as a function of AKT activation state (Laplante and Sabatini, 2009). The greater activation of AKT induced by increased Leu and Ile supplementation in the present study suggested that these EAA contribute (at least in vitro) to maintaining insulin signaling in SAT. Eukaryotic translation elongation factor 2, a downstream target of the mTORC1 signaling pathway, controls protein synthesis (Kaul et al., 2011). Although in the present study we did not measure proliferation or apoptosis, the fact that greater supply of Leu or Ile led to activation of AKT (p-AKT/total AKT) and eEF2 (p-eEF2/total eEF2) led us to speculate that mTORC2 rather than mTORC1 might have been the primary branch responding to the supply of BCAA. Thus,

these results suggest that greater activation of mTOR in SAT might play a more important role in controlling cell survival and proliferation rather than protein synthesis.

At least in non-ruminants, the mTOR signaling pathway seems to exert some control on adipose biology and function via regulating aspects of lipid metabolism and adipokine synthesis/secretion (Cai et al., 2016). For instance, adipocyte-specific *mTOR*-silencing in mice led to insulin resistance and inhibited adipocyte differentiation via the peroxisome proliferator-activated receptor γ signaling pathway (Shan et al., 2016). In another study, silencing of eukaryotic translation initiation factor 2 alpha kinase 4 (a.k.a. general control nonderepressible 2) in mice led to reduced adipose tissue mass when fed a Leu-deficient diet (Guo and Cavener, 2007). The degradation of BCAA produces acetyl-CoA and succinyl-CoA both of which are important intermediates in the TCA cycle and contribute carbon for lipogenesis in adipose tissue (Sears et al., 2009, Song et al., 2018). Together, these data agree with the fact that 3T3-L1 pre-adipocytes consume greater amounts of BCAA during differentiation (Green et al., 2016). From a mechanistic standpoint, the fact that BCAA, particularly Leu, can activate mTORC1 in mammalian cells (Lynch and Adams, 2014) including adipose (Lynch et al., 2002) led us to speculate a direct effect of Leu on mTOR in the present study. Thus, the greater activation of mTOR (p-mTOR/total mTOR) in response to Leu and Ile supplementation suggested that BCAA might play a dual-role as regulators of mTOR and stimulators of lipogenesis, i.e. they could play dual functions in SAT.

Except for BCAA, Gln also plays an important role in regulating the mTOR signaling pathway, with several AA transporters (e.g., SLC38A1, solute carrier family 1 member 5, **SLC1A5**; solute carrier family 1 member 5, **SLC7A5**) being responsible for cellular Gln uptake or export (Nicklin et al., 2009). For instance, SLC38A1, a neutral AA transporter, controls Gln

transport into cells (Mackenzie and Erickson, 2004). The inhibition of SLC1A5 prevents L-Gln uptake resulting in a reduction in mTOR signaling; SLC7A5, a heterodimeric bidirectional antiporter, mediates the exchange of intracellular L-Gln for extracellular L-Leu (Nicklin et al., 2009). Greater BCAA supply upregulated mRNA abundance of AA transporters in MAC-T cells (Dong et al., 2018). Thus, we speculate that reduced SLC38A1 in response to Leu might contribute to maintaining intracellular Leu and Gln homeostasis. In non-ruminant cells, BCKDK, a rate-limiting enzyme of BCAA catabolism, regulates intracellular concentrations of BCAA via inactivation and phosphorylation of the BCKD complex (Shimomura et al., 2001). Thus, the greater protein abundance of BCKDK in response to increased BCAA supplementation in the present study implies greater intracellular BCAA availability. Such a response also helps explain the greater activation of mTOR. The similar pattern of BCKDK and SLC38A1 suggests that Gln along with BCAA might potentially regulate mTOR signaling in bovine SAT. However, the exact mechanisms whereby Gln and BCAA interact in bovine SAT are unknown and merit further study.

Overall, increased Leu or Ile supply contributes to greater activation of mTOR without impairing insulin signaling, which might be partly explained by increased AA transport and reduced BCAA catabolism in SAT (Figure 8.4). Because of the potential practical applications of enhancing the post-ruminal supply of BCAA via feeding in rumen-protected form, in vivo studies are warranted. For example, abomasal infusions of BCAA under negative energy balance would help assess the benefit of post-ruminal BCAA on adipose function. Those data could help guide studies with periparturient cows.

TABLE AND FIGURES

Table 8.1. Amino acid (AA) composition of the culture media with an ideal AA profile (IPAA; Lys:Ile ratio of 1.29:1; Lys:Val ratio of 1.12:1; Lys:Leu ratio of 0.78:1) and treatment media supplemented with greater amounts of Leu (incLeu), Ile (incIle), or Val (incVal) to alter ratios of Lys:Leu, Lys:Ile, or Lys:Val relative to IPAA.

	Treatment[1]			
Item[2]	IPAA	incLeu	incIle	incVal
L-Lys (µg/mL)	175	175	175	175
L-Met (µg/mL)	60	60	60	60
Lys:Met	2.9:1	2.9:1	2.9:1	2.9:1
L-Leu (µg/mL)	206	225	206	206
Lys:Leu	0.85:1	0.78:1	0.85:1	0.85:1
L-Ile (µg/mL)	121	121	136	121
Lys:Ile	1.45:1	1.45:1	1.29:1	1.45:1
L-Val (µg/mL)	142	142	142	156
Lys:Val (µg/mL)	1.23:1	1.23:1	1.23:1	1.12:1
L-Arg (µg/mL)	84	84	175	175
L-His (µg/mL)	74	74	74	74
L-Phe (µg/mL)	93	93	93	93
L-Thr (µg/mL)	97	97	97	97
L-Trp (µg/mL)	16	16	16	16

[1]IPAA = ideal AA profile, used as control medium. Ratios of essential AA are as follows: Lys:Met = 2.9, Lys:Thr = 1.8, Lys:His = 2.38, Lys:Val = 1.23, and Thr:Phe = 1.05 were based on NRC (2001), Haque et al. (2012), and our previous studies [Dong et al. (2018)].
[2]Composition of AA in the medium was prepared as described by Dong et al. (2018).

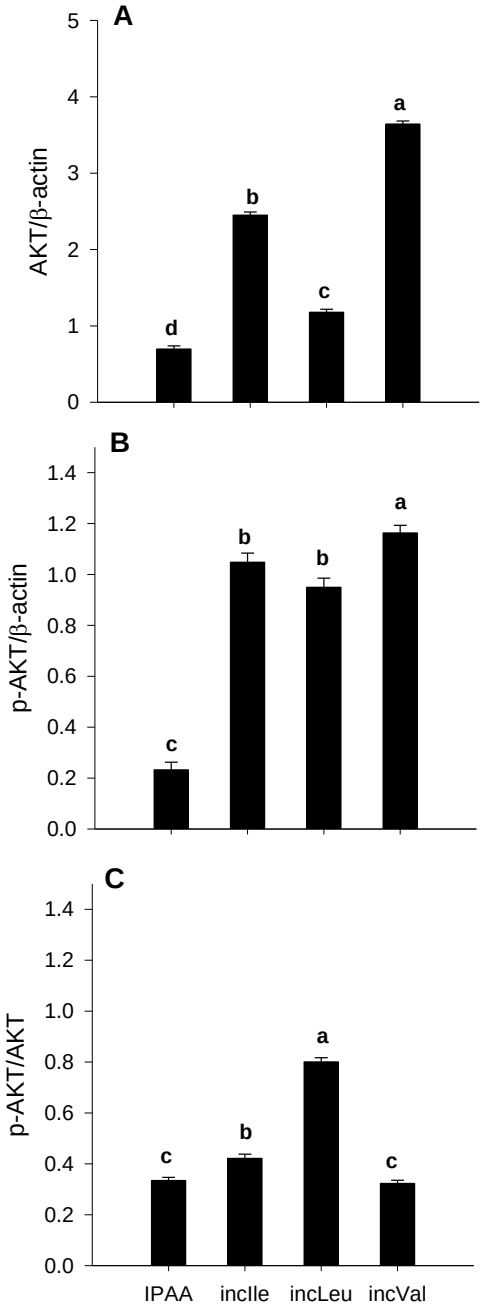

Figure 8.1. Protein abundance (relative to β-actin) of protein kinase B (AKT; total, panel A), p-AKT (active, panel B), ratio of p-AKT/AKT (panel C) in s.c. adipose tissue cultured with different levels of Leu, Ile, or Val. Control media contained an ideal AA profile (IPAA; Lys : Met 2.9 : 1, Lys:Val 1.23:1; Lys:Ile 1.45:1; Lys:Leu 0.85:1). Treatment media was supplemented with greater amounts of Leu, Ile, or Val to achieve ratios of Lys:Leu 0.78:1 (incLeu), Lys:Ile 1.29:1(incIle), or Lys:Val 1.12:1 (incVal). Different letters indicate differences between treatments ($P < 0.05$). Data are LS means, n = 4 cows per group, ± pooled SEMs.

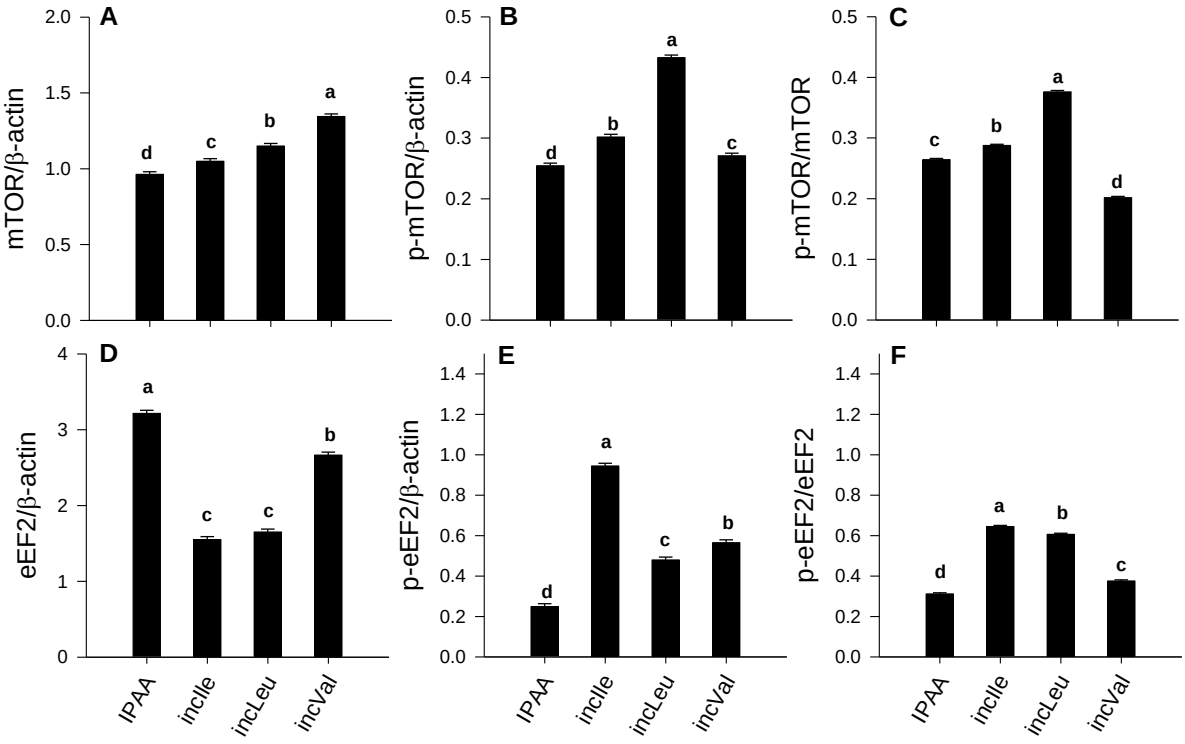

Figure 8.2. Protein abundance (relative to β-actin) of mechanistic target of rapamycin (mTOR; total, panel A), p-mTOR (active, panel B), ratio of p-mTOR/mTOR (panel C), eukaryotic elongation factor 2 (eEF2; total, panel D), p-eEF2 (active, panel E), and ratio of p-eEF2/eEF2 (panel F) in s.c. adipose tissue cultured with different levels of Leu, Ile, or Val. Control media contained an ideal AA profile (IPAA; Lys : Met 2.9 : 1, Lys:Val 1.23:1; Lys:Ile 1.45:1; Lys:Leu 0.85:1). Treatment media was supplemented with greater amounts of Leu, Ile, or Val to achieve ratios of Lys:Leu 0.78:1 (incLeu), Lys:Ile 1.29:1(incIle), or Lys:Val 1.12:1 (incVal). Different letters indicate differences between treatments ($P < 0.05$). Data are LS means, n = 4 cows per group, ± pooled SEMs.

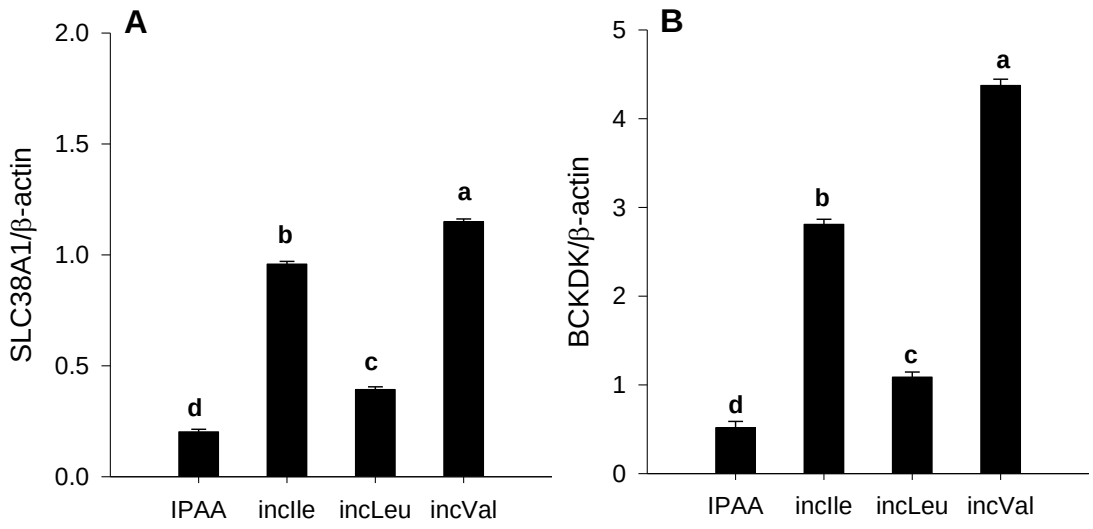

Figure 8.3. Protein abundance (relative to β-actin) of the Gln transporter SLC38A1 (panel A) and branched-chain keto acid dehydrogenase kinase (BCKDK, panel B) in s.c. adipose tissue cultured with different levels of Leu, Ile, or Val. Control media contained an ideal AA profile (IPAA; Lys:Met 2.9:1, Lys:Val 1.23:1; Lys:Ile 1.45:1; Lys:Leu 0.85:1). Treatment media was supplemented with greater amounts of Leu, Ile, or Val to achieve ratios of Lys:Leu 0.78:1 (incLeu), Lys:Ile 1.29:1(incIle), or Lys:Val 1.12:1 (incVal). Different letters indicate differences between treatments ($P < 0.05$). Data are LS means, n = 4 cows per group, ± pooled SEMs.

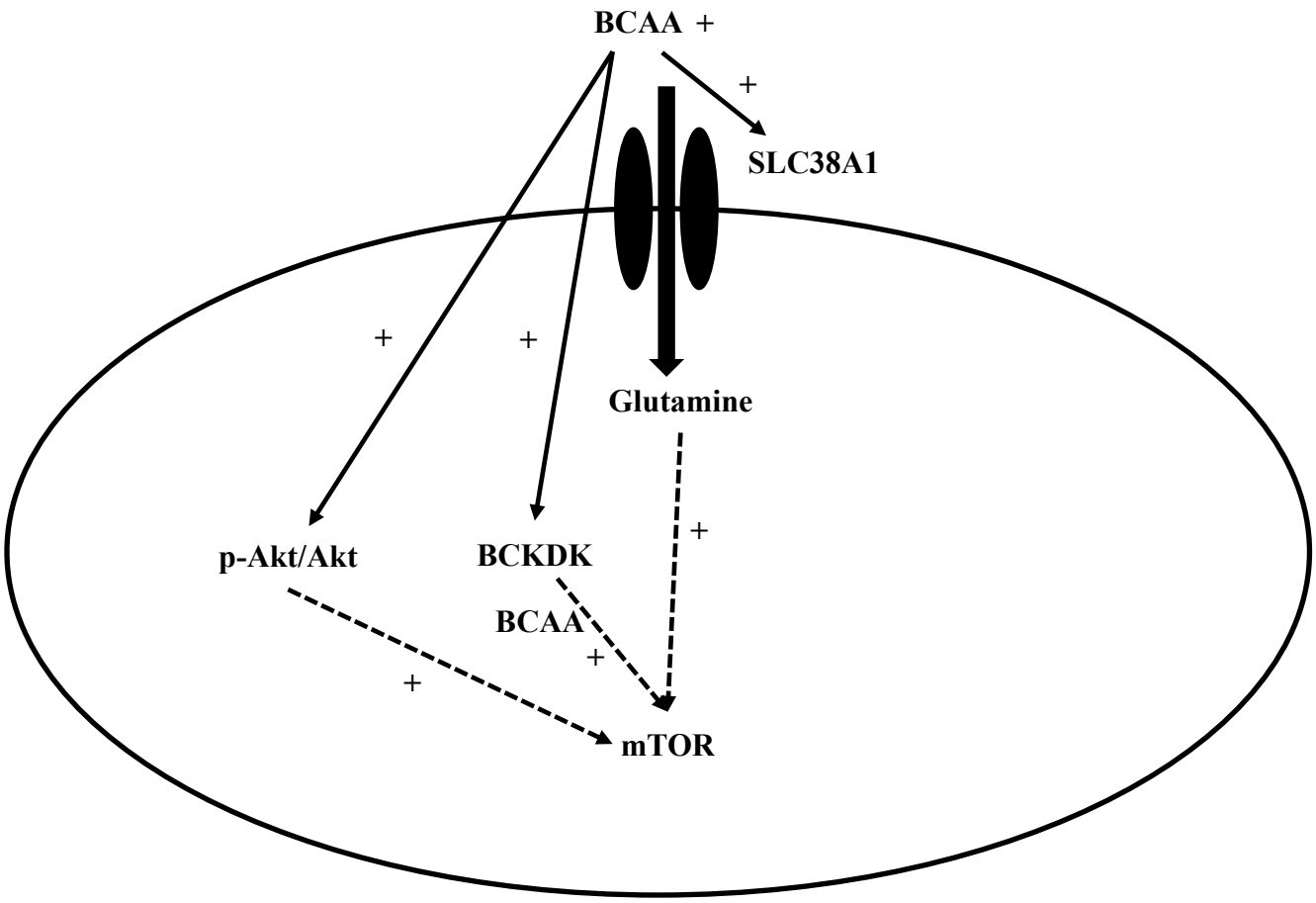

Figure 8.4. Putative model based on available data of enhanced branched-chain amino acids supply on adipose tissue function. AKT = protein kinase B; BCAA= branched-chain amino acids; BCKDK = branched-chain α-keto acid dehydrogenase kinase; mTOR = mechanistic target of rapamycin; SLC38A1= solute carrier family 38 member 1; + = increase; - = decrease.

REFERENCES

Adeva, M. M., J. Calviño, G. Souto, and C. Donapetry. 2012. Insulin resistance and the metabolism of branched-chain amino acids in humans. Amino Acids 43:171-181.

Appuhamy, J. A. D. R. N., J. R. Knapp, O. Becvar, J. Escobar, and M. D. Hanigan. 2011. Effects of jugular-infused lysine, methionine, and branched-chain amino acids on milk protein synthesis in high-producing dairy cows. J. Dairy Sci. 94:1952-1960.

Appuhamy, J. A. D. R. N., N. A. Knoebel, W. A. D. Nayananjalie, J. Escobar, and M. D. Hanigan. 2012. Isoleucine and leucine independently regulate mTOR signaling and protein synthesis in MAC-T cells and bovine mammary tissue slices. J. Nutr. 142:484-491.

Blanchard, P.-G., R. J. Moreira, É. Castro, A. Caron, M. Côté, M. L. Andrade, T. E. Oliveira, M. Ortiz-Silva, A. S. Peixoto, F. A. Dias, Y. Gélinas, R. Guerra-Sá, Y. Deshaies, and W. T. Festuccia. 2018. PPARγ is a major regulator of branched-chain amino acid blood levels and catabolism in white and brown adipose tissues. Metabolism 89:27-38.

Burgos, S. A., M. Dai, and J. P. Cant. 2010. Nutrient availability and lactogenic hormones regulate mammary protein synthesis through the mammalian target of rapamycin signaling pathway. J. Dairy Sci. 93:153-161.

Cai, H., L. Q. Dong, and F. Liu. 2016. Recent advances in adipose mTOR signaling and function: therapeutic prospects. Trends Pharmacol. Sci. 37:303-317.

Contreras, G. A., C. Strieder-Barboza, and J. De Koster. 2018. Symposium review: Modulating adipose tissue lipolysis and remodeling to improve immune function during the transition period and early lactation of dairy cows. J. Dairy Sci. 101:2737-2752.

De Koster, J. D. and G. Opsomer. 2013. Insulin resistance in dairy cows. Vet. Clin. North Am. Food Anim. Pract. 29:299-322.

Dong, X., Z. Zhou, L. Wang, B. Saremi, A. Helmbrecht, Z. Wang, and J. J. Loor. 2018. Increasing the availability of threonine, isoleucine, valine, and leucine relative to lysine while maintaining an ideal ratio of lysine:methionine alters mammary cellular metabolites, mammalian target of rapamycin signaling, and gene transcription. J. Dairy Sci. 101:5502-5514.

Ghaffari, M. H., A. Jahanbekam, H. Sadri, K. Schuh, G. Dusel, C. Prehn, J. Adamski, C. Koch, and H. Sauerwein. 2019. Metabolomics meets machine learning: Longitudinal metabolite profiling in serum of normal versus overconditioned cows and pathway analysis. J. Dairy Sci. 102:11561-11585.

Green, C. R., M. Wallace, A. S. Divakaruni, S. A. Phillips, A. N. Murphy, T. P. Ciaraldi, and C. M. Metallo. 2016. Branched-chain amino acid catabolism fuels adipocyte differentiation and lipogenesis. Nat. Chem. Biol. 12:15-21.

Guo, F. and D. R. Cavener. 2007. The GCN2 eIF2α kinase regulates fatty-acid homeostasis in the liver during deprivation of an essential amino acid. Cell Metab. 5:103-114.

Haque, M. N., H. Rulquin, A. Andrade, P. Faverdin, J. L. Peyraud, and S. Lemosquet. 2012. Milk protein synthesis in response to the provision of an “ideal” amino acid profile at 2 levels of metabolizable protein supply in dairy cows. J. Dairy Sci. 95:5876–5887.

Herman, M. A., P. She, O. D. Peroni, C. J. Lynch, and B. B. Kahn. 2010. Adipose tissue branched chain amino acid (BCAA) metabolism modulates circulating BCAA levels. J. Biol. Chem. 285:11348-11356.

Ji, P., J. K. Drackley, M. J. Khan, and J. J. Loor. 2014. Inflammation- and lipid metabolism-related gene network expression in visceral and subcutaneous adipose depots of Holstein cows. J. Dairy Sci. 97:3441-3448.
Ji, P., J. S. Osorio, J. K. Drackley, and J. J. Loor. 2012. Overfeeding a moderate energy diet prepartum does not impair bovine subcutaneous adipose tissue insulin signal transduction and induces marked changes in peripartal gene network expression1. J. Dairy Sci. 95:4333-4351.
Kaul, G., G. Pattan, and T. Rafeequi. 2011. Eukaryotic elongation factor-2 (eEF2): its regulation and peptide chain elongation. Biochem. Funct. 29:227-234.
Laplante, M. and D. M. Sabatini. 2009. mTOR signaling at a glance. J. Cell Sci. 122:3589.
Liang, Y., F. Batistel, C. Parys, and J. J. Loor. 2019. Methionine supply during the periparturient period enhances insulin signaling, amino acid transporters, and mechanistic target of rapamycin pathway proteins in adipose tissue of Holstein cows. J. Dairy Sci. 102:4403-
Lynch, C. J. and S. H. Adams. 2014. Branched-chain amino acids in metabolic signalling and insulin resistance. Nat. Rev. Endocrinol. 10:723-736.
Lynch, C. J., B. J. Patson, J. Anthony, A. Vaval, L. S. Jefferson, and T. C. Vary. 2002. Leucine is a direct-acting nutrient signal that regulates protein synthesis in adipose tissue. Am. J. Physiol. Endocrinol. Metab. 283:E503-E513.
National Research Council. 2001. Nutrient requirements of dairy cattle. 7th rev. ed. Natl. Acad. Press, Washington, DC.
Mackenzie, B. and J. D. Erickson. 2004. Sodium-coupled neutral amino acid (System N/A) transporters of the SLC38 gene family. Pflugers Arch. 447:784-795.
McCormack, S. E., O. Shaham, M. A. McCarthy, A. A. Deik, T. J. Wang, R. E. Gerszten, C. B. Clish, V. K. Mootha, S. K. Grinspoon, and A. Fleischman. 2013. Circulating branched-chain amino acid concentrations are associated with obesity and future insulin resistance in children and adolescents. Pediatr. Obes. 8:52-61.
Minuti, A., M. Bionaz, V. Lopreiato, N. A. Janovick, S. L. Rodriguez-Zas, J. K. Drackley, and J. J. Loor. 2020. Prepartum dietary energy intake alters adipose tissue transcriptome profiles during the periparturient period in Holstein dairy cows. J. Anim. Sci. Biotechnol. 11:1.
Mukesh, M., M. Bionaz, D. E. Graugnard, J. K. Drackley, and J. J. Loor. 2010. Adipose tissue depots of Holstein cows are immune responsive: Inflammatory gene expression in vitro. Domest. Anim. Endocrinol. 38:168-178.
Nichols, K., J. J. M. Kim, M. Carson, J. A. Metcalf, J. P. Cant, and J. Doelman. 2016. Glucose supplementation stimulates peripheral branched-chain amino acid catabolism in lactating dairy cows during essential amino acid infusions. J. Dairy Sci. 99:1145-1160.
Nicklin, P., P. Bergman, B. Zhang, E. Triantafellow, H. Wang, B. Nyfeler, H. Yang, M. Hild, C. Kung, C. Wilson, V. E. Myer, J. P. MacKeigan, J. A. Porter, Y. K. Wang, L. C. Cantley, P. M. Finan, and L. O. Murphy. 2009. Bidirectional transport of amino acids regulates mTOR and autophagy. Cell 136:521-534.
Sears, D. D., G. Hsiao, A. Hsiao, J. G. Yu, C. H. Courtney, J. M. Ofrecio, J. Chapman, and S. Subramaniam. 2009. Mechanisms of human insulin resistance and thiazolidinedione-mediated insulin sensitization. Proc. Natl. Acad. Sci. U. S. A. 106:18745.
Shan, T., P. Zhang, Q. Jiang, Y. Xiong, Y. Wang, and S. Kuang. 2016. Adipocyte-specific deletion of mTOR inhibits adipose tissue development and causes insulin resistance in mice. Diabetologia 59:1995-2004.

Shimomura, Y., M. Obayashi, T. Murakami, and R. A. Harris. 2001. Regulation of branched-chain amino acid catabolism: nutritional and hormonal regulation of activity and expression of the branched-chain α-keto acid dehydrogenase kinase. Opin. Clin. Nutr. Metab. Care 4:419-423.

Song, Z., A. M. Xiaoli, and F. Yang. 2018. Regulation and metabolic significance of de novo lipogenesis in adipose tissues. Nutrients 10:1383.

Webb, L. A., H. Sadri, K. Schuh, S. Egert, P. Stehle, I. Meyer, C. Koch, G. Dusel, and H. Sauerwein. 2020. Branched-chain amino acids: Abundance of their transporters and metabolizing enzymes in adipose tissue, skeletal muscle, and liver of dairy cows at high or normal body condition. J. Dairy Sci.103:2847-2863.

Wullschleger, S., R. Loewith, and M. N. Hall. 2006. TOR signaling in growth and metabolism. Cell 124:471-484.

Yang, X., C. Yang, A. Farberman, T. C. Rideout, C. F. M. de Lange, J. France, and M. Z. Fan. 2008. The mammalian target of rapamycin-signaling pathway in regulating metabolism and growth1,2. J. Anim. Sci. 86:E36-E50.

Yoneshiro, T., Q. Wang, K. Tajima, M. Matsushita, H. Maki, K. Igarashi, Z. Dai, P. J. White, R. W. McGarrah, O. R. Ilkayeva, Y. Deleye, Y. Oguri, M. Kuroda, K. Ikeda, H. Li, A. Ueno, M. Ohishi, T. Ishikawa, K. Kim, Y. Chen, C. H. Sponton, R. N. Pradhan, H. Majd, V. J. Greiner, M. Yoneshiro, Z. Brown, M. Chondronikola, H. Takahashi, T. Goto, T. Kawada, L. Sidossis, F. C. Szoka, M. T. McManus, M. Saito, T. Soga, and S. Kajimura. 2019. BCAA catabolism in brown fat controls energy homeostasis through SLC25A44. Nature 572:614-619.

Zachut, M., H. Honig, S. Striem, Y. Zick, S. Boura-Halfon, and U. Moallem. 2013. Periparturient dairy cows do not exhibit hepatic insulin resistance, yet adipose-specific insulin resistance occurs in cows prone to high weight loss. J. Dairy Sci. 96:5656-5669.

Zhang, S., X. Zeng, M. Ren, X. Mao, and S. Qiao. 2017. Novel metabolic and physiological functions of branched chain amino acids: a review. J. Anim. Sci. Biotechnol. 8:10.

Zhou, Y., J. Ren, T. Song, J. Peng, and H. Wei. 2016. Methionine regulates mTORC1 via the T1R1/T1R3-PLCβ-Ca2+-ERK1/2 signal transduction process in C2C12 cells. Int. J. Mol. Sci. 17:1684.

CHAPTER 9: CONCLUSIONS

The periparturient period is a critical stage for dairy cows during their production cycle. Peripartal cows experience systemic oxidative stress, inflammation, and insulin resistance, which contribute to increased incidence of metabolic disorders. During the periparturient period, adipose tissue is highly mobilized to meet the increased energy demands due to fetal growth and milk production. It is noteworthy that peripartal cows with HBCS accumulate more body fat and exhibit a greater extent of fat mobilization and oxidative stress. Both in vivo and in vitro studies suggest that enhanced post-ruminal AA supply (e.g., Met and Arg) not only improves milk protein synthesis, but also helps alleviate oxidative stress and inflammation via alterations in NFE2L2 and mTOR pathways in the bovine liver and mammary gland. However, the role of NFE2L2 and mTOR pathways in bovine adipose tissue is largely unknown. Essential AA play multiple roles in mammalian cells. For example, Met, one of the limiting AA in lactating cows, plays a critical role in regulating antioxidant (e.g., GSH) synthesis via the transsulfuration pathway. Amino acids transporters are responsible for regulating AA availability within the intracellular space. Changes in AA transporter abundance in bovine adipose tissue during the periparturient period are not well known. Additionally, whether adipose tissue is responsive to enhanced AA profiles also is unclear. Therefore, the objectives of the experiments of the dissertation were to (1) investigate changes of NFE2L2, mTOR, and AA transporters in bovine SAT during the periparturient period, (2) evaluate whether NFE2L2 and mTOR are responsive to enhanced AA supply, (3) investigate whether body condition prepartum affects oxidative stress in adipose tissue, (4) evaluate the effect of essential AA supply (e.g., Met and Arg) on protein abundance associated with mTOR and AA transporters in bovine adipose explants challenged

with C2:0-ceramide or H_2O_2, (5) analyze protein abundance associated with insulin signaling, mTOR, and AA transporters in bovine adipose explants incubated with BCAA.

(1) Several components of GSH metabolism and NFE2L2 antioxidant signaling pathways and various components of insulin and mTOR signaling pathways are expressed in SAT and respond to the change in physiological state from late pregnancy to early lactation. The gradual increase in protein abundance of key components of the NFE2L2 pathway reflects the state of oxidative stress experienced by cows. The mTOR signaling pathway seems responsive to DMI and the systemic availability of key nutrients (e.g., AA).

(2) Supplementation of Met led to lower MDA and greater activity of GSH antioxidant enzymes in SAT. In addition, enhanced RPM supply increased mRNA and protein abundance of some AA transporters along with greater abundance of p-AKT and p-mTOR.

(3) Both HBCS and NBCS cows experience oxidative stress during the periparturient period. However, HBCS cows had lower overall plasma β-carotene and ROS concentrations in SAT especially after parturition, suggesting HBCS might experience prolonged oxidative stress postpartum. Activation of NFE2L2 in SAT might partly explain the reduced oxidative stress in dairy cows with NBCS. Interestingly, SAT in overconditioned cows might trigger compensatory mechanisms leading to upregulation of AA transport and activation of mTOR signaling.

(4) C2:0-ceramide challenge led to lower protein abundance of AA transporter and reduced insulin signaling in adipose tissue. In addition, enhancing the supply of Arg or Met alone contributed to altering AA metabolism by increasing the protein abundance of BCKDK and mTOR pathway activity. Unique responses to Arg and Met supply during ceramide stimulation included greater activation of mTOR by Arg, while Met increased the antioxidant response through upregulation of GSTM1. The short-term stimulation of adipose tissue with

H_2O_2 had a negative effect on some of the components of insulin signaling. Overall, increasing the supply of Met attenuated the decrease in abundance of insulin signaling-related proteins and seemed to enhance NFE2L2 and GSH-related anti-oxidant responses.

(5) In vitro data suggest that increased Leu or Ile supply resulted in greater activation of mTOR without impairing insulin signaling, which might be partly explained by increased AA transport and reduced BCAA catabolism in SAT.

Overall, data indicate that NFE2L2 and mTOR signaling pathways in adipose tissue adapt to the change in physiologic state during the periparturient period. These pathways are not only responsive to AA supply (e.g., Met) both in vivo and in vitro but also are influenced by energy reserves in prepartal cows. Further in vivo research is warranted to investigate the role of Met and other AA in regulating immune, antioxidant, and metabolic systems in bovine adipose tissue using mass spectrometry and isotopic tracing technologies to understand AA metabolism in bovine adipose tissue.

APPENDIX A: CHAPTER 2 - SUPPLEMENTAL MATERIAL

Supplemental Table A.1. Gene symbol, primer features, and qPCR performance for genes measured in periparturient dairy cow subcutaneous adipose tissue.

Gene symbol (GenBank number)	Primer sequence (5'-3')	Product length (bp)	Slope[1]	(R^2)[2]	Efficiency[3]	Gene name
GCLC (NM_001083674)	CACAAATTGGCAGACAATGC GGCGACCTTCATGTTCTCAT	211	-3.138	0.998	2.083	Glutamate-cysteine ligase catalytic subunit
GCLM (NM_001038143)	TGGAGCAGCTGTATCAGTGG GAATGTCAGGGATGCTCTCC	198	-3.265	0.996	2.024	Glutamate-cysteine ligase modifier subunit
GPX1 (NM_174076)	CCCCTGCAACCAGTTTGG GAGCATAAAGTTGGGCTCGAA	106	-3.590	0.994	1.899	Glutathione peroxidase 1
GSR (NM_001114190)	GAGAACGCTGGCATTGAG AGCAGGCAGTCAACATCT	143	-3.338	0.930	1.993	Glutathione reductase
GSTM1 (NM_175825)	ATCTGCTACAGCCCTGACTTTGA AAGGCCTCTTCCCCAGAAAC	100	-3.328	0.986	1.997	Glutathione S-transferase M1
ME1 NM_001144853	CCAACTGCCCTCATTGGAGT CGCGACCCTTGGTCAGTTTA	166	-3.214	0.950	2.047	Malic enzyme 1
TALDO1 NM_001035283	GCGGATGCTGAGAGAACGA AAGCATGTGCAATTAGGCCC	111	-3.112	0.989	2.096	Transaldolase 1
MTR NM_001030298	ATA CCG CCA ATG CCA AGG ATG AGA CAC GCT GAT GAC AA	136	-3.058	0.939	2.038	5-methyltetrahydrofolate-homocysteine methyltransferase
CDO NM_001034465	GTGTGAATGTGGGTTGCATACC TCCTCGACGTTCCACCCATA	100	-3.021	0.990	2.062	Cysteine dioxygenase
CBS NM_001102000	GCC ACC ACC TCT GTC AAA TTC GGA CAG AAA GCA GAG TGG TAA CTG	120	-3.553	0.993	1.912	Cystathionine β-synthase
BHMT NM_001011679	GCT CTC CTC GTC CAT CCT CAT CCG TTC TAG GAT GCC CTT CTT	81	-3.198	0.959	2.054	Betaine homocysteine methyltransferase
NFE2L2 (NM_001011678)	AGGACATGGATTTGATTGAC TACCTGGGAGTAGTTGGCA	272	-3.529	0.987	1.920	Nuclear factor, erythroid 2 like 2
KEAP1 (NM_001101142)	ACAACAGTGTGGAGAGGTATGAGC AGAGCAGACGGTTGAGGACAG	108	-3.524	0.982	1.922	Kelch-like ECH-associated protein1
CUL3 (NM_001192806)	CTTTCCGATGACCATGGATGAA GCTCCTCAAAACTAAGACCACTG	110	-3.388	0.992	1.973	Cullin3

[1]Slope of the standard curve.

[2]R^2 stands for the coefficient of determination of the standard curve.

[3]Efficiency is calculated as $[10^{(-1 / \text{Slope})}]$.

Supplemental Table A.2. Antibody symbol, catalog number, company, dilution ratio, and antibody name for antibodies measured in periparturient dairy cow subcutaneous adipose tissue.

Antibody	Catalog Number	Company	Dilution ratio	Antibody Name
HCAR2	ARP63888_P050	Aviva Systems Biology	1:200	Hydroxycarboxylic acid receptor 2
GPX1	ab22604	Abcam	1:500	Glutathione peroxidase 1
GPX3	ARP41491_P050	Aviva Systems Biology	1:500	Glutathione peroxidase 3
GSTM1	ARP41769_P050	Aviva Systems Biology	1:500	Glutathione S-transferase Mu 1
GSTA4	ARP48555_P050	Aviva Systems Biology	1:500	Glutathione S-transferase A4
KEAP1	ARP34727_P050	Aviva Systems Biology	1:1000	Kelch like ECH associated protein 1
HMOX1	ARP45222_P050	Aviva Systems Biology	1:1000	Heme oxygenase 1
ERK1	OASE00362	Aviva Systems Biology	1:1000	Extracellular signal-regulated kinase 1
Phospho-ERK1(Thr202)	4370T	Cell Signaling Technology	1:1000	Phosphorylated extracellular signal-regulated kinase 1
NFE2L2	137550	Abcam	1:1000	Nuclear factor erythroid 2-like 2
Phospho-NFE2L2(Ser40)	PA5-67520	Invitrogen	1:500	Phosphorylated nuclear factor erythroid 2-like 2

Supplemental Figure A.1. Representative blots with band size information.

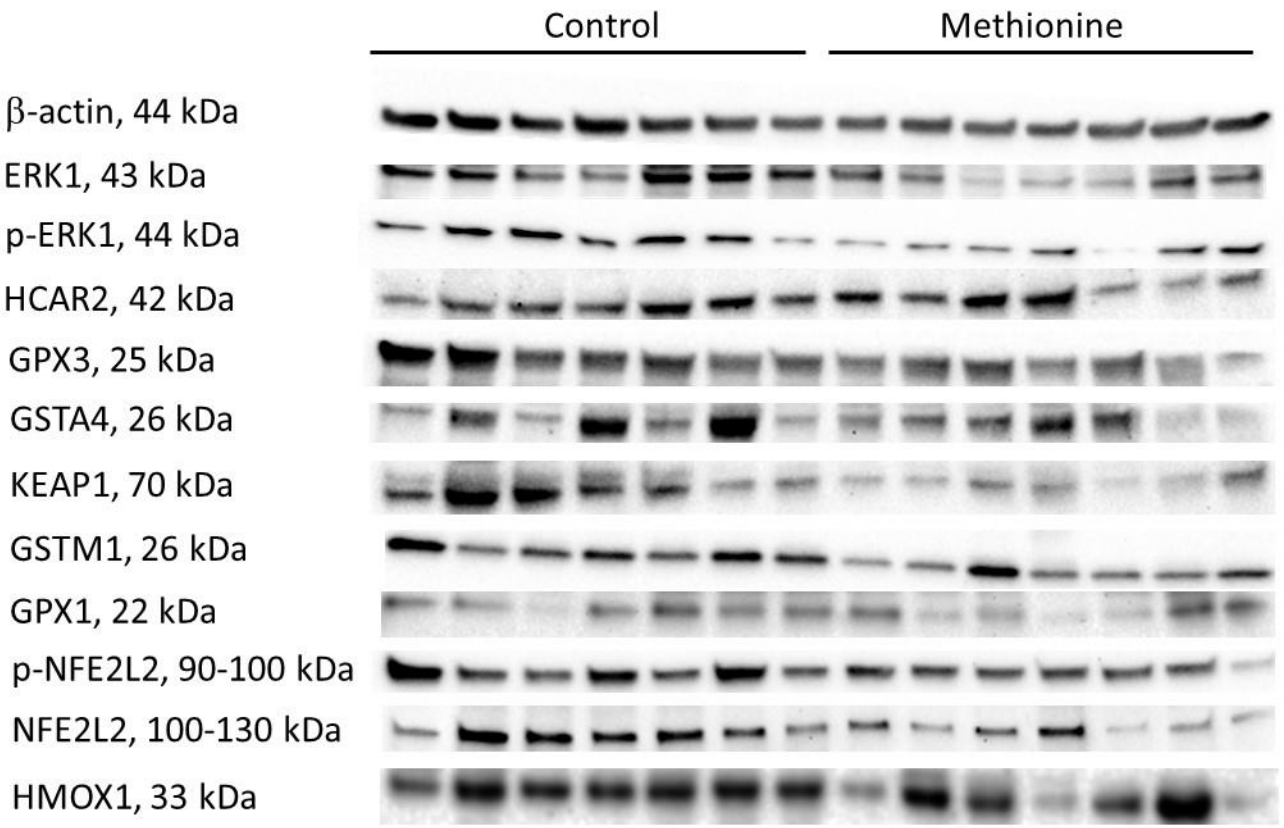

APPENDIX B: CHAPTER 3 - SUPPLEMENTAL MATERIAL

Supplemental Table B.1. Gene symbol, primer features, and qPCR performance for genes measured in periparturient dairy cow subcutaneous adipose tissue.

Gene	Primers (5'-3')	bp	Slope[1]	(R^2)[2]	Efficiency[3]	Gene name
Amino acid transporters						
SLC1A1	GGTGATTGTGCTGAGTGCTG	133	-3.117	0.992	2.093	Glutamate transporter
NM_174599.2	CTCCACAATGCCAGTCCCAA					
SLC1A5	GGCTAGCAGCTGTTTACTCCT	129				Neutral amino acid transporter
NM_174601.2	AGTCTGGGGGCTAGAAGACG					
SLC3A2	GAGCATTCCCTTGCTTGCAC	175	-3.152	0.983	2.076	Heavy-chain amino acid transporter
NM_001024488.2	GCTCATGGTGCCTGAGTCG					
SLC7A5	CCGTACCCTCACTGGTGTTC	181	-3.068	0.972	2.118	Branched-chain and aromatic amino acid transporter
NM_174613.2	AGATGAACCTTGATGGGCCG					
SLC7A1	CTTCGACCTGAAGGACCTGG	101	-3.506	0.982	1.929	High affinity cationic amino acid transporter
NM 001135792.1	GCTCGGGCTGGTATCGTAAG					
SLC36A1	GGCTATCGTCACTGCCCTCTA	100	-3.114	0.974	2.095	Neutral and cationic amino acid transporter
NM 001192498.1	ACAGTTGGGCAGGTTGAGAGTT					
SLC38A1	GGAAGGGCGGATACCACTTT	168	-2.729	0.975	2.325	Neutral amino acid transporter
XM_010827702.2	TGACACCCCTGTTATCTCAGC					
mTOR pathway						
AKT1	CTGCACAAGCGAGGTGAGTA	134	-3.256	0.987	2.208	Protein kinase B
NM_173986.2	GAGAAGTTGTTGAGGGGCGA					
RPS6KB1	ACAGCCTGCTTTTACTTGGC	178	-3.112	0.990	2.096	Ribosomal protein S6 kinase B1
NM_205816.1	AGGTGTGTGTGACTGTTCCG					
EIF4EBP1	GGAGTGTCGGAACTCACCTG	162	-3.008	0.980	2.150	Eukaryotic translation initiation factor 4E-binding protein
NM_001077893.2	AACTGTGACTCTTCACCGCC					

[1]Slope of the standard curve.
[2]R^2 stands for the coefficient of determination of the standard curve.
[3]Efficiency is calculated as $[10^{(-1 / \text{Slope})}]$.

Supplemental Table B.2. Antibody symbol, catalog number, company, dilution ratio, and antibody name for antibodies measured in periparturient dairy cow subcutaneous adipose tissue.

Antibody	Catalog Number	Company	Dilution ratio	Antibody Name
mTOR	2972S	Cell Signaling Technology	1:200	Mechanistic target of rapamycin
Phospho-mTOR(Ser2448)	2971S	Cell Signaling Technology	1:200	Phosphorylated mechanistic target of rapamycin
AKT	9272S	Cell Signaling Technology	1:1000	Protein kinase B
Phospho-AKT(Ser473)	9271S	Cell Signaling Technology	1:1000	Phosphorylated protein kinase B
INSR	ab190734	Abcam	1:200	Insulin receptor
GLUT4	ARP43785_P050	Aviva Systems Biology	1:1000	Glucose transporter 4
Phospho-4-EBP1(Thr37/46)	9459S	Cell Signaling Technology	1:1000	Phosphorylated eukaryotic translation initiation factor 4E-binding protein
Phospho-EEF2(Thr56)	2331S	Cell Signaling Technology	1:1000	Phosphorylated eukaryotic elongation factor 2
SLC3A1	ab41751	Abcam	1:200	Solute carrier family 3 member 1
SLC38A1	ab60145	Abcam	1:200	Solute carrier family 38 member 1
SLC1A5	ab84903	Abcam	1:200	Solute carrier family 1 member 5
BCKDK	ab151297	Abcam	1:500	Branched-chain α-keto acid dehydrogenase kinase
RPS6	2217s	Cell Signaling Technology	1:500	S6 ribosomal protein
Phospho-RPS6 (Ser235/236)	2211s	Cell Signaling Technology	1:500	Phosphorylated S6 ribosomal protein
FASN	3180S	Cell Signaling Technology	1:1000	Fatty acid synthase
HSL	4107	Cell Signaling Technology	1:1000	Hormone-sensitive lipase
Phospho-HSL(Ser563)	4139	Cell Signaling Technology	1:200	Phospho-hormone-sensitive lipase
PPARG	ARP32880_T100	Aviva Systems Biology	1:1000	Peroxisome proliferator-activated receptor gamma
IRS1	ab52167	Abcam	1:200	Insulin receptor substrate 1

APPENDIX C: CHAPTER 4 - SUPPLEMENTAL MATERIAL

Supplemental Table C.1. Gene symbol, primer features, and qPCR performance for genes measured in periparturient dairy cow subcutaneous adipose tissue.

Gene symbol (GenBank number)	Primer sequence (5'-3')	Product length (bp)	Slope[1]	(R^2)[2]	Efficiency[3]	Gene name
GCLC (NM_001083674)	CACAAATTGGCAGACAATGC GGCGACCTTCATGTTCTCAT	211	-3.37	0.991	1.980	Glutamate-cysteine ligase catalytic subunit
GCLM (NM_001038143)	TGGAGCAGCTGTATCAGTGG GAATGTCAGGGATGCTCTCC	198	-3.51	0.996	1.926	Glutamate-cysteine ligase modifier subunit
GPX1 (NM_174076)	CCCCTGCAACCAGTTTGG GAGCATAAAGTTGGGCTCGAA	106	-3.67	0.983	1.873	Glutathione peroxidase 1
GSR (NM_001114190)	GAGAACGCTGGCATTGAG AGCAGGCAGTCAACATCT	143	-3.38	0.965	1.977	Glutathione reductase
ME1 NM_001144853	CCAACTGCCCTCATTGGAGT CGCGACCCTTGGTCAGTTTA	166	-3.56	0.98	1.911	Malic enzyme 1
TALDO1 NM_001035283	GCGGATGCTGAGAGAACGA AAGCATGTGCAATTAGGCCC	111	-3.26	0.997	2.028	Transaldolase 1
NFE2L2 (NM_001011678)	AGGACATGGATTTGATTGAC TACCTGGGAGTAGTTGGCA	272	-3.63	0.969	1.886	Nuclear factor, erythroid 2 like 2
KEAP1 (NM_001101142)	ACAACAGTGTGGAGAGGTATGAGC AGAGCAGACGGTTGAGGACAG	108	-3.21	0.977	2.046	Kelch-like ECH-associated protein1
CUL3 (NM_001192806)	CTTTCCGATGACCATGGATGAA GCTCCTCAAAACTAAGACCACTG	110	-2.98	0.974	2.165	Cullin3

[1]Slope of the standard curve.
[2]R^2 stands for the coefficient of determination of the standard curve.
[3]Efficiency is calculated as $[10^{(-1 / \text{Slope})}]$.

Supplemental Table C.2. Antibody symbol, catalog number, company, dilution ratio, and antibody name for antibodies measured in periparturient dairy cow subcutaneous adipose tissue.

Antibody	Catalog Number	Company	Dilution ratio	Antibody Name
GSTM1	ARP41769_P050	Aviva Systems Biology	1:250	Glutathione S-transferase Mu 1
KEAP1	ARP34727_P050	Aviva Systems Biology	1:250	Kelch-like ECH associated protein 1
ERK1/2	OASE00362	Aviva Systems Biology	1:250	Extracellular signal-regulated protein kinases 1 and 2
Phospho-ERK1/2(Thr202)	4370T	Cell Signaling Technology	1:250	Phosphorylated extracellular signal-regulated protein kinases 1 and 2
NFE2L2	137550	Abcam	1:250	Nuclear factor erythroid 2-like 2
Phospho-NFE2L2(Ser40)	PA5-67520	Invitrogen	1:250	Phosphorylated nuclear factor erythroid 2-like 2

Supplemental Figure C.1. Plasma biomarkers of inflammation and oxidative stress at-10, 7, 15 and 30 d relative to calving in Holstein cows with prepartum (28d before expected parturition) high (HBCS, BCS ≥3.5) or normal body condition sore (NBCS, BCS≤3.25) (panel A= Albumin; panel B=NO_3^-; panel C= NO_2^-; panel D= NO; panel E= Paraoxonase; panel F= Retinol; panel G= Tocopherol; panel H= Alkaline phosphatase). Data are LS means, n = 11 cows per group, ± pooled SEMs. [ab]Means differ (BCS × Day, $P \leq 0.05$).

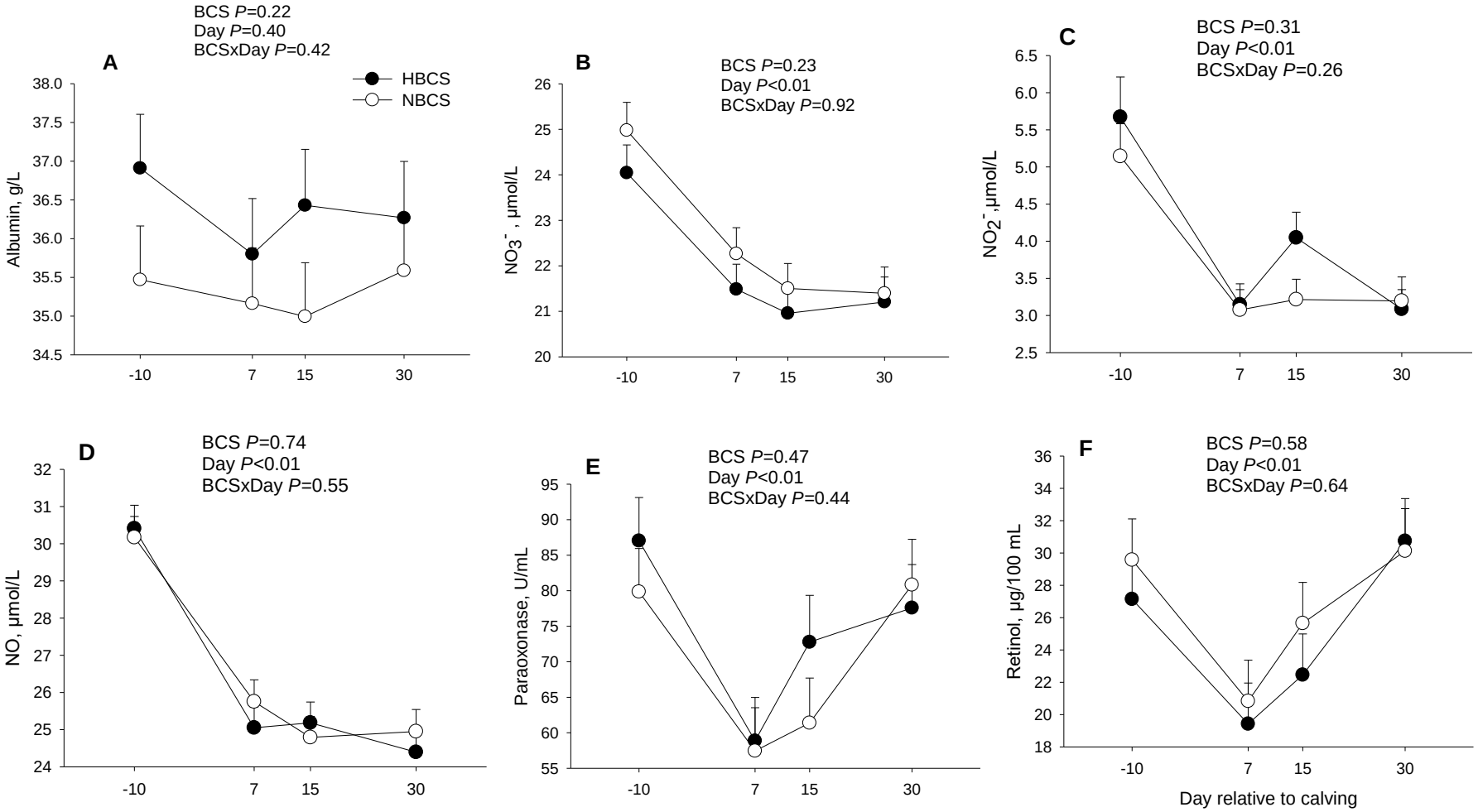

Supplemental Figure C.1. (cont.)

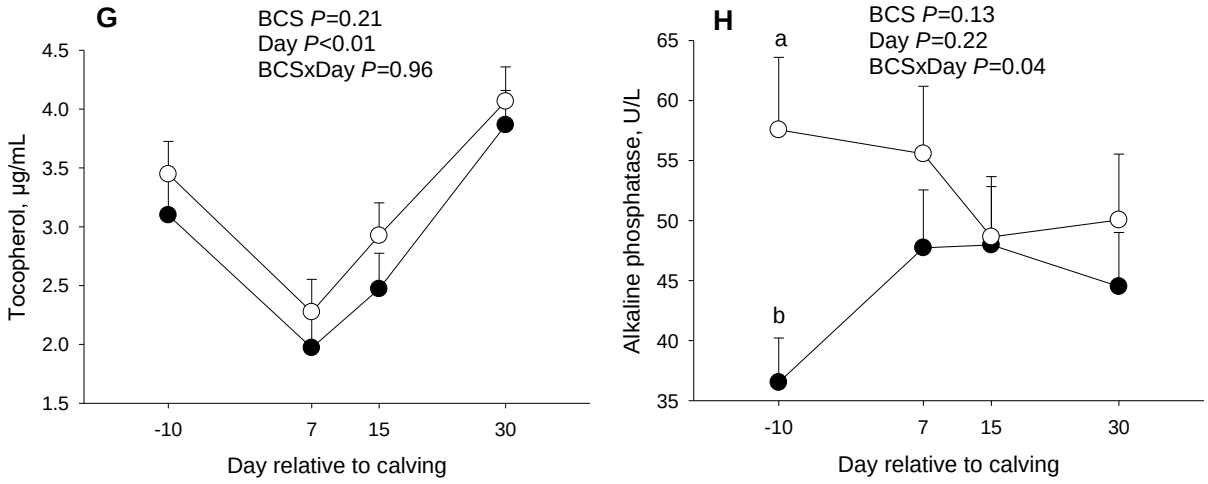

Supplemental Figure C.2. Representative blots with band size information.

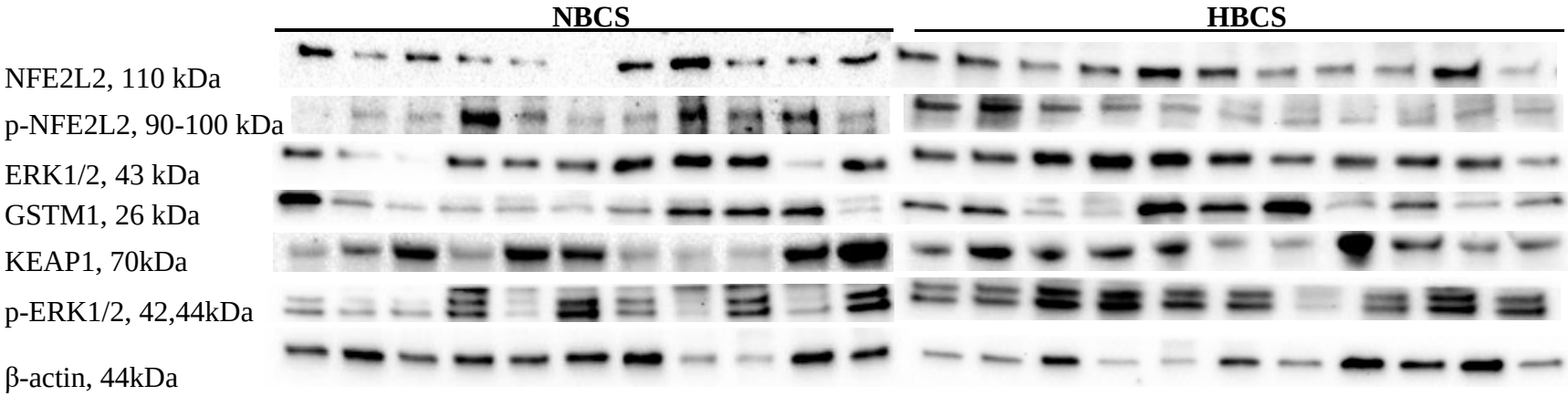

APPENDIX D: CHAPTER 5 - SUPPLEMENTAL MATERIAL

Supplemental Table D.1. Gene symbol, primer features, and qPCR performance for genes measured in periparturient dairy cow subcutaneous adipose tissue.

Gene	Primers (5'-3')	bp	Slope[1]	$(R^2)^2$	Efficiency[3]	Gene name
Amino acid transporters						
SLC1A1	GGTGATTGTGCTGAGTGCTG	133	-3.102	0.995	2.101	Glutamate transporter
NM_174599.2	CTCCACAATGCCAGTCCCAA					
SLC1A5	GGCTAGCAGCTGTTTACTCCT	129	-3.184	0.996	2.061	Neutral amino acid transporter
NM_174601.2	AGTCTGGGGGCTAGAAGACG					
SLC7A5	CCGTACCCTCACTGGTGTTC	181	-3.701	0.980	1.863	Branched-chain and aromatic amino acid transporter
NM_174613.2	AGATGAACCTTGATGGGCCG					
SLC7A1	CTTCGACCTGAAGGACCTGG	101	-3.473	0.962	1.941	High affinity cationic amino acid transporter
NM 001135792.1	GCTCGGGCTGGTATCGTAAG					
SLC36A1	GGCTATCGTCACTGCCCTCTA	100	-3.313	0.973	2.004	Neutral and cationic amino acid transporter
NM 001192498.1	ACAGTTGGGCAGGTTGAGAGTT					
SLC38A2	TGAAAAGCCATTATGCCGATGT	148	-3.287	0.987	2.015	Sodium-coupled neutral amino acid transporter 2
NM_001082424.1	CCCACAATCGCATTGCTCAG					
mTOR and insulin signaling pathway						
AKT1	CTGCACAAGCGAGGTGAGTA	134	-3.682	0.998	1.869	Protein kinase B
NM_173986.2	GAGAAGTTGTTGAGGGGCGA					
RPS6KB1	ACAGCCTGCTTTTACTTGGC	178	-3.509	0.983	1.927	Ribosomal protein S6 kinase B1
NM_205816.1	AGGTGTGTGTGACTGTTCCG					
EIF4EBP1	GGAGTGTCGGAACTCACCTG	162	-3.615	0.997	1.891	Eukaryotic translation initiation factor 4E-binding protein
NM_001077893.2	AACTGTGACTCTTCACCGCC					
INSR	CCCTTCGAGAAAGTGGTGAACA	84	-3.435	0.990	1.955	Insulin receptor
AY574999	AGCCTGAAGCTCGATGCGATAG					
IRS1	CTCAAGAGTGCCCACCTCAA	187	-3.791	0.992	1.882	Insulin receptor substrate 1
XM_003581871.4	AGGTCTTCATTCTGCTGTGAT					

Supplemental Table D.1. (cont.)

Urea cycle						
ASL	CGAGCACCTACAACAAGGAC	158	-3.476	0.990	1.939	Argininosuccinate lyase
XM_590345	GGCTAGCATGTCAGGACTCA					
ARG1	CCATCTTTCACGCCAGCTAC	224	-3.736	0.993	1.852	Arginase 1
XM_591315	CCATCTTTCACGCCAGCTAC					
ASS1	GAAGAAGGCGCTGAAGCTTG	250	-3.569	0.993	1.906	Argininosuccinate synthetase
M26198	GGTGAGCTCAAACCGGATCT					

[1]Slope of the standard curve.
[2]R^2 stands for the coefficient of determination of the standard curve.
[3]Efficiency is calculated as [$10^{(-1 / \text{Slope})}$].

Supplemental Table D.2. Antibody symbol, catalog number, company, dilution ratio, and antibody name for antibodies measured in periparturient dairy cow subcutaneous adipose tissue.

Antibody	Catalog Number	Company	Dilution ratio	Antibody Name
mTOR	2972S	Cell Signaling Technology	1:200	Mechanistic target of rapamycin
Phospho-mTOR (Ser2448)	2971S	Cell Signaling Technology	1:200	Phosphorylated mechanistic target of rapamycin
AKT	9272S	Cell Signaling Technology	1:1000	Protein kinase B
Phospho-AKT (Ser473)	9271S	Cell Signaling Technology	1:1000	Phosphorylated protein kinase B
GLUT4	ARP43785_P050	Aviva Systems Biology	1:1000	Glucose transporter 4
SLC38A1	ab60145	Abcam	1:200	Solute carrier family 38 member 1
BCKDK	ab151297	Abcam	1:500	Branched-chain α-keto acid dehydrogenase kinase

Supplemental Figure D.1. Representative blots with band size information.

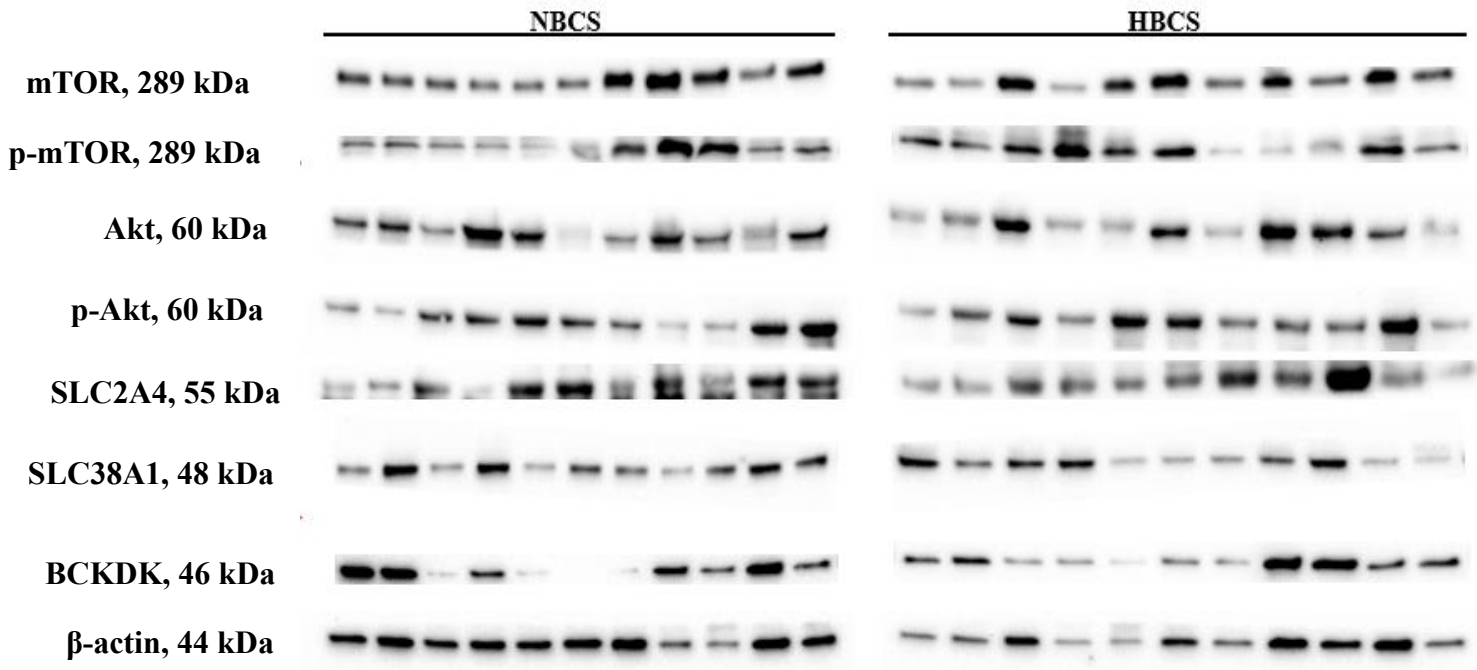

APPENDIX E: CHAPTER 6 - SUPPLEMENTAL MATERIAL

Supplemental Table E.1. Ingredient composition of the lactation diet fed to cows prior to slaughter.

Ingredient	% of DM
Corn silage	40.2
Dry ground corn grain	17.3
Canola meal expelled	5.6
Alfalfa hay	18.4
Corn gluten feed pellets	7.9
Vitamin and mineral mix[1]	4.4
Blood meal[2]	0.4
Rumen-protected lysine[3]	0.4
Rumen-protected methionine[4]	0.1
Urea 281 CP	0.4
Rumen inert fat[5]	1.5
Molasses	3.4

[1]Mineral and vitamin mix was formulated to contain 12.51% Ca, 14.06% Na, 9.60% Cl, 3.18% Mg, 6.48% K, 0.19% S, 26.93 mg/kg Co, 301.01 mg/kg of Cu, 40.22 mg/kg of I, 678.25 mg/kg Fe, 1,519.35 mg/kg Mn, 8.62 mg/kg Se, 4.47 mg/kg of organic Se, 1621.05 mg/kg of Zn, 43.34 kIU/kg Vitamin A, 10.89 kIU/kg of Vitamin D_3, 466.41 IU/kg of Vitamin E, 4.23 mg/kg of biotin, 46.65 mg/kg of thiamine, and 0.35 g/kg of monensin (Rumensin, Elanco, Greenfield, IN)
[2]ProVAAl AADvantage (Perdue AgriBusiness, Salisbury, MD)
[3]Ajipro-L Generation 3 (Ajinomoto Heartland, Inc., Chicago, IL)
[4]Smartamine M (Adisseo, Alpharetta, GA).
[5]Energy Booster 100 (Milk Specialties Global, Eden Prairie, MN)

Supplemental Table E.2. Chemical composition and associated standard deviations for diets fed to cows prior to slaughter.

Item	Mean	SD
DM, %	49.83	3.74
CP, % of DM	15.74	0.75
ADF, % of DM	20.21	1.92
NDF, % of DM	30.66	1.80
Lignin, % of DM	3.74	0.70
NFC, % of DM	41.81	2.22
Starch, % of DM	27.19	3.23
Crude fat, % of DM	4.30	0.32
Ash, % of DM	7.44	0.90
NE_L, Mcal/kg of DM	1.67	0.02
Ca, % of DM	0.82	0.13
P, % of DM	0.44	0.03
Mg, % of DM	0.29	0.02
K, % of DM	1.59	0.14
Na, % of DM	0.56	0.08
S, % of DM	0.25	0.01
Fe, ppm	260	81
Zn, ppm	101.86	14.44
Cu, ppm	13.57	1.72
Mn, ppm	76.14	7.08
Mo, ppm	1.03	0.36

Supplemental Table E.3. Catalog number and source, dilution ratios, and target protein antibodies used in the present study.

Antibody	Catalog Number	Company	Dilution ratio	Antibody Name
mTOR	2972S	Cell Signaling Technology	1:500	Mechanistic target of rapamycin
Phospho-mTOR (Ser2448)	2971S	Cell Signaling Technology	1:250	Phosphorylated mechanistic target of rapamycin
AKT	9272S	Cell Signaling Technology	1:500	Protein kinase B
Phospho-AKT (Ser473)	9271S	Cell Signaling Technology	1:250	Phosphorylated protein kinase B
GSTM1	ARP41769_P050	Aviva Systems Biology	1:500	Glutathione S-transferase Mu 1
SLC38A1	ab60145	Abcam	1:250	Solute carrier family 38 member 1
BCKDK	ab151297	Abcam	1:500	Branched-chain α-keto acid dehydrogenase kinase
eEF2	2332s	Cell Signaling Technology	1:500	Eukaryotic elongation factor 2
Phospho-eEF2 (Thr56)	2331s	Cell Signaling Technology	1:250	Phosphorylated eukaryotic elongation factor 2

Supplemental Figure E.1. Representative blots with band size information.

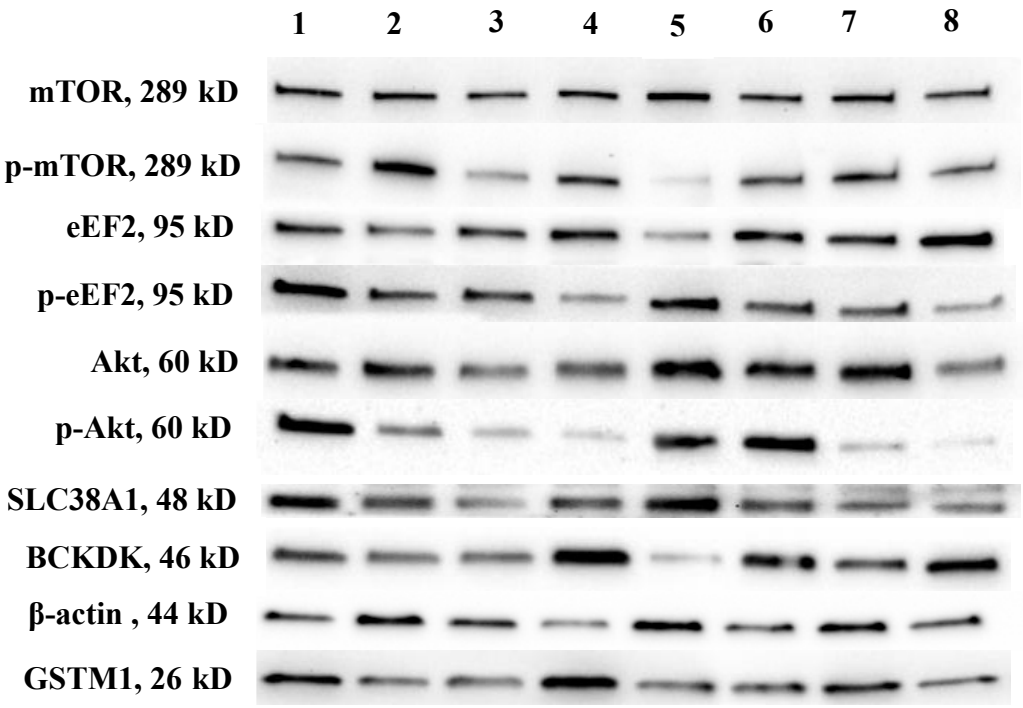

1. -Met,-Arg, -C2:0-ceramide 2. +Met,-Arg, -C2:0-ceramide 3. -Met,-Arg, +C2:0-ceramide
4. +Met,-Arg,+C2:0-ceramide 5. -Met,+Arg,-C2:0-ceramide 6.+Met,+Arg, -C2:0-ceramide
7. -Met,+Arg,+C2:0-ceramide 8.+Met,+Arg, +C2:0-ceramide

APPENDIX F: CHAPTER 7 - SUPPLEMENTAL MATERIAL

Supplemental Table F.1. Gene symbol, accession number, and forward and reverse primer sequence of the analyzed genes.

Gene[1]	Accession #	Forward sequence	Reverse sequence
GAPDH	NM_001034034.2	TGGAAAGGCCATCACC	CCCACTTGATGTTGGCAG
RPS9	NM_001101152.2	CCTCGACCAAGAGCTG	CCTCCAGACCTCACGTTTGTTC
ACTB	NM_173979.3	ACCAACTGGGACGACA	GTCTCGAACATGATCTGGGTC
IL6	NM_173923.2	CCAGAGAAAACCGAAG	CCTTGCTGCTTTCACACTCATC
TNF	NM_173966.3	CCAGAGGGAAGAGCAG	TCGGCTACAACGTGGGCTAC
IL10	NM_174088.1	GAAGGACCAACTGCAC	AAAACTGGATCATTTCCGACA
IL1B	NM_174093.1	TCCACCTCCTCTCACAG	TACCCAAGGCCACAGGAATCT
SOD1	NM_174615.2	GGCTGTACCAGTGCAG	GCTGTCACATTGCCCAGGT
SOD2	NM_201527.2	TGTGGGAGCATGCTTAT	TGCAGTTACATTCTCCCAGTTG
CAT	NM_001035386.2	TTCAGTGATCGAGGGAT	TGCAATAAACTGCCTCTCCATT

[1] *ACTB* = Actin beta; *CAT* = Catalase; *GAPDH* = Glyceraldehyde-3-phosphate dehydrogenase; *IL6* = Interleukin 6; *IL10* = Interleukin 10; *IL1B* = Interleukin 1β; *RPS9* = Ribosomal protein S9; *SOD1* = Superoxide dismutase 1; *SOD2* = Superoxide dismutase 2, mitochondrial *TNF* = Tumor necrosis factor.

Supplemental Table F.2. RT-qPCR performance among genes measured.

Gene symbol	Median Ct[1]	Median ΔCt[2]	Slope[3]	(R^2)[4]	Efficiency[5]
IL6	19.34	-1.16	-3.338	0.999	1.993
TNF	29.08	8.91	-3.222	0.997	2.043
IL10	29.69	9.54	-3.131	0.990	2.086
IL1B	24.19	4.30	-3.313	0.983	2.004
SOD1	23.29	3.06	-3.364	0.997	1.983
SOD2	22.24	2.04	-3.329	0.997	1.997
CAT	21.85	1.46	-3.326	0.996	1.998

[1]The median was calculated considering all cows.

[2]The median of ΔCt was calculated as [Ct gene – geometrical mean of Ct internal controls] for samples.

[3]Slope of the standard curve.

[4]R^2 stands for the coefficient of determination of the standard curve.

[5]Efficiency was calculated as [$10^{(-1/Slope)}$].

Supplemental Table F.3. Antibody symbol, catalog number, company, dilution ratio, and full name of antibodies used.

Antibody	Catalog Number	Company	Dilution ratio	Full name
SAMTOR	HPA050733	Sigma-Aldrich	1:200	S-adenosylmethionine sensor upstream of TORC1;
p-AKT	9271	Cell signaling	1:200	Phosphorylated AKT serine/threonine kinase
p-mTOR	2971	Cell signaling	1:200	Phosphorylated mechanistic target of rapamycin
p-AMPK	2535	Cell signaling	1:200	Phosphorylated 5'-prime-AMP-activated protein kinase
PPARG	ARP32880-T100	AVIVA systems biology	1:250	Peroxisome proliferator activated receptor gamma
p-ACACA	PA5-17725	Thermo Fisher	1:200	Phosphorylated acetyl-CoA carboxylase alpha
FASN	3180	Cell signaling	1:200	Fatty acid synthase
LIPE	ab103281	Abcam	1:50	Hormone-sensitive lipase
CBS	AV45746	Sigma-Aldrich	1:200	Cystathionine β-synthase
SLC1A3	ab41751	Abcam	1:200	Solute carrier family 1 member 3 (EAAT1)
SLC2A4	ARP43785_P050	AVIVA systems biology	1:200	Solute carrier family 2 member 4(GLUT4)
NFE2L2	ab137550	Abcam	1:200	Nuclear factor, erythroid 2 like 2
KEAP1	8047	Cell signaling	1:200	Kelch like ECH associated protein 1
GPX1	ab22604	Abcam	1:200	Glutathione peroxidase 1
GSTM1	ARP41769_P050	AVIVA systems biology	1:500	Glutathione S-transferase mu 1
RELA	4764	Cell signaling	1:200	Nuclear factor kappa B subunit p65

Supplemental Figure F.1. Representative blots of proteins in subcutaneous adipose tissue (SAT; n = 4/treatment) cultured in media with an "ideal" profile of essential amino acids (CTR; Lys: Met 2.9:1), SAT incubated with CTR plus 100 μM H_2O_2 (HP), or SAT incubated with CTR plus enhanced Met supply plus 100 μM H_2O_2 (HPMET; Lys:Met 2.5:1).

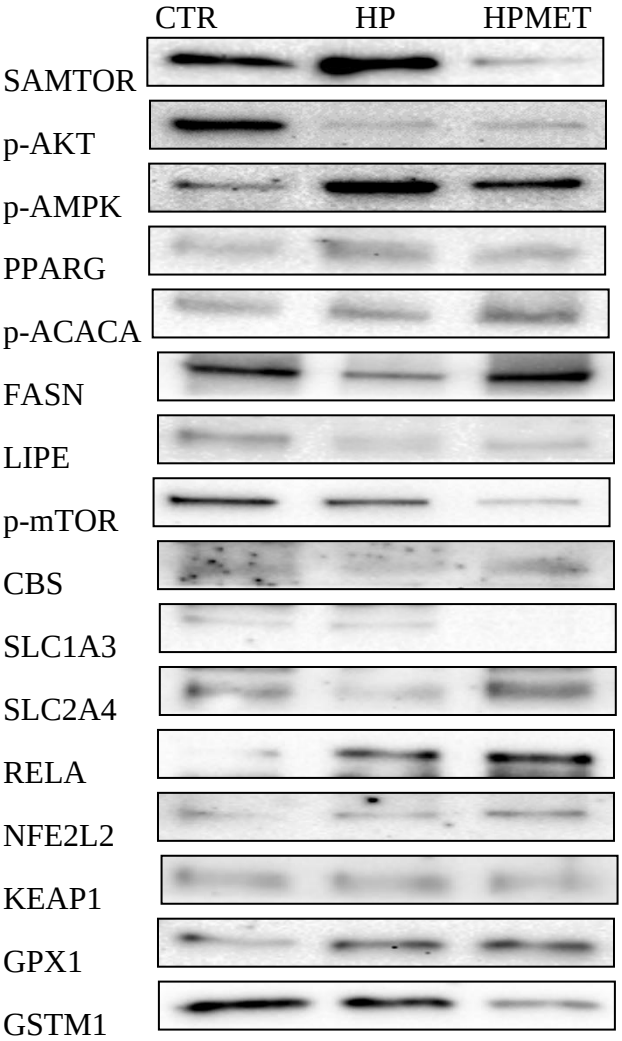

APPENDIX G: CHAPTER 8 - SUPPLEMENTAL MATERIAL

Supplemental Table G.1. Catalog number and source, dilution ratios, and target protein antibodies used in the present study.

Antibody	Catalog Number	Company	Dilution ratio	Antibody Name
mTOR	2972S	Cell Signaling Technology	1:500	Mechanistic target of rapamycin
Phospho-mTOR (Ser2448)	2971S	Cell Signaling Technology	1:250	Phosphorylated mechanistic target of rapamycin
AKT	9272S	Cell Signaling Technology	1:500	Protein kinase B
Phospho-AKT (Ser473)	9271S	Cell Signaling Technology	1:250	Phosphorylated protein kinase B
SLC38A1	ab60145	Abcam	1:250	Solute carrier family 38 member 1
BCKDK	ab151297	Abcam	1:500	Branched-chain α-keto acid dehydrogenase kinase
eEF2	2332s	Cell Signaling Technology	1:500	Eukaryotic elongation factor 2
Phospho-eEF2 (Thr56)	2331s	Cell Signaling Technology	1:250	Phosphorylated eukaryotic elongation factor 2